The University Of Sheffield.

INTEGRATION OF BIOLOGICAL WASTEWATER TREATMENT AND ALGAL GROWTH FOR BIOFUELS

A thesis submitted to The University of Sheffield by

Philippa Jane Uttley

For the degree of

Doctor of Philosophy

APRIL 2014

Department of Chemical and Biological Engineering

Sir Robert Hadfield Building

Mappin Street

Sheffield S1 3JD

UK

For Graham and Jennie,

with love

ABSTRACT

This thesis is concerned with the production of biofuels from microalgae that can be grown in wastewater on marginal land. Algal-derived biodiesel is a promising alternative to both the finite reserves of fossil fuels and also the current biofuel crops that take up agricultural land. The case for coupling biological wastewater treatment to the production of algal biodiesel is a compelling one that is explored in this research using a combination of mathematical modelling and laboratory experiments.

Algae utilise by-products of the wastewater treatment process such as carbon dioxide, nitrate and ammonia. In this work, a mathematical model of an integrated wastewater treatment and algal cultivation system is presented. The model contains two units: an activated sludge unit for secondary wastewater treatment and a pond for the cultivation of algae. These units have both liquid phase and gas phase integration. For the liquid phase, the treated effluent from the activated sludge unit is transferred to the algal pond to provide nutrients for algal growth. The model also incorporates gas-phase integration whereby the CO_2 rich off-gas from the activated sludge unit is captured and used to enhance the algal growth. In addition, the O_2 enriched off-gas from the algal pond is recycled back to improve dissolved oxygen levels in the activated sludge unit.

The mathematical model uses equations for algal growth that were developed using laboratory experiments to measure the effect of dissolved CO_2, nitrate and ammonia on the growth kinetics of a typical strain of freshwater alga: *Chlorella sp*.. The model includes the industry standard Activated Sludge Model No. 3 for wastewater treatment. An economic profit function is used in the model to find the optimal pattern of gas phase integration to maximise Net Present Value over a specified project lifetime. For the case considered, the model predicts that integration using the gas and liquid exchange described above is necessary for a profitable outcome. This is a general approach that can be used to retrofit biofuel production onto an existing wastewater site, or design a new integrated system from first principles.

ACKNOWLEDGEMENTS

I would like to take this opportunity to extend my gratitude to my primary supervisor, Dr Stephen Wilkinson, whose encouragement and guidance made this work possible. His enthusiasm in explaining concepts that were completely new to me has been very much appreciated. Steve's innovative approach to problem-solving and experimentation always kept things interesting; I feel lucky to have had such an imaginative supervisor throughout the course of this research.

I am very grateful to my secondary supervisor, Dr Jim Gilmour, from the Department of Molecular Biology and Biotechnology for advising me on all things algal. Jim has shown great patience in explaining fundamental biology to a chemist, even when I've asked for clarification on the most basic of concepts. I very much appreciate the time and knowledge afforded to me, as well as the space to work in a very busy laboratory.

I would further like to thank: Dr Stephen Palmer and MWH, for funding; The E-Futures Doctoral Training Centre, its Director, Prof Geraint Jewell, Programme Manager, Dr Neil Lowrie, and former Director, Prof Tony West; The Engineering and Physical Sciences Research Council (EPSRC) and the RCUK Energy Programme.

Thanks also to my E-Futures colleagues for advising me on subjects outside my own expertise, and to the members of Jim's group who helped me in the lab with equipment and algae.

Last but not least, my husband and daughter – thanks for making me smile at the end of each day.

TABLE OF CONTENTS

LIST OF FIGURES

LIST OF TABLES

NOMENCLATURE

Activated Sludge Model No. 3

$b_{A,NOx}$	Anoxic endogenous respiration rate of X_A (d^{-1})
$b_{A,O2}$	Aerobic endogenous respiration rate of X_A (d^{-1})
$b_{H,NOx}$	Anoxic endogenous respiration rate of X_H (d^{-1})
$b_{H,O2}$	Aerobic endogenous respiration rate of X_H (d^{-1})
$b_{STO,NOx}$	Anoxic respiration rate of X_{STO} (d^{-1})
$b_{STO,O2}$	Aerobic respiration rate of X_{STO} (d^{-1})
$K_{A,ALK}$	Bicarbonate saturation for nitrifiers (mol HCO_3^- m^{-3})
K_{ALK}	Saturation constant for alkalinity for X_H (mol HCO_3^- m^{-3})
$K_{A,NH4}$	Ammonium substrate saturation for X_A (g N m^{-3})
$K_{A,NOx}$	Saturation constant for S_{NOx} for X_A (g NO_3^- -N m^{-3})
$K_{A,O2}$	Oxygen saturation for nitrifiers (g O_2 m^{-3})
k_H	Hydrolysis rate constant (g COD_{XS} g COD_{XH}^{-1} d^{-1})
K_{NH4}	Saturation constant for S_{NH4} (g N m^{-3})
K_{NOx}	Saturation constant for S_{NOx} (g NO_3^- N m^{-3})
K_{O2}	Saturation constant for S_{O2} (g O_2 m^{-3})
K_S	Saturation constant for S_S (g COD_{SS} m^{-3})
K_{STO}	Saturation constant for X_{STO} (g COD_{XSTO} (g COD_{XH})$^{-1}$)
k_{STO}	Storage rate constant (g COD_{SS} (g COD_{XH})$^{-1}$ d^{-1})
K_X	Hydrolysis saturation constant (g COD_{XS} (g COD_{XH})$^{-1}$)
S_{ALK}	Alkalinity (mol HCO_3^- m^{-3})
S_I	Inert soluble organic material (g COD m^{-3})
S_{N2}	Dinitrogen (g N_2 m^{-3})
S_{NH4}	Ammonium plus ammonia nitrogen (g N m^{-3})
S_{NOX}	Nitrate plus nitrite nitrogen (g N m^{-3})
S_{O2}	Dissolved oxygen (g O_2 m^{-3})
S_S	Readily biodegradable organic substrates (g COD m^{-3})
X_A	Nitrifying organisms (g COD m^{-3})
X_H	Heterotrophic organisms (g COD m^{-3})

X_I	Inert particulate organic material (g COD m^{-3})
X_S	Slowly biodegradable substrates (g COD m^{-3})
X_{SS}	Suspended solids (g (SS) m^{-3})
X_{STO}	Cell internal storage product of heterotrophic organisms (g COD m^{-3})
η_{NOx}	Anoxic reduction factor (–)
μ_A	Autotrophic maximum growth rate of X_A (d^{-1})
μ_H	Heterotrophic maximum growth rate of X_H (d^{-1})

Activated Sludge Algal Pond Models

alpha	Settling constant (-)
B	Constant (3000^{-1} (kg O_2) d (h m^3)$^{-1}$)
c	Cost parameter (€)
days	Number of days process operational (d)
feed	Substrate concentration in primary effluent (g m^{-3})
G_{ps}	Gas flow from algal pond to sludge tank (m^3 d^{-1})
G_{sp}	Gas flow from sludge tank to algal pond (m^3 d^{-1})
H_{CO2}	Henry's Constant for carbon dioxide (atm^{-1})
H_{N2}	Henry's Constant for nitrogen (atm^{-1})
H_{O2}	Henry's Constant for oxygen (atm^{-1})
i	Stoichiometric conversion factor (g g^{-1})
IC	Investment Cost
K_{CO2}	Saturation constant for elevated carbon dioxide (g m^{-3})
K_{CO2atm}	Saturation constant for atmospheric carbon dioxide (g m^{-3})
k_La	Oxygen mass transfer coefficient (d^{-1})
K_{NH4alg}	Saturation constant for NH_4 (g NH_4 m^{-3})
K_{NOXalg}	Saturation constant for NO_3 (g NO_3 m^{-3})
K_{O2alg}	Saturation constant for O_2 for algae (g O_2 m^{-3})
k_{O2pond}	Rate constant (d^{-1})
kWh	Energy term (kWh m^{-3})
L_{sp}	Liquid flow from sludge tank to algal pond (m^3 d^{-1})
n_{co2}	Co-operative exponent for atmospheric CO_2 (-)
n_{nh}	Co-operative exponent for ammonium (-)

n_{no}	Co-operative exponent for nitrate (-)
$O2_{req}$	Aerobic yield (g O_2 (g COD)$^{-1}$)
oil_{pc}	Fraction of algal biomass available as lipid
OC	Operating Cost
Out	Outflow from compartment (m^3 d^{-1})
pg	Algal pond gas compartment
pl	Algal pond liquid compartment
Pres	Pressure check function
r	Revenue parameter (€ g^{-1})
S_{CO2}	Dissolved carbon dioxide (g m^{-3})
sg	Activated sludge tank gas compartment
sl	Activated sludge tank liquid compartment
V	Volume in compartment (m^3)
X_{Algae}	Algal biomass (g m^{-3})
XS_{hyd}	Hydrolysis reaction involving X_S
Y	Yield parameter (g g^{-1})
α_E	Unitary annual operation cost (€ d kWh^{-1})
Γ	Updating term (year)
δ	Cost parameter (–)
μ_{CO2}	Algal max growth rate for elevated CO_2 (d^{-1})
μ_{CO2atm}	Algal max growth rate at atmospheric CO_2 (d^{-1})
μ_{NH4}	Factor for algal growth rate on NH_4 (d^{-1})

Simple Steady-State

A_{feed}	Bulk transfer of A (g m^{-3})
K_A	Saturation constant for species A (g m^{-3})
k_{La}	Oxygen mass transfer coefficient (d^{-1})
K_{O2}	Saturation constant for oxygen (g O_2 m^{-3})
O_{2sol}	Air saturation constant of O_2 (g O_2 m^{-3})
X_H	Biomass involved in the process (g m^{-3})
μ_{max}	Maximum growth rate (d^{-1})

Acronyms

3N-BBM+V	Bold's Basal Medium with 3-fold Nitrogen plus Vitamins
AD	Anaerobic Digestion
ASAPM	Activated Sludge Algal Pond Model
AS[M]	Activated Sludge [Model]
BOD	Biochemical Oxygen Demand
CHP	Combined Heat and Power
COD	Chemical Oxygen Demand
CSTR	Continuously Stirred Tank Reactor
GAMS®	General Algebraic Modelling System
HRAP[M]	High Rate Algal Pond [Model]
HRT	Hydraulic Retention Time
IEA	International Energy Agency
IWA	International Water Association
LLS	Linear Least Squares
LP	Linear Programming
NLP	Non-Linear Programming
NPV	Net Present Value
ODE	Ordinary Differential Equation
PAO	Phosphorus-Accumulating Organism
PPT	Proximate Parameter Tuning
RWQM	River Water Quality Model
SBML	Systems Biology Mark-up Language
SLP	Sequential Linear Programming
SRT	Solids Retention Time
TAG	Triacylglycerol
WWT[P]	Wastewater Treatment [Plant]

CHAPTER 1 - INTRODUCTION

1.1 Background

1.1.1 The fuels crisis and climate change

It is now widely accepted that fossil fuels, such as oil, gas and coal, are finite resources and will, eventually, run out. Fossil oil is arguably the most at risk of impending exhaustion, with calculations from the International Energy Agency (IEA 2008) predicting that there are approximately 40 years of oil reserves remaining, given current rates of consumption. Since Aleklett et al. (2010) argued that the IEA did not consider the full implications of peak oil in their prediction of 2008, and that future supply may not equal current production rates, the IEA have now conceded that an average conventional oil field can expect to see annual declines in output of around 6% per year (IEA 2013a) once production has peaked. The world is heavily dependent upon oil, with fossil oil representing over 40% of global fuel consumption in 2011 (IEA 2013b), over 60% of which was used as transport fuel, highlighting the growing dependence on and expectation of automobility (see Figures 1-1 and 1-2 below).

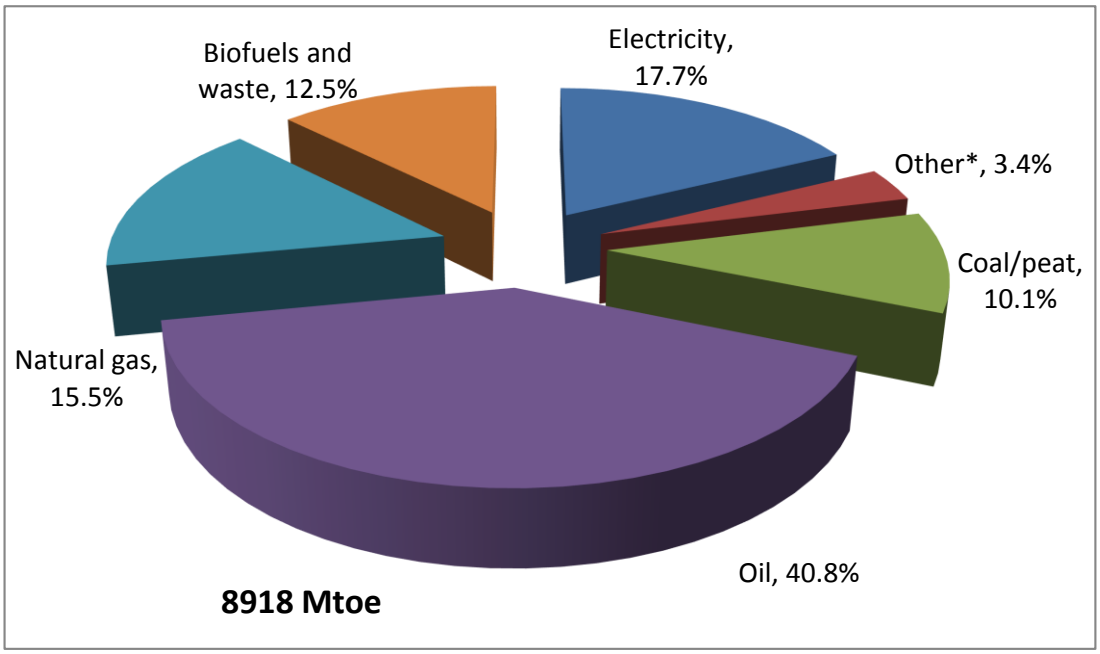

Figure 1-1 2011 Fuel Shares of Total Final Consumption – World (IEA 2013b)

*Includes geothermal, solar, wind, heat, etc.

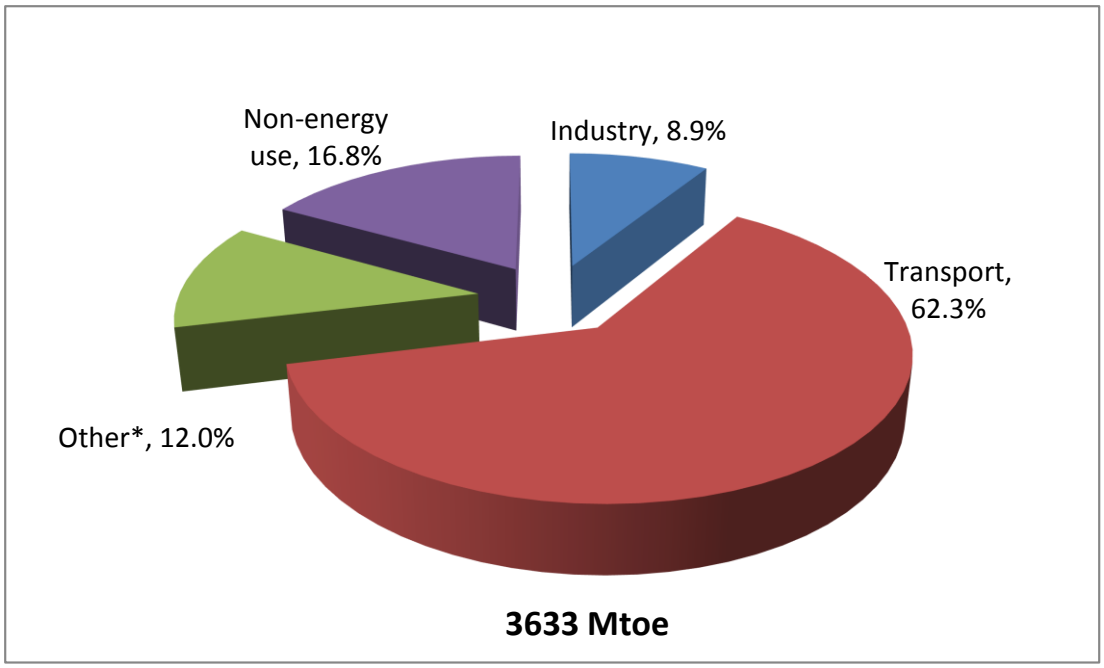

Figure 1-2 2011 Shares of World Oil Consumption (IEA 2013b)

*Includes agriculture, commercial and public services, residential, and non-specified other

As it is unlikely that the world's dependence upon oil will alter significantly in the near future, it is of great importance that provision of liquid fuels, and energy in general, is guaranteed in order to maintain, and improve, current standards of living (IEA 2010). Another matter of concern is the future supply of oil to the petrochemicals industry, which is in direct competition with energy providers for the same raw material. Only 10% of crude oil worldwide is used for the manufacture of petrochemicals (Keim 2010) with 90% being used for the provision of energy. Many everyday products, from plastics to pharmaceuticals, are derived from oil and their paucity could have serious global implications. As petroleum contains hydrocarbon units in the form they are required by the chemicals industry, it has been proposed that supplies should be safeguarded for that purpose. This is not a new concept; the interrelationship between fossil fuels and organic raw materials was highlighted by Weissermel (1980) more than thirty years ago and is an issue yet to be resolved.

Political issues can greatly affect the availability of resources from oil-rich regions, such as the Middle East, Russia and sub-Saharan Africa (Kjarstad and Johnsson 2009). This is due in part to the unwillingness of OECD countries to rely upon

nations where there is the potential for disruption to supply, following political arguments or civil unrest. Ethical issues also form part of this argument, and include concerns such as widespread fuel poverty in resource-rich countries, where the benefits of hydrocarbon wealth are not shared out equally among the nations' citizens. Internal politics can also affect oil production with political leaders being unwilling to hand control of oil reserves over to international companies (IEA 2008), having the belief that national companies will better serve the interests of their nation.

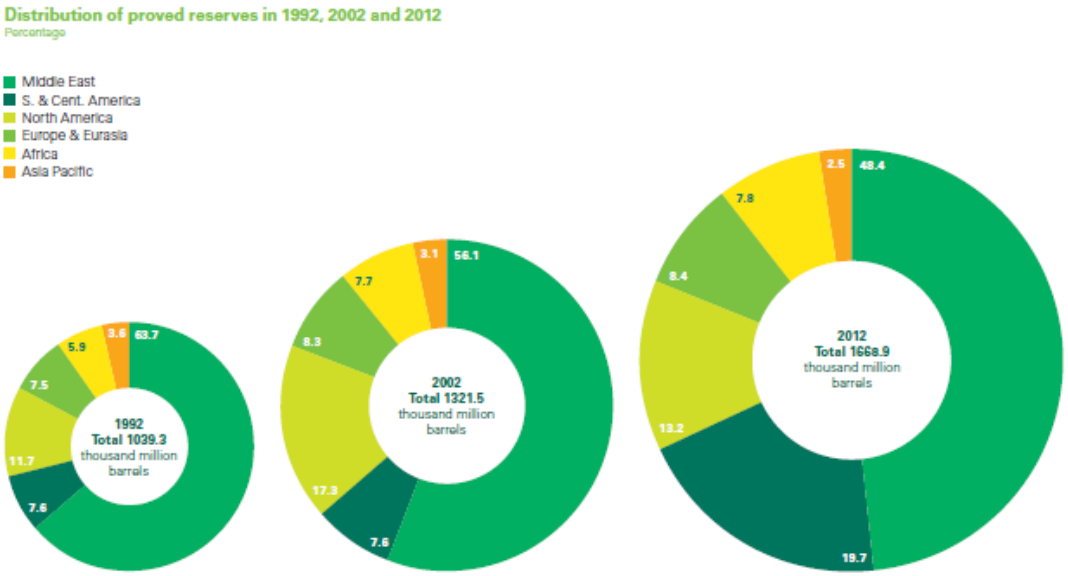

Figure 1-3 Distribution of proved oil reserves in 1992, 2002 and 2012 (BP 2013)

Recently, technologies to exploit new types of resources – such as light tight oil, ultra-deepwater fields and bituminous sands – have advanced greatly (IEA 2012; IEA 2013a) but this in itself raises concerns about greenhouse gas emissions and climate change. The greenhouse effect, caused by water vapour and carbon dioxide, plays an important part in maintaining the earth at its natural temperature (Le Treut et al. 2007). Historically, the earth's climate system has gone through periods of heat and cold along with fluctuating carbon dioxide levels (Petit et al. 1999; Raynaud et al. 2000) and is influenced by its own internal dynamics. However, the burning of fossil fuels has led to a higher concentration of carbon dioxide in the atmosphere than would naturally be found, with a steep and continuing rise since the Industrial Revolution (MacKay 2009; Kone and Buke 2010), causing an increase in the earth's

temperature, which may be further exacerbated by the melting of snow and reduction of albedo (Cubasch et al. 2013).

Regulations limiting the amount of carbon dioxide that can be released into the atmosphere have been set by means of the Kyoto Protocol (United Nations 1998). This was followed up in the UK by the Climate Change Act (Great Britain 2008) stating that the net UK carbon account for the year 2050 will be at least 80% lower than the 1990 baseline. As well as emissions and carbon trading schemes, the Act covers other provisions such as waste reduction and recycling but the Department of Energy and Climate Change predict that the UK will remain dependent upon fossil fuels, particularly oil for transport and gas for electricity generation, for some time to come (Department for Energy and Climate Change 2013). The British Government does, however, remain committed to the use of renewable energy with the pursuance of policies that support emissions reduction and bioenergy use (Department for Energy and Climate Change 2009; Department for Energy and Climate Change 2012). Nevertheless, as the UK's carbon dioxide emissions represented approximately 1.6% of the global total in 2010 (United Nations 2013), cooperation and agreement between all countries of the world will be required before significant reductions in global greenhouse gas emissions can be made.

1.1.2 Biofuels

One possible solution to the problems outlined above is the development of sustainable biofuels extracted from plant biomass. Demirbas (2009) describes the major benefits of biofuels, detailing positive economic and environmental impacts, as well as providing energy security. Biofuels have the advantage of global availability – occurrence of fossil fuels is localised – and countries without traditional oil resources have the potential to grow biofuel crops. Another advantage is the opportunity to be carbon-neutral; carbon dioxide emitted on combustion of a biofuel has only recently been absorbed from the atmosphere – unlike fossil fuels, which were formed from atmospheric carbon millions of years ago. In addition to these advantages, biofuels would not suffer from the same

depletion rates as traditional fuels as biomass can be continually grown and harvested.

Several types of liquid biofuel can be synthesised, such as biodiesel, bioethanol, biokerosene and biobutanol, all of which can be used as replacements for the fossil-derived liquid fuels currently in use. Ethanol and butanol can be produced from cereals and sugar beet or cane, while biodiesel and biokerosene are derived from oils, such as palm or rapeseed (Bellarby et al. 2010; Swana et al. 2011; Llamas et al. 2012); these are examples of 1st generation biofuels where the plant products are commonly found in the human food chain. More interesting, perhaps, are the 2nd generation biofuels – grown in the same way as 1st generation fuels but are either non-edible residues of food crop production or lignocellulosic biomass that is not used for human consumption (Nigam and Singh 2011). Examples of these are *Miscanthus*, which is used to produce bioethanol, and *Jatropha*, for biodiesel (Chisti 2007; Bellarby et al. 2010). Another crop of interest is hemp, as it is well suited to UK growing conditions and the whole plant can be utilised – i.e. the stems, leaves, flowers and seeds. A range of products can be obtained from hemp, including essential oils, nutritional supplements, high quality fibres, animal feed and low carbon construction materials (Lanot and McQueen-Mason 2011). Following extraction of high-value products, the residual biomass is then suitable for biofuel production.

A successful example of biofuel use is the Brazilian project ProAlcohol, which uses bioethanol from sugarcane as an alternative to gasoline (Matsuoka et al. 2009; Solomon 2010; Demirbas 2011). Brazil's experience of bioethanol spans over 30 years, making it the third largest global producer of ethanol after North and Central America and South America (RFA 2014). Pure gasoline is no longer sold in Brazil's filling stations – a blend containing 20-25% of locally-produced ethanol is available as a replacement – and electricity is generated from the combustion of spent biomass; it is envisaged that sugarcane will supply approximately 30% of Brazil's energy needs by 2020 (Matsuoka et al. 2009). In contrast, Germany was the top biodiesel-producing nation in 2008, with approximately 75% of all biodiesel being produced in Europe (Solomon 2010). Choice of feedstock is made based on

government policies, the overall transportation fuel consumption of the country in question, as well as geographic distribution of resources and climate.

Despite these successes, the use of 1st and 2nd generation fuel crops does pose significant questions. Perhaps most importantly is the food versus fuel argument – what are the moral and ethical implications of using foodstuffs to generate transport fuels? Many hectares of land are used that may, in fact, be needed to feed an increasing global population. Add to this the issues of soil degradation, eutrophication and the requirement for water and fertiliser (Rowe et al. 2009; Clarens et al. 2010; Solomon 2010), and the case for biofuels becomes less convincing. Nevertheless, there is another alternative: a 3rd generation biofuel in the form of oil derived from microbial biomass, such as fungi or algae. Recent research demonstrates that certain strains of filamentous fungi may contain almost 50% lipid, making them of great interest for the production of biodiesel (Sergeeva et al. 2008; Strobel et al. 2008; Lunin et al. 2013). However, this thesis will concentrate on microalgae, which will be discussed in the next chapter.

1.2 Project Aims

This project aims to explore the possibilities for process integration between existing wastewater treatment processes and the next generation of technology to produce biodiesel from microalgae, investigating the benefits of these complementary processes via the construction of a mathematical model. Biological wastewater treatment is an established biochemical process that utilises microorganisms to reduce the contaminants in domestic and industrial effluents to acceptable levels for discharge. Photosynthetic microalgae are autotrophic organisms that fix carbon dioxide from the atmosphere in order to grow; they are actively under consideration for large scale biodiesel production since, under the right conditions, some strains of algae produce high levels of lipid that are suitable for conversion to biodiesel.

The project is sponsored by the MWH Group, who is interested in both the economics of massive scale production of microalgae for biodiesel and improving

the environmental impact of wastewater treatment. MWH is a global organisation within the wet infrastructure sector that is involved in a variety of management and engineering schemes, including: water supply, treatment and storage, hydropower and renewable energies, and environmental services.

This thesis aims to build upon the commercially available mathematical models that are used within the wastewater treatment industry by coupling the Activated Sludge Model No. 3 (ASM3) with a model of algal growth, thereby utilising the by-products of wastewater treatment as a source of nutrients. The Activated Sludge suite of models (Henze et al. 2000) are designed to characterise the biological processes within an activated sludge tank, with a view to predicting total wastewater treatment times for a given wastewater composition. The integrated model of biological wastewater treatment and algal growth should combine mathematical sub-models of both individual processes and bulk transfer expressions between the separate units.

Once an understanding of the interactions of each dynamic process within the model is reached, the master model will be coupled to a mathematical optimisation algorithm to consider the financial implications of such a project. Inbuilt cost functions can be optimised for minimum cost and maximum algal growth and profit. Parameters for optimisation may include flow rates and the interconnections between bioreactors. Because of the problem complexity, a nonlinear programming problem is proposed to obtain some insights for future models. This work is not intended as a platform for a novel method of optimisation and an optimal model of the integrated process is not anticipated. The aim of this work is to produce an economic model that is relevant to the wastewater treatment industry and a useful tool in the decision-making process when gauging the feasibility of an algal pond extension to a WWTP using the activated sludge process. This work outlines a whole-process model that combines wastewater treatment, carbon capture and algal growth of a design that has not previously been seen in the literature.

It is clear that the use of liquid fossil fuels is unsustainable for reasons of both resource depletion and environmental considerations. Although there may be several years' of oil reserves remaining, these stocks cannot be exploited without major investment and multi-national cooperation. Furthermore, the pledge of the UK Government to drastically reduce its carbon dioxide emissions by 2050 makes the continued use of fossil fuels increasingly controversial. Nevertheless, the requirement remains to provide a renewable and sustainable source of liquid fuels for the global population. There are many excellent ideas currently under consideration with regard to algal biofuels, including ways in which to minimise cost by using as much of the algal cell as possible. However, there is a lack of research linking all of the possible processes that could result in maximum profitability for the biofuels industry, and it has already been suggested that the treatment of wastewater should form the basis for this research. Industrial symbiosis, the co-existence of two or more mutually-beneficial processes, is becoming increasingly significant as industry comes to terms with the concept of enhanced waste utilisation. Progress is being made in the area of process integration and it is now being recognised that wider implications, such as sustainability, should be built into the integration studies.

To fully understand the process design the parameters required for the provision of nutrients to algae from wastewater, for example, mathematical modelling is of utmost importance. Businesses will be reluctant to invest in such a novel scheme unless there are strong indications of a profitable outcome, in addition to the knowledge that wastewater treatment targets will be met. Mathematical modelling and optimisation provide the best methods for exploring various plant configurations and the costs and profits associated with every possible design.

1.3 Contributions and Thesis Structure

The contributions of this thesis are as follows:

- a modelling framework of an integrated activated sludge-algal pond system, based on a detailed representation of wastewater treatment, enabling economic analysis
- experimental work, providing important parameters for algal growth
- results that suggest the profitability of such a system.

These contributions are presented and discussed throughout the thesis. To begin with, Chapter 2 provides a review of the relevant literature. Chapter 3 describes the methods used for computational modelling, and Chapter 4 covers materials and methods for the laboratory experiments with microalgae. Chapters 5 and 6 provide the results of the Activated Sludge Algal Pond Model (ASAPM) versions 1 and 2. Chapter 7 presents the results of the laboratory work, and Chapter 8 details the results of ASAPM v3. Conclusions and further work are discussed in Chapter 9.

CHAPTER 2 - LITERATURE REVIEW

2.1 Microalgae

2.1.1 Characteristics and requirements for growth

Algae belong to a group of eukaryotic organisms (Madigan et al. 2003) that carry out oxygenic photosynthesis and include great diversity across thousands of species. Such is their diversity that algae can be found in the oceans, lakes, rivers, rocks and soil, and in extremes of temperature from permanent snow and ice to deserts (Belcher and Swale 1976). Algae are either unicellular or colonial and most are microscopic, although seaweeds, which also belong to this group, can grow to over 50 m in length. Green algae are related to green plants and each algal cell contains one or more chloroplasts, which holds the photosynthetic pigments. Alongside the usual cell activities, certain strains of microalgae produce lipids, hydrocarbons, or other complex oils. This is well known in *Botryococcus braunii*, a colonial alga, which excretes long-chain hydrocarbons; up to 75% (Chisti 2007) of its dry weight can be attributed to oil content. Other oil-producing algae include species of *Chlorella*, *Nannochloropsis* and *Dunaliella*, and there is some evidence to suggest that certain types of oil shale originated from green algae growing in lake beds in prehistoric times (Madigan et al. 2003). Further beneficial features of microalgae are their ability to grow rapidly, often doubling their mass within 24 h, and high photosynthetic yields of approximately 3-8% solar energy conversion (Chisti 2007; Lardon et al. 2009).

The adaptable nature of algae is demonstrated across its many species, some of which can grow in extreme environments. For example, Gilmour (1990) describes the habitats of organisms found in shoreline rockpools where salinity and temperature can increase significantly at low tide. An incoming tide then causes an abrupt change in conditions, which the rockpool organisms must withstand in order to survive. These survival mechanisms are of interest when considering the utilisation of microalgae for biodiesel – specifically, the production of a compatible solute. With the purpose of maintaining cell volume and function, and to prevent

sodium-ion poisoning of cells and cell membranes, starch is converted into a compatible solute, often glycerol, when intracellular water is reduced due to high external salinities. Consequently, glycerol production is a rapid process seen in actively growing cells and allows photosynthesis to recommence under non-ideal conditions.

Another, slower, mechanism seen in cells that are no longer growing rapidly produces triacylglycerol (TAG) in response to growth inhibition. This mechanism is of interest when using microalgae to produce biofuels and research is ongoing to understand how TAG could be synthesised preferentially within the cell (Liu, Y.M. et al. 2013). Nutrient deprivation, in the form of nitrogen starvation, may be used to trigger the formation of lipid in certain species (Lardon et al. 2009; Stephenson et al. 2010; Liu, J.Y. et al. 2013) as may the use of certain drugs that induce neutral lipid accumulation as result of stress in the endoplasmic reticulum (Kim et al. 2013). Another more novel technique to encourage TAG accumulation is the air-drying of algal cells that have been fixed onto a microfibre surface by filtration (Shiratake et al. 2013). Although this technique is in its early stages of development, it could prove useful for the industrial production of TAG in the future. However, the focus of this thesis is the integration of algal growth with wastewater treatment and targeted lipid production will not be considered in further detail.

Commercially, algae can be grown in either photobioreactors or raceway ponds (Chisti 2007; Clarens et al. 2010; Stephenson et al. 2010); both utilise natural light and each offer various pros and cons. Photobioreactors are tubular arrays of glass or plastic solar collectors, which are filled with the microalgal culture. These may prove useful for growing small volumes of concentrated algal culture, but the assembly is difficult to scale up beyond a tube length of 80 m. This restriction is due to a requirement to return the culture to a degassing zone to extract the oxygen produced in photosynthesis, in order to avoid photo-oxidative damage to cells. Raceway ponds are closed-loop recirculation channels that are open to the atmosphere and very simple to construct. Production volumes from the ponds can be negatively affected by contamination with adventitious microorganisms as well as poor growth rates caused by dark zones at the bottom of the channels.

However, the use of raceway ponds has been shown to be the least energy-intensive (Lardon et al. 2009; Stephenson et al. 2010) and likely to be used in preference to the photobioreactor for algal production on a large scale.

Both methods of cultivation require a source of carbon dioxide and other nutrients, such as nitrogen and phosphorus, for growth – the challenge being to find the best source for these. Indeed, a life-cycle assessment by Clarens et al. (2010) judged the provision of renewable sources of nutrients and carbon dioxide to be the most important factors in the viability of algal biodiesel. Kadam (2002) proposed that location of an algal farm adjacent to a coal-fired power station would provide a convenient source of carbon dioxide from flue gases, and co-firing with algal biomass would be financially and environmentally advantageous. Additionally, Lizzul et al. (2014) found a reduction in the nitrogen oxide content of exhaust gases when supplied to a culture of *Chlorella sorokiniana*.

In a comprehensive report by Lundquist et al. (2010), where a cost analysis of algal biofuel production has been undertaken, four out of the five cases studied used offsite flue gases to provide CO_2 to the algal pond. This report goes so far as to suggest that new-build industrial projects that produce carbon dioxide should be accompanied by algal ponds to negate emissions by producing valuable biomass. This is not the first time that microalgae have been used as a way to absorb evolved CO_2, having been researched as part of the Russian space programme in the 1960s and '70s (Gitelson et al. 1976). In the experiments, gases were exchanged between the four compartments of a hermetically sealed unit, with a compartment each for wheat, vegetables and *Chlorella sp*., and one for human operatives. One object of the experiment was to measure the removal of carbon dioxide by plants to replace it with oxygen for human consumption; it is this concept that is adopted in this research – the transfer of evolved CO_2 to an algal pond and return of O_2 for use in the activated sludge process.

As mentioned previously, a build-up of oxygen in the medium can inhibit algal growth and cause photo-oxidative damage to cells, resulting in a low density culture. Marquez et al. (1995) worked on experiments to investigate the inhibitory

effect of oxygen accumulation on the growth of algae. This work produced a reciprocal plot of dissolved oxygen concentration versus the rate of photosynthesis, from which a value for the inhibition constant, K_i, was obtained. This value has proved useful in this research for the modelling of algal growth, where the concentration of oxygen in the algal pond is taken into consideration along with substrates necessary for growth. Recent research at the University of Sheffield has found a way to counteract this inhibitory effect. In a pilot scale study by Zimmerman et al. (2011), the use of microbubbles have the ability to both deliver CO_2 rich gas to an algal culture and strip evolved O_2 from the medium at the same time. In order to take advantage of the high carbon dioxide content of steel plant exhaust gases, a fluidic oscillator was used to produce very small bubbles to increase the mass transfer of CO_2 into the culture medium. Not only was this intention met but the algal culture showed exponential growth of biomass, consistent with the removal of the inhibitory effect of dissolved oxygen.

As algae are highly adept in the uptake of nitrogen and phosphorus, municipal or agricultural wastewater could provide a convenient water source for a freshwater alga. In the aforementioned life-cycle assessment by Clarens et al. (2010), three different types of wastewater effluents were investigated and their use, when compared with freshwater, was shown to have a beneficial effect on the burdens considered in their research. The concept of using algae to treat wastewater is not new and was a matter of interest for the California State Water Pollution Control Board in the 1950s (Allen 1956). Research into this area was continued to gain more insight into the uptake of nitrate and phosphate in secondary effluents (Kawasaki et al. 1982), therefore establishing the use of algae as a tertiary treatment in dealing with domestic and agricultural wastewater. The luxury uptake of phosphorus has also been shown to occur under conditions relevant to waste stabilisation ponds (Powell et al. 2008), although this thesis will focus on nitrogen uptake in secondary effluent following treatment by the activated sludge process. Recent research tends to concentrate on how the tertiary treatment of wastewater with algae can be optimised for biomass production as well as nutrient removal (Ji et al. 2013; Osundeko et al. 2013; Arbib et al. 2014). Still, more work is needed to

connect all of the above ideas to give a more complete picture of the commercial cultivation of biofuel feedstocks from algae.

2.1.2 Algal biofuels

Following algal growth, downstream processing is required to manufacture the final biodiesel product. The steps required for production of biodiesel are harvesting, lipid extraction and conversion, and each of these steps can be made up of two or more processes (Brennan and Owende 2010). An assessment of algal biodiesel production by Stephenson et al. (2010) goes into some detail on downstream processing and describes the steps from cultivation to lipid extraction. For example, the process may comprise: flocculation using aluminium sulphate and dewatering; cell disruption and lipid extraction; transesterification of TAG to biodiesel. According to Cao et al. (2009), one of the main challenges to algal biofuels is the cost of energy intensive harvesting and drying techniques. One possible solution to that is the use of textured, stainless steel sheets submerged in the medium to which the algae can attach, then to be scraped off once a thick layer of cells has accumulated. A similar approach has been adopted by Johnson and Wen (2010), using polystyrene foam but it is yet unclear how these methods could be used on an industrial scale.

Unfortunately, triacylglycerol cannot be used directly in diesel engines due to its high viscosity and low volatility (Demirbas 2005). Additionally, the presence of polyunsaturated fatty acids in algal lipid makes the oil susceptible to oxidation and would not, therefore, comply with existing standards for biodiesel intended for vehicle use (Chisti 2007). However, triacylglycerol can be converted to methyl esters (biodiesel) via transesterification using monohydric aliphatic alcohols (Brennan and Owende 2010). Methanol is commonly used due to its low cost and physico-chemical advantages, e.g. reactivity and low boiling point. Although the stoichiometry of the reaction is 3:1 alcohol to TAG, the alcohol is added in excess to drive the equilibrium to the right and the reaction to completion (see Figure 2-1, below). The reaction can be either acid- or base-catalysed, however base catalysis

is normally preferred due to faster reaction rates, lower reaction temperatures and higher conversion efficiency (Fukuda et al. 2001).

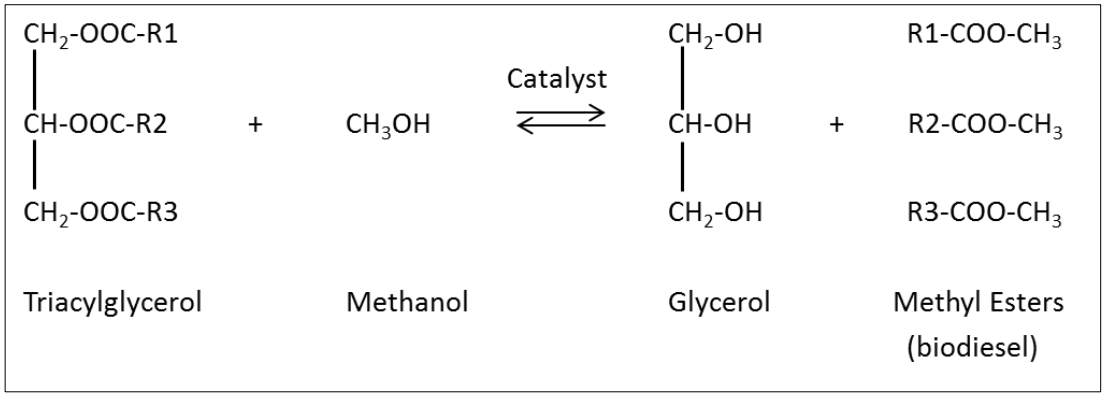

Figure 2-1 Transesterification of TAG with alcohol (Fukuda et al. 2001)

Alternatively, the transesterification reaction can be catalysed enzymatically. Disadvantages associated with base catalysts – such as saponification and subsequent catalyst recovery and biofuel separation – can be avoided with the use of lipases. Reactions using biocatalysts generally take place under mild conditions and therefore have a lower energy requirement. In addition to this, no separation step is needed following transesterification when lipases are used in packed bed reactors, and some have the ability to convert both triacylglycerol and polyunsaturated fatty acids into biodiesel (Yan et al. 2014). Large-scale application of enzyme catalysed transesterification is less common than chemical procedures due to the high cost of lipases. However, costs are now decreasing and biocatalysts may be the future for biodiesel production due to the advantages outlined here.

As well as lipids for biodiesel, algal biomass can be used to produce biogas in the form of methane. Situation of anaerobic digestion (AD) alongside algal biodiesel production is another way to maximise the total energy output from an algal cell (Brune et al. 2009; Sialve et al. 2009): following lipid extraction, the remaining biomass is fed into the digestion vessel, from which methane and liquid digestate is collected. Methane may be used to fire a generator, from which the electricity for liquid pumping, etc. may be obtained, and liquid digestate is a convenient source of nutrients. Of course, lipid removal will reduce the overall methane productivity from digestion of the biomass, so the aims of the process must be decided

beforehand. If the aim of algal growth is biodiesel production, then biogas yield would be reduced; on the other hand, if biodiesel is not required, the whole algal cell would be available for AD, therefore maximising biogas production. This introduces the concept of a biorefinery, which will be discussed further throughout the chapter.

2.2 Biological Wastewater Treatment

2.2.1 Overview

For reasons of public health and environmental protection, regulations are in place to control the quality of wastewater that is released into the UK's watercourses, and biological wastewater treatment often forms the basis for compliance. Detailed information regarding wastewater treatment can be found in selected texts, including Metcalf and Eddy's Wastewater Engineering (Tchobanoglous et al. 2004), Environmental Engineering (Kiely 1998), Wastewater Treatment Plant Design (Vesilind 2003), Activated Sludge (Gray 1990), and sections in Basic Biotechnology (Vandevivere and Verstraete 2006) and Brock's Biology of Microorganisms (Madigan et al. 2003). Untreated wastewater can contain organic and inorganic compounds, nutrients and pathogenic microorganisms – each having their own associated risks. If wastewater is allowed to stand and decompose, problems can arise with regard to odour, which is one of the main concerns raised by the general public (Tchobanoglous et al. 2004). If it is to be re-used as drinking water, proper treatment and disinfection is required to eliminate all toxins and pathogens to avoid risk of disease. Wastewater containing nutrients should be carefully treated to prevent eutrophication upon release into rivers; algal blooms disrupt photosynthesis in plants that grow on riverbeds and can also encourage bacterial growth, which in turn causes a reduction in the amount of dissolved oxygen in the water, leading to negative impacts on fish and other aquatic life.

The level of contamination by carbonaceous compounds, and the efficiency of treatment, is measured in terms of the biochemical oxygen demand (BOD). This measure describes the amount of dissolved oxygen required by aerobic biological

organisms to oxidise the organic matter in the water sample. As the measurement relies upon biological processes, it typically takes five days to complete and is known as the BOD_5. An alternative measurement, the chemical oxygen demand (COD), uses potassium dichromate in an acid solution to obtain the oxygen demand value in around 2 hours. However, as the digestion procedure can oxidise more compounds than would be oxidised biologically, it must be taken into account that the COD value is frequently higher than the BOD value. Put simply, the BOD_5 is a measure of biodegradable organic carbon, and the COD a measure of the total organic carbon in a sample of wastewater (Kiely 1998).

In addition to organic compounds, two key nutrients found in wastewater are nitrogen and phosphorus. While both elements are essential for the growth of plants and microorganisms and are necessary for the biological wastewater treatment process to proceed, if released in large quantities, the environmental effects outlined in earlier paragraphs may arise. Both nitrogen and phosphorus exist in wastewater in various forms, making measurement more challenging. For example, nitrogen is commonly present as ammonia, ammonium, nitrite and nitrate. While nitrite (NO_2^-) is an unstable intermediate, nitrate (NO_3^-) is a useful measure of the stability of the water with respect to oxygen demand. Likewise, phosphorus can exist as orthophosphate, polyphosphates and organic phosphate. Orthophosphate is the only form that can be measured directly; polyphosphates and organic phosphates must undergo acid digestion prior to analysis. Nitrogen can be removed in properly designed biological treatment plants; phosphorous removal is achieved by addition of iron or aluminium salts prior to settlement, or by assigning additional controls in the activated sludge process.

2.2.2 The Activated Sludge Process

Municipal wastewater treatment usually consists of primary and secondary treatments – primary treatment being the physical separation of solid and liquid wastes. One type of secondary treatment is the activated sludge (AS) process and approximately half of the UK's wastewater is treated this way – the rest being treated by the older, more land-intensive system of biological filtration

(Staffordshire University 2011). While activated sludge is more technically demanding, it requires a fraction of the land area and is more effective in removing nitrogen and phosphorus.

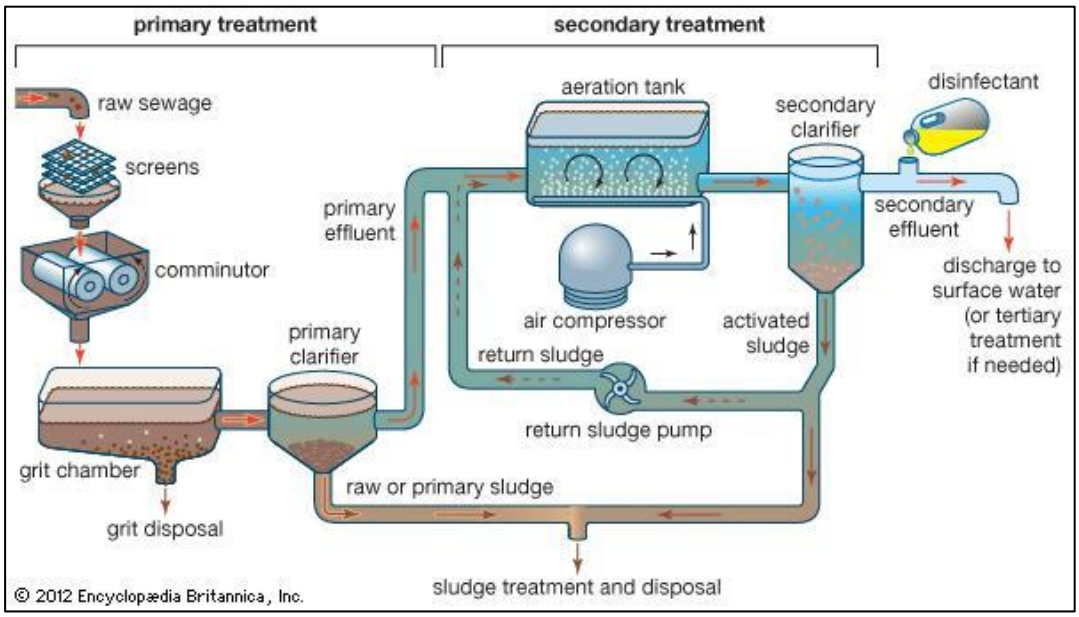

Figure 2-2 Primary and secondary treatment of sewage, using the activated sludge process (Encyclopedia Britannica 2014)

The activated sludge process is a suspended growth process, which uses a consortium of bacteria and other microorganisms to transform dissolved biodegradable constituents into acceptable end products. The liquid suspension is maintained by appropriate mixing methods and aerated to achieve a positive dissolved oxygen concentration (Tchobanoglous et al. 2004). A general formula for the biological process is as follows:

$$\nu_1(organic\ material) + \nu_2 O_2 + \nu_3 NH_3 + \nu_4 PO_4^{3-} \xrightarrow{microorganisms} \nu_5(biomass) + \nu_6 CO_2 + \nu_7 H_2O$$

Equation 2-1

where ν_i is the stoichiometric coefficient.

This formula describes how microorganisms, largely bacteria, can be employed to convert organic material (ν_1) into simple end products such as carbon dioxide, water and new cells (ν_5). Oxygen (O_2), ammonia (NH_3) and phosphate (PO^{3-}_4) are the nutrients required by the microorganisms. During the process, bacteria aggregate

into flocs that act as a platform upon which other bacteria and protozoa can grow to produce an activated sludge.

An important parameter in process control is the Solids Retention Time (SRT), which describes the average time, in days, that solids spend in the system. These solids are mainly the sludge which comprises cell biomass that has grown in the system. Flow rates can be adjusted to increase or decrease the SRT, and a longer residence time will lead to more complete treatment of the wastewater. At a rate determined by the treatment goal, the mixed liquor is fed into the secondary clarifier where the activated sludge is allowed to settle; clarification may be aided by species of protozoa that consume bacteria, therefore effectively 'polishing' the secondary effluent. Some of the settled sludge is returned to the aeration tank and acts as an inoculum to treat a continuous flow of wastewater; the wasted sludge is either dried and burned or used for fertiliser, or directed to AD. The treated water is then discharged into watercourses or sent for further purification treatments. Although the wastewater constituents are not completely removed by the activated sludge process, residual levels are low enough to meet local and national quality standards.

The biological mechanisms within the AS process are many and complex. For example, certain bacteria will be responsible for the conversion of ammonia to nitrate under aerobic conditions, while another species will convert nitrate to nitrogen gas under anoxic conditions. Likewise, the activated sludge process may be configured such that specific bacteria store large amounts of phosphorus to facilitate phosphate removal. In order to model the activated sludge process mathematically, key reactions must be isolated and simplified and ASM3 (Gujer et al. 2000) can be adopted as a general description of the biological process as a whole. For example, Figure 2-3 illustrates how nitrifying and heterotrophic organisms work independently of each other to decay slowly biodegradable substrates and ammonium into inert particulate biomass.

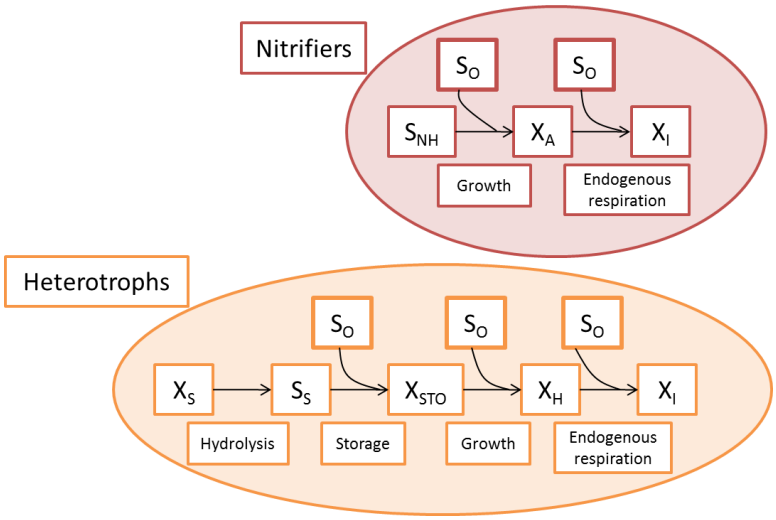

Figure 2-3 Flow of COD in ASM3 (Gujer et al. 2000)

Within the model, concentrations of soluble compounds are characterised by S and particulate compounds by X. The process is initiated by the hydrolysis of X_S (slowly biodegradable substrates) to S_S (readily biodegradable organic substrates). Following hydrolysis, a series of reactions describes the activity of heterotrophic organisms (X_H) via the production of cell internal storage products (X_{STO}) to yield inert particulate organic material (X_I). The nitrifying activity of autotrophic organisms (X_A) produces dissolved nitrate-nitrogen (S_{NO3}), used by heterotrophic organisms in denitrification, and ultimately X_I, in what is an entirely separate but complementary process. While this description may seem rather simplistic, with no detailed information on specific organisms beyond auto- or heterotrophy, the model does produce results in keeping with measured secondary effluent characteristics and has been extensively used in the calculation of treatment times for wastewater of varying compositions.

2.3 Process Integration and Energy from Waste

In essence, process integration is a simple concept whereby a waste stream from one part of a chemical process can provide value to another part of the process. The most common example is heat duty in which heat is transferred from one stream to another. Another important example is when waste water produced by cleaning one process unit can be used to provide some of the cleaning resource for another 'dirtier' cleaning task. For cases in which there are many possible matches

between streams, specialist algorithms, such as the pinch method, have been devised. Although only a simple two-way exchange of gases is considered in this work, a brief review of the literature in this area is provided. These techniques would be appropriate for more complex integration between wastewater treatment and algal cultivation such as, for example, more aerobic/anoxic units for wastewater treatment, or AD as another source of CO_2.

2.3.1 History and use of process integration methods

From a process engineering point of view, the manufacture of chemical products can be divided into three general classes: commodity chemicals, fine chemicals, and speciality chemicals (Smith 2005). As the eventual aim must be to produce algal biodiesel as a commodity chemical – produced in large volumes and undifferentiated from other biodiesels – the process design should reflect this objective. The key to successful manufacture of commodity chemicals is to make the process as cost-effective as possible. This means that capital and operating costs should be evaluated, and process integration techniques employed to optimise production. A breakthrough in process integration was pinch technology, developed by Linnhoff in the 1970s (Kemp 2007), which focused on the thermodynamics of a process with a view to improving efficiency in the supply of heat to cold streams. The technique uses a plot of temperature vs. change in enthalpy (heat flow) to set energy targets based on the minimum temperature difference between hot and cold streams; where a process employs multiple streams, heat loads over a given temperature range are added together to form a composite curve.

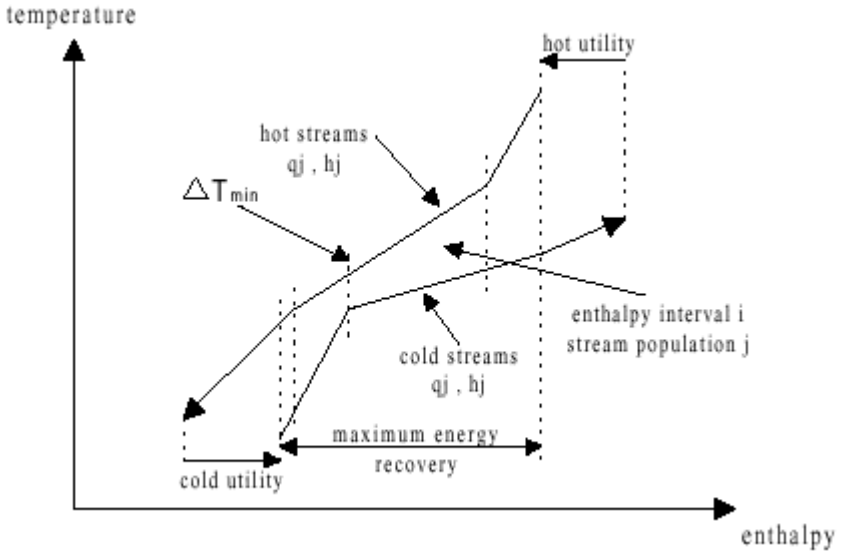

Figure 2-4 Example diagram of composite curves and enthalpy intervals (Santos and Zemp 2000)

For feasible heat exchange, the hot stream must always be hotter than the cold stream; in order to maintain this rule, either curve may be shifted along the enthalpy axis providing that the slope, supply and target temperatures remain the same. The pinch represents the point at which the two streams are closest and is determined by the minimum temperature difference at which the heat exchanger can operate. The first industrial example (Kemp 2007) of pinch analysis was undertaken by ICI plc, when a fractionating plant required an upgrade to handle increased throughput of 25%. As there was insufficient space to install a new fired heater to provide the increased capacity, new technologies were consulted to find a novel solution. Upon analysis by Linnhoff's method, a maximum energy recovery (MER) network was designed and installed, which included enlarged exchangers and rerouted pipe-work but no additional heater. This lead to an energy saving of approximately 35% when compared to the installation of a fired heater; this equated to an approximate annual saving of £1 million at 1982 prices.

As pinch analysis matured, the general principles were employed on a wider scale to solve different types of problems. Another case study from Kemp (2007) provides details of how the technology was used to save energy on a hospital site. This particular example illustrates how pinch techniques can be applied to non-process plants by examining the energy demands of a group of buildings and the times at

which energy is required. Energy-saving measures included the rescheduling of incinerator operation to provide heat for cold streams, the inclusion of municipal waste as an incinerator feedstock, and the conversion of standby generators to combined heat and power (CHP). Further extensions of pinch technology have included the development of mass exchange networks (El-Halwagi and Manousiouthakis 1989) and the minimisation of wastewater effluents (Wang and Smith 1994) in chemical processes. These extensions have led to the concept of clean process technology, where the environment is considered alongside the traditional chemical and thermal processes. Staine and Favrat (1996) are among researchers who have extended pinch analysis to include thermodynamic, economic and environmental factors, with a view to achieving life-cycle and environomic optimisation for industrial processes, and Frangopoulos and Keramioti (2010) have built upon this work, highlighting the requirement to include social indicators to reach full sustainability. Pinch analysis techniques have recently been applied to the management of CO_2 emissions with the development of the Carbon Emission Pinch Analysis (CEPA) method, which was designed for use in the energy planning sector to calculate the amount of zero-carbon energy sources needed to offset the carbon footprint of fossil-based energy generation (Tjan et al. 2010).

2.3.2 Energy from waste

A novel example of process integration is a project run by WarmCO_2 in The Netherlands. The project operates within the province of Zeeland and brings together the greenhouse horticulture and chemical industries, using waste products from the chemical industry to support horticultural growth. Water that has been used as a coolant on an ammonia manufacturing plant is piped to an aubergine farm three miles away, at a temperature of around 90 °C, providing heating for its greenhouses; the water is later returned to the factory for re-use. In addition to maintaining greenhouse temperature at a constant 20 °C, the ammonia plant also provides carbon dioxide, maintaining a concentration inside the greenhouses that is three times above atmospheric levels. According to the plantation owner (Rijckaert 2009), the increased level of carbon dioxide can lead to a crop yield that is two to three times greater than would normally be expected. As well as increased revenue

from a greater yield, the owner has negotiated a fixed price for heat and carbon dioxide with WarmCO_2 over a fifteen year term, which will provide greater financial security in the face of fluctuating energy costs. According to the Dutch horticultural association LTO Glaskracht, the greenhouse horticulture industry was responsible for 63% of the agriculture sector's carbon emissions in 2008. As LTO Glaskracht is committed to reducing emissions by 30% of 1990 levels by 2020, this type of process integration is of great importance to the industry if this target is to be achieved.

A method of obtaining energy from waste that is gaining popularity is AD – a biological process of decomposition of organic waste, which occurs in the absence of oxygen. It is similar in principal to composting but is carried out in a sealed vessel, thus collecting gaseous by-products from the process and reducing greenhouse gas emissions from landfill. Any biodegradable material is suitable for AD; however the best is material that is putrescible, such as grass clippings, wastewater sludge, food waste and some plant materials, including algae and oil-extracted algae (Olguin 2012). AD consists of four stages and the final stage – methanogenesis – is the stage of interest in terms of energy from waste, as it produces biogas with a methane content of up to 75% (Cantrell et al. 2007; Friends of the Earth 2007; Park and Craggs 2007). Following digestion and the collection of biogas, digestate remains in two forms: liquid and solid. The liquid digestate is suitable as a fertiliser, and the solid as a soil improver (Morken et al. 2013). Prior to use, the biogas should be scrubbed to remove contaminants such as hydrogen sulphide, ammonia and carbon monoxide (Morgan 2008). This step is also necessary to remove carbon dioxide to leave pure methane, before it can be used commercially for fuel. The concentrated biogas can also be used to run a combined heat and power unit to produce heat and electricity that can be used for adjacent plant processes, thereby reducing the need for energy from the national grid.

The ideas of carbon sequestration, use of wastewater and AD can be applied to the cultivation of algae. Kadam (2002) explored the environmental implications of the use of algae as a carbon sequestration medium alongside a coal-fired power plant; the plant was then co-fired with the algal biomass. Whilst it was found that co-

firing reduced fossil fuel consumption and emissions, such as carbon dioxide, methane and sulphates, it was also found that energy and fertiliser inputs were required. In a more recent paper, Rosenberg et al. (2011) discuss the use of carbon dioxide emissions from an ethanol biorefinery to enhance algal growth but, disappointingly, stops short of integrating the algal biomass into the biorefinery's output. Sialve et al. (2009) argue that AD is necessary to make algal biodiesel production economically and energetically favourable. The paper tackles a number of issues with the technology, including low biodegradability, release of ammonia, and sodium toxicity and suggests some solutions to these problems. Woertz et al. (2009) and Clarens et al. (2010) have addressed the issue of the water sources for algal growth, in combination with the idea of supplementation with carbon dioxide from flue gases. The water burden associated with algal growth is reduced upon use of municipal and dairy farm wastewaters, in addition to the water undergoing treatment for nutrient removal. To this end, Fortier and Sturm (2012) have analysed the feasibility of co-locating algal biomass production with wastewater treatment plants in Kansas, USA, using geospatial theory. The investigation studied available areas by land cover type, within set radial extents of wastewater treatment plants, and concluded that 29% of Kansas' liquid fuel demand could be met in this way without diverting freshwater and fertiliser from the agricultural sector.

Several authors in the field of algal biofuels have considered the amalgamation of processes to improve economics and sustainability in the form of a biorefinery. In his paper of 2007, Chisti discusses the concept where all components of the biomass are fully utilised. For example, not only may microalgal lipids be used as a feedstock for biodiesel but long chain fatty acids may be used for health food supplements, and carbohydrates, pigments and proteins for chemical and medical applications (Yen et al. 2013). Following lipid extraction, the remaining biomass can potentially be used as animal feed (Brune et al. 2009), or used as a feedstock for AD (Sialve et al. 2009; Olguin 2012). AD can be considered a useful tool in the recycling of important nutrients such as phosphorus, as the liquid digestate produced can be used instead of industrially-manufactured fertiliser. The integrated biorefinery has

already been established in Canada, the USA, and Germany to obtain maximum yield from biofuel crops; however, Chisti (2007), Brune et al. (2009), and Heaven et al. (2011) have warned that algal biomass may not be the ideal candidate for AD and that methane content will be reduced following extraction of lipid from the cells. Contrary to this opinion, recent results from a simulation model by Morken et al. (2013) show that the integrated algal cultivation/AD biorefinery could be totally independent of external energy supplies. Hence, it remains the belief that algal biodiesel production must be integrated with other processes to attain maximum profitability and sustainability.

2.3.3 Algae and industrial wastewater treatment

The use of algae, in consortium with bacteria, is an accepted method of wastewater treatment in what is known as the high-rate algal pond (HRAP). This concept was developed from the use of suspended growth wastewater treatment lagoons, where the appearance of algae was considered to be a disadvantage (Tchobanoglous et al. 2004). The HRAP combines the growth of bacteria and algae in a symbiotic relationship, whereby the bacteria digest dissolved organic compounds with oxygen produced by the photosynthesising algae which in turn consume carbon dioxide produced by the bacteria (Yang 2011). When relying on this process for industrial cultivation of algae, however, the species must be chosen carefully to ensure that the alga will thrive in an ammonium-rich environment. As ammonium uptake in algal cells is not well controlled, NH_4 may quickly reach toxic levels within the organism if its metabolism cannot be rapidly adjusted to assimilate ammonium as it enters the cell (Tam and Wong 1996; Giordano et al. 2007).

Another key problem for algal cultivation using HRAPs is the specific harvesting of the algal biomass in preference to bacteria. Although technically feasible, it is costly due to the requirement of expensive flocculants (Lundquist et al. 2010). Consequently, it may be prudent for the production of biofuels to consider algae as a tertiary treatment. We know that secondary effluent is a suitable medium for algal growth, as algal blooms are common in settling basins following wastewater treatment in aerobic flow-through partially mixed lagoons (Tchobanoglous et al.

2004). Additionally, in a recent study by Osundeko et al. (2013), five strains of algae were isolated from secondary effluent tanks at a wastewater treatment works in Ellesmere Port, UK, demonstrating that secondary effluent is a natural environment in which algae may grow. This idea has also been supported by Wang et al. (2010), Li et al. (2011a) (2011b) and Mutanda et al. (2011). The use of algae in simple waste stabilisation ponds, used in small communities around the world, has also been suggested for the removal of phosphorus to reduce the variability of P removal from this type of system (Powell et al. 2008).

In an assessment of the algal biofuel industry by Lundquist et al. (2010), it is stated that algal cultivation would be uneconomic without wastewater treatment being the primary goal. Income from the treatment of wastewater would significantly reduce the cost of a barrel of algal oil, to a point where it becomes competitive with fossil oil. In addition to the treatment of wastewater, biodiesel production is combined with supplementation with carbon dioxide from a natural gas-fired power station and an onsite generator driven by methane obtained from anaerobic digestion of waste algal biomass. AD also provides nutrients to the algal ponds in the form of liquid digestate. However, the delivery of carbon dioxide represents a major expense at a capital cost of $594,000 for a 100 ha facility. Although some carbon dioxide is provided from an onsite generator, the process could become even more efficient if increased levels of carbon dioxide were provided from another onsite, renewable source. This example serves to highlight the requirement for further research to explore supply of gases and nutrients to the process of algal cultivation for biofuels, preferably in a multi-disciplinary manner that combines biology, engineering and modelling.

2.4 Modelling and Optimisation of Biological Processes

2.4.1 Mathematical Modelling

Mathematical models can be used for a wide range of tasks, from air quality analysis to optimising routes for haulage vehicles, and their fundamental purpose is to determine the output, or to forecast what might occur, if a particular set of

inputs were applied (Kiely 1998). Models, however, are particularly useful in quantitative descriptions of biological processes, to predict how yield and productivity may be affected by a change in an operating condition, such as temperature or medium composition. To begin with, the model complexity should be decided by studying the process in question to determine the dominant mechanisms that should be included (Kiely 1998; Nielsen 2006). In the case of a biological or chemical process, the substrates involved in the reactions and their stoichiometry should also be specified. Once this has been resolved, kinetic expressions are used to describe the rates of reaction within the process. This is a key step in the development of the model and many kinetic expressions may be evaluated before an adequate description is found. A control volume for the reactor should also be established and a set of balance equations used to show how material flows in and out of the control volume. The kinetic rate and mass balance equations together make up the complete model. However, operating and kinetic parameters are also required, for which experimental data is often necessary. The simulation of the process is compared to the experimental data and the fit of the model evaluated. If the fit of the model is deemed to be poor, revision of the model and its parameters is required until a satisfactory description of the whole process is obtained.

Some popular processes benefit from published models that have been produced following years of research; one example is biological wastewater treatment – specifically, models of the activated sludge process. The International Association on Water Pollution Research and Control (IAWPRC) formed a task group in 1982 to assimilate and simplify the various models of the activated sludge process that were in use at the time (Henze et al. 2000). Modelling of the process had been underway for approximately 15 years but there was little confidence in the models due, in part, to their complexity. The result of five years' research and development was the Activated Sludge Model No. 1 (ASM1), published in 1987, which has been widely used as a basis for further modelling development. ASM1 was based on eight processes, including hydrolysis, growth and decay of heterotrophs and autotrophs, and ammonification. A discussion of the Monod expressions used in the biological

models can be found in Chapter 3 (Section 3.3 Modelling Wastewater Treatment and Algal Growth).

As interest in biological phosphorus removal was increasing, the model was revised and ASM2 published in 1995. This model included process rate equations for phosphorus-accumulating organisms (PAOs), although some aspects of their activity was still unclear; the model was extended to $ASM2_D$ in 1999 as a greater understanding of denitrification by PAOs was reached. Over years of use, it became apparent that there were a number of defects with ASM1, and ASM3 was published in 2000 to address these issues. Like ASM1, ASM3 relates to the core processes of domestic wastewater treatment: oxygen consumption, sludge production, nitrification and denitrification. It was felt that decay processes should be described in more detail, as computing power was considered insufficient to support more than one lysis rate equation at the time of the publication of ASM1. The intention with ASM3 was to provide a basis for further work and is, therefore, adaptable to different situations; for example, it does not include a module for biological phosphorus removal, but this detail may be taken from ASM2 and connected to ASM3. Indeed, the model has been further developed by both Iacopozzi et al. (2007) and Hiatt and Grady (2008) who propose that nitrification and denitrification should be considered separately, for use in applications where the nitrification dynamics become more important.

With the same intentions as the group tasked with modelling the activated sludge process, the International Water Association (IWA, formerly IAWPRC) set up two further groups to collate information that would lead to the development of river water quality and AD models. With respect to river water, the IWA's aim was to propose a basic model, specific for carbon, oxygen, nitrogen and phosphorus, that could be linked to the ASM series; the outcome was RWQM1 (Reichert et al. 2001; Shanahan et al. 2001; Vanrolleghem et al. 2001). Although not immediately apparent, RWQM1's relevance to this research is its inclusion of rate equations for the growth of algae – the biochemical process parameters of which may be applied to an algal pond model and hydrodynamic parameters added to suit the geometry of the reactor (Jupsin et al. 2003). However, while RWQM1 includes expressions for

growth of algae on ammonium and nitrate, it does not include carbon dioxide within the expressions. This omission is also seen in some high-rate algal pond models, such as that by Gehring et al. (2010), which uses RWQM1 as its basis. Other HRAP models may describe growth on CO_2 but do not differentiate between nitrate-nitrogen and ammonium-nitrogen (Buhr and Miller 1982; Yang 2011; Nauha and Alopaeus 2013). Other researchers have focused on photosynthetic terms (Sukenik et al. 1991) and on oxygen levels, temperature and pH of the growth medium (Jimenez et al. 2003), or have described algal growth as an function of light intensity and activation energy (Bordel et al. 2009). While this provides a more complete picture of algal growth, it does not deliver a model that that can be used within a wastewater treatment setting where the utilisation of carbon dioxide is a key process.

The Anaerobic Digestion Model (ADM1), published in 2002 (Batstone et al.), has also been designed to complement the activated sludge models, with biochemical Monod-type kinetics being presented in the same format as ASM1. However, though the same type of rate equation is employed, some complications have been encountered with plant-wide modelling due to the fact that not all unit processes use the same state variables. A benchmark simulation model has been proposed (Copp et al. 2003) and a further, refined, model developed (Nopens et al. 2009; 2010) to facilitate conversion of state variables to and from activated sludge and AD. Recently, an extension to BSM2 has been proposed to include greenhouse gas emissions, namely N_2O from the treatment of wastewater and CH_4 emissions from sewers, to test mitigation strategies for minimisation of these pollutants (Guo et al. 2012). The model has been used to track the progress of N, P and C compounds throughout the activated sludge and AD processes (Ekama 2009), commonly combined for the digestion of waste sludge, to help plan the most efficient layout of WWTPs. Corominas et al. (2012) have also used BSM2 to model GHG emissions from an integrated AS/AD process. In this work, the authors have emphasised the importance of using process-based dynamic models over models based on empirical factors to better evaluate GHG emissions from WWTPs, and this is a concept adopted in this research.

Several authors have used modelling methods to estimate the costs associated with the construction of wastewater treatment plants. In 1999, Gillot et al. presented a model-based simulation system for cost calculation that included both the integration of the plant design and the plant's dynamic behaviour and integration of investment and operating costs to evaluate different scenarios. This early work proposed the use of ASM1 and a settler model and it was later was developed to include a Robustness Index to assess the transferability of control strategies to different scenarios, as costs and effluent quality criteria may vary from one country to another (Vanrolleghem and Gillot 2002). More recently, Alasino et al. (2007;2010) have extended this idea to optimise both process configuration and equipment dimensions with Net Present Value (NPV) as the objective function, embedding up to five reactors and a secondary settler in a flowsheet structure that uses ASM3 and the Takács model. These principles have been employed by Gebreslassie et al. (2013), who propose a superstructure model for an algae-based biorefinery that simultaneously maximises the NPV and minimises the global warming potential of the processes. The major processing steps include carbon capture and algal productivity, harvesting and dewatering, lipid extraction, AD and power generation, and algal oil processing technologies to produce biodiesel. However, much more work is required to produce a superstructure that includes biological descriptions of algal growth and the activated sludge process, alongside AD, CHP and other biorefinery activities to model an extended waste treatment plant/algae-based biorefinery system.

2.4.2 Mathematical Optimisation

The aim of mathematical optimisation is to find the best available value of a function, within a defined domain. Alternatively, one might say that a problem may be solved in order to minimise or maximise an element, such as cost or productivity, by systematically analysing a given set of variables. This set of variables may be obtained as outputs from a mathematical model, as one or more parameter is adjusted. It is a natural progression, therefore, that computational modelling software should be coupled with mathematical optimisation software, and this practice is particularly applicable to biochemical engineering processes where

vessel sizes, flow rates and temperatures may all be adjusted to reach a specific target and process engineering tools employed to improve energy and economic efficiency (Hosseini and Shah 2011). A multi-objective optimisation may be used, where more than one element is considered for a solution – for example, cost *and* productivity (Hager et al. 1993). Multi-modal optimisations give more than one valid solution, where small changes to one area of a series of processes may be more effective than the use of a more general solution. There are very many optimisation techniques that can be employed, all of which are based upon logical, mathematical, and probabilistic theory (Rao 1965); however, such detailed mathematical argument is beyond the scope of this report, the main focus of the project being the integration of biochemical processes.

The optimisation technique chosen to solve the optimisation problem in this research is based on a sequential linear programming (SLP) algorithm called Proximate Parameter Tuning (PPT), which was originally designed for parameter estimation problems. Linear programming (LP) is a well-established method that is widely used in many engineering applications and also in biological and metabolic modelling (Nolan and Lee 2011). The LP algorithm is often embedded within algorithms aimed at more complex non-linear problems – such as the SLP algorithm used in this work. Although details of this algorithm are beyond the scope of this work, a comparison of a non-linear optimisation problem with one of the simplest optimisation procedures for parameter estimation – the linear least squares algorithm – is provided in the next chapter. This is done purely for illustrative purposes. Despite that it is a simple linear method with only two fitted parameters, the least squares procedure has been used to solve a variety of mathematical problems from diverse disciplines, including analytical chemistry (Cruwys et al. 2002), electronics engineering (Cirrincione et al. 2002) and the food science industry (Dingstad et al. 2004). Based on experimental data, a conditional probability distribution value, y, is assigned for a given value of x, and this information can be used in two ways. In analytical chemistry, for example, the predicted value of y is compared to the experimental value, and the correlation coefficient used to analyse the properties of the experimental method under test. Alternatively, a trend line

can be fitted to experimental data and the equation for the line used to predict values for which there is no measured data. It is this second use of the algorithm that will be employed for this research.

Both wastewater treatment systems and biochemical modelling have previously been subject to optimisation procedures, leading to improvements in the understanding of biological processes. For example, Balku and Berber (2006) employed an evolutionary algorithm to identify an optimum aeration schedule for nitrification and denitrification in activated sludge systems. The research used ASM3 to model the biological processes in aeration and settling tanks and applied periods of aeration and non-aeration, via an aeration device, to a single aeration tank. This enabled continuous operation of the system, satisfied carbon and nitrogen effluent limits, and was optimised for minimal energy use. In addition to this work, research has been undertaken to optimise the size and configuration of bioreactor systems. While not solely for use by the wastewater treatment sector, Harmand et al. (2003) sought to adapt developments made within the chemical engineering industry to cope with complex biological systems. Given a specific biological process and flow rate, to be treated at steady-state operation for a given duration, the minimum required volume can be calculated, using a combination of a continuous stirred-tank reactor (CSTR) and recirculation loops. This enabled intelligent distribution and re-distribution of the input flow between increasingly smaller tanks to obtain the same results as would be expected from a much less flexible arrangement.

Perhaps more relevant to this project are the works of Mussati et al. (2005) and Alasino et al. (2007), who addressed the simultaneous optimisation of the process configuration and equipment dimensions of a WWTP. The aim of the research was to minimise the investment and operating costs of new plants comprising up to five reactors and a secondary settler, with varying flow distribution along the reaction zone. The use of ASM3 to describe the biochemical processes results in a non-linear system – the NLP problems being solved in both cases using GAMS® (General Algebraic Modelling System). Similarly, El-Shorbagy et al. (2011) present a formulation to find the optimal sizes of WWT units to meet effluent requirements

but with the least cost. The optimisation algorithm used in the work of El-Shorbagy et al. identifies one or more design alternatives that may fulfil specific criteria by assessing the sensitivity of the model output to the parameters in question. The authors propose that this method may be extended to provide system-wide optimisation where all of the plant's processes are optimised together, and that same method is employed in this research.

As well as wastewater treatment, mathematical optimisation is now being applied to sustainable energy systems, some of which have been discussed in this chapter. For example, He et al. (2012) used a dynamic optimisation framework to profile the optimal carbon dioxide concentration for a microalgal culture in a photobioreactor. This resulted in the design of an on-off pulse mode for delivery of flue gases whereby the Monod-based microalgal growth model was verified by experimental results. Some recent work has focused on bioethanol production and supply systems with a view to GHG reduction (Zamboni et al. 2011; Akgul et al. 2012). Although this research is not based upon biodiesel from microalgae, similar principles might be applied in the future to the integration of wastewater treatment with 3rd generation biomass for biofuel systems. These papers acknowledge the need for a fully integrated analysis of all steps associated with biofuel production including land use requirements, global warming mitigation and economic and financial feasibility. Zamboni et al. (2011) recommend the use of waste biomass from ethanol production in CHP to meet emissions targets, and this may well be the case for spent algal biomass. The use of 2nd generation biomass in biofuel systems is preferable to 1st generation in terms of reducing costs and imports of biomass to the UK (Akgul et al. 2012); as microalgae grown in wastewater has a reduced dependency upon land and water, an assessment of this type of biofuel supply chain could be vital to the decision-making process for 3rd generation biofuels.

Sensitivity analysis is an important tool in mathematical optimisation and has been used to assist in the design of wastewater treatment plants. A sensitivity analysis by Mussati et al. (2002) of ASM3, conducted shortly after its publication in 2000, identified the most significant of the kinetic parameters, providing a focus for experimental investigation on a real wastewater treatment plant. This enabled

further analysis of significant parameters and how these may affect plant control strategies when disturbances in wastewater load are experienced. Further, more recent, work confirms that ASM3 is sensitive to variability in influent characteristics and this may have an effect on WWTP design (El-Shorbagy et al. 2011). For example, an increase in the concentration of readily biodegradable substrate in the wastewater would require longer retention times and/or an increase in air flow rates, and allowances for this scenario should be built into new WWTPs. Modellers are also using sensitivity analysis to measure the viability of biorefineries and to identify which processes have the greatest effect on the system as a whole. Brownbridge et al. (2014) consider the production of algal biodiesel under a biorefinery scenario using concentrated solar power for heat and power to cultivate algae and manufacture a number of products from the biomass. The sensitivity analysis yielded a biodiesel production cost and predicted that algal lipid content had the greatest effect on this value. However, and somewhat disappointingly, the model stopped short of using a biological model for algal growth and instead used a productivity expression. This highlights the necessity to combine engineering and biological models of numerous processes into one superstructure to best optimise and analyse the viability of wastewater treatment with integrated algal biofuel production. To date, and to the best of my knowledge, this is a challenge that remains unmet.

CHAPTER 3 - MODELLING METHODS

3.1 Introduction

Many interesting ideas were introduced in Chapter 2 in a review of the literature. In this chapter those ideas are assembled into a workable model that is of use to the wastewater treatment industry. This chapter will be organised in a way that best represents the thought processes required to reach the final Activated Sludge Algal Pond Model, which was built up over three versions. Therefore, the different concepts associated with the construction of the model will be discussed, rather than presenting the work in a chronological order. However, results of the three versions of the model will be presented chronologically in Chapters 5, 6 and 8. This chapter begins with an examination of materials used in the modelling work.

3.2 Modelling Software

3.2.1 CellDesigner

The software used to produce the initial models was CellDesigner (Funahashi et al. 2010), which is a free-to-download simulation engine for the modelling of gene-regulatory and biochemical networks. It has a structured diagram editor, and networks can be drawn based on the process diagram. Although it is intended for detailed modelling of intracellular processes, CellDesigner is used in a different way for modelling process units. It provides an excellent graphical representation for navigating complex models and has a good solver for integrating the ordinary differential equations (ODEs) that comprise the models presented in this work. The software is used to model continuous, well mixed process units. Balance equations on state variables are built up from actual reactions and also 'pseudo-reactions' that represent physical flows in and out of process units through pipelines. The software is well-established and is SBML-compatible, allowing for easy transfer of processes into other modelling programmes.

A full array of species types is available in CellDesigner, from simple molecules to antisense RNA, reflecting its origin as a biological modelling programme. In

addition, there are numerous transition and reaction tools, compartments, and operator buttons. Simple molecules, state transitions, association and dissociation reactions were sufficient for the type of macro-processes described in this work; kinetic rates and stoichiometry are entered into the Reaction module within the model. Simulation results are accessed via the Simulation Control Panel.

3.2.2 Sentero

For the later models, a bespoke software package was used. Sentero (Wilkinson 2009) is another SBML-compliant modelling system, created for the dynamic analysis of cellular signalling and metabolic pathways. In a similar way to CellDesigner, species and reactions are modelled using nodes that are joined by flux links. Reaction nodes contain the kinetic expression for the reaction, and the corresponding stoichiometric information is stored within the flux link that joins the reaction node to the species being consumed or produced; global parameters are stored in dataset nodes. It is also possible to group together a number of species and reaction nodes to form a compartment or process unit.

The functionality of Sentero is threefold: modelling, simulation, and analysis. The modelling and simulation components are very similar to CellDesigner and allow the user to create a graphical representation of the process, and then solve the underlying system of differential equations to yield the result. The analysis component provides a suite of algorithms that can be applied to the model; for example, Sentero includes a parameter tuning algorithm (Wilkinson et al. 2008) that uses a nominal parameter value, with upper and lower bounds, and sensitivity analysis to assign parameter values for which there may be little or no experimental data.

Sentero's proximate parameter tuning algorithm can be used to fit a model to raw time series data. It is, however, essentially a general purpose optimiser based on sequential linear programming. This is the functionality that is utilised in this process synthesis research. Since the optimisation requires repeated simulations, Sentero uses MATLAB (MathWorks 2013), specifically its *ode15s* solver, to provide a computationally efficient simulation engine. Sentero also provides parameter

sampling functionality which makes it possible to find multiple solutions using a range of different starting values for the decision variables. The flexibility of choice with respect to the model's reaction kinetics and stoichiometry means that Sentero lends itself equally well to both cellular signalling pathways and chemical engineering processes.

3.2.3 Biological models

The activated sludge models, specifically ASM3, were used as described by the IWA's Scientific and Technical Report No. 9 (Henze et al. 2000). Further details defining the application of the models were obtained from: Balku and Berber (2006), for design parameters and final species concentrations; and Hauduc et al. (2010), for ASM3 stoichiometric values.

Algal growth expressions were written with Monod kinetics in mind and based on the ASM3 style. Jupsin et al. (2003) provided stoichiometry for algal growth on NH_4 and NO_3.

3.2.4 Plant synthesis and design

For the basic principles of wastewater treatment plant design, including gas utilisation and production, and Henry's Law for dissolved gases, Wastewater Engineering: Treatment and Reuse (Tchobanoglous et al. 2004) was consulted. Economic functions and cost parameters for the net present value were extracted from Alasino et al. (2007; 2010). Information was obtained regarding: oil price and carbon trading value from Oil-Price.net (2011), Intercontinental Exchange (2011) and Bloomberg (2013); wastewater treatment revenue from Lundquist et al. (2010); and the carbon footprint of wastewater treatment from Lavigne and Gloger (2006).

3.3 Modelling Wastewater Treatment and Algal Growth

The fundamental concept of this research is the integration of biological wastewater treatment and algal growth. It is important, therefore, that a robust description of all biological processes is adopted, in order to accurately track the influx, consumption and generation of substrates during wastewater treatment and

through to the algal pond. Because this research aims to provide a model that can be used by industry, the industry-standard activated sludge models were the obvious choice in representing biological wastewater treatment. As discussed in Chapter 2, these models have been developed over time and in this work the most recent version of the model – the Activated Sludge Model No. 3 (ASM3) – is used.

The activated sludge models use Monod kinetics to describe the major events occurring during biological wastewater treatment. The equation is a mathematical model for the growth of microorganisms and is a homologue of the Michaelis-Menten expression (Doran 2006). While Michaelis-Menten kinetics represents enzyme reactions in constant populations, Monod kinetics relates microbial growth to the concentration of a growth-limiting substrate in an aqueous environment. The form of the equation is thus:

$$\mu = \mu_{max} \frac{S}{K_S + S} \qquad \textbf{Equation 3-1}$$

where:

- μ is the specific growth rate of the microorganism
- μ_{max} is the maximum specific growth rate of the microorganism
- S is the concentration of the limiting substrate for growth
- K_S is the half-saturation coefficient, i.e. the value of S when $\mu/\mu_{max} = 0.5$.

K_S and μ_{max} are empirical coefficients, which differ between species, and must be determined experimentally. They are calculated by way of a double-reciprocal, or Lineweaver-Burk, plot; the full details of this method are explained in Chapter 7, which includes examples of the empirical coefficients that have been generated for this research.

As well as growth-limiting substrates, there are other factors that can affect the growth of microbial cultures. In the case of biological wastewater treatment, this may be the presence or absence of oxygen in the activated sludge tank. For example, nitrifying bacteria require oxygen to convert ammonium into nitrate and the nitrification rate will decrease as the concentration of dissolved oxygen

approaches zero. The opposite is true for denitrifying bacteria, which grow under anoxic conditions. The kinetic expressions in the activated sludge models have been written to include an oxygen switching function to either facilitate or inhibit a reaction according to the dissolved oxygen concentration. For a process that requires oxygen, the switching function, which forms one part of the overall process rate, is:

$$\frac{S_O}{K_O+S_O} \qquad \textbf{Equation 3-2}$$

and for an anoxic process is:

$$\frac{K_O}{K_O+S_O} \qquad \textbf{Equation 3-3}$$

In the case of biological wastewater treatment, where there is a mixture of different bacteria in one vessel, it is necessary to specify the growing substrate for each process; to do this, the process rate is multiplied by the organism involved. An example that draws together all of these components is the very first process in ASM1 – aerobic growth of heterotrophs – and this process rate is presented below:

$$\mu = \mu_H \left(\frac{S_S}{K_S+S_S}\right)\left(\frac{S_O}{K_O+S_O}\right) X_{B,H} \qquad \textbf{Equation 3-4}$$

The first part of the expression is in the basic Monod format (see Equation 3-1), which relates the specific growth rate of the organism (μ_H) to its growth-limiting substrate S_S. A switching function (as Equation 3-2) is also present, which tells us the process is aerobic and will slow as the dissolved oxygen concentration approaches zero. Finally, we can see by the first order multiplier at the end of the process rate that heterotrophic biomass ($X_{B,H}$) is the growing substrate, tying in with the use of the growth rate μ_H in the first part of the expression. This is a relatively simple example of the type of process rate used in the activated sludge models, and the biological processes and corresponding rates do increase in complexity from ASM1 to ASM3. Many of ASM3's expressions include more than one growth-limiting substrate, illustrating the complex nature of interactions occurring in biological wastewater treatment.

As I wanted the final model to be as up-to-date as possible the first step was to build ASM3, for which the Sentero modelling software was used. Figure 3-1 shows a screenshot of the ASM3 model.

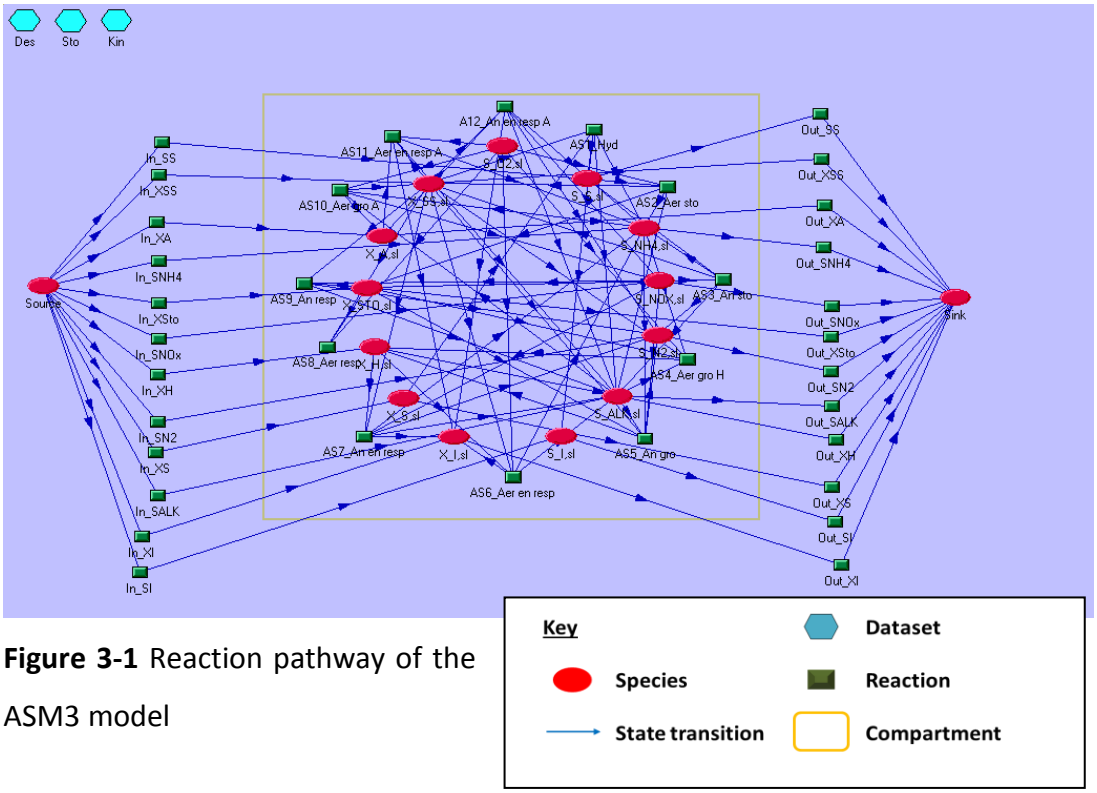

Figure 3-1 Reaction pathway of the ASM3 model

The results of this model were verified against Balku and Berber (2006) from which the reactor volume, influent flow and initial conditions were taken. To validate the isolated ASM3 network, feeds flowing to and from each species were required to simulate the flow of wastewater in and out of the aeration tank; the modelling of continuous processes will be discussed in more detail in Section 3.4 below and the results of the validation are presented in Chapter 6 (Section 6.3.1). The published process rates, stoichiometry and parameter values for ASM3 are provided in Appendices A-C and have been taken from the work of Gujer et al. (2000) and Hauduc et al. (2010).

The growth of algal biomass was modelled in the same way as biological wastewater treatment, using Monod kinetics. Based on processes found in the River Water Quality Model (Reichert et al. 2001) and high-rate algal ponds (Jupsin et al. 2003), algal growth expressions were formulated to utilise the carbon dioxide and nitrogen compounds found in treated wastewater and used parameters

calculated from laboratory experiments; the construction of these expressions is discussed more fully in Chapters 7 and 8. Because the gas exchange system proposed in this work relies upon the organisms being grown in a vessel with an enclosed headspace, an inhibition term for oxygen was written into the algal growth expression based on the findings of Marquez et al. (1995). An example of one of the expressions, growth on ammonium, is shown below:

$$\mu = \left(\left(\mu_{CO2atm}\frac{S_{CO2\_pl}^{nco2}}{K_{CO2atm}^{nco2}+S_{CO2\_pl}^{nco2}}\right)+\mu_{CO2}\left(\frac{S_{CO2\_pl}}{K_{CO2}+S_{CO2\_pl}}\right)\right)\left(\mu_{NH4}\frac{S_{NH4\_pl}^{nnh}}{K_{NH4alg}^{nnh}+S_{NH4\_pl}^{nnh}}\right)\left(\frac{K_{O2alg}}{K_{O2alg}+S_{O2\_pl}}\right)X_{Algae}$$

Equation 3-5

This expression is quite complex when compared to the expression taken from ASM1 (Equation 3-4). Here growth is limited by the concentrations of carbon dioxide and ammonium and is inhibited by the presence of dissolved oxygen. Growth on carbon dioxide was observed in the laboratory to proceed at two rates – up to atmospheric concentration and above atmospheric concentration. These rates are reflected by the inclusion of two growth rates: μ_{CO2atm}, for growth at atmospheric levels of carbon dioxide; and μ_{CO2}, for growth at elevated levels of CO_2. In both expressions, the growth-limiting substrate is dissolved carbon dioxide in the algal pond, S_{CO2_pl}. The expression for growth on CO_2 is then multiplied by growth on NH_4 and inhibition by O_2; the growing substrate is X_{Algae}. As stated in the previous paragraph, Equation 3-5 is shown here as an example of how Monod kinetics are employed to describe algal growth. The derivation of parameter values is discussed in Chapter 7 and the formulation of the algal growth expressions is described in detail in Chapter 8. The use of the co-operative exponent, *n*, is also discussed in these later chapters.

3.4 Modelling Continuous Processes

The modelling of continuous processes is another key concept in this research. As WWTPs have a constant influx of wastewater to be treated, it is necessary to model

the activated sludge process as such rather than as a batch reactor, and this idea was introduced in Section 3.3, above. In addition to this, a constant supply of nutrients to the algal pond is required and this is only possible through a continuous process. This concept is illustrated by the following model, developed using CellDesigner, which uses a combination of bulk transfer expressions and a biochemical process rate expression (Figure 3-2).

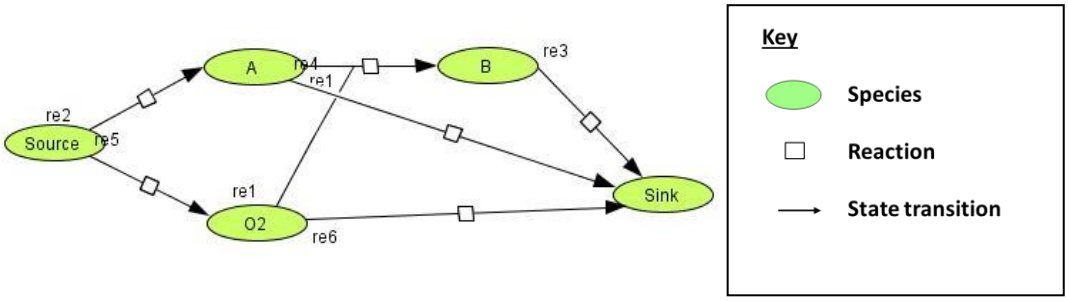

Figure 3-2 Simple continuous process model

The starting point for the model was a state transition from species A to species B – a theoretical reaction based on Monod kinetics. A source was added to the model, from which there was a constant supply of species A, representing the flow of wastewater to an aeration tank. A sink was included to accept species B and any surplus reactants at a rate corresponding to the hydraulic retention time – this represented the flow of effluent from the aeration tank. In a more complex system, where solids are settled out and recycled during the process, a parameter describing the net removal rate of insoluble components can be added to the wash-out of particulate species. By adding this extra parameter, the particulates are removed more slowly than soluble species at a rate corresponding to the solids retention time.

The intention to mimic the activated sludge process and, to this end, dissolved oxygen was added to reaction of A to B to represent the use of O_2 by bacteria in biological wastewater treatment. Dissolved oxygen was introduced from the source, with a fixed concentration of 8.9 g O_2 m^{-3}; the dissolved oxygen concentration was calculated using Henry's Constant (Plambeck 1995) at 25 °C:

$$c = \frac{p}{H} \qquad \textbf{Equation 3-6}$$

$$H_{O2} = 756.7 \frac{atm}{\frac{mol}{L}} \times \frac{1\ mol}{32\ g} = 23.6 \frac{atm}{\frac{g}{L}}$$

$$p_{O2} = 1\ atm \times 21\% = 0.21\ atm$$

$$c = \frac{0.21\ atm}{23.6 \frac{atm}{\frac{g}{L}}} = 8.9 \times 10^{-3} \frac{g}{L} \times \frac{1000\ L}{1\ m^3} = 8.9\ g\ O_2\ m^{-3}$$

Process rate expressions and parameter values can be seen in Tables 1 and 2. In keeping with the simplicity of the model, all stoichiometric values were set to 1 and initial concentrations were set to 0 g m^{-3} (the source and sink being fixed).

Table 1 Process rates for the simple steady-state model

Process	**Process Rate**
1. Conversion of A to B	$\mu_{max} \frac{A}{K_A + A} \frac{O_2}{K_{O2} + O_2} X_H$
2. Flow of A from source	$\frac{\mathrm{A_{feed}}}{\mathrm{HRT}}$
3. Flow of B to sink	$\frac{\mathrm{B}}{\mathrm{HRT}}$
4. Flow of A to sink	$\frac{\mathrm{A}}{\mathrm{HRT}}$
5. Aeration	$k_{\mathrm{La}}(\mathrm{O_{2sol}} - \mathrm{O_2})$
6. Flow of O_2 to sink	$\frac{\mathrm{O_2}}{\mathrm{HRT}}$

Table 2 Parameter values for the simple steady-state model

Parameter ID	**Value**	**Units**		**Parameter ID**	**Value**	**Units**
μ_{max}	1.0	d^{-1}		A_{feed}	100.0	g m^{-3}
K_A	20.0	g m^{-3}		HRT	0.5	d
K_{O2}	0.5	g m^{-3}		$k_L a$	30.0	d^{-1}
X_H	1000.0	g m^{-3}		O_{2sol}	8.9	g m^{-3}

This simple model was not results-orientated and full results will not, therefore, be reported in this thesis. However, to ascertain that the theories upon which the model had been built were correct, the simulation programme was used as a way to illustrate the concepts of steady-state processes and mass balance. Values taken from the simulation (Appendix D) were used to demonstrate that the mass within

the reactor is balanced and conforms to the general mass-balance analysis, which is shown below in a simplified word statement:

Rate of accumulation = inflow – outflow + generation – consumption **Equation 3-7**

The mass balance of any substrate is calculated by using the parameters and process rate written into the model to describe each reaction; in a steady state, accumulation of any compound must be zero. For example, the mass balance for substrate A can be calculated using Equation 3-7:

$$0 = \mathrm{QA_{feed}} - \mathrm{QA} + 0 - \left(\mu_{\max}\left(\frac{\mathrm{A}}{\mathrm{K_A + A}}\right)\left(\frac{\mathrm{O_2}}{\mathrm{K_{O2} + O_2}}\right)\mathrm{X_H V}\right)$$

$$0 = \frac{\mathrm{QA_{feed} - A}}{\mathrm{V}} - \left(\mu_{\max}\left(\frac{\mathrm{A}}{\mathrm{K_A + A}}\right)\left(\frac{\mathrm{O_2}}{\mathrm{K_{O2} + O_2}}\right)\mathrm{X_H}\right)$$

where Q is the flow of species A and V is the volume in the reactor. As:

$$\mathrm{HRT} = \frac{\mathrm{V}}{\mathrm{Q}} \qquad \textbf{Equation 3-8}$$

Q and V can be substituted for HRT and the mass balance equation rearranged as follows:

$$0 = \frac{\mathrm{A_{feed} - A}}{\mathrm{HRT}} - \left(\mu_{\max}\left(\frac{\mathrm{A}}{\mathrm{K_A + A}}\right)\left(\frac{\mathrm{O_2}}{\mathrm{K_{O2} + O_2}}\right)\mathrm{X_H}\right)$$

$$\frac{\mathrm{A_{feed} - A}}{\mathrm{HRT}} = \left(\mu_{\max}\left(\frac{\mathrm{A}}{\mathrm{K_A + A}}\right)\left(\frac{\mathrm{O_2}}{\mathrm{K_{O2} + O_2}}\right)\mathrm{X_H}\right)$$

By inserting the final steady-state concentrations for species A and O_2 (6.4 g m^{-3} and 1.7 g m^{-3} respectively – see Appendix D) into the equation, it can be demonstrated that the mass of the substrate flowing in and out of the reactor is equal to its consumption.

$$\frac{100 - 6.4}{0.5} = 1.0 \times \left(\frac{6.4}{20 + 6.4}\right) \times \left(\frac{1.7}{0.5 + 1.7}\right) \times 1000$$

$$187\ \frac{g\ m^{-3}}{d} = 187\ \frac{g\ m^{-3}}{d} \quad \therefore \textit{the mass of species A is balanced}$$

This process was repeated for all substrates by substituting the relevant process rate expression into the mass-balance equation. The simple activated sludge model

was used as a basis for later models, in which compartments relating to the different phases of an aeration tank and algal pond were introduced; this work is presented in more detail in Section 3.5 Modelling Units Using Separate Gas and Liquid Compartments.

3.5 Modelling Units Using Separate Gas and Liquid Compartments

As stated previously, the fundamental concept of this research is the integration of wastewater treatment and algal growth. It is intended that treated wastewater should be used as the growth medium for algae, thereby reducing the life cycle burden with respect to water. It is anticipated that nutrients remaining in the secondary effluent will be used by the algae to grow and the effluent will therefore be directed from the aeration tank to the algal pond. Furthermore, cellular respiration of the bacteria in biological wastewater treatment results in the evolution of carbon dioxide, which is required by algae to grow. Conversely, algae release oxygen as a product of photosynthesis, which can be used by the bacteria in the activated sludge process. To make use of this, a novel gas exchange system has been designed that links the headspaces of the two vessels. This research seeks to explore the benefit of such an exchange system by using gases that would otherwise be emitted as waste.

For this work, four separate units made up of liquid phases for biological wastewater treatment and algal growth and their corresponding gas phases are required. In practice, selected substrates and processes can be grouped together to form a compartment, which can then be linked by mass and bulk transfer expressions. The four compartments are separated thus:

1. Activated sludge liquid phase, including ASM3 substrates and processes
2. Activated sludge gas phase, containing atmospheric and evolved gases
3. Algal pond liquid phase, with algal growth processes
4. Algal pond gas phase, as sludge gas phase above.

An illustration of the separate units and their connections can be seen in Figure 3-3, which shows the full Activated Sludge Algal Pond Model (ASAPM).

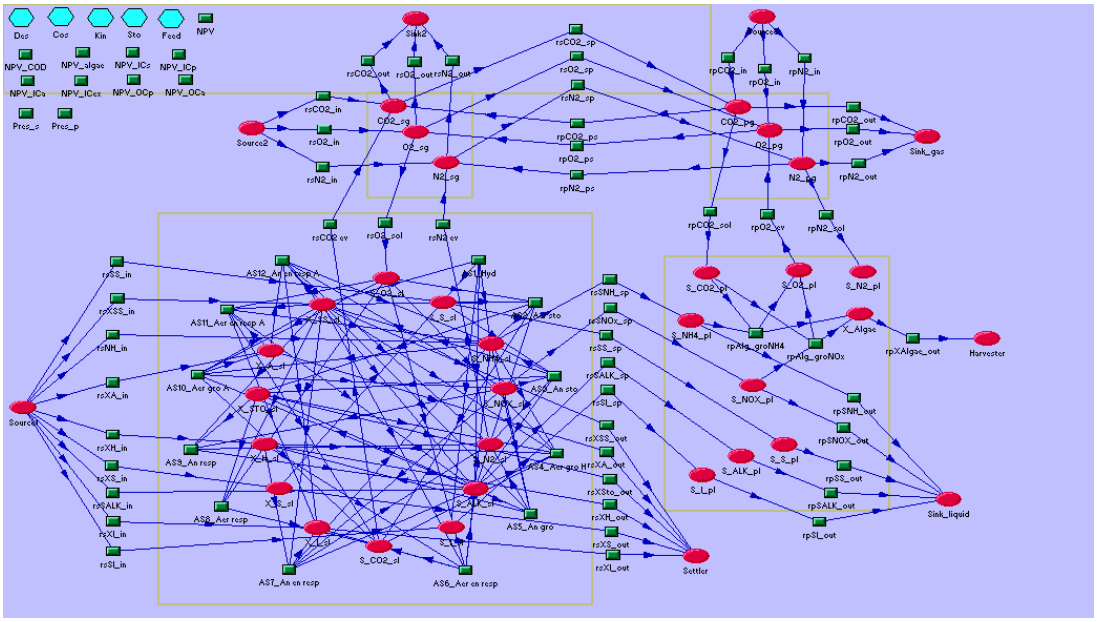

Figure 3-3 ASAPM showing compartments, biological processes, bulk and mass transfer

Each compartment is linked to a sink and a source, to and from which substrates can flow; the activated sludge liquid phase acts as the source for the algal pond. Bulk transfer expressions are written in the general form of *concentration* multiplied by *flow*; for example, carbon dioxide gas flowing from the source into the activated sludge gas phase:

$$rsCO2_{in} = CO2_{feed}.In_{sg}$$

where $CO2_{feed}$ is the CO_2 concentration in air and In_{sg} is the gas flow from air to the sludge tank. An extra parameter, *alpha*, is added when describing the outflow of particulate substrates. For example, the flow of inert particulate organic material (X_I) from the sludge tank to the settler is modelled as follows:

$$rsXI_{out} = X_I.Out_{sl}.alpha$$

where *alpha*, the settling parameter, is equal to the quotient of the hydraulic retention time and the solids retention time. The hydraulic retention time is calculated as shown in Equation 3-8, above, and the solids retention time used in this work is 20 days.

In addition to bulk transfer in and out of the system, there is also bulk transfer between the compartments. This uses the same format as described in the previous paragraph but parameters that link the corresponding phases of the separate vessels are used. The novel gas exchange system uses the parameters G_{sp} and G_{ps} to describe the flow of gaseous substrates from the sludge tank to the algal pond and vice versa. Also, the parameter L_{sp} describes the flow of wastewater substrates from the sludge liquid phase into the algal pond. As the liquid flow is one-way, a parameter describing liquid flow from the algal pond to the sludge liquid is unnecessary.

Mass transfer expressions describe the flow of constituents across the gas/liquid interface. The solubility of gas in a liquid is directly proportional to the partial pressure of the gas above the liquid, and Henry's Law is employed to determine the rate of transfer of gases to and from the liquid phase. The flux of gas from the gas phase to the liquid phase can be approximated by the equation:

$$r = k_L(C_i - C_L) \qquad \textbf{Equation 3-9}$$

where r = rate of mass transferred per unit area per unit time

k_L = liquid film mass transfer coefficient

C_i = concentration at the interface in equilibrium with partial pressure in the gas

C_L = concentration in the bulk liquid phase (Tchobanoglous et al. 2004).

This equation can be used to formulate expressions that suit the four-compartment model, using Henry's Law Constants specific to the gas in question. For example, the expression for the dissolution of O_2 in the sludge tank is:

$$rsO2_{sol} = V_{sl}.kLa_s\left(O2_{sg}.H_{O2} - O2_{sl}\right)$$

where V_{sl} is the liquid volume in the sludge tank, k_La_s is the oxygen mass transfer coefficient in the sludge tank, $O2_{sg}$ is the O_2 concentration in the activated sludge gas phase, H_{O2} is Henry's Constant for O_2 and $O2_{sl}$ is the concentration of dissolved oxygen in the activated sludge liquid phase. The expression can be rearranged for evolution of a gas; for example, evolution of CO_2 from the sludge liquid phase:

$$rsCO2_{ev} = V_{sl}(kLa_s \times 0.91)\left(CO2_{sl} - CO2_{sg}.H_{CO2}\right)$$

where $CO2_{sl}$ is the concentration of dissolved carbon dioxide in the sludge liquid phase, $CO2_{sg}$ is the CO_2 concentration in the sludge gas phase and H_{CO2} is Henry's Constant for CO_2. In the reactions describing the dissolution and evolution of carbon dioxide, the oxygen transfer coefficient, k_La, was multiplied by 0.91 to reflect the difference in diffusivities between oxygen and carbon dioxide (Sperandio and Paul 1997).

As ASM3 is not concerned with carbon dioxide evolved from the activated sludge, an additional component, S_{CO2_sl}, was added as a product to each biological process in which oxygen was consumed. The stoichiometry for the evolution of carbon dioxide was assumed to be equal but opposite to that for oxygen, based on the general equation for cellular respiration:

$$C_5H_7NO_2 + 5O_2 \rightarrow 5CO_2 + NH_3 + 2H_2O$$

where the stoichiometry of the consumption of O_2 is equal to the generation of CO_2 (Tchobanoglous et al. 2004). The addition of this substrate is clearly necessary in this work due to my intention to transfer carbon dioxide for use in the algal pond. The stoichiometric expressions for the consumption of oxygen were copied for the production of carbon dioxide, and the parameters $Y_{STO,O2}$ and $Y_{H,O2}$ for oxygen were named $Y_{STO,CO2}$ and $Y_{H,CO2}$ for carbon dioxide. Values for these parameters can be found in Chapters 6 and 8 and the stoichiometry of the processes is included in Appendix B.

By creating separate gas phase compartments, it was necessary to include a function that could evaluate the concentration of gases in the vessels' headspaces. The expression used to calculate this concentration, shown here for the algal pond, is:

$$Pres_p = \frac{O2_{pg}}{32} + \frac{CO2_{pg}}{44} + \frac{N2_{pg}}{28} \qquad \textbf{Equation 3-10}$$

In Equation 3-10, the weight compositions used in the model are converted into molar concentrations using the molecular weights of each gaseous species. As the

concentration of each gas is measured in g m^{-3}, the resultant $Pres_p$ value will be given in mol m^{-3}. Note that the pressures inside the vessels must be considered when altering gas flows to the headspace. In this model, the two most abundant atmospheric gases (nitrogen and oxygen) are included as well as the gas of interest (carbon dioxide). The molar concentration of an ideal gas (=P/RT) which, at atmospheric pressure and a temperature of 293 K, is approximately 41 mol m^{-3}. Therefore, as well as setting a target value for the total Net Present Value, two additional targets are set that stipulate $Pres_s$ and $Pres_p$ should both produce a value of 41 mol m^{-3}. The pseudo-reactions $Pres_s$ and $Pres_p$ were modelled for use as soft constraints in model optimisation. With a target value 41 mol m^{-3}, the objective function is penalised to maintain this pressure constraint. In this work, the objective function is NPV, which is discussed in the next section.

3.6 Process Economics

The aim of this research is an economic model that allows capital costs and operating costs to be represented so as to minimise their impact on the overall Net Present Value (NPV) for the integrated process design. Operating costs account for the electrical energy requirement of the unit and include an updating term for the life span of the WWTP; capital costs are calculated using the equipment characteristic dimension, i.e. the volume of the compartment. Costs are represented in the standard way by cost curves. Considering the investment cost of an activated sludge tank, the volume of the tank is multiplied by parameters that have been calculated to take into account the cost of materials and construction. As the unit increases in size, the capital costs will increase accordingly. A typical curve, using parameters to calculate investment cost according to size, can be seen in Figure 3-4 below.

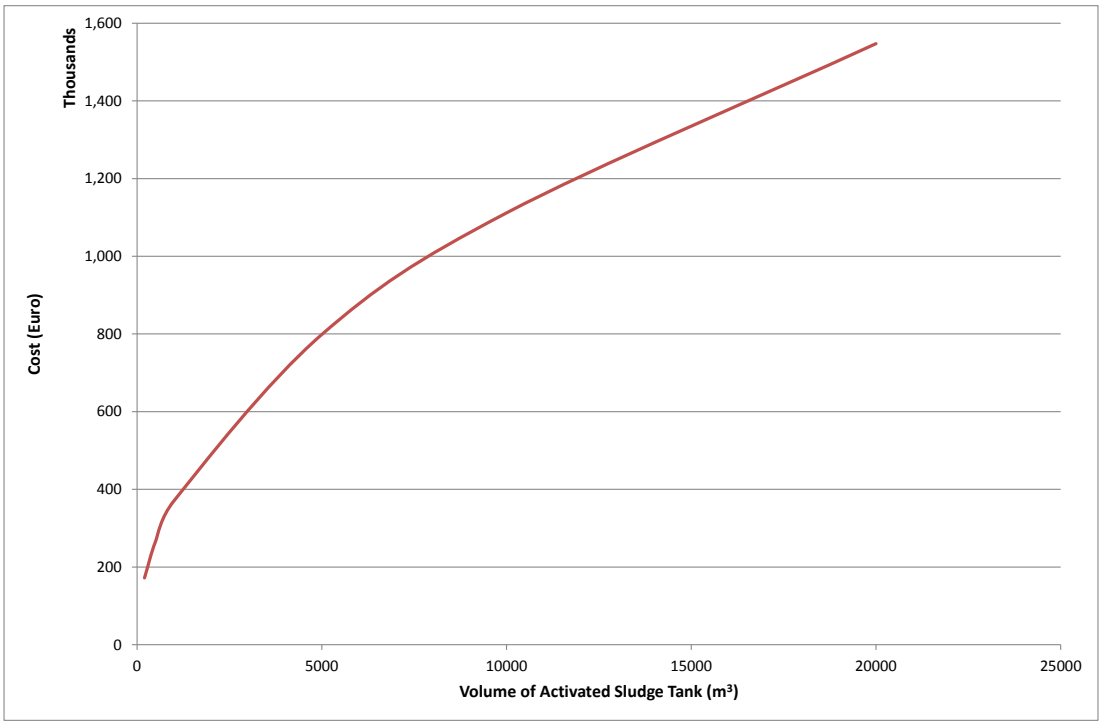

Figure 3-4 Capital costs of activated sludge tank according to unit volume

The model presented in this work was developed to include economic functions as a type of pseudo-reaction. Sentero has only two entities: species and reactions, with reactions being the only objects that can contain algebraic expressions involving state variables. This is why the overall economic objective function was modelled as a pseudo-reaction which could then be optimised. Also, for reporting purposes, each cost component making up the objective function was split into its own pseudo-reaction. Revenue functions include the income from treatment of wastewater and the sale of algal lipid; cost functions include investment costs of the vessels and aeration systems, and the operating costs for liquid pumping and aeration.

Investment cost functions, IC_p for unit p, have the basic structure of $IC_p = b_p.Z_p^{\delta p}$ where b and δ are cost parameters and Z_p is the equipment characteristic dimension (Alasino et al. 2007). In this work, I have adopted the letter c instead of b for the cost parameter, to avoid confusion with the endogenous respiration parameter b in ASM3. Typically, the value for Z is a volume – i.e. the volume of an activated sludge tank – but also applies here to the gas flows of the novel gas exchange system. It was anticipated that costs would increase with flow rate to

reflect the extra strength required to withstand higher pressures and should, therefore, not be priced at a flat rate. The capital cost of the aeration system is slightly more complex and takes into account the oxygen transfer coefficient, k_La. For example, the capital cost of the aeration system is modelled as follows:

$$NPV_{ICa} = -c_a\left(B\left((k_L a_s.V_{sl})^{\delta_a} + \left(k_L a_p.V_{pl}\right)^{\delta_a}\right)\right)$$

In the work of Alasino et al., the expression $B.k_L$a.V is used to calculate the oxygen capacity of the aeration system, where B is a constant. The example above consists of two aeration systems – one for the activated sludge tank and another for the algal pond.

Operating costs were also taken from the work of Alasino et al. and have the basic structure of $OC_p^T = \Gamma(\alpha.E)$ for unit *p* over the lifespan, T, of the WWTP. The parameters *Γ*, *α* and *E* represent the updating term, unitary operation costs and the energy demand of the unit, respectively. The updating term is used to compute costs to the present value and is calculated thus:

$$\Gamma = \sum_{j=1}^{n} \frac{1}{(1+id)^j} = \frac{1-(1+id)^{-n}}{id} \qquad \textbf{Equation 3-11}$$

where *id* is the interest (discount) rate and *n* is the lifespan of the plant. The term *E* is calculated by multiplying the flows to and from the compartment by a parameter for energy demand, in units of kWh m^{-3}, which I have named *kWh*. The operating cost of liquid pumping is modelled as follows:

$$NPV_{OCp} = \Gamma\,.\,days_{COD}\left(-\alpha_E\left(kWh\left(In_{sl} + Out_{sl} + L_{sp} + Out_{pl}\right)\right)\right)$$

In this model an additional term, $days_{COD}$, represents the number of days that the plant is operational and wastewater is being treated. This parameter was included to give more flexibility to this novel integrated process, as the plant may not be fully operational all year round. If such a plant were built in the UK, it is entirely feasible that algal growth may be limited to only 6-9 months of the year; the plant operators may decide in that scenario to close down the wastewater treatment arm of the integrated process, and this additional term provides that option. The unitary

operation cost parameter, α_E, has been adjusted from the annual value quoted in Alasino et al. to a daily value, to accommodate the $days_{COD}$ parameter.

The revenue functions presented in this work are based upon the concepts of the aforementioned paper but, given that Alasino et al. do not consider revenue, the expressions used here are written specifically for this research. For example, the function that models revenue from algal growth is:

$$NPV_{algae} = \Gamma . days_{algae} \left(\left(r_{algae} . Harvester . oil_{pc} \right) + \left(r_{CO2} \left(\left(CO2_{sg} \left(In_{sg} - Out_{sg} \right) \right) - \left(CO2_{pg} \left(In_{pg} - Out_{pg} \right) \right) \right) \right) \right)$$

This function uses two familiar parameters – Γ and $days_{algae}$ – the updating term and the number of days per year that algae to grow is expected to grow. The expression takes into account both revenue from the sale of algal oil and revenue from carbon capture. The mass of algae in the Harvester is multiplied by the term r_{algae}, which represents the revenue from the sale of algal lipid and is based on the current price of fossil oil. This is further multiplied by the oil_{pc} parameter, which is an estimation of the lipid fraction of the algal cell. In this work, the percentage is set at 0.25, as seen in the report by Lundquist et al. (2010); rather than setting this fraction at a fixed value, my intention was to provide flexibility in the model and the potential to grow an alga with a higher lipid content. The latter part of the expression calculates the carbon dioxide sequestered by algal growth and this is multiplied by r_{co2}, a revenue parameter based on the current carbon trading price.

The function NPV represents the total Net Present Value of the process as a whole and is simply the sum of all of the individual NPV functions. It is this pseudo-reaction that is used as the objective function in optimising the model, and a target value can be specified that the optimisation software will aim to reach. Model optimisation will be discussed in greater detail in the next section of this chapter.

3.7 Optimisation

The model in this work is a set of ordinary differential equations representing dynamic mass balances and follows the key modelling paradigm of:

1. Construct a mathematical model
2. Fit the model to data (parameter estimation)
3. Optimise the decision variables.

To begin with, a set of nominal design parameters is chosen with the intention to optimise them to maximise the net present value (NPV) of the integrated process. In order to illustrate the concept of model optimisation, the linear least squares (LLS) problem is discussed, which is frequently chosen as the approximation criterion to find solutions in an over-determined system (Rao 1965; Lawson and Hanson 1974; Barlow 1993). Although the optimisation problems developed in this research are far more complex (including non-linear differential equations and many parameters), didactic comparisons can be made with the least squares formula as seen in Table 3 below.

Table 3 Comparison of the LLS and model-based algorithms

	Least Squares	**Model-Based Optimisation**
1. Mathematical model equation	$y = mx + c$	Rate of change of O_2 equals O_2 supplied by mass transfer minus O_2 consumed by growth, e.g. $\frac{dS_{O2,sl}}{dt} = kLa_s(O2_{sg}.H_{O2} - S_{O2,sl}) - k_{STO}\frac{S_{O2,sl}}{K_{O2}+S_{O2,sl}}\frac{S_{S,sl}}{K_S+S_{S,sl}}X_{H,sl}$
2. Model parameters		
a) Fitted parameters	m, c	Kinetic parameter, e.g. K_{O2}
b) Design parameters	-	In_{sg}, G_{ps}, k_La, etc.
3. Optimisation		
a) Objective function	Minimise residuals $\min_{m,c}\sum_i(\hat{y}_i - y_i)^2$	Maximise profit, e.g. revenue from WWT minus aeration costs
b) Constraints	$c = 0$	Concentration of gases in headspace (41 mol m^{-3})
c) Method of optimisation	Calculus (see below)	Numerical

The algebraic expressions to follow show the derivation of the linear least squares algorithm, which is a method commonly used in statistical analysis to produce a closed-form analytical solution to a given problem. If the model assumed a linear dependence of algal growth on nutrients, for instance, the resultant plot would be a straight line of the form $y = mx + c$. In an ideal case, the model and experimental results would be in complete agreement; i.e. the error in the residuals would be equal to zero, and $\hat{y}_i = y_i$ for all values of i. The least squares algorithm, below, can be used to find expression for m and c such that the residuals are minimised.

$$\min_{m,c} \sum_i (\hat{y}_i - y_i)^2$$

The equation of the line from the plotted experimental data can be expressed as *mx + c = ŷ*, which can then be substituted into the algorithm:

$$\min_{m,c} \sum_i (mx_i + c - y_i)^2$$

The brackets can be expanded to give:

$$\begin{aligned}(mx_i + c - y_i)(mx_i + c - y_i) \\ &= m^2x_i^2 + mx_ic - mx_iy_i + mx_ic + c^2 - y_ic - mx_iy_i - y_ic + y_i^2 \\ &= m^2x_i^2 + 2mx_ic - 2mx_iy_i + c^2 - 2y_ic + y_i^2\end{aligned}$$

This expression can be differentiated for *m*:

$$2mx_i^2 + 2x_ic - 2x_iy_i$$

and for c: $2mx_i + 2c - 2y_i$

The sum of squared errors can be expressed as:

$$E = \min_{m,c} \sum_i (m^2x_i^2 + 2mx_ic - 2mx_iy_i + c^2 - 2y_ic + y_i^2)$$

which, when plotted, produces a curve. Taking the gradient at the bottom of the curve, when the sum of the squared errors is at its lowest point, the rate is zero, and:

$$\left.\frac{dE}{dm}\right|_c = \sum(2mx_i^2 + 2x_ic - 2x_iy_i) = 0$$

$$= 2m\sum x_i^2 + 2c\sum x_i - 2\sum x_iy_i = 0$$

$$= m\sum x_i^2 + c\sum x_i - \sum x_iy_i = 0 \qquad \textbf{Equation 3-12}$$

and

$$\left.\frac{dE}{dc}\right|_m = \sum(2mx_i + 2c - 2y_i) = 0$$

$$= 2m\sum x_i + n2c - 2\sum y_i = 0$$

$$= m\sum x_i + nc - \sum y_i = 0 \qquad \textbf{Equation 3-13}$$

Rearranging Equation 3-13 provides an expression for *m*:

$$m = \frac{\sum y_i - nc}{\sum x_i} \qquad \textbf{Equation 3-14}$$

To find an expression for c, substitute Equation 3-14 into Equation 3-12:

$$\left(\frac{\sum y_i - nc}{\sum x_i}\right)\sum x_i^2 + c\sum x_i - \sum x_i y_i = 0 \qquad \textbf{Equation 3-15}$$

Multiplying Equation 3-15 by $\sum x_i$, rearrange for *c*:

$$(\sum y_i - nc)\sum x_i^2 + c(\sum x_i)^2 - (\sum x_i y_i)\sum x_i = 0$$

$$(\sum y_i)(\sum x_i^2) - nc(\sum x_i^2) + c(\sum x_i)^2 - (\sum x_i y_i)\sum x_i = 0$$

$$-nc(\sum x_i^2) + c(\sum x_i)^2 = -(\sum y_i)(\sum x_i^2) + (\sum x_i y_i)\sum x_i$$

$$c((\sum x_i)^2 - n\sum x_i^2) = -(\sum y_i)(\sum x_i^2) + (\sum x_i y_i)\sum x_i$$

$$c = \frac{-\sum y_i(\sum x_i^2) + \sum x_i(\sum x_i y_i)}{(\sum x_i)^2 - n\sum x_i^2} \qquad \textbf{Equation 3-16}$$

The problem can also be solved by using a numerical, rather than calculus-based method – i.e. by manually estimating values for *m* and *c* and checking for goodness of fit.

This is illustrated by the graph shown in Figure 3-5, where the sum of squared errors for a range of estimated *m* and *c* values has been calculated for a set of hypothetical experimental results. The hypothetical data presented can be seen to reach a minimum point where the value of *m* is approximately 0.2 and *c* approximately 2.0. The mathematical algorithm to be used for the model-based optimisation will follow this procedure of searching an *n*-dimensional space for the lowest (or highest, depending on the objective function) point. However, as biological systems are more complex than the example shown here, the resultant surface plot may have numerous hills and valleys, and the challenge of the algorithm is to find the optimum point in the entire search space.

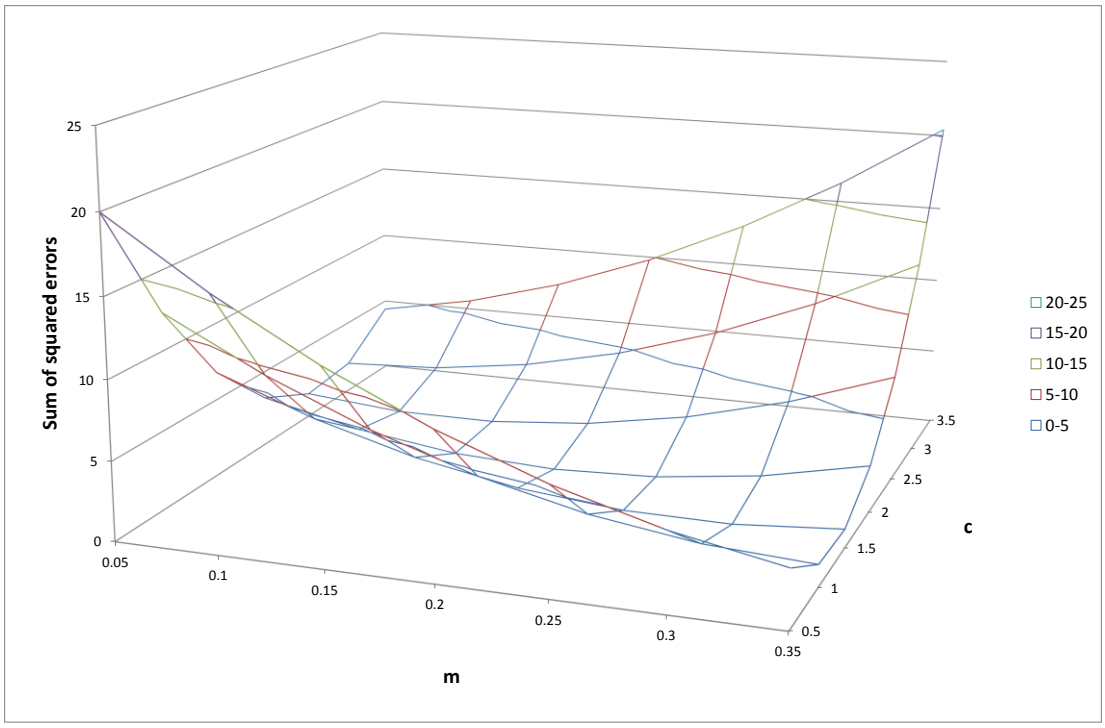

Figure 3-5 Sum of squared errors vs. estimated *m* and *c* values

In this work, optimisation was carried out using Sentero's Proximate Parameter Tuning (PPT) algorithm (Wilkinson et al. 2008; Wilkinson 2009). This is a sequential linear programming method that was originally written for the estimation of kinetic parameters in intracellular processes but can be used for optimising economic objectives. For example, certain key design parameters may be specified in order to maximise NPV; however, there may be numerous combinations of parameter values that may achieve the target value. Sentero's PPT algorithm seeks parameter values that are closest to the nominal values rather than those at the extremes of the parameter space. With respect to this model, where design parameters represent gas flows, Sentero's optimisation method prevents flows from becoming unmanageably high. This is very important from a practical point of view but also in that costs will increase with the complexity of the engineering project. Several economic functions have been included in the model to keep a track of investment and operating costs.

It is anticipated that the novel gas transfer system proposed in this work will be crucial to the profitability of the process. Although there are investment and operating costs attached to this additional gas transfer system, it is the hope that

optimisation will find the balance between successfully recycling the carbon-rich off-gases from the activated sludge process and the ensuing pumping costs. With NPV as the objective function, the optimiser will find the best values of design variables in order to maximise the net worth of the project. Use of the optimisation software will be described in detail in Chapter 5 (Section 5.3.2).

The methods presented here have been presented in a logical, rather than chronological, order. The Activated Sludge Algal Pond Model was constructed over three iterations, i.e. versions 1, 2 and 3. The results of these models will be shown in Chapters 5, 6 and 8, along with a full and comprehensive description of each model. The following chapter – Materials and Methods: Microalgae – describes the laboratory work undertaken to provide the kinetic parameters for algal growth required by the model.

CHAPTER 4 - MATERIALS AND METHODS: MICROALGAE

The aim of these experiments was to determine parameters that could be used in expressions of algal growth within the algal pond liquid compartment. In particular, growth on nitrate, ammonium and carbon dioxide were investigated for compatibility with ASM3 employed in the activated sludge liquid phase.

4.1 Materials

4.1.1 Chemicals

The primary chemicals for the growth medium (stock solutions 1-6, see Table 4) were sourced from Fisher Scientific UK Ltd. The trace elements and vitamins (for solutions 7-9) were obtained from Sigma Aldrich. Ammonium chloride was sourced from Sigma Aldrich. Life sparkling mineral water (Princes Gate Spring Water) was purchased locally.

4.1.2 Algal species

The microalga used in this study was of the *Chlorella* genus and was isolated from a freshwater pond in Weston Park, Sheffield. The organism was identified to the genus level by 18S DNA sequencing by Jasem Almohsen (laboratory of Dr D J Gilmour, Department of Molecular Biology and Biotechnology, University of Sheffield). Although the species remains unidentified at present, it was decided that this alga should be used for two reasons: being a freshwater organism, it would be complementary to the concept of integration with domestic wastewater treatment; it is native to Britain and therefore able to grow successfully in the climate for which this research is written.

4.1.3 Algal culture medium

Chlorella sp. was cultured in a modified Bold's basal medium with 3-fold nitrogen and vitamins (3N-BBM+V), the basic composition of which can be seen in Table 4. However, individual methods should be consulted for the exact quantities of stock solutions used, as they were varied according to the aims of the experiment; also,

ammonium chloride (NH_4Cl) was used in one instance as an alternative to sodium nitrate ($NaNO_3$). Stock solutions were made up with deionised water; media solutions were autoclaved at 121 °C for 15 minutes and allowed to equilibrate to room temperature prior to use. Life sparking mineral water was assumed to be free of bacteria.

Table 4 Stock solutions for the preparation of 3N-BBM+V

Stock	Concentration ($g\ L^{-1}$)	Compound	Volume for 1 L medium (mL)	Concentration in final medium (M)
1	25.0	$NaNO_3$	30.0	8.82×10^{-3}
2	2.5	$CaCl_2.2H_2O$	10.0	1.70×10^{-4}
3	7.5	$MgSO_4.7H_2O$	10.0	3.04×10^{-4}
4	7.5	$K_2HPO_4.3H_2O$	10.0	3.29×10^{-4}
5	17.5	KH_2PO_4	10.0	1.29×10^{-3}
6	2.5	NaCl	10.0	4.2×10^{-4}
7	**Trace element solution**		6.0	-
8	1.2	Vitamin B_1	1.0	3.56×10^{-6}
9	0.01	Vitamin B_{12}	1.0	7.38×10^{-9}

Trace element solution: in 1 L deionised water, add Na_2 EDTA (0.75 g) and the minerals in exactly the following sequence: $FeCl_3.6H_2O$ (97.0 mg), $MnCl_2.4H_2O$ (41.0 mg), $ZnCl_2$ (5.0 mg), $CoCl_2.6H_2O$ (2.0 mg) and $NaMoO_4.2H_2O$ (4.0 mg). Fe EDTA (131.72 mg) was used in place of $FeCl_3.6H_2O$ for the experiment in Section 4.2.3, below.

4.1.4 Growth conditions

Algal growth was carried out in a temperature-controlled growth room at 25°C, with 24 h illumination; the cultures were not shaken. Light measurements were taken with a SKP200/SKP216 hand-held photometer (SKYE Instruments Ltd) fitted with a Hansatech QSRED Quantum sensor. Different flask positions received slightly different quantities of light – see Figure 4-1, below.

35	55	67	72	68	68
42	72	85	92	92	87
35	45	54	56	56	53

Figure 4-1 Light levels in different areas of illuminated shelving (values shown in µmol photons m^{-2} s^{-1})

Measurements were taken at various intervals on the shelving, although the values given above are by no means limited in area to one flask per measurement. For this study, the shaded area only was used due to utilisation by other researchers for algal cultures. To reduce the effects of differing light levels, flask positions were rotated on a regular basis; therefore, the algal cultures received a mean illumination of 72 µmol photons m^{-2} s^{-1}.

Figure 4-2 Illuminated algal cultures in temperature-controlled growth room

Figure 4-2, above, is a typical example of illuminated shelving where algal cultures can be grown. Note that the arrangement of flasks does not necessarily correspond to the positions indicated in Figure 4-1.

4.1.5 Spectroscopy

UV-Vis spectroscopy was carried out using a Unicam Helios alpha spectrophotometer. Cell density was measured at an absorbance of 600 nm (OD_{600}) using standard disposable cuvettes (pathlength = 1 cm). To determine the nitrate

content in the algal culture, the supernatant was measured at an absorbance of 232 nm (OD_{232}) using a glass cuvette (pathlength = 1 cm). The system was calibrated by first inserting a blank (deionised H_2O) before measuring samples.

4.1.6 Data processing

All numerical data was processed in Microsoft Excel (Office 2010) to produce growth curves and calculate kinetic parameters for the mathematical model.

4.2 Methods

4.2.1 Cultivation of Chlorella sp. with varying concentration of $NaNO_3$

To assess the effect of nitrate concentration on the growth of *Chlorella sp*., algal culture was grown in modified BBM+V with varying concentrations of nitrate. For this experiment, a nitrate-free medium was made up – i.e. as per Table 4 but omitting Stock 1, $NaNO_3$. Instead, a separate sodium nitrate solution was made up, at a target concentration of 1 g/L, by dissolving 152.5 mg $NaNO_3$ in 150 mL of the nitrate-free medium, for later use (actual concentration 1.02 g/L). Prior to inoculation, algal culture (*Chlorella sp*., 100 mL) was split into four 50 mL Falcon tubes and centrifuged at 3000 *g* for 10 minutes; the supernatant fluid was discarded. Nitrate-free medium (25 mL) was added to one Falcon tube and the pellet re-suspended; this culture was used to re-suspend all four pellets to obtain a culture that was four times denser than the original. The culture was washed a further two times in nitrate-free BBM+V; 1 ml aliquots of this culture were transferred into a volume of nitrate-free medium. Sodium nitrate (1 g/L $NaNO_3$ solution) was added to the algal subcultures to represent concentration of 0, 5, 10, 20, 50, 100, and 200 mg/L $NaNO_3$ (see Table 5, below). Triplicate subcultures of each concentration were prepared in autoclaved 250 mL conical flasks, made up to 100 mL with nitrate-free BBM+V and sealed with sponge bungs; aseptic conditions were maintained throughout. The optical density of the original algal culture was 0.280 AU at 600 nm, which had been concentrated to produce an inoculum. The optical density of the subcultures was estimated as follows:

$$Conc_{stock} \times Vol_{stock} = Conc_{dil} \times Vol_{dil}$$ **Equation 4-1**

$$Conc_{dil} = \frac{0.280\ AU \times 100\ mL}{25\ mL} = 1.12\ AU$$

$$Conc_{dil\,2} = \frac{1.120\ AU \times 1\ mL}{100\ mL} = 0.011\ AU$$

Table 5 Preparation of cultures with varying concentrations of $NaNO_3$

Culture ID (A-C)	Volume $NaNO_3$ Stock Solution (mL)	$NaNO_3$ Concentration in Culture (mg/L)	$NaNO_3$ Concentration in Culture (mM)	Nitrogen Content of Culture (mg/L)
0	0.00	0	0	0
5	0.50	5.08	0.06	0.84
10	1.00	10.17	0.12	1.67
20	2.00	20.33	0.24	3.35
50	5.00	50.83	0.60	8.37
100	10.00	101.67	1.20	16.75
200	20.00	203.33	2.39	33.49

The above volumes were calculated using Equation 4-1, e.g.

$$Vol_{stock} = \frac{5\ mg\ L^{-1} \times 100\ mL}{1000\ mg\ L^{-1}} = 0.5\ mL$$

The flasks were transferred to the growth room and, at intervals, 1.5 mL samples taken from each subculture for OD_{600} measurements.

The concentration of residual nitrogen in the algal cultures was tracked by spectroscopy, for which a calibration curve was required. Sodium nitrate standard solutions were prepared in the range of 0-3 mM, by dissolving 170.3 mg of $NaNO_3$ in 100 mL nitrate-free BBM+V medium to produce a 20 mM $NaNO_3$ solution. This stock solution was diluted to produce solutions of 0.2, 0.4, 0.6, 0.8, 1.0, 1.5, 2.0, 2.5 and 3.0 mM $NaNO_3$ in nitrate-free BBM+V medium (10.0 mL). The optical density at

232 nm of each solution was measured and the data was plotted to produce a calibration curve (Bumadian 2011).

Table 6 Calibration curve for NO_3-N concentration determination by spectroscopy

$NaNO_3$ Standard Solution Concentration (mM)	**Volume of $NaNO_3$ Stock Solution (mL)**	**OD_{232} (AU)**
Blank	0	0.000
0.2	0.1	0.171
0.4	0.2	0.348
0.6	0.3	0.375
0.8	0.4	0.494
1.0	0.5	0.608
1.5	0.75	0.867
2.0	1.0	1.169
2.5	1.25	1.397
3.0	1.5	1.551

Following the measurement of optical density at 600 nm, the algal samples were prepared for measurement of nitrate-nitrogen by transferring the samples to 1.5 mL Eppendorf tubes and centrifuging in the microfuge at 3000 *g* for 2 minutes. An aliquot (0.9 mL) of the supernatant was transferred to a glass cuvette and measured at 232 nm.

4.2.2 Cultivation of Chlorella sp. with varying concentration of NH_4Cl

The aim of this experiment was to assess the utility of ammonium by *Chlorella sp*., as residual dissolved ammonium may remain in treated wastewater. Again, a nitrate-free medium was made up – i.e. as per Table 4 but omitting Stock 1, $NaNO_3$. A separate ammonium chloride solution was made up, at a target concentration of 629 mg/L, by dissolving 94.3 mg NH_4Cl in 150 mL of the nitrate-free medium, for later use. Prior to inoculation, algal culture (*Chlorella sp*., 100 mL) was washed and concentrated using the method described in Section 4.2.1. 1 ml aliquots of the concentrated culture were transferred into a volume of nitrate-free medium. Ammonium chloride (629 mg/L NH_4Cl solution) was added to the algal subcultures

to represent concentration of 0, 3, 6, 13, 31, 63, and 126 mg/L NH_4Cl (see Table 7, below). Triplicate subcultures of each concentration were prepared in autoclaved 250 mL conical flasks, made up to 100 mL with nitrate-free BBM+V and sealed with sponge bungs; aseptic conditions were maintained throughout. The optical density of the original algal culture was 0.495 AU at 600 nm, which had been concentrated to produce an inoculum. Using Equation 4-1, the optical density of the subcultures was estimated as follows:

$$Conc_{dil} = \frac{0.495\ AU \times 100\ mL}{25\ mL} = 1.980\ AU$$

$$Conc_{dil} = \frac{1.980\ AU \times 1\ mL}{100\ mL} = 0.020\ AU$$

Table 7 Preparation of cultures with varying concentrations of NH_4Cl

Culture ID (A-C)	Volume NH_4Cl Stock Solution (mL)	NH_4Cl Concentration in Culture (mg/L)	NH_4Cl Concentration in Culture (mM)	Nitrogen Content of Culture (mg/L)
0	0.00	0	0	0
3	0.50	3.14	0.06	0.82
6	1.00	6.29	0.12	1.65
12	2.00	12.57	0.24	3.29
31	5.00	31.43	0.59	8.23
62	10.00	62.87	1.18	16.45
125	20.00	125.73	2.35	32.90

The above volumes were calculated using Equation 4-1, e.g.

$$Vol_{stock} = \frac{3\ mg\ L^{-1} \times 100\ mL}{629\ mg\ L^{-1}} = 0.5\ mL$$

The flasks were transferred to the growth room and, at intervals, 1.0 mL samples taken from each subculture for OD_{600} measurements.

4.2.3 Cultivation of Chlorella sp. with varying concentration of CO_2

The aim of this experiment was to measure the effect of carbon dioxide on the growth of *Chlorella sp*., as carbon dioxide produced during the activated sludge process could be used to feed algae in an adjacent pond. This was assessed by the novel method of adding commercially available sparkling mineral water (for human consumption) to the growth medium. To start with, a double-strength 3N-BBM+V solution was made up, to allow for addition of carbonated/deionised water to formulate media representing approximately 20, 40, 80, 200, and 400 times atmospheric CO_2 concentration. As water will already contain carbon dioxide at a concentration of 0.6 mg L^{-1} at standard temperature and pressure, aliquots of carbonated water were added to the algal cultures to represent increasing concentrations of dissolved CO_2 in in the medium. To illustrate:

$$H = \frac{p}{c} \qquad \textbf{Equation 4-2}$$

Where H is Henry's Constant, *p* is the partial pressure and *c* is concentration.

For CO_2, H = 29.76 atm $(mol/L)^{-1}$ or 0.68 atm $(g/L)^{-1}$, and *p* = 4 x 10^{-4} atm. Therefore, the concentration of CO_2 in water at STP will be:

$$c = \frac{4 \times 10^{-4} atm}{0.68 \frac{atm}{g/L}} = 5.88 \times 10^{-4} \frac{g}{L} = 0.6\ mg\ L^{-1}$$

The manufacturing process of Life sparkling mineral water achieves 3.5 volumes of CO_2 per volume of water, under ideal conditions; i.e. carbon dioxide is present in at a concentration of 0.7% by mass (Cloud 2013). Assuming 1 mole of CO_2 gas occupies 22.4 L, then:

$$\frac{3.5\ L}{22.4\ L\ mol^{-1}} = 0.156\ mol\ CO_2\ in\ 1\ L\ water$$

Since CO_2 has a molecular weight of 44 g mol^{-1}, then:

$$0.156\ mol\ \times 44\ g\ mol^{-1} = 6.864\ g\ CO_2\ per\ 1000\ g\ water$$

However, as the CO_2 concentration will vary according to the environmental conditions at the time of manufacture, a bottle of sparkling water from the same batch was weighed and shaken to expel the gas – this was repeated until a consistent value was achieved; the concentration for the batch was determined to be 6.42 g CO_2 L^{-1}. This value can then be used to calculate the volume of sparkling water required to achieve the required levels of CO_2 in the media. For example, 18 times the level of carbon dioxide in water would equate to a concentration of 10.8 mg L^{-1}; subtracting the concentration naturally occurring in water, 0.6 mg CO_2 L^{-1}, a spike of 10.2 mg CO_2 L^{-1} would be required. Using Equation 4-1:

$$Vol_{stock} = \frac{10.2\ mg\ L^{-1} \times 100\ mL}{6420\ mg\ L^{-1}} = 0.16\ mL$$

To prepare the cultures: 50 mL double-strength 3N-BBM+V, deionised and carbonated water according to Table 8 below, and 1 mL aliquots of algal culture were transferred into 250 mL conical flasks and sealed with sponge bungs. Triplicates of each concentration were prepared, and aseptic conditions were maintained as far as practicable to minimise bacterial contamination. It was envisaged that CO_2 may desorb from the cultures over a number of hours; comparing this to the conceptual integrated wastewater treatment plant, where the algal pond would be fed continuously with CO_2-rich gases from the activated sludge tank, the cultures were fed daily with carbonated water to mimic this process and maintain the required levels of CO_2.

Table 8 Preparation of cultures with varying concentrations of CO_2

Culture ID (A-C)	Volume 2x Strength 3N-BBM+V (mL)	Volume Deionised Water (mL)	Daily Volume of Carbonated Water (mL)	Additional CO_2 (mg/L)	Total CO_2 Concentration (mg/L)
1	50	50	0.00	0	0.6
18	50	49.84	0.16	10.3	10.9
40	50	49.64	0.36	23.1	23.7
82	50	49.24	0.76	48.8	49.4
210	50	48.04	1.96	125.8	126.4
425	50	46.04	3.96	254.2	254.8

The optical density of the original culture was 1.765 AU at 600 nm; the optical density of the subcultures was estimated as follows:

$$Conc_{dil} = \frac{1.765\ AU \times 1\ mL}{100\ mL} = 0.018\ AU$$

The flasks were transferred to the growth room and, at intervals, 1.0 mL samples taken from each subculture for OD_{600} measurements. The daily volume of carbonated water was added to each culture before returning to the growth room.

The results of these experiments are reported in Chapter 7; however, early versions of the integrated model were produced prior to the application of these results and ASAPM versions 1 and 2 are presented in the following chapters.

CHAPTER 5 - ACTIVATED SLUDGE ALGAL POND MODEL VERSION 1

In this chapter, the first version of the integrated Activated Sludge Algal Pond Model is introduced. The results presented here chart the development of the model, delivering four separate sets of results from non-integrated and integrated systems, and economic and optimised models. Initially, the model was constructed with simplified expressions for wastewater treatment and algal growth, and the model had the flexibility to operate with or without gas exchange between the two vessels. It was demonstrated that gas exchange was indeed beneficial to both processes, after which economic functions were added to the model to predict capital and operating costs as well as revenue streams. The economic model was used as the basis for optimisation, using nominal design parameter values from which to find a good solution. However, a globally optimal solution is difficult to achieve and proving optimality is, therefore, beyond the scope of this research.

5.1 Introduction

Drawing together the concepts presented in Chapter 3, a model was constructed using Sentero that consisted of: four interconnected compartments to form a continuous process; Monod expressions for wastewater treatment and algal growth; and economic functions. A screenshot of the model, ASAPM v1, can be seen in Figure 5-1. The model was built in stages, however, beginning with a model of integrated wastewater treatment and algal growth to determine the significance of gas exchange on the two biological processes. Only once this utility had been explored were economic functions added, which enabled optimisation of the model.

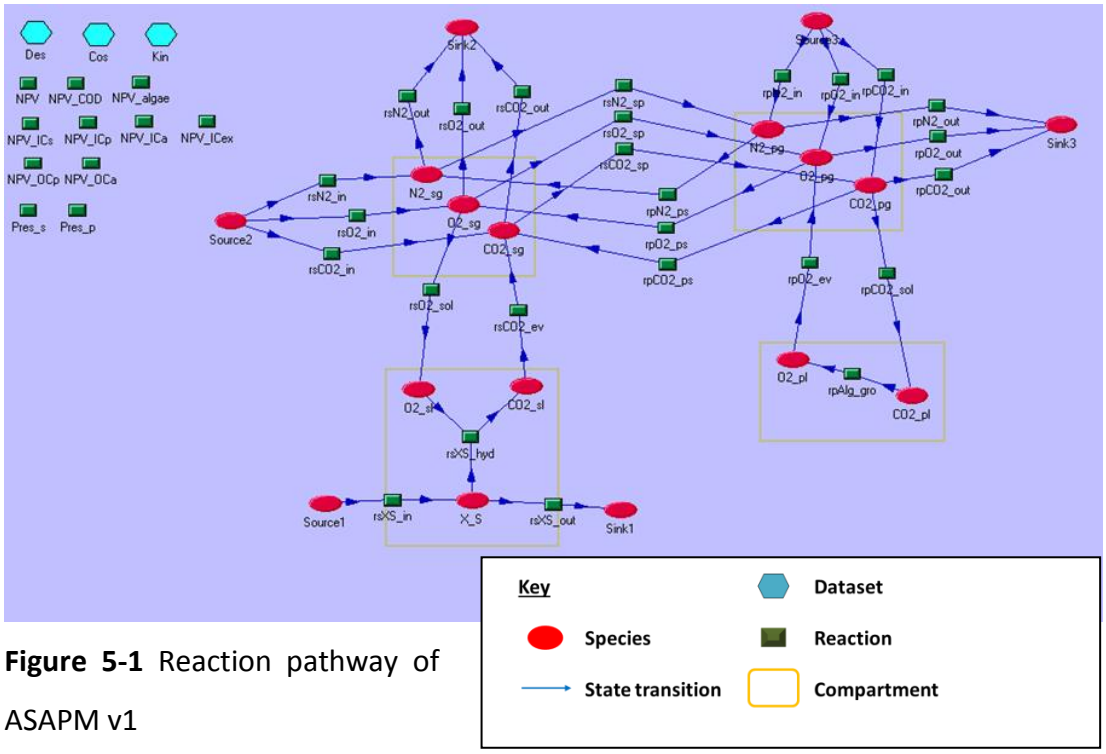

Figure 5-1 Reaction pathway of ASAPM v1

This first version of the integrated model allowed exploration of the benefits of an integrated activated sludge-algal growth process, with particular emphasis on the novel gas exchange system; a comparison of gas exchange on/off will be discussed in Section 5.3.1, below. The inclusion of economic functions provided the ability to optimise the model with Net Present Value (NPV) as the objective function; the optimisation procedure and results are explained in Section 5.3.2. The model in its entirety is presented in the following section.

5.2 The Model

The thought processes involved in the production of the integrated model are discussed fully in Chapter 3; the process rates, economic functions and parameter values that make up the model are presented here. The stoichiometric matrix for this model can be seen in Appendix E. Table 9 details the process rates of the model – a collection of bulk and mass transfer and Monod-type expressions. The 17 species are interconnected by 26 reactions that are named according to the process being described, with the prefix *rs* denoting a reaction in the sludge tank and *rp* a reaction in the pond.

Table 9 Process rates for ASAPM v1

ρ	Process	Process Rate
$rsN2_{in}$	N_2 feed into AS tank	$N2_{feed}.In_{sg}$
$rsO2_{in}$	O_2 feed into AS tank	$O2_{feed}.In_{sg}$
$rsCO2_{in}$	CO_2 feed into AS tank	$CO2_{feed}.In_{sg}$
$rsN2_{out}$	N_2 flow out of AS tank	$N2_{sg}.Out_{sg}$
$rsO2_{out}$	O_2 flow out of AS tank	$O2_{sg}.Out_{sg}$
$rsCO2_{out}$	CO_2 flow out of AS tank	$CO2_{sg}.Out_{sg}$
$rsN2_{sp}$	N_2 flow from AS tank to algal pond	$N2_{sg}.G_{sp}$
$rsO2_{sp}$	O_2 flow from AS tank to algal pond	$O2_{sg}.G_{sp}$
$rsCO2_{sp}$	CO_2 flow from AS tank to algal pond	$CO2_{sg}.G_{sp}$
$rpN2_{ps}$	N_2 flow from pond to AS tank	$N2_{pg}.G_{ps}$
$rpO2_{ps}$	O_2 flow from pond to AS tank	$O2_{pg}.G_{ps}$
$rpCO2_{ps}$	CO_2 flow from pond to AS tank	$CO2_{pg}.G_{ps}$
$rpN2_{in}$	N_2 feed into algal pond	$N2_{feed}.In_{pg}$
$rpO2_{in}$	O_2 feed into algal pond	$O2_{feed}.In_{pg}$
$rpCO2_{in}$	CO_2 feed into algal pond	$CO2_{feed}.In_{pg}$
$rpN2_{out}$	N_2 flow out of algal pond	$N2_{pg}.Out_{pg}$
$rpO2_{out}$	O_2 feed out of algal pond	$O2_{pg}.Out_{pg}$
$rpCO2_{out}$	CO_2 flow out of algal pond	$CO2_{pg}.Out_{pg}$
$rsO2_{sol}$	Dissolution of O_2 in AS tank	$V_{sl}.kLa_s(O2_{sg}.H_{O2} - O2_{sl})$
$rsCO2_{ev}$	Evolution of CO_2 from AS tank	$V_{sl}(kLa_s \times 0.91)(CO2_{sl} - CO2_{sg}.H_{CO2})$
$rpO2_{ev}$	Evolution of O_2 from algal pond	$V_{pl}.kLa_p(O2_{pl} - O2_{pg}.H_{O2})$
$rpCO2_{sol}$	Dissolution of CO_2 in algal pond	$V_{pl}(kLa_p \times 0.91)(CO2_{pg}.H_{CO2} - CO2_{pl})$
$rpAlg_{gro}$	Algal growth	$k_{O2pond}\frac{CO2_{pl}}{K_{CO2} + CO2_{pl}}X_{Algae}$
$rsXS_{in}$	X_S feed into AS tank	$XS_{feed}.In_{sl}$
$rsXS_{hyd}$	Hydrolysis of X_S and aerobic growth	$\mu_H\frac{O2_{sl}}{K_{O2} + O2_{sl}}\frac{X_S}{K_S + X_S}X_H$
$rsXS_{out}$	X_S flow out of AS tank	$X_S.Out_{sl}$

The reactions $rpAlg_{gro}$ and $rsXS_{hyd}$ are simplified descriptions of algal growth and wastewater treatment. The intention of this exploratory model was to observe the effect of enclosed headspaces on biological processes and it was felt that a full set of growth expressions was unnecessary at this stage. Reaction $rpAlg_{gro}$ is a very crude description of algal growth, whereby the only consideration is the conversion of carbon dioxide into oxygen. Similarly, reaction $rsXS_{hyd}$ is a simplified version of the hydrolysis of trapped organics in wastewater. ASAPM v1 also includes pseudo-reactions as economic functions and these are shown in Table 10.

Table 10 Economic and pressure constraint functions for ASAPM v1

f	**Function**	**Expression**
NPV	Total Net Present Value	Sum of individual NPV expressions below
NPV_{algae}	Value of biodiesel and CO_2 sequestration	$\Gamma . days_{algae}\left(V_{pl}\left(k_{O2pond}\left(\frac{CO2_{pl}}{K_{CO2}+CO2_{pl}}\right)X_{Algae}\right)(r_{algae}.Y_{algae}+ r_{CO2}.Y_{CO2})\right)$
NPV_{COD}	Value of COD treatment	$\Gamma . days_{COD}\left(r_{COD}\left(V_{sl}\left(\mu_H\left(\frac{O2_{sl}}{K_{O2}+O2_{sl}}\right)\left(\frac{X_S}{K_S+X_S}\right)X_H\right)\right)\right)$
NPV_{ICa}	Investment cost of aeration system	$-c_a\left(B\left((kLa_s.V_{sl})^{\delta_a}+\left(kLa_p.V_{pl}\right)^{\delta_a}\right)\right)$
NPV_{ICex}	Investment cost of gas exchange system	$-c_{ex}\left(G_{sp}^{\delta_{ex}}+G_{ps}^{\delta_{ex}}\right)$
NPV_{ICp}	Investment cost of algal pond	$-c_p\left(V_{pl}^{\delta_p}+V_{pg}^{\delta_p}\right)$
NPV_{ICs}	Investment cost of sludge tank	$-c_s\left(V_{sl}^{\delta_s}+V_{sg}^{\delta_s}\right)$
NPV_{OCa}	Operating cost of aeration	$\Gamma . days_{COD}\left(-\alpha_E\left(kWh(In_{sg}+Out_{sg}+In_{pg}+Out_{pg}+ G_{sp}+G_{ps})\right)\right)$
NPV_{OCp}	Operating cost of liquid pumping	$\Gamma . days_{COD}\left(-\alpha_E\left(kWh(In_{sl}+Out_{sl})\right)\right)$

f	Function	Expression
$Pres_p$	Algal pond pressure check	$\frac{O2_{pg}}{32} + \frac{CO2_{pg}}{44} + \frac{N2_{pg}}{28}$
$Pres_s$	Sludge tank pressure check	$\frac{O2_{sg}}{32} + \frac{CO2_{sg}}{44} + \frac{N2_{sg}}{28}$

The structures of the economic functions are discussed in Chapter 3. While investment and operating costs have their origins in the work of Alasino et al. (2007), revenue functions have been modelled according to the rate of the reactions in the liquid phases. As reactions $rpAlg_{gro}$ and $rsXS_{hyd}$ were written in terms of the dissolution or evolution of carbon dioxide and oxygen, there are no measureable particulate substrates upon which to calculate revenue. Instead, revenue increases correspondingly with the rate of the reaction. An estimate of algal productivity and CO_2 evolution is built into NPV_{algae} using the yield parameters Y_{algae} and Y_{CO2}. The parameter Y_{algae} is estimated from the fraction of C that makes up the algal cell, $C_{106}H_{263}O_{110}N_{16}P$ – i.e. in 3,550 g of algae there are 1,272 g of CO_2-C, therefore it was estimated that the productivity of the reaction would be 2.791 g algae (g CO_2-C)$^{-1}$. Lavigne and Gloger (2006) calculate that 18,250 kg BOD produces 26,767 kg CO_2; it is from here that I derived the parameter Y_{CO2}, which has a value of 1.467 g CO2 g BOD^{-1}. A full list of starting parameter values is given in Table 11 below.

Table 11 Parameter values for ASAPM v1

Parameter ID	Description	Value	Units
Design Parameters			
G_{ps}	Gas flow from pond to sludge tank	1000	$m^3\ d^{-1}$
G_{sp}	Gas flow from sludge tank to pond	2000	$m^3\ d^{-1}$
In_{sg}	Gas flow from air to sludge tank	1000	$m^3\ d^{-1}$
Out_{sg}	Gas flow from sludge tank to air	1000	$m^3\ d^{-1}$
In_{pg}	Gas flow from air to pond	1000	$m^3\ d^{-1}$
Out_{pg}	Gas flow from pond to air	3000	$m^3\ d^{-1}$
In_{sl}	Liquid flow into sludge tank	3000	$m^3\ d^{-1}$
Out_{sl}	Liquid flow from sludge tank	3000	$m^3\ d^{-1}$
k_La_p	Oxygen transfer coefficient (pond)	120	d^{-1}

Parameter ID	Description	Value	Units
k_La_s	Oxygen transfer coefficient (sludge)	120	d^{-1}
V_{pg}	Volume of gas in pond headspace	500	m^3
V_{sg}	Volume of gas in sludge tank headspace	50	m^3
V_{pl}	Volume of liquid in pond	4000	m^3
V_{sl}	Volume of liquid in sludge tank	400	m^3
Feed Parameters			
$O2_{feed}$	O_2 content in air	276	g m^{-3}
$CO2_{feed}$	CO_2 content in air	0.722	g m^{-3}
$N2_{feed}$	N_2 content in air	897	g m^{-3}
XS_{feed}	COD content in primary effluent	115	g m^{-3}
Kinetic Parameters			
H_{CO2}	Henry's Constant for CO_2	0.81	atm^{-1}
H_{O2}	Henry's Constant for O_2	0.03	atm^{-1}
k_{O2pond}	Rate constant	1	d^{-1}
K_{CO2}	Saturation constant for CO_2	0.5	g m^{-3}
X_{Algae}	Algal biomass	100	g m^{-3}
μ_H	Heterotrophic max growth rate for X_H	1	d^{-1}
K_{O2}	Saturation constant for O_2	0.1	g m^{-3}
K_S	Saturation constant for X_S	1	g m^{-3}
X_H	Heterotrophic biomass	1000	g m^{-3}
$O2_{req}$	Aerobic yield	0.5	g O_2 (g COD) $^{-1}$
Cost Parameters			
Γ	Updating term	12.462	year
$days_{algae}$	Number of days pond operational	365	days
$days_{COD}$	Number of days sludge tank operational	365	days
kWh	Energy term	0.04	kWh m^{-3}
r_{COD}	Revenue parameter, COD treatment	0.001229	€ g^{-1} COD_{XS}
r_{algae}	Revenue parameter, algal lipid	0.0005	€ g^{-1}
Y_{algae}	Algal yield	2.791	g algae (g CO_2-C)$^{-1}$
r_{CO2}	Revenue parameter, carbon trading	0.0001	€ g^{-1} C
Y_{CO2}	CO_2 yield from wastewater treatment	1.467	g CO_2 (g BOD)$^{-1}$
c_s	Cost parameter, sludge tank	10304	€
δ_s	Cost parameter, sludge tank	0.477	-
c_p	Cost parameter, pond	10304	€
δ_p	Cost parameter, pond	0.477	-
B	Constant	0.0003	kg O_2 d (h m^3)$^{-1}$
c_a	Cost parameter, aeration	8590	€
δ_a	Cost parameter, aeration	0.433	-
c_{ex}	Cost parameter, gas exchange	8590	€
δ_{ex}	Cost parameter, gas exchange	0.433	-
α_E	Unitary operation cost	0.068	€ d kWh^{-1}

The design parameter values presented here were chosen arbitrarily as start-up values for the model, as were the kinetic parameter values for reactions $rpAlg_{gro}$ and $rsXS_{hyd}$. As the model is improved, in both complexity and accuracy, parameters values will be updated accordingly; Chapters 6 and 8 discuss these improved models. Below are the results from this first version of the model.

5.3 Results

5.3.1 Process with integrated gas phase

The aim of the integrated ASAPM is to investigate the benefits of gas transfer between vessels, particularly with respect to algal growth. To ascertain whether CO_2-rich gas improved the rate of algal growth, two separate simulations were run using design parameters chosen to test this concept prior to the inclusion of economic functions. The first simulation included no transfer of gas into the algal pond from the activated sludge tank but obtained atmospheric air from a source; the second simulation included transfer of gases between the sludge vessel and the algal pond. The simulation results from Sentero were downloaded into Excel and the pertinent data plotted for comparison – refer to Figures 5-2 and 5-3, below. Note that time courses are plotted to illustrate the important point that the model is a dynamic one; however, it is the steady state values reached soon after 2 days and summarised in Table 12 that are important.

The data shown to be most affected by the change in the source of gas was the concentration of dissolved CO_2 in the algal pond and the rate of the reaction for algal growth, $rpAlg_{gro}$. Both of these sets of data are greatly improved by aeration of the algal pond from the activated sludge tank, with the concentration of CO_2 in the algal pond being increased by approximately 30 times. It was anticipated that by improving the availability of CO_2 in the pond medium, an increase in algal growth would occur. This expectation was demonstrated by the results of the simulation, with an increase in the concentration of algal biomass in the pond (please note that tabulated results are quoted as productivities for a 4,000 m^3 algal pond, in kg d^{-1}).

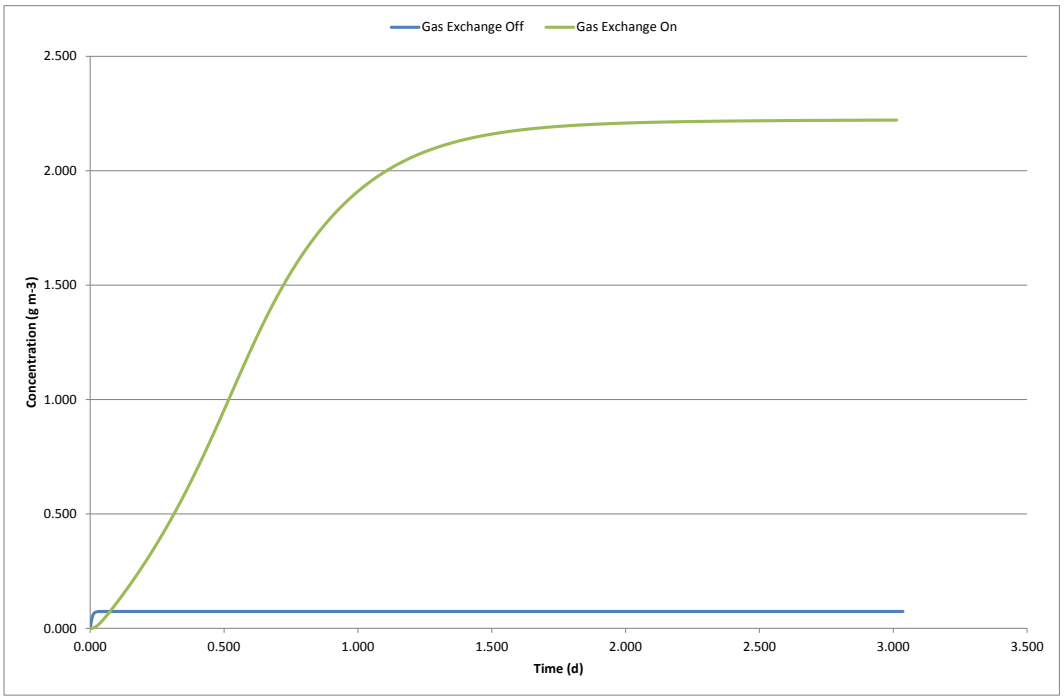

Figure 5-2 Comparison of CO_2 concentration in the algal pond liquid phase with gas exchange on and off

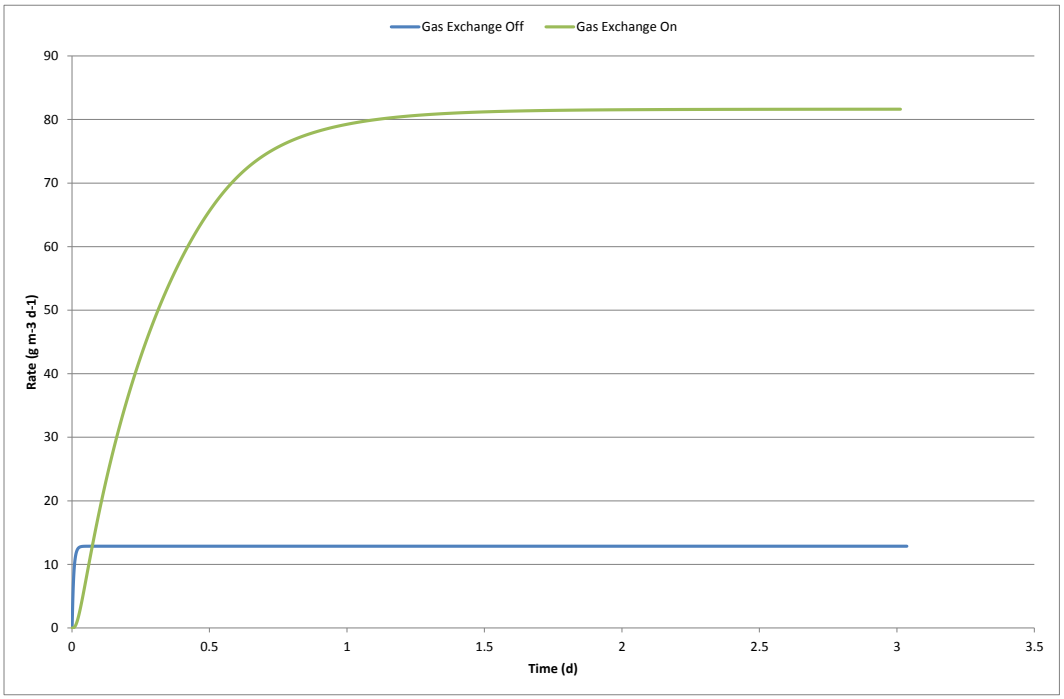

Figure 5-3 Comparison of algal growth rate with gas exchange on and off

The design variables used in these simulations are shown in Table 12, below. Note that the gas flows were manually selected rather than being the result of an optimisation process. It is noteworthy that the concentration of dissolved CO_2 is

greatly improved by a relatively small inflow of gas from the sludge tank; a gas flow of 100,000 m^3 d^{-1} was deemed to be a reasonable estimate for an algal pond of 4,000 m^3 but the concentration of dissolved CO_2 remained low at 0.07 g m^{-3}. By changing the configuration of the algal pond to receive gas from the sludge tank, the dissolved CO_2 concentration increased to over 2 g m^{-3}. There was also a slight increase in the removal of COD due to the transfer of O_2-rich gas from the algal pond into the sludge tank; these results are also shown in the table below.

Table 12 Comparison of results of two scenarios from ASAPM v1

	Parameter/Variable	Units	Scenario 1: Gas Exchange OFF	Scenario 2: Gas Exchange ON
Design Parameters	G_{ps}	m^3 d^{-1}	0	1,000
	G_{sp}	m^3 d^{-1}	0	2,000
	In_{pg}	m^3 d^{-1}	100,000	0
	In_{sg}	m^3 d^{-1}	1,000	1,000
	Out_{pg}	m^3 d^{-1}	100,000	1,000
	Out_{sg}	m^3 d^{-1}	1,000	0
	Total gas pumping flow	m^3 d^{-1}	**202,000**	**5,000**
Steady State Variables	COD Removal	%	91.13	95.48
	Rate of algal biomass production	kg d^{-1}	51.44	326.56
	Sludge dissolved O_2	g m^{-3}	0.63	5.43
	Pond dissolved CO_2	g m^{-3}	0.07	2.22

The total gas pumping requirement for Scenario 1 amounts to 202,000 m^3 d^{-1}; this value represents the worst case scenario where gases are pumped both in and out – in practice, less out pumping should be required. With the gas exchange on, however, the total gas pumping requirement is reduced to 5,000 m^3 d^{-1}. This reduction is achieved by the use of gas transfer flow between the activated sludge and algal pond – atmospheric air is no longer required by the algal pond, as all gases are provided from the sludge tank. In Scenario 2, the activated sludge no longer discharges gases to the atmosphere – the off-gas is diverted to the algal pond – and while some O_2-rich off gas is released to atmosphere from the pond, half is recycled back to the activated sludge vessel.

Because atmospheric CO_2 levels are particularly low, a very high gas flow rate into the algal pond was needed in Scenario 1 to provide the algae with sufficient CO_2 for growth. In Scenario 2, a low gas flow is sufficient to provide the algae with their CO_2 requirements because the expression for biological wastewater treatment has been crudely modelled as a producer of carbon dioxide and, therefore, the off-gas from the activated sludge process will be rich in CO_2. As the rate of gas flowing into the pond from the sludge is much lower, the rate flowing out of the algal pond is also much lower to maintain the mass balance. This reduction in flow could have a major economic impact on the operating costs of such a system, as all pumped processes carry the financial burden of electrical energy requirements. This reduction of almost 98% in pumping requirement would equate to a significant saving in energy cost, and this will be discussed in the following sections.

5.3.2 Optimisation with NPV as objective function

Once it had been demonstrated that gas transfer was an effective tool in increasing the rate of biological processes and decreasing aeration rates, the economic functions detailed in Table 10 were added to enable optimisation with respect to the Net Present Value. In order to do this, the Proximate Tuning Analysis function on Sentero was employed. There are various considerations that should be taken into account when preparing the optimisation – these include: objective function(s) and weighting, design parameters and range, step length, and number of iterations; each of these considerations will be explained in the following paragraphs.

Firstly, the objective function is chosen to be maximum project Net Present Value, which is made up of all the NPV components given in Table 10. Since the PPT algorithm in Sentero was designed for parameter estimation, it works in terms of minimising the deviation between the model output (in this case NPV) and a specified target value. In order to maximise NPV, therefore, a high target value is specified that can never be reached. This has the effect of maximising NPV as, at each iteration, the PPT algorithm tries to minimise the deviation between the actual NPV and the target value. Target values are also used for constraints whose violation should be penalised to ensure a feasible solution. Two such constraints

are included to ensure that atmospheric pressure is maintained in both the activated sludge and algal gas compartments. These equality constraints include the last two expressions given in Table 10, which relate to the headspace pressure in each of the process units as discussed earlier at the end of Section 3.5. The concentration of an ideal gas at atmospheric pressure and a temperature of 293 K is approximately 41 mol m^{-3}. Therefore, as well as setting a target value for the total NPV, two additional targets are set that stipulate that the $Pres_s$ and $Pres_p$ functions both produce a value of 41 mol m^{-3}. Clearly, it is also possible to investigate higher than atmospheric pressure in the headspace of the units but this was not included as a design variable in this study. The overall objective function is therefore a weighted combination of the total NPV and the two pressure functions.

In preparation for optimisation, a simulation of the non-optimised economic model was run. In this simulation, all of the gas inlets were opened up using nominal values – i.e. the design parameters Out_{sg} and In_{pg}, previously set to zero in the integrated 'gas exchange on' scenario, were given a starting value of 1,000 m^3 d^{-1}. This was a necessary step to enable optimisation of all design parameters associated with the gas exchange system. The optimisation itself is presented as a sequence of runs, each run being a randomly selected set of starting values for the design parameters specified. As an optimal value will be obtained from a given range for each parameter, the nominal parameter value may not be equal to zero as this would not provide the parameter tuning algorithm with a sample space from which to calculate a locally optimal solution. For completeness, the results were compared with a simulation whereby the gas exchange was turned off. Both sets of results are shown in the Table 13.

Table 13 Results of simulation of non-integrated and integrated systems

	Parameter/Variable		Units	Non-Integrated System	Integrated System
Design Parameters	G_{ps}		$m^3 d^{-1}$	0	1,000
	G_{sp}		$m^3 d^{-1}$	0	2,000
	In_{pg}		$m^3 d^{-1}$	100,000	1,000
	In_{sg}		$m^3 d^{-1}$	1,000	1,000
	Out_{pg}		$m^3 d^{-1}$	100,000	3,000
	Out_{sg}		$m^3 d^{-1}$	1,000	1,000
	Total gas pumping flow		$m^3 d^{-1}$	**202,000**	**9,000**
Steady State Variables	COD Removal		%	91.13	82.18
	Rate of Algal Biomass Production		$kg\ d^{-1}$	51.44	186.75
	$O2_{sl}$		$g\ m^{-3}$	0.63	0.29
	$CO2_{pl}$		$g\ m^{-3}$	0.07	0.44
	$Pres_s$		$mol\ m^{-3}$	43.86	21.78
	$Pres_p$		$mol\ m^{-3}$	41.63	21.69
Costs	NPV:	**Total**	€	**-1,440,160**	**1,322,962**
Project Term 20 y Discount Rate 0.05		COD	€	1,757,559	1,584,866
		Algae	€	361,093	1,310,913
		ICa	€	-1,017	-1,017
		ICex	€	0	-401,854
		ICp	€	-738,220	-738,220
		ICs	€	-246,142	-246,142
		OCa	€	-2,499,199	-111,350
		OCp	€	-74,234	-74,234
	Annual Revenue		€	-115,564	106,160

Perhaps unsurprisingly, the model indicates that to build an algal pond that is not supported by another process would make a loss due to the amount of energy required for aeration. We can see from these results that although it is profitable, the COD removal and rate of algal biomass production are both poor. In addition to this, the concentration of gases in the sludge and pond headspaces is not at the expected atmospheric value of 41 mol m^{-3}. For optimisation purposes, only the integrated process is considered. Bearing in mind a total NPV of €1,322,962, it did not seem unreasonable to set a target value of €4,000,000; the final required values for $Pres_s$ and $Pres_p$ were set to 41 mol m^{-3}. As well as setting targets, these values

can also be given a weighting according to the importance of the outcome. In this example, all weightings were left to their nominal value of 10. All of these values may be seen in Figure 5-4, below. However, the pressure relation, since it is a constraint, could be deemed to be of greater importance than NPV. To reflect this, the weighting was set to 1,000 in Chapter 8 (see Section 8.3.4). In setting NPV as the objective function, it is assumed that sludge dissolved oxygen and pond dissolved carbon dioxide will both improve, therefore increasing COD removal and the rate of algal biomass production.

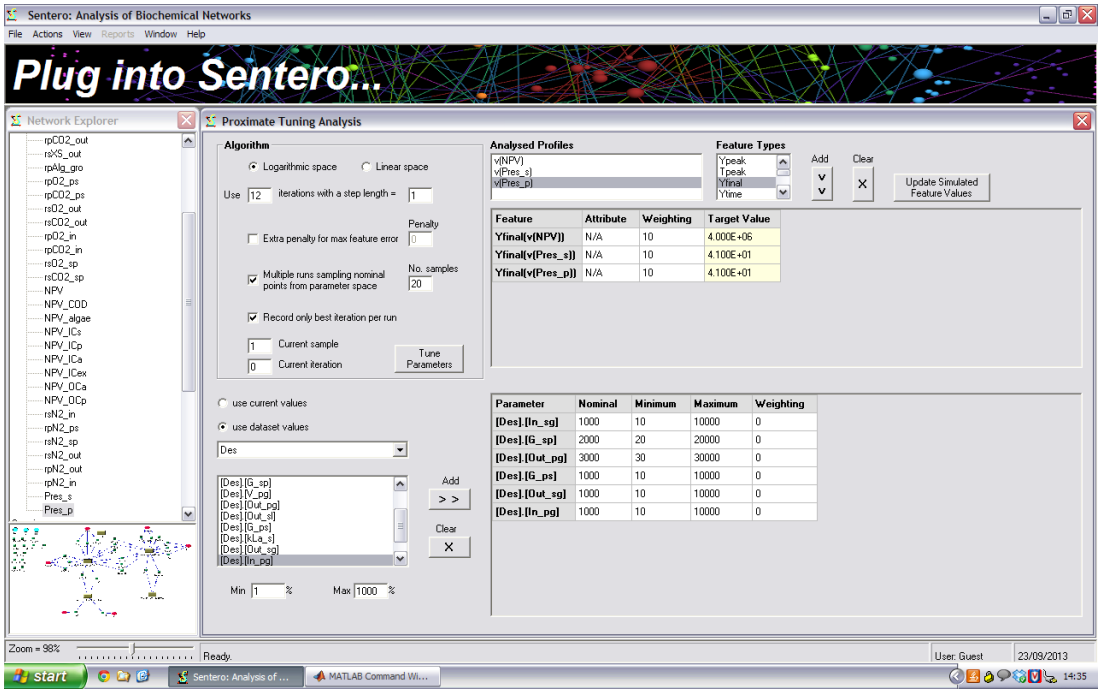

Figure 5-4 Screen shot of Proximate Tuning Analysis

Once the objective function has been set up, the parameters to achieve this target are selected. As the focus of this model is the novel gas exchange system, it is natural that this set of design parameters should be chosen to optimise the model. The design parameters are those detailed in Table 13, above. The range of parameter variance is also specified – in this optimisation, a range of 1-1000% of the nominal value was chosen – providing a parameter space in which to generate a locally optimal solution for each parameter. If we knew that a particular wastewater treatment plant had an upper limit for gas pumping flows, the upper range of parameter variance could be set to a much lower value; as this work is to

produce a proof-of-concept model, no such restrictions are in place at present. Again, these values can be seen in Figure 5-4, above.

In Sentero's proximate tuning analysis function, it is possible to specify a step length for the optimiser, for which the default setting is 1. The step length is how far away from the nominal parameter value the optimiser will look for its optimum and may be adjusted to search the n-dimensional space in large strides or more carefully. For example, if the nominal parameter values were thought to be already quite close to the optimum, a step length of 0.5 or less may be specified, to ensure that the optimiser searched only the immediate space around these values. Conversely, if the step length is too small in the first instance, the optimiser may never take a big enough step to find the true optimum and may be confined to a search space in an area that is good but not necessarily the best solution. Finally, the number of samples and iterations are selected but the time taken to complete the run should be considered. In the analysis shown above, I chose to run 20 samples, each with 12 iterations. This is quite a time-consuming request, although the run can be made longer still by increasing the number of samples and perhaps leaving the analysis to run overnight. The results of the analysis are shown, for example, as Run 2.10 – being the 10^{th} iteration of the 2^{nd} sample – and each run being a randomly selected set of starting values for the design parameters specified.

The best results from the optimisation are shown in Table 14, below. Please note that values for the investment costs of the sludge tank, algal pond and aeration system (ICs, ICp and ICa), and the operating cost of liquid pumping (OCp) are not included in Table 14. These values remain the same as detailed in Table 13 because only the gas exchange investment and operating costs (ICex and OCa) will differ from one scenario to the next on account of the design parameters chosen for the optimisation.

Table 14 Results of optimisation of ASAPM v1

	Parameter/Variable		Units	Run 2.10	Run 3.12	Run 6.12	Run 18.12	Run 19.12
Design Parameters	G_{ps}		$m^3\ d^{-1}$	4,250.00	323.60	1,806.00	48.48	1,343.00
	G_{sp}		$m^3\ d^{-1}$	4,495.00	1,529.00	1,994.00	2,265.00	1,960.00
	In_{pg}		$m^3\ d^{-1}$	2,238.00	96.85	1,140.00	734.80	100.30
	In_{sg}		$m^3\ d^{-1}$	141.20	1,141.00	139.30	2,137.00	560.90
	Out_{pg}		$m^3\ d^{-1}$	2,600.00	1,370.00	1,413.00	3,028.00	786.00
	Out_{sg}		$m^3\ d^{-1}$	20.00	10.00	10.00	10.00	10.00
	Total gas pumping flow		$m^3\ d^{-1}$	**13,744.20**	**4,470.45**	**6,502.30**	**8,223.28**	**4,760.20**
Steady State Variables	COD Removal		%	95.45	94.89	95.45	95.11	95.51
	Rate of Algal Biomass Production		kg d-1	321.09	321.65	323.80	319.18	325.59
	Species $O2_{sl}$		$g\ m^{-3}$	5.10	2.26	5.02	2.87	5.90
	Species $CO2_{pl}$		$g\ m^{-3}$	2.03	2.05	2.12	1.97	2.19
	$Pres_s$		$mol\ m^{-3}$	39.23	40.99	41.01	41.00	40.99
	$Pres_p$		$mol\ m^{-3}$	39.74	41.01	41.00	41.01	41.00
Costs Project Term 20 y Discount Rate 0.05	NPV:	**Total**	€	**2,217,379**	**2,662,539**	**2,522,219**	**2,623,739**	**2,585,874**
		COD	€	1,840,961	1,830,079	1,840,828	1,834,377	1,842,060
		Algae	€	2,253,843	2,257,809	2,272,886	2,240,465	2,285,456
		ICex	€	-674,765	-310,426	-451,433	-289,749	-423,134
		OCa	€	-170,047	-55,310	-80,448	-101,741	-58,894
	Annual Revenue		€	177,931	213,653	202,393	210,539	207,501

Comparing the best results from the optimisation, Run 3.12 appears to be the closest to the optimal solution. Just taking into consideration total NPV and annual revenue, Run 3.12 performs better than the other solutions. It is noteworthy that the values for COD removal and the rate of algal biomass are not the best in this solution but can be improved upon, as seen in Run 19.12. This is a result of $O2_{sl}$ and $CO2_{pl}$ both being higher in Run 19.12, although an increase of 261% in $O2_{sl}$ from Run 3.12 to Run 19.12 equates to only a very slight improvement in COD removal. A small increase in $CO2_{pl}$ from Run 3.12 to Run 19.12 provides a corresponding increase in the rate of algal biomass production. The $Pres_s$ and $Pres_p$ values are broadly similar across all runs at around the 41 mol m^{-3} mark. Moving on to the cost functions, NPV_{COD} and NPV_{Algae} reflect the efficiency of COD removal and rate of biomass production with Run 19.12 being the highest. However, considering the total gas pumping flows and their associated costs, Run 3.12 provides the lowest values. It is this balance between process efficiency and expenditure that puts Run 3.12 closest to the optimal – this solution may not be the most productive but the lower investment and operating costs lead to a higher overall NPV.

Demonstrating precise optimality is not the aim of this research – in this thesis, I aim to demonstrate good solutions for a model that can be applied to a real wastewater treatment plant, rather than finding a globally optimal solution to a theoretical problem. With this in mind, the design parameters obtained from Run 3.12 were accepted as adequate for the aims of this research, and entered into the final version of ASAPM v1. This model used as the basis for ASAPM v2, which is explored in greater detail in the next chapter.

5.4 Discussion

5.4.1 Gas phase integration is necessary to make the process profitable

The simulation results obtained from ASAPM v1, and shown in Table 13, indicate that the idea of integration of algal growth with biological wastewater treatment is certainly worthy of further research. However, gas exchange is necessary to make the process profitable. The results outlined in Section 5.3.2 show that a separate

algal pond, which is not connected to biological wastewater treatment, may prove to be quite a burden with respect to operating costs. The model predicts that to provide aeration sufficient for algal growth would be prohibitively expensive. By integrating the gas phases of the two processes, a greater concentration of CO_2 can be delivered to the algal pond; although an increase in CO_2 availability will not necessarily result in an equal increase in the rate of algal growth in practice, a moderate increase in algal growth could certainly be expected.

Without gas exchange, the concentration of carbon dioxide in the algal pond falls below the value expected of dissolved CO_2 at atmospheric pressure (0.6 g m^{-3}); this is due to the use of CO_2 by the algal growth model, $rpAlg_{gro}$, with supply unable to match demand. Using the CO_2 evolved during growth of biomass in the activated sludge process, the dissolved concentration can be increased to around 2 g CO_2 m^{-3} in the algal pond. This increase, from 0.07 g CO_2 m^{-3}, increases the growth rate from approximately 50 to 320 kg algal biomass d^{-1}. However, this model does not at present represent realistic algal growth; algal growth is modelled merely as a consumer of carbon dioxide and a producer of oxygen. It is not anticipated that the values obtained in this first version will be retained in the final version of the model but rather act as an indicator for future patterns.

The transfer of gases from the algal pond to the activated sludge vessel seems to be of lesser importance in this early version of the model. Similarly, growth of biomass in the activated sludge process is modelled as a consumer of oxygen and a producer of carbon dioxide; however, as oxygen is more abundant in the atmosphere, it is easy to provide enough oxygen for the process to proceed unhindered. Looking at the results of optimisation in Table 14, we see the concentration of species $O2_{sl}$ increase from 2.26 to 5.90 g O_2 m^{-3}, with a corresponding increase in COD removal from 94.89 to 95.51%. Although the increase in dissolved oxygen is significant, the rate of COD removal is not – this suggests that the reaction $rsXS_{hyd}$ is much less sensitive to oxygen that its counterpart in the algal pond is to carbon dioxide. Again, it is anticipated that this early model will act only as an indicator for future patterns as the model grows in complexity.

One consideration with the novel concept of gas exchange between activated sludge and algal growth is how best to model the operating costs of this facility – specifically with respect to NPV_{OCa}, which describes the operating cost of aeration. One could argue that exhaust from the vessels would flow directly to atmosphere from the headspace without the need for pumping; however, this would only occur if the headspace were above atmospheric pressure in the first instance. More energy would be then required to maintain this elevated pressure. This balance could be quite complex to calculate within the model, so it was decided to use a flat rate for all pumping flows and include the pumping of exhaust gases instead of increasing the cost of gas inflow.

5.4.2 Summary

These initial results highlight the requirement for an extended model with more accurate kinetic rates and parameters to obtain a model that realistically reflects what could be expected from an existing wastewater treatment plant with an algal pond extension. The use of CO_2-rich gas from the sludge tank may certainly prove to be the factor that makes the production of algal biofuels more cost-effective. Note that Lundquist et al. (2010) calculates how much it would cost to produce a barrel of algal oil, rather than specifying a sale price, and this production cost is more than the value of a standard barrel of fossil oil. However, I have based revenue from algal lipid on the cost of fossil oil because it would be unrealistic to attempt to sell algal oil for a higher price than standard fossil oil. The amount of algal biomass available for sale is based upon the rate of the reaction, $rpAlg_{gro}$. In addition to revenue from algal lipid, I have included in the NPV_{algae} function the ability to claim a subsidy for carbon sequestration, which is based on the trading price of carbon on the open market (Intercontinental Exchange 2011). Although this source of income may be speculative at present, its inclusion provides the model with greater flexibility towards future legislation and incentives with regard to carbon emissions and sequestration.

Like the function for algal revenue, the value of COD treatment is based upon the rate of the reaction $rsXS_{hyd}$; the revenue for wastewater treatment is calculated

from values provided by Lundquist et al. (2010). As the model is built up to greater complexity, the wastewater revenue function will not focus on just one reaction and will be calculated on the disappearance of certain substrates – this will be addressed in Chapter 6. I have assumed that the costs associated with constructing an algal pond will be the same as those for activated sludge as detailed in Alasino et al. (2007), which is focused upon wastewater treatment rather than algal growth. As the market for algal biofuels expands, more accurate cost values may emerge; as I have distinguished between the sludge tank and algal pond in naming my parameters, model values will be easy to update as new data becomes available.

CHAPTER 6 - ACTIVATED SLUDGE ALGAL POND MODEL VERSION 2

6.1 Introduction

Following on from the construction of ASAPM v1 detailed in Chapter 5, the next stage of the modelling process was to extend the activated sludge reactions to include an industry standard activated sludge model. The biological reactions in the liquid phases of the first version of the model were highly simplified but served to demonstrate that integration of activated sludge and algal growth were worthy of further research. For the next version of the integrated model, the industry standard activated sludge model, ASM3 (Gujer et al. 2000), was inserted to improve the reactions in the activated sludge liquid phase. A screenshot of ASAPM v2 is shown in Figure 6-1, below.

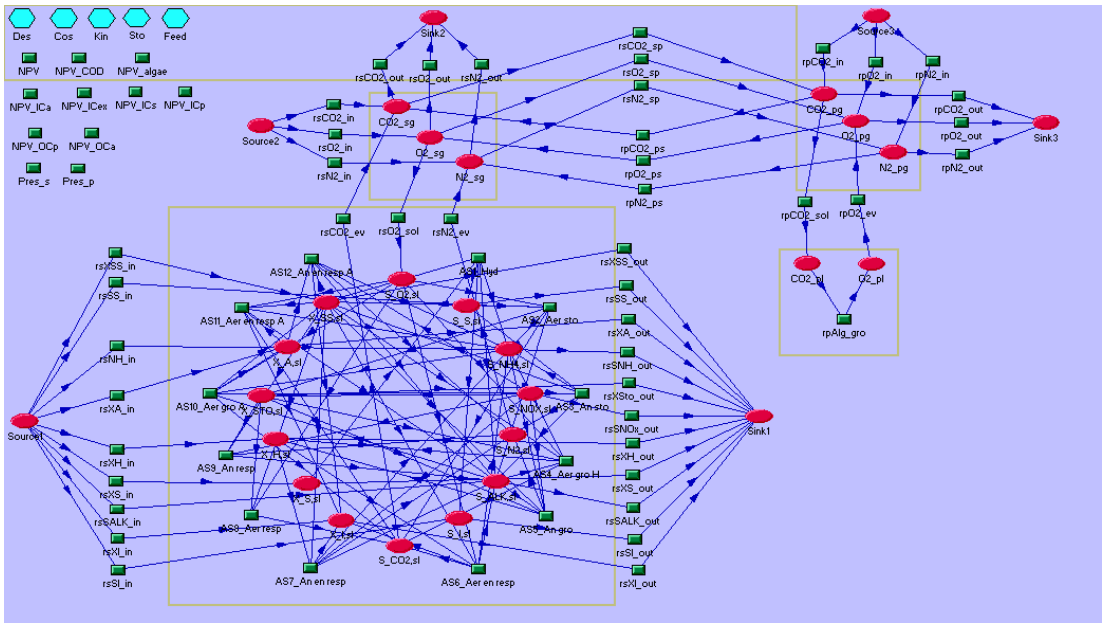

Figure 6-1 Reaction pathway of ASAPM v2

ASM3 is a description of the microbiological transformation processes observed in suspended growth biological wastewater treatment and consists of three main reaction types: hydrolysis, growth of heterotrophic organisms and growth of nitrifying organisms. Hydrolysis is a single reaction in which slowly biodegradable substrates, X_S, are made available to the activated sludge system as readily

biodegradable organic substrates. Eight processes are dedicated to describing the life-cycle of heterotrophic organisms (X_H), which are able to metabolise all degradable organic substrates; these organisms grow under aerobic conditions and some also under anoxic conditions, leading to denitrification. The final three processes describe the life-cycle of nitrifying organisms (X_A) that oxidise ammonium directly to nitrate. Endogenous respiration of both X_H and X_A produces inert particulate organic material (X_I) that is not degraded in activated sludge systems. This inert material is flocculated onto the activated sludge, which is then settled to produce treated wastewater and a thickened sludge that can be further processed.

6.2 The Model

The basic structure of the model remains the same from version 1 to version 2 – the difference being the integration of an industry standard activated sludge model. In this section, process rates, economic functions and parameter values are presented that are new to this version but the full model will not be displayed to avoid repetition of material already presented in Chapter 5. Published material – i.e. ASM3, its parameter values and stoichiometry – will not be presented here but is given in Appendices A-C; additional stoichiometry pertaining to ASAPM v2 is shown in Appendix F.

ASM3 was built into the existing Sentero ASAPM v1 file. Connections to the original activated sludge gas and liquid compartments were replaced with links to the new ASM3 compartment; the redundant activated sludge liquid compartment was then deleted from the model. The removal of the original activated sludge liquid phase meant that the existing economic function for NPV_{COD} no longer applied, as it was based on the rate of the simplified reaction in version 1. The function was updated to measure the reduction in concentration of wastewater components, taking into account the soluble organic compounds that remain untreated in the activated sludge tank while collecting revenue for the treated species. As ASM3 includes the production of N_2, a mass transfer expression was required to describe its evolution from the sludge liquid to the sludge gas phase. New bulk transfer processes were

written as discussed in Chapter 3, and all of these new expressions are shown in Table 15 below.

Table 15 New reactions and pseudo-reactions for ASAPM v2

ρ/*f*	**Process/Function**	**Expression**
rsN2$_{ev}$	Evolution of N_2 from AS tank	$V_{sl}.kLa_s\left(S_{N2,sl} - N2_{sg}.H_{N2}\right)$
In$_z$	Inflow of substrates	$substrate_{feed}.In_{sl}$
Out$_{Sz}$	Outflow of soluble substrates	$S_{substrate}.Out_{sl}$
Out$_{Xz}$	Outflow of particulates	$X_{substrate}.Out_{sl}.alpha$
NPV$_{COD}$	Value of COD treatment	$\Gamma.days_{COD}.r_{COD}.In_{sl}.\Big((SS_{in} + SI_{in} + XI_{in} + XS_{in} + XH_{in}) - \left(S_{I\_sl} + S_{S\_sl}\right)\Big)$

New parameter values required for these expressions are given below (Table 16) and are used in combination with existing parameter values shown in Table 11, Chapter 5. Here, design parameter values for the gas exchange system that were obtained as a result of the optimisation of ASAPM v1 are shown here; these will be used as start-up parameters for version 2 and will be optimised in Section 6.3.3 of this chapter.

Table 16 Additional parameters for ASAPM v2

Parameter	**Description**	**Value**	**Units**
G_{ps}	Gas flow from pond to sludge tank	323.60	$m^3\ d^{-1}$
G_{sp}	Gas flow from sludge tank to pond	1,529.00	$m^3\ d^{-1}$
In_{sg}	Gas flow from air to sludge tank	1,141.00	$m^3\ d^{-1}$
Out_{sg}	Gas flow from sludge tank to air	10.00	$m^3\ d^{-1}$
In_{pg}	Gas flow from air to pond	96.85	$m^3\ d^{-1}$
Out_{pg}	Gas flow from pond to air	1,370.00	$m^3\ d^{-1}$
H_{N2}	Henry's Constant for N_2	0.015	atm-1
In_{sl}	Liquid flow into sludge tank	1000	$m^3\ d^{-1}$
Out_{sl}	Liquid flow from sludge tank	1000	$m^3\ d^{-1}$
alpha	Settling parameter	0.0225	-

Parameter	Description	Value	Units
V_{sl}	Volume of liquid in the sludge tank	450	m^3
Feed Parameters			
SI_{feed}	Concentration of S_I in primary effluent	30.0	g m^{-3}
SS_{feed}	Concentration of S_S in primary effluent	100.0	g m^{-3}
SNH_{feed}	Concentration of S_{NH4} in primary effluent	16.0	g m^{-3}
$SALK_{feed}$	Concentration of S_{ALK} in primary effluent	5.0	g m^{-3}
XI_{feed}	Concentration of X_I in primary effluent	25.0	g m^{-3}
XS_{feed}	Concentration of X_S in primary effluent	75.0	g m^{-3}
XH_{feed}	Concentration of X_H in primary effluent	30.0	g m^{-3}
XA_{feed}	Concentration of X_A in primary effluent	0.1	g m^{-3}
XSS_{feed}	Concentration of X_{SS} in primary effluent	125.0	g m^{-3}

Following completion of the model, everything other than ASM3 and its bulk transfer processes were removed to enable the independent verification of ASM3 against the literature – this is discussed in the next section.

6.3 Results

6.3.1 ASM3 and model verification

ASM3 was built in a stepwise manner into the ASAPM v1 file, before isolating the activated sludge liquid phase in order to verify the simulation results. The results of the simulation were compared to the results given by Balku and Berber (2006); however, in some ways the results are difficult to compare due to differences in the aeration sequence used to feed the vessel. Balku and Berber employ an alternating aeration sequence of 0.9 h non-aerated followed by a 1.8 h aerated period, reaching a final dissolved oxygen concentration of 2.6 g m^{-3}; I adopted a fixed S_O concentration of 2.6 g m^{-3} in an attempt to mimic the aeration conditions of Balku and Berber's model as closely as possible. The HRT and SRT for this simulation were 0.45 and 20 d respectively, and the settling parameter, *alpha*, was calculated accordingly. The results of the simulation are shown in Table 17, below.

Table 17 Simulated concentrations of ASM3 components

ASM3 components ($g\ m^{-3}$)	Primary effluent	Aeration tank after 20 days	
		Balku and Berber	My model
S_{O2}	0.0	2.6	2.6
S_I	30.0	30.0	30.0
S_S	100.0	0.1	0.2
S_{NH4}	16.0	0.3	0.4
S_{N2}	0.0	-	2.7
S_{NOX}	0.0	6.3	18.7
S_{ALK}	5.0	3.4	2.2
X_I	25.0	1,390.7	1,156.6
X_S	75.0	57.7	57.6
X_H	30.0	1,414.8	1,037.8
X_{STO}	0.0	124.7	114.4
X_A	0.1	68.7	54.7
X_{SS}	125.0	3,312.9	7,101.3

The aim of Balku and Berber's study was to produce a model of a completely stirred alternating aerobic-anoxic process, in which carbon removal, nitrification and denitrification proceeds in a single vessel. In contrast, the aim of this research is less about denitrification and the production of N_2 but more concerned with aerobic reactions and the production of CO_2. However, as no other sample output detailing all ASM3 components was found in the literature, it was necessary to compare these results to a study with slightly different aims.

Several processes in the activated sludge model obtain energy from denitrification rather than aerobic respiration, and these processes are inhibited by S_O. As Balku and Berber's model employs a sequence of aerated/non-aerated periods, the non-aerated periods would allow the anoxic processes to proceed fully and efficiently. When compared to this system, where dissolved oxygen was present at all times, we can see the difference in the dissolved nitrate concentration, S_{NOX}. Due to the constant presence of dissolved oxygen, it was not possible for this model to

produce a dissolved nitrate concentration of less than 18.7 g S_{NOX} m^{-3}, compared with 6.3 g S_{NOX} m^{-3} in Balku and Berber's model. This incomplete denitrification will have a knock-on effect with regard to the production of other components, namely: heterotrophic organisms (X_H) and inert particulate organic compounds (X_I). The value for cell internal storage product of heterotrophic organisms (X_{STO}) is also slightly lowered since a fraction of this is produced under anoxic conditions, and the elevated concentration of NO_3^- ions can be seen to have an effect on pH by the slight decrease in the value of S_{ALK}.

The aeration sequence employed by Balku and Berber will also have an effect on the aerobic reactions of ASM3, although these differences are less marked upon comparison of both model outputs. For example, the concentration of S_S and S_{NH4} are slightly higher than Balku and Berber's; this can be explained by the probability that, during aerated periods, the concentration of S_O will be much higher than the fixed value of 2.6 g O_2 m^{-3}. This elevated dissolved oxygen concentration will provide the system with the energy for aerobic reactions to go further towards completion – thereby removing more S_S and S_{NH4} and producing more X_H and X_A.

Overall, the differences were either small enough to be deemed insignificant, or can be explained by the novel aeration sequence used by Balku and Berber. The values of slowly biodegradable substrates (X_S) are equal, validating the hydrolysis reaction from which other reactions originate. Another notable difference is that between the concentrations of X_{SS}, with my simulated value being significantly higher. This is due to Balku and Berber's model having an inbuilt function to limit the concentration of particulates to 3,000 g m^{-3}, whereas my model has no such restriction.

The aim of the verification was to ensure that no structural or other mistake had been made in the modelling of ASM3. As a definitive set of output values is unavailable in the literature, it is very difficult to guarantee the absolute accuracy of the values obtained here. However, the similarities are enough that we can infer no major errors have been built into the model, and the model is robust enough to continue into extended versions. As stated previously, it is the intention that the

simplified activated sludge liquid compartment of ASAPM v1 will be replaced with the new ASM3 compartment; improvements in the detail of the model will produce a more realistic outcome and give the financial functions more credibility.

6.3.2 Integrated model with ASM3

Once the ASM3 model had been verified, the full integrated model was reopened and links from the simplified activated sludge liquid phase replaced with links to the new ASM3 compartment; the redundant liquid phase was deleted and this file renamed ASAPM v2. One of these new links included dissolved carbon dioxide (S_{CO2_sl}), which was added as a product of aerobic reactions. To reflect the change in the activated sludge liquid phase, the NPV_{COD} function was updated to reflect the concentration of COD (g m^{-3}) that has been treated in the activated sludge process. The model contained design parameters carried over from v1, in addition to new parameters added for ASM3. A simulation of this model was run to assess the suitability of v1 parameters in v2 with ASM3 and the results can be seen in Table 18, below.

Table 18 Simulation results from ASAPM v2 using design parameters from v1

Design Parameter (m^3 d^{-1})			
G_{ps}			323.60
G_{sp}			1,529.00
In_{pg}			96.85
In_{sg}			1,141.00
Out_{pg}			1,370.00
Out_{sg}			10.00
ASM3 Component (g m^{-3})			
S_{O2_sl}	4.2 x10^{-3}	X_{I_sl}	1,143.8
S_{I_sl}	30.0	X_{S_sl}	56.2
S_{S_sl}	84.0	X_{H_sl}	1,969.0
S_{NH4_sl}	18.3	X_{STO_sl}	1,958.8
S_{N2_sl}	12.5	X_{A_sl}	4.7
S_{NOX_sl}	0.0	X_{SS_sl}	6,392.8
S_{ALK_sl}	5.2	S_{CO2_sl}	17.3

Steady State Variables			
$CO2_{pl}$ (g m^{-3})			0.04
Rate of Algal Biomass Production (kg d^{-1})			31.26
$Pres_s$ (mol m^{-3})			33.81
$Pres_p$ (mol m^{-3})			33.01
NPV (€)			
Total	-350,480	Annual	-28,124
COD	816,366	Algae	219,405
ICa	-1,032	ICex	-310,426
ICp	-738,220	ICs	-256,519
OCa	-55,310	OCp	-24,745

The results using the design parameters carried over from v1 do not suit the new extended model with ASM3 at all – the ASM3 components in the sludge liquid are not in agreement with the isolated model, dissolved CO_2 in the pond is very low, the pressure constraint is below the atmospheric level of 41 mol m^{-3}, and the overall process is running at a loss. The starting concentration of dissolved oxygen in the sludge liquid was 8.9 g m^{-3}, the concentration of O_2 in water calculated using Henry's Law, and has reduced to almost nothing. It is postulated that the reactions in the activated sludge cannot proceed at such a low concentration of S_{O2_sl}, giving poor results for the other ASM3 components and, in turn, the revenue for wastewater treatment, NPV_{COD}. However, the concentration of dissolved carbon dioxide in the sludge liquid (S_{CO2_sl}) is high at 17.3 g m^{-3} but the design parameters do not facilitate its transfer to the algal pond, where the concentration of dissolved CO_2 remains low. This has the obvious impact on the rate of algal growth and the cost function NPV_{algae}.

One important parameter in the provision of oxygen to the liquid phase is the oxygen transfer coefficient, $k_L a$, and is determined by considering the uptake of oxygen by microorganisms. Normally, on a wastewater treatment plant, the $k_L a$ is ascertained experimentally and depends upon the quality of the water to be treated. For example, if the water quality is poor and an excess of oxygen is required to fully treat the influent, the $k_L a$ value would be higher than if the water quality were already quite good. This would be determined by the concentration of suspended solids and biodegradable organic compounds – sufficient oxygen would be required for nitrification and as an energy source for aerobic processes for conversion to inert material. Until now, the $k_L a$ value has been set to 120 d^{-1}; a typical maximum operating limit is considered to be 360 d^{-1} (Alasino et al. 2007). With this in mind, the $k_L a$ was increased to 240 d^{-1}, although this alone had limited effect on the results using the design parameters from v1. It was clear that optimisation of the model using Sentero's parameter tuning facility was required to determine the correct gas flows for v2.

6.3.3 Optimisation

As demonstrated in the previous section, successful transfer of design parameters from one model to the next is not guaranteed. In this case however, transfer was not to be expected considering the vast change in reactions within the sludge liquid phase from an over-simplified model to an industry standard one. The oxygen demand of the new sludge liquid model is great and the existing gas transfer values insufficient to meet demand; microorganisms in the sludge liquid use oxygen as rapidly as it is supplied and it is important that the concentration should be maintained at 1-3 g O_2 m^{-3} (Tchobanoglous et al. 2004). Two parameter tuning analyses of ASAPM v2 were carried out according to the description in Section 5.3.2 with Total NPV, $Pres_s$ and $Pres_p$ as the objective functions. In addition to these targets, the first optimisation included dissolved oxygen in the sludge liquid, S_{O2_sl} as an objective function, with a target concentration of 3 g m^{-3}. The second optimisation included the product of hydrolysis, S_{S_sl}, with a target concentration of 0.1 g m^{-3}. An example of the proximate tuning analysis can be seen in Figure 6-2,

below. Many of the results from the optimisation runs were quite similar and the best are shown in Table 19.

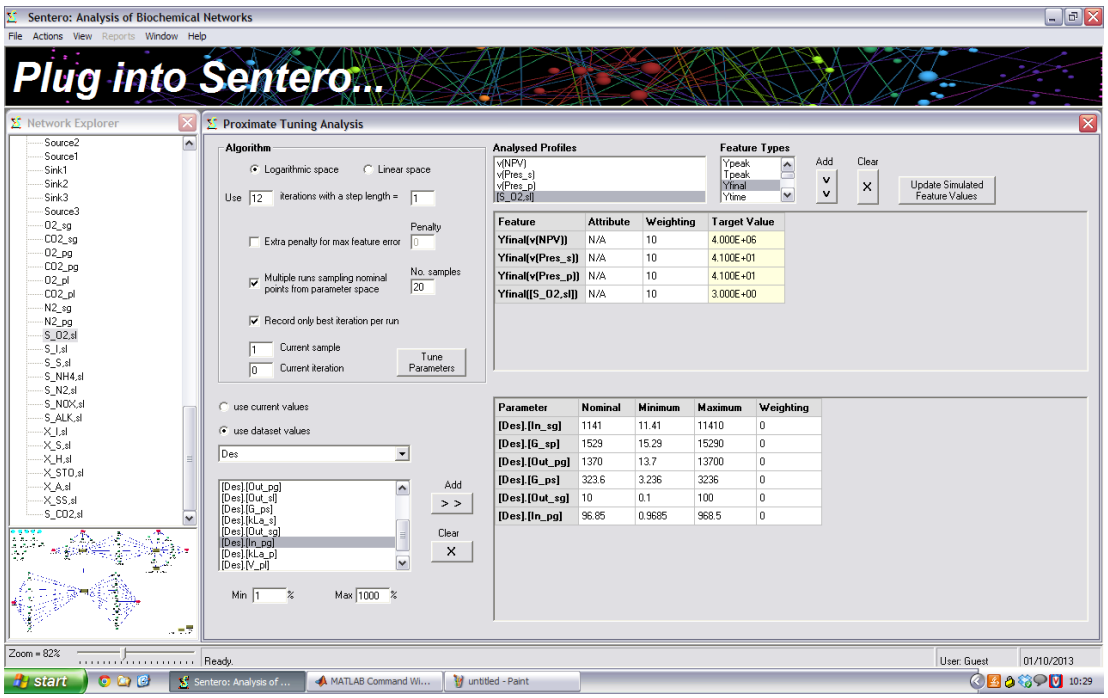

Figure 6-2 Screen shot of Proximate Tuning Analysis

Table 19 Results of parameter tuning analysis

	Parameter/Variable/Function	Units	Run 1.1	Run 16.12	Run 20.11
Design Parameters	G_{ps}	$m^3\ d^{-1}$	647.60	32.36	3.97
	G_{sp}	$m^3\ d^{-1}$	7,709.00	10,950.00	6,686.00
	In_{pg}	$m^3\ d^{-1}$	286.50	9.69	0.97
	In_{sg}	$m^3\ d^{-1}$	7,478.00	11,410.00	7,100.00
	Out_{pg}	$m^3\ d^{-1}$	7,428.00	11,100.00	6,846.00
	Out_{sg}	$m^3\ d^{-1}$	22.80	1.00	0.41
	Total gas pumping flow	$m^3\ d^{-1}$	**23,571.90**	**33,503.05**	**20,637.35**
Objective Function	Sludge-dissolved O_2 (S_{O2_sl})	$g\ m^{-3}$	1.4	-	1.3
	Organic substrates (S_{S_sl})	$g\ m^{-3}$	-	0.2	-
	$Pres_s$	$mol\ m^{-3}$	41.27	41.40	41.48
	$Pres_p$	$mol\ m^{-3}$	41.09	41.02	40.78
	Total NPV	€	**1,065,001**	**986,300**	**1,251,000**

Of the results presented here, it was decided to take Run 1.1 as the optimum. Although Run 1.1 does not provide the greatest NPV, it does provide the closest result with respect to $Pres_s$ and $Pres_p$. Of the three sets of results, Run 6.12 provides the lowest NPV because of the high total gas pumping requirement. Although Run 20.11 has the lowest total gas pumping flow and the highest NPV, the balance is not quite right to provide the correct mole values in the headspaces – therefore illustrating that optimisation is a balancing act between profitability and physical restrictions. The value of sludge-dissolved oxygen in Run 20.11 is also lower than in Run 1.1, which would lead to a reduction in the rate of all aerobic reactions in the activated sludge. A full steady-state simulation was run with the design parameters of Run 1.1 to assess the effect of the increased concentration of sludge-dissolved oxygen on the ASM3 components (see Table 20).

Table 20 Simulation results of ASAPM v2 with optimisation Run 1.1

ASM3 Component (g m^{-3})			
S_{O2_sl}	1.4	X_{I_sl}	1,943.1
S_{I_sl}	30.0	X_{S_sl}	57.5
S_{S_sl}	0.2	X_{H_sl}	1,064.4
S_{NH4_sl}	0.5	X_{STO_sl}	116.3
S_{N2_sl}	14.2	X_{A_sl}	58.7
S_{NOX_sl}	16.7	X_{SS_sl}	10,769.2
S_{ALK_sl}	2.1	S_{CO2_sl}	28.4
Algal Pond			
Pond-dissolved CO_2 (g m^{-3})			0.71
Rate of Algal Biomass Production (kg d^{-1})			234.80
NPV (€)			
Total	1,065,001	Annual	85,460
COD	1,284,836	Algae	1,648,153
ICa	-1,133	ICex	-555,734
ICp	-738,220	ICs	-256,519
OCa	-291,638	OCp	-24,745

The final concentrations of ASM3 components in the optimised model are now very similar to those obtained for the isolated ASM3 model and are, therefore, in broad agreement with Balku and Berber's alternating aerobic-anoxic process. The differences between the integrated model, ASAPM v2, and the results from the literature are again explained by the reasons set out in Section 6.3.1 – i.e. the absence of an anoxic period in the model leads to elevated concentrations of dissolved nitrate and reduced concentrations of heterotrophic organisms and their internal storage product (X_{H_sl} and X_{STO_sl}), and nitrifying organisms (X_{A_sl}). However, the production of these particulate substrates and inert material (X_{I_sl}) has improved slightly, which may be due to the level of dissolved oxygen in the sludge liquid; the starting concentration in the integrated model was 8.9 g O_2 m^{-3}, increasing the rate of the aerobic reactions in the initial stages of the simulation, before reducing to a steady-state value of 1.4 g O_2 m^{-3}. Remembering that the isolated ASM3 model had a fixed value of 2.6 g O_2 m^{-3}, there are bound to be slight differences in the reaction rates and substrate concentrations between the two models.

Following optimisation, the model has now found a profitable outcome for the integrated activated sludge and algal pond process, with a total NPV of €1,065,001. This provides an annual income of €85,460 and the investment and operating costs are almost covered by the revenue from the sale of algal biomass. This is in sharp contrast to the non-optimised model that used design parameters from ASAPM v1, which ran at an overall loss of €350,480. Clearly, the investment costs for the activated sludge tank and algal pond are the same, as is the operating cost for the algal pond, because these parameters are not affected by the optimisation; conversely, the investment costs for the gas exchange and aeration systems, and the operating cost of these, are noticeably higher in the optimised version. However, this extra expense is justified by the improvement in levels of necessary dissolved gases in the vessels, leading to a great improvement in wastewater treatment, algal growth and their associated revenues.

6.4 Discussion

6.4.1 Production of model using recognised kinetic expressions

The production of a model that includes an industry-standard description of biological wastewater treatment marks an important stage in the progress of this research project. While the simplified model, ASAPM v1, was important in demonstrating that evolved carbon dioxide from the wastewater treatment process could prove useful for algal growth in a connected vessel, it was impossible to know this for certain until a realistic model of the activated sludge process was built in. By including the evolution of carbon dioxide from the aerobic reactions of microorganisms in the activated sludge, we are able to measure, transfer and sequester this resource in the form of biomass for biofuels.

The activated sludge model was built using kinetic rate expressions and values from ASM3 (Gujer et al. 2000), stoichiometry from Hauduc et al. (2010) and simulation results from Balku and Berber (2006); unfortunately, the Scientific and Technical Report (Henze et al. 2000) that features the activated sludge models did not include all components with which to build and compare a model, and was missing stoichiometric expressions and parameters, and a sample output. It was this lack of joined-up information that formed an obstacle to verification and meant that it was necessary to verify using a model with a slightly different focus to the results. However, as the majority of the simulated results agreed, and those that didn't can be explained, it was reasonable to assume that the ASM3 part of ASAPM v2 was functioning as intended by the authors. Indeed, it is accepted that the ASM3 results are very unlikely to be the same as values found in the literature due to the omission of pertinent data, differences in software, design parameters and project focus.

The results provided in Table 18 demonstrate how important dissolved oxygen is for the reactions in the activated sludge. When the oxygen content is low, the microorganisms cannot function; while hydrolysis, which is not oxygen-dependent, can go ahead, the product of hydrolysis, S_S, cannot be converted to inert material by aerobic processes and the chemical oxygen demand of the sludge remains high. It

has been demonstrated how this can be overcome by using a model that includes process flows in addition to biological reactions – employing the modelling software's parameter tuning algorithm provides design parameters that not only suit the activated sludge processes but also the plant's physical restraints. By optimising the model, a solution can be found that takes advantage of the oxygen-rich gas evolved in the algal pond by transferring it to the sludge tank; the gas flow in from the atmosphere is also tuned to the oxygen requirement of the microorganisms in the activated sludge.

The data given in Tables 18 and 20 shows that transfer of CO_2-rich gas from the activated sludge to the algal pond is still relevant and necessary for the growth of algae. By applying a set of design parameters that do not suit the model well, it can be seen how the concentration of dissolved carbon dioxide can fall quite sharply – thereby reducing production of algae and revenue from the sale of biomass. By employing design parameters yielded from the use of NPV as an objective function, the dissolved CO_2 content of the algal pond has increased by default, as the parameter tuning algorithm recognises this as a way to increased revenue. However, the algal growth reaction in the pond liquid phase is still highly simplified and the results from this part of the model remain uncertain. This uncertainty in addressed in the next two chapters.

6.4.2 Summary

Looking back to the results obtained in Chapter 5, the predicted NPV of the two model versions can be compared. In ASAPM v1, the Total NPV was €2,662,539; in this model the Total NPV has been reduced to €1,065,001. This difference is mainly due to a reduction in revenue from algae arising from a reduction in the concentration of pond-dissolved carbon dioxide. This indicates that the simplified activated sludge reaction produced an excess of CO_2 compared to the more realistic ASM3 reactions and, therefore, too much carbon dioxide was then transferred to the algal pond. However, when the revenue from treatment of wastewater are compared (NPV_{COD}), the values are much closer: €1,830,079 in v1 and €1,284,836 in v2. This suggests that the simplified model was quite accurate in predicting COD

removal, although it was somewhat lacking in its requirement for oxygen – this became apparent upon using design parameters meant for v1 in v2. This hurdle was overcome by setting dissolved oxygen as one of the objective functions in the parameter tuning analysis to increase its concentration in the sludge liquid.

This extension of the integrated activated sludge algal pond model is a step on the path towards producing a model relevant to the wastewater treatment industry – the next step being extension of the algal pond with process rate expressions that reflect the growth of algae on wastewater nutrients. The first version of the model, ASAPM v1, was intended to act as an indicator for future patterns and predicted that exhaust gases from activated sludge would be useful in growing algae in a connected pond. With this second iteration of the model we can see that this is still the case, with the exchange of gases from the sludge tank to the algal pond being one of the dominant flows. As discussed at the end of Chapter 5, the transfer of gas from the pond to the sludge tank is of lesser importance and this effect is again observed in this updated version of the model. It may or may not be the case that this flow becomes more significant as the algal growth model is extended. The extension of ASAPM v2 to a version that includes liquid integration and experimentally derived algal growth models is discussed in the following chapters.

CHAPTER 7 - GROWTH KINETICS OF *Chlorella sp.* UNDER NITROGEN AND CARBON DIOXIDE LIMITATION

7.1 Introduction

Laboratory experiments were required to aid in the determination of certain model parameters and were designed to reflect not only the resources available at a typical wastewater treatment plant but also those detailed in the Activated Sludge Model 3. The growth of algae is dependent upon the provision of nutrients and a suitable environment; factors that may be monitored experimentally include nitrogen, phosphorus and sodium chloride concentrations, and levels of dissolved gases within the culture. As ASM3 tracks the consumption of ammonium and nitrates, data on how these nutrients could be used by algae growing in treated wastewater was deemed to be of the greatest interest. Since it is the aim of this research to use carbon dioxide generated during the activated sludge process to feed the algae, experimentation on the utilisation of CO_2 by algae was also crucial.

The growth of the algal culture can be measured over a number of days and the rate of growth plotted to determine the Monod constant, K_S, and the maximum growth rate, μ_{max}. These parameter values can then be included in the process rate expression for algal growth in the computational model. The growth rate, μ, can be derived by differentiation, which can then be used in a double-reciprocal (Lineweaver-Burk) plot to find μ_{max} and K_S. To illustrate:

$$\frac{dx}{dt} = \mu t \qquad \textbf{Equation 7-1}$$

and

$$x_t = x_0 e^{\mu t} \qquad \textbf{Equation 7-2}$$

As growth is measured by optical density over time, the optical density values can be substituted into Equation 7-2 and rearranged to find the specific growth rate, μ.

$$OD_2 = OD_1 e^{\mu(t2-t1)}$$

$$\frac{OD_2}{OD_1} = e^{\mu(t2-t1)}$$

$$ln\left(\frac{OD_2}{OD_1}\right) = \mu(t2 - t1)$$

$$ln\left(\frac{OD_2}{OD_1}\right) \times \frac{1}{(t2-t1)} = \mu \qquad \textbf{Equation 7-3}$$

Taking reciprocals of both μ and substrate concentration, S, the resultant plot produces a trendline from which the half-saturation coefficient, K_S, and maximum specific growth rate, μ_{max}, can be derived.

Monod equation: $$\mu = \mu_{max}\frac{S}{K_S+S} \qquad \textbf{Equation 7-4}$$

Taking reciprocals: $$\frac{1}{\mu} = \frac{1}{\mu_{max}}\left(\frac{K_S+S}{S}\right)$$

$$\frac{1}{\mu} = \frac{K_S}{\mu_{max}}\frac{1}{S} + \frac{1}{\mu_{max}} \qquad \textbf{Equation 7-5}$$

Equation 7-5 is an expression in the form of *y = mx + c*, so Monod parameters can be calculated as follows:

$$c = \frac{1}{\mu_{max}} \qquad \therefore \quad \mu_{max} = c^{-1}$$

$$m = \frac{K_S}{\mu_{max}} \qquad \therefore \quad K_S = \mu_{max} \times m$$

Experimentally derived parameters are used as the foundation for rate expressions of biological processes within a mathematical model. Hill type kinetics are frequently used for the fitted rate equations and a co-operative exponent, n, which is greater than unity, is used to give a sigmoidal or switch-like dependence for the influence of substrate on growth rate. In fact, these results often seem to follow a sigmoid, and such Hill type kinetics for uptake of nitrogen containing species have been previously used in the pioneering modelling work of Flynn et al. (1997).

In order to gather the required data, numerous algal cultures should be grown in media containing different concentrations of the substrate of interest – in this case, nitrate and ammonium. The concentrations of these compounds in wastewater were considered prior to designing experiments using values around the typical

nitrogen contents of primary and secondary effluents. In the literature (Gujer et al. 2000; Balku and Berber 2006), a typical initial ammonium concentration is 16.0 g N m^{-3}, reducing to 0.3 g N m^{-3} following treatment; nitrate is typically not present in primary effluent but present in secondary effluent at approximately 6.3 g N m^{-3}, depending on the design of wastewater treatment plant. Experiments were designed to explore algal growth around these concentrations, with nitrogen content being equal in both nitrate and ammonium experiments, to enable easier comparisons. This is illustrated in the table below.

Table 21 Concentrations of nitrogen in experimental algal cultures

$NaNO_3$ (mg L^{-1})	**$NaNO_3$ (mM)**	**NO_3-N (mg N L^{-1})**	**NO_3-N (mM N)**		**NH_4Cl (mg L^{-1})**	**NH_4Cl (mM)**	**NH_4-N (mg N L^{-1})**	**NH_4-N (mM N)**
0.00	0.00	0.00	0.00		0.00	0.00	0.00	0.00
5.10	0.06	0.84	0.06		3.15	0.06	0.82	0.06
10.2	0.12	1.68	0.12		6.29	0.12	1.65	0.12
20.4	0.24	3.36	0.24		12.6	0.24	3.29	0.24
51.0	0.60	8.40	0.60		31.5	0.59	8.23	0.59
102	1.20	16.8	1.20		62.9	1.18	16.5	1.18
204	2.40	33.6	2.40		126	2.35	32.90	2.35

Triplicate cultures of each concentration were prepared in order to verify density measurements made by spectroscopy; the standard error of each dataset was determined.

As explained in Chapter 4, the microalga used in this study was an unidentified species of *Chlorella*, isolated from a freshwater pond in Weston Park, Sheffield. The organism was cultured in the laboratory by Jasem Almohsen (laboratory of Dr D J Gilmour, Department of Molecular Biology and Biotechnology, University of Sheffield) and had been found to grow well in media with nitrate as the nitrogen source (3N-BBM+V). This species, therefore, fits well with growth in treated wastewater as ammonium is converted to nitrate during the activated sludge

process. However, experiments were also designed using NH_4Cl with the intention to model growth on residual ammonium in the secondary effluent.

7.2 Results

7.2.1 Effect of nitrate concentration on the growth of cells

The strategy followed had the intention to establish the relationship between the growth of *Chlorella sp*. and the concentration of nitrate in the growth medium. In order to assess this relationship, the cultures were sampled at intervals for a total of 35 days and both the growth rate and nitrate-nitrogen concentration were evaluated by measurement of the optical density of each sample at wavelengths of 600 and 232 nm respectively. It was anticipated that measurements continued over a protracted period may give some indication as to whether nitrate-nitrogen was the limiting factor in sustained growth, or if other nutrients played a more significant role in extended growth. The mean optical density of the triplicate cultures (cultures A-C) was calculated and the values plotted against time (days); the mean experimental data can be seen in Table 22 (full raw data can be seen in Appendix H).

Table 22 Mean optical density of triplicate cultures of *Chlorella sp*. grown with different concentrations of sodium nitrate

ID*	Mean OD_{600} at day:											
	3	**5**	**7**	**10**	**12**	**14**	**18**	**20**	**24**	**26**	**28**	**35**
0	0.034	0.044	0.056	0.073	0.077	0.096	0.091	0.090	0.086	0.089	0.082	0.089
5	0.040	0.071	0.094	0.128	0.130	0.165	0.173	0.184	0.208	0.233	0.237	0.268
10	0.045	0.087	0.132	0.168	0.185	0.234	0.257	0.291	0.340	0.371	0.391	0.454
20	0.042	0.078	0.124	0.191	0.217	0.275	0.294	0.327	0.374	0.411	0.430	0.484
50	0.052	0.092	0.148	0.256	0.319	0.402	0.478	0.537	0.610	0.663	0.697	0.798
100	0.040	0.070	0.112	0.218	0.269	0.345	0.444	0.513	0.654	0.752	0.818	1.036
200	0.052	0.110	0.159	0.362	0.465	0.561	0.672	0.811	1.040	1.226	1.381	1.699

* ID column shows mg $NaNO_3$ L^{-1}

The graph shown in Figure 7-1 illustrates that the cultures of *Chlorella sp*. began to grow at a rate seemingly independent of nitrate concentration, i.e. all cultures

followed roughly the same growth rate up to an age of 7 days (with the exception of the culture grown in 0 mg $NaNO_3$ L^{-1} medium). By day 10 the culture densities were spread out according to the initial concentration of sodium nitrate. From this point, the cultures containing $NaNO_3$ at a concentration of 50 mg/L and above grew more rapidly that those with less sodium nitrate. By day 14, the separation was much more pronounced, with the culture containing the most $NaNO_3$ being the fastest-growing. This trend continued until the end of the experiment, when the growth of cultures containing less than 50 mg/L $NaNO_3$ had levelled off.

The results obtained followed the general pattern that was expected from such an experiment – that sustained growth of an algal culture was dependent upon provision of nitrogen within the growth medium. It was, however, not expected that the culture with no, or very low, concentrations of nitrate should grow at all; this may suggest that excess nitrogen is stored within the cell, which enabled recovery from the lag-phase and growth to continue thereafter. An alternative source of nitrogen may have originated from the lag-phase itself, where decomposition of dead cells released available nitrogen into the medium for uptake by surviving algal cells. However, the data implies that a minimum of 50 mg/L of nitrate is required for sustained growth over several days.

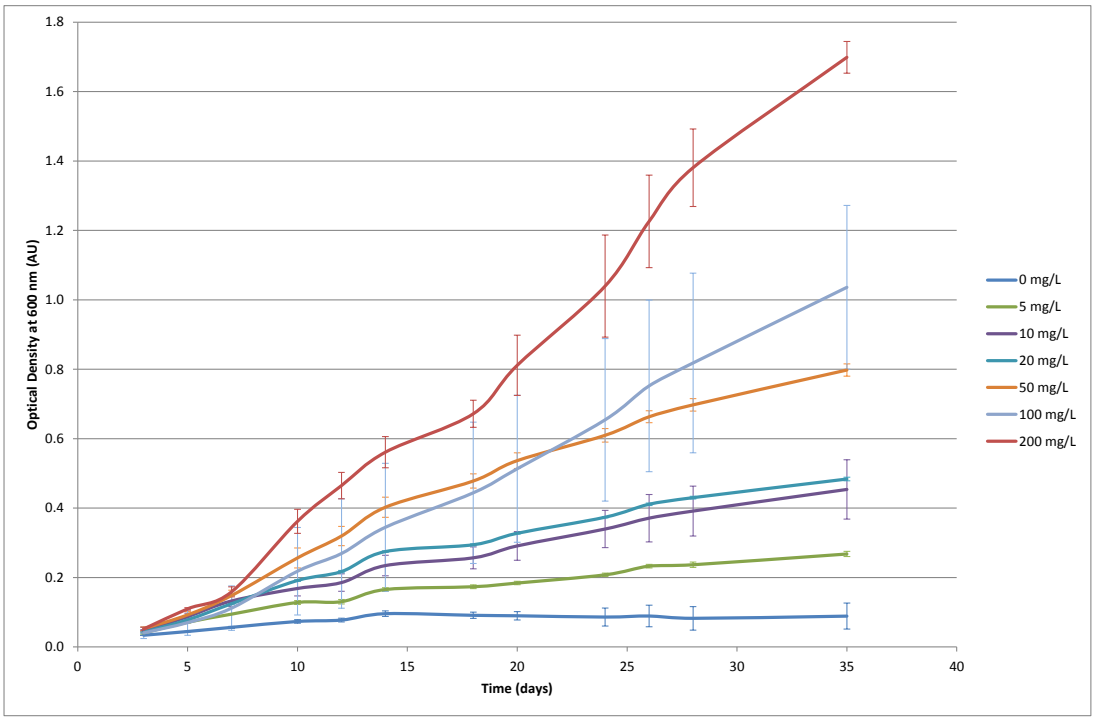

Figure 7-1 Growth of *Chlorella sp*. with different concentrations of $NaNO_3$ (bars represent standard error)

The standard error of the triplicate measurements were calculated and are illustrated in Figure 7-1. It should be noted that the standard error in the measurements for the cultures grown in 100 mg $NaNO_3$ L^{-1} is larger than the errors in the other concentrations. During the experiment, it was observed that the culture 100-A did not grow at the same rate as cultures 100-B and 100-C and it was assumed that its growth had been inhibited by residual detergent in the flask. After 18 days, culture 100-A did show signs of growth and for the remainder of the experiment made a good recovery. However, measurements for culture 100-A will not be included in the calculation of the Monod parameters as this culture did not exhibit a typical growth pattern.

These experimental data can be used to find parameter values for the model with respect to nitrate, which are included in the process rate expression for the growth of algae. Two ways of finding the growth parameters on nitrate, which give very different equations, are presented below. In the first instance, the growth rate information was adjusted to represent the fact that there is residual growth, even without any nitrate in the media. The second method adopted is far more satisfactory since it employs the additional measurements of nitrate in the media

and is, therefore, able to use more data points to give a much better consensus rate equation that takes into account the actual nitrate level that the cells experience. The results show that nutrient release and re-use by microalgal cells is a very important factor to take into consideration when investigation the kinetics of algal growth.

For the first method of characterising the growth kinetics on nitrate, the parameter values were found via a double-reciprocal plot of growth rate vs. substrate concentration, as discussed in Section 7.1. Remembering Equation 7-3, growth, μ, is calculated directly from the experimental data and, in this case, uses the mean measurements from day 3 to day 12. As seen in Figure 7-1, there is some residual growth in nitrate-free medium and, in order to correct for this, growth rates were normalised by subtracting the growth seen for zero initial nitrate, [S] = 0 (see Table 23). This normalised growth rate, Nμ, was used in the Lineweaver-Burk plot (Figure 7-2) to determine μ_{max} and K_S.

Table 23 Growth rates of *Chlorella sp*. at different values of [S]

$NaNO_3$ Concentration ([S], mg/L)	**Experimental Growth Rate (μ, d^{-1})**	**Normalised Growth Rate (Nμ, d^{-1})**	**1/[S]**	**1/Nμ**
0.000	0.092	0.000	0.000	0.000
5.083	0.130	0.038	0.197	26.370
10.167	0.156	0.064	0.098	15.612
20.333	0.182	0.089	0.049	11.212
50.833	0.201	0.109	0.020	9.212
101.667	0.223	0.130	0.010	7.675
203.333	0.244	0.152	0.005	6.594

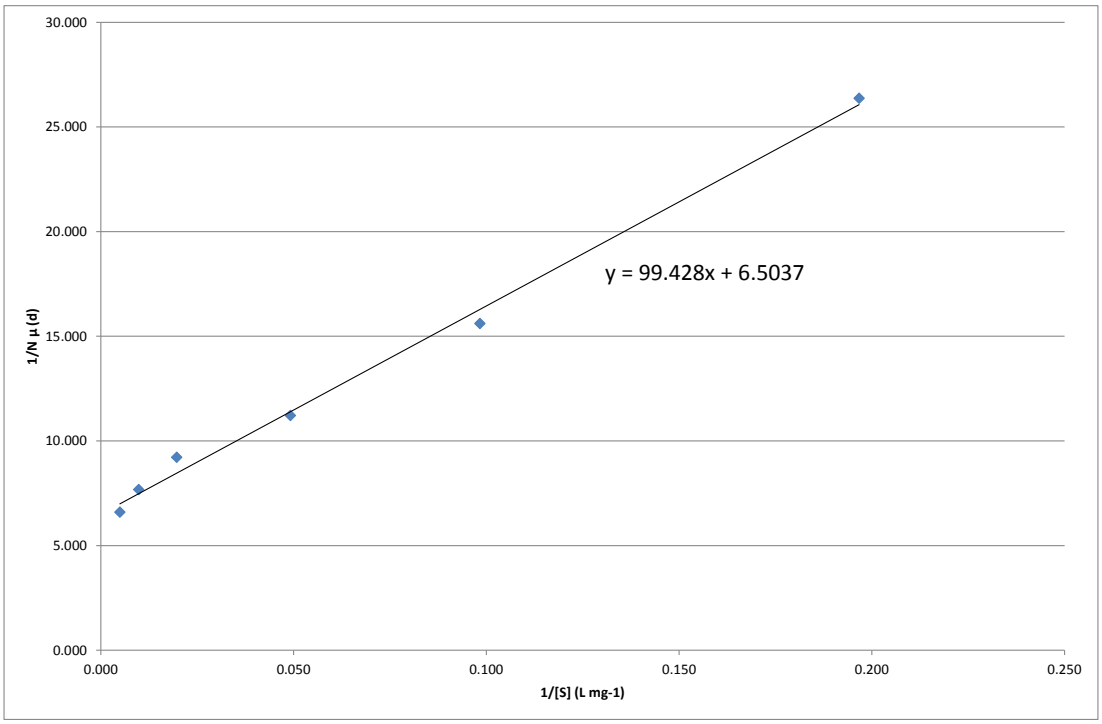

Figure 7-2 Double-reciprocal plot of *Chlorella sp*. growth data with $NaNO_3$

Considering Equation 7-5, the intercept is equal to μ_{max}^{-1}:

$$\mu_{NO3} = c^{-1} = \frac{1}{6.5037\ d} = 0.154\ d^{-1}$$

This value, in combination the gradient, can then be used to calculate the Monod constant for nitrate dependency, K_{NO3}.

$$K_{NO3} = \mu_{max} \times m = 0.154\ d^{-1} \times 99.428\ d\ mg\ L^{-1} = 15.288\ mg\ L^{-1}$$

Using the Monod expression, Equation 7-4, the calculated values of μ_{NO3} and K_{NO3} can be employed to find a predicted growth rate for all values of [S].

$$\mu = 0.154\ \frac{[S]}{15.288 + [S]}$$

Figure 7-3, below, compares the normalised experimental growth rate and that predicted by the equation above. The agreement is good as one would expect, given the good straight line fit apparent in Figure 7-2.

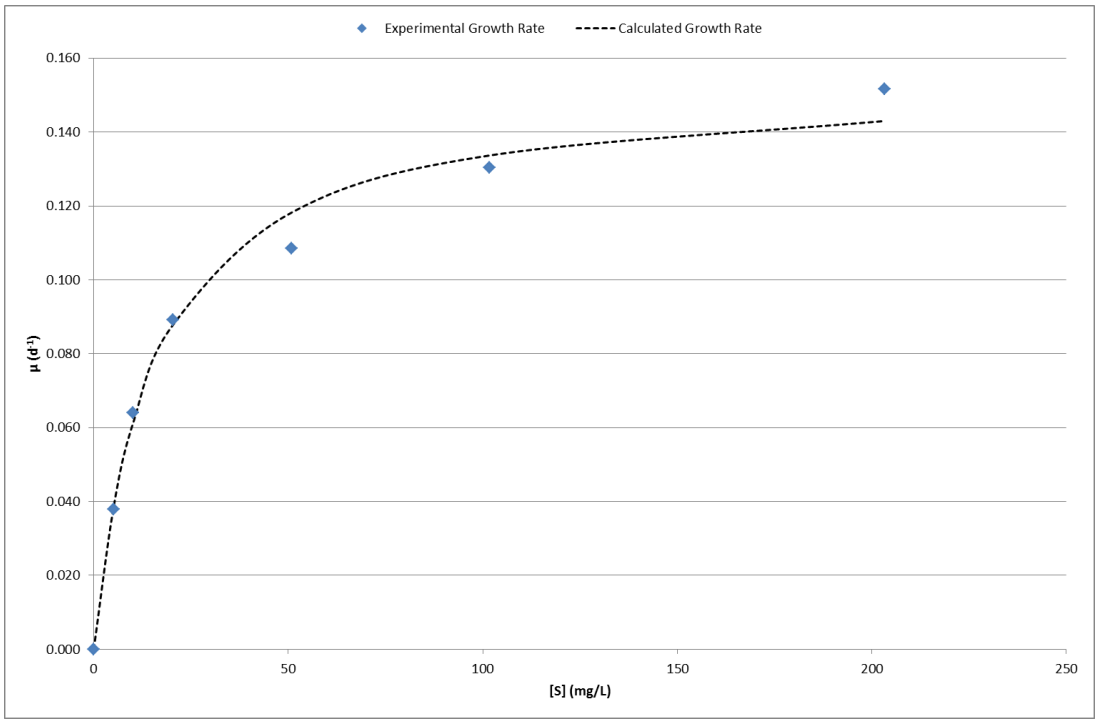

Figure 7-3 Comparison of experimental growth rate of algae on nitrate (diamonds) and the calculated values (continuous dashed line)

The approach just described, however, does not take account of the fact that the actual concentration of nitrate in the media during culture might be quite different from the initial value at inoculation. Nitrate will be consumed by cell growth and produced by lysis of dead cells. Since the nitrate concentration in the media was tracked throughout the experiment at the same time as biomass, many more data points were available for analysis. For each time interval the growth rate was calculated and plotted against the average nitrate concentration in the media during that interval. The results are shown in Figure 7-6. Before discussing the growth equation inferred by using this second approach, the experimental details of the nitrate measurements made during cell culture will be discussed.

Nitrate can be reliably detected by absorption at 232 nm and a calibration curve was constructed as shown in Figure 7-4 (data in Table 24).

Table 24 Calibration values for NO_3-N concentration determined by spectroscopy at 232 nm

$NaNO_3$ Standard Solution Concentration (mM)	**OD_{232} (AU)**
Blank	0.000
0.2	0.171
0.4	0.348
0.6	0.375
0.8	0.494
1.0	0.608
1.5	0.867
2.0	1.169
2.5	1.397
3.0	1.551

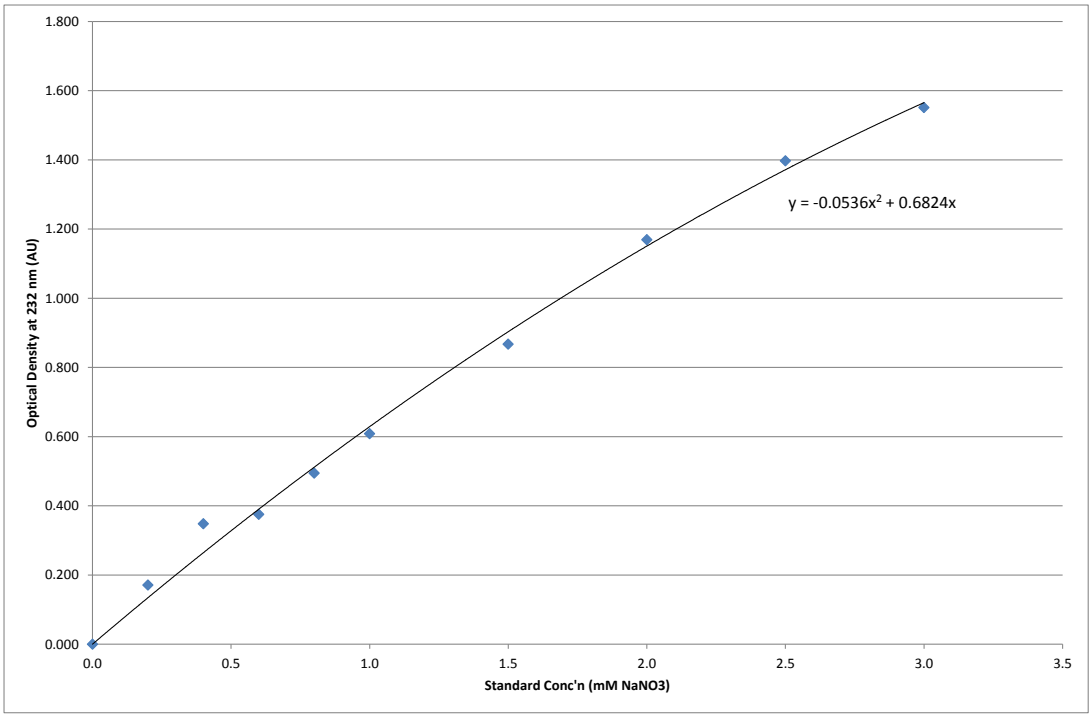

Figure 7-4 Calibration curve of $NaNO_3$ standard solutions

Using OD_{232} measurements, the sodium nitrate concentrations were found for all cultures by application of the quadratic formula to the equation of the calibration curve, $y = -0.0536x^2 + 0.6824x$. The mean optical density measurements are given

in Table 25, and mean values of sodium nitrate concentration in the triplicate cultures can be seen in Table 26. Tables of raw data can be found in Appendices I and J.

Table 25 Mean optical density of triplicate cultures of *Chlorella sp*. for the determination of sodium nitrate concentration

Culture ID	**Mean OD_{232} at day:**											
	3	**5**	**7**	**10**	**12**	**14**	**18**	**20**	**24**	**26**	**28**	**35**
0 mg/L	0.086	0.112	0.100	0.105	0.078	0.120	0.129	0.130	0.112	0.132	0.116	0.152
5 mg/L	0.077	0.099	0.063	0.071	0.062	0.085	0.095	0.098	0.117	0.108	0.098	0.120
10 mg/L	0.111	0.092	0.064	0.073	0.073	0.104	0.106	0.116	0.140	0.124	0.117	0.148
20 mg/L	0.182	0.167	0.095	0.085	0.084	0.113	0.127	0.133	0.157	0.149	0.136	0.171
50 mg/L	0.453	0.441	0.356	0.239	0.190	0.175	0.194	0.183	0.219	0.227	0.216	0.268
100 mg/L	0.824	0.858	0.796	0.691	0.665	0.638	0.554	0.484	0.444	0.438	0.423	0.414
200 mg/L	1.484	1.544	1.469	1.346	1.325	1.270	1.191	1.058	0.837	0.731	0.606	0.881

Table 26 Mean sodium nitrate concentration (mg $NaNO_3$ L^{-1}) calculated using $y = -0.0536x^2 + 0.6824x$

Culture ID	Mean $NaNO_3$ (mg/L) concentration at day:											
	3	**5**	**7**	**10**	**12**	**14**	**18**	**20**	**24**	**26**	**28**	**35**
0 mg/L	7.211	10.312	8.664	9.044	7.337	10.884	11.393	11.775	11.457	13.624	10.886	15.040
5 mg/L	9.686	12.525	7.947	8.875	7.737	10.736	12.008	12.391	14.818	13.582	12.390	15.117
10 mg/L	14.050	11.542	7.989	9.128	9.213	13.071	13.411	14.648	17.731	15.718	14.821	18.809
20 mg/L	23.168	21.175	11.967	10.693	10.566	14.263	16.019	16.786	19.923	18.890	17.257	21.694
50 mg/L	59.722	58.053	46.388	30.711	24.280	22.263	24.691	23.350	28.056	29.061	27.657	34.485
100 mg/L	114.664	118.408	105.442	81.359	75.813	70.070	53.299	41.361	36.949	40.167	41.177	54.571
200 mg/L	236.636	250.090	233.261	207.650	203.483	192.609	178.195	154.545	117.744	100.526	81.933	124.325

The concentration values in Table 26 do not include the measurements for culture 100-A, for the reasons outlined previously. Also, the measurements for culture 0-A were excluded from the concentration calculations as the OD_{232} measurements were much higher than those for 0-B and 0-C. It was assumed that contamination, which did not affect the growth of the culture, caused interference with the optical density measurement at 232 nm to produce an artificially high result. It was not thought to be a true reading as culture 0-A did not grow any faster than cultures 0-B and 0-C, which would have been the case if the nitrate concentration had in fact been elevated. These discrepancies can be examined in the raw data, which includes standard error calculations, and is presented in full in the Appendices. A plot of OD_{232} against time (days) can be seen in Figure 7-5, below.

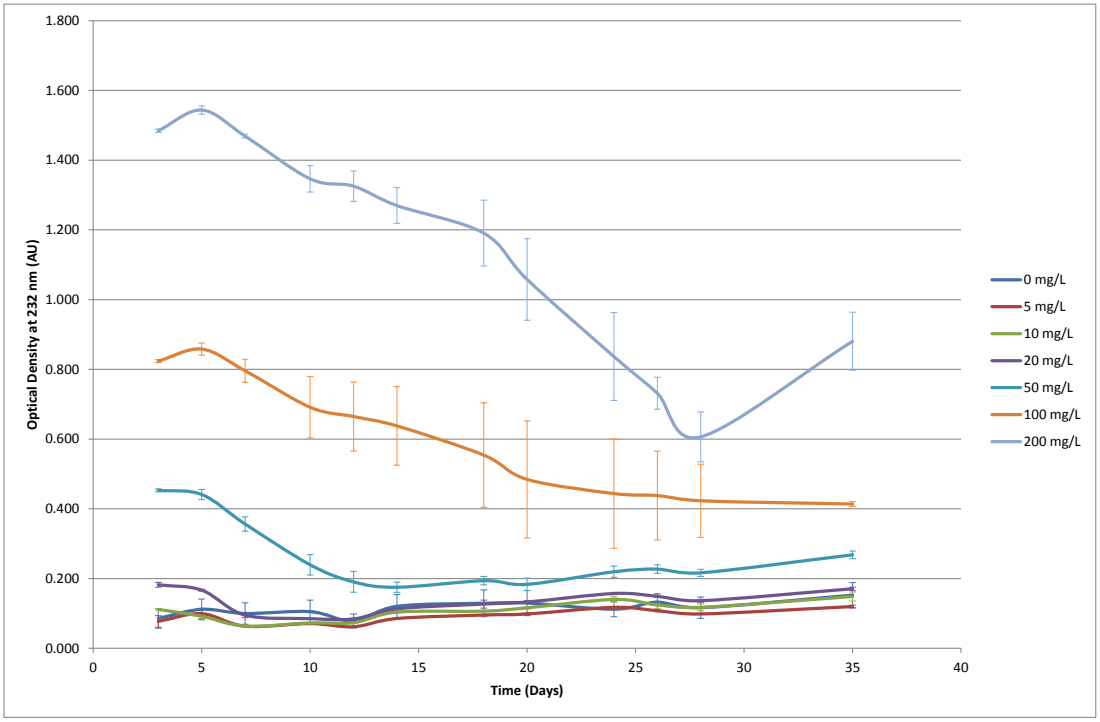

Figure 7-5 Disappearance of nitrate in cultures of *Chlorella sp*. (bars represent standard error)

We can see from this graph that, after a brief initial increase, the nitrate concentration decreases with time – a pattern that was expected as nitrate is used for growth. The initial increase in nitrate corresponds to the theory of cells dying during the lag phase and releasing nitrate into the medium for use by living cells. Towards the end of the measurements, nitrate again increases for some of the

profiles. Again, this could be explained by cell death within an aging culture, and nitrate being released from ruptured cells. So, although nitrate plays an important part in the growth of *Chlorella sp*., the cultures can be considered to be self-sustaining to a degree, as nitrogen from dead cells is reused by living cells.

Each of the data points shown in Figure 7-6 is the average growth rate between two consecutive sampling points versus the average nitrate concentration during the same period. As an example, consider the data for the first two sample points in the cultures inoculated into media with 0 mg/L of sodium nitrate. Between Day 3 and Day 5 the optical density increases from 0.086 AU to 0.112 AU (Table 25) and so, using Equation 7-3, the average growth over this period is calculated thus:

$$\mu = ln\left(\frac{0.112}{0.086}\right) \times \frac{1}{(5-3)} = 0.132\ d^{-1}$$

During this same interval, the sodium nitrate concentration increases from 7.211 mg/L to 10.312 mg/L so the mean concentration over the interval is calculated as

$$\frac{7.211 + 10.312}{2} = 8.76\ mg\ NaNO_3 L^{-1}$$

So the point (8.76, 0.132) is one of the data points plotted on Figure 7-6.

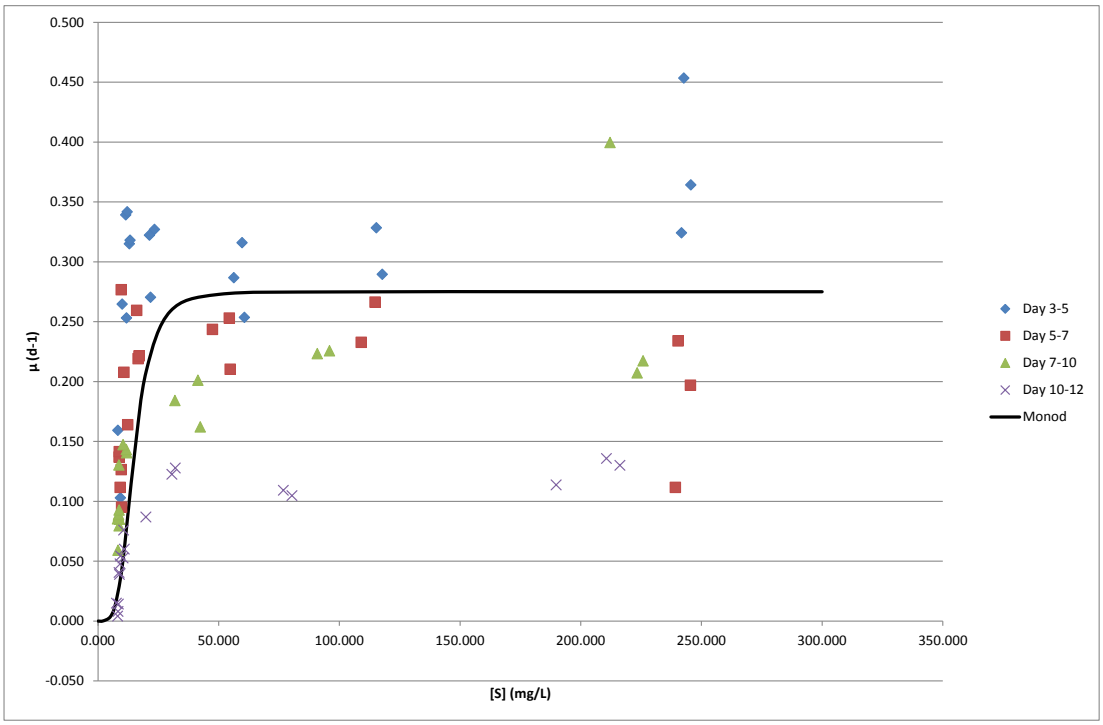

Figure 7-6 Scatter graph of growth rate vs. measured concentration of $NaNO_3$ including fitted Monod term for specific growth rate of *Chlorella sp*.

The data points are distinguished according to the time in culture at which the measurements were recorded and it can therefore be seen that growth rates at later times (e.g. Day 10-12) tend to be less than those at earlier times (e.g. Day 3-5). This illustrates that growth of algae is often sub-exponential – i.e. growth rate decreases with higher cell concentration. Although this effect can be modelled with so-called logistic type equations, these are not used for this data set since it would require a far more comprehensive set of experiments that are beyond the scope of this work. Instead, the continuous line in Figure 7-6 was fitted manually, and has the following Hill type kinetic equation for the growth of *Chlorella sp*. on sodium nitrate:

$$\mu = 0.27 \frac{[S]^4}{15.0^4 + [S]^4} \qquad \textbf{Equation 7-6}$$

where [S] is the concentration of sodium nitrate in mg/L. The K_{NO3} value used above (15 mg NO_3 L^{-1}) is in agreement with the value obtained earlier from the Lineweaver-Burk plot shown in Figure 7-2. Following analysis of this data, it can be seen that growth is strongly switched on at this value, where the curve is at its

steepest, and a cooperative exponent of $n = 4$ was chosen to provide the highly sigmoidal shape suggested by the data. Interestingly, similar Hill type kinetics with exactly the same cooperative exponent of 4 have been previously published for uptake of nitrogen containing species of microalgae in the modelling work of (Flynn et al. 1997). This growth equation also has the big advantage over the first approach in that the growth rate drops to zero for a zero nitrate concentration as required; this important result of the experimental work is utilised in the computational modelling.

A close-up of the graph at the lower end of the concentration [S] scale can be seen in Figure 7-7.

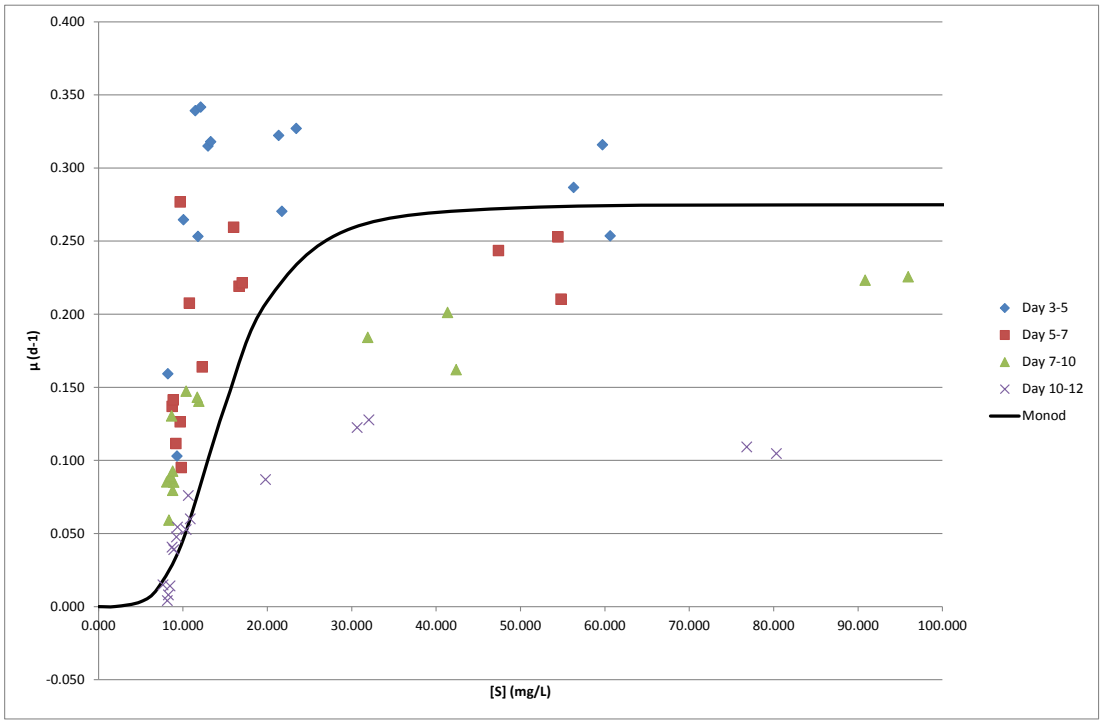

Figure 7-7 Close-up of sigmoidal shape observed in graph of growth rate vs. measured concentration of $NaNO_3$ (see Figure 7-6)

In accordance with ASM3 conventions, the K_S value was adjusted to reflect the nitrogen content of the growth medium, i.e. the relative atomic mass of nitrogen with respect to the relative molecular mass of sodium nitrate.

$$K_{NO3} = \frac{15\ mg\ NaNO_3 L^{-1}}{85} \times 14 = 2.47\ mg\ N\ L^{-1}$$

The model (Equation 7-6) and its parameters were used to produce a mathematical description of algal growth on nitrates in the integrated activated sludge and algal pond model.

7.2.2 Effect of ammonium concentration on the growth of cells

The intention of this experiment was to establish the relationship between the growth of *Chlorella sp*. and the concentration of ammonium in the growth medium. In order to assess this relationship, the cultures were sampled at intervals for a total of 20 days and the growth rate determined by measurement of the optical density of each sample at a wavelength of 600 nm. Optical density measurements were not taken to ascertain the ammonium concentration in the cultures as it was not anticipated that there would be a meaningful change over the course of the experiment; this was due to anecdotal evidence of preferred growth on nitrate from early experiments, as stated in the Introduction to this chapter (Section 7.1). The mean optical density of the triplicate cultures of the same NH_4Cl concentration (cultures A-C) was calculated and the values plotted against time (days). The mean experimental data can be seen in Table 27 and a table of raw data is shown in Appendix K.

Table 27 Mean optical density of triplicate cultures of *Chlorella sp*. grown with different concentrations of ammonium chloride

Culture ID	**Mean OD_{600} at day:**						
	3	**5**	**7**	**11**	**13**	**17**	**20**
0 mg/L	0.039	0.051	0.053	0.075	0.091	0.104	0.119
3 mg/L	0.041	0.061	0.073	0.104	0.131	0.156	0.177
6 mg/L	0.036	0.052	0.062	0.098	0.122	0.154	0.181
12 mg/L	0.040	0.058	0.075	0.160	0.195	0.226	0.253
31 mg/L	0.036	0.051	0.060	0.138	0.195	0.226	0.221
62 mg/L	0.037	0.048	0.054	0.110	0.141	0.172	0.189
125 mg/L	0.033	0.042	0.046	0.093	0.131	0.166	0.175

The data shown above suggests that growth rate on ammonium is much less than on nitrate for this species of *Chlorella*. It can be seen in Figure 7-8 that higher

concentrations of NH_4Cl appear to inhibit growth rate - the fastest-growing culture is in the medium containing 12 mg NH_4Cl L^{-1}, with 31 mg NH_4Cl L^{-1} a close second. Until day 5, the cultures of *Chlorella sp*. grew at a similar rate for all concentrations; by day 11 the culture densities were more spread out but not in accordance with the initial concentration of ammonium chloride. In fact, the only culture that grew less well than the culture with the most ammonium (125 mg NH_4Cl L^{-1}) was the culture in nitrogen-free medium. The experiment was terminated at day 20 as the algal cultures did not appear healthy and had formed clumps that produced a grainy suspension upon mixing.

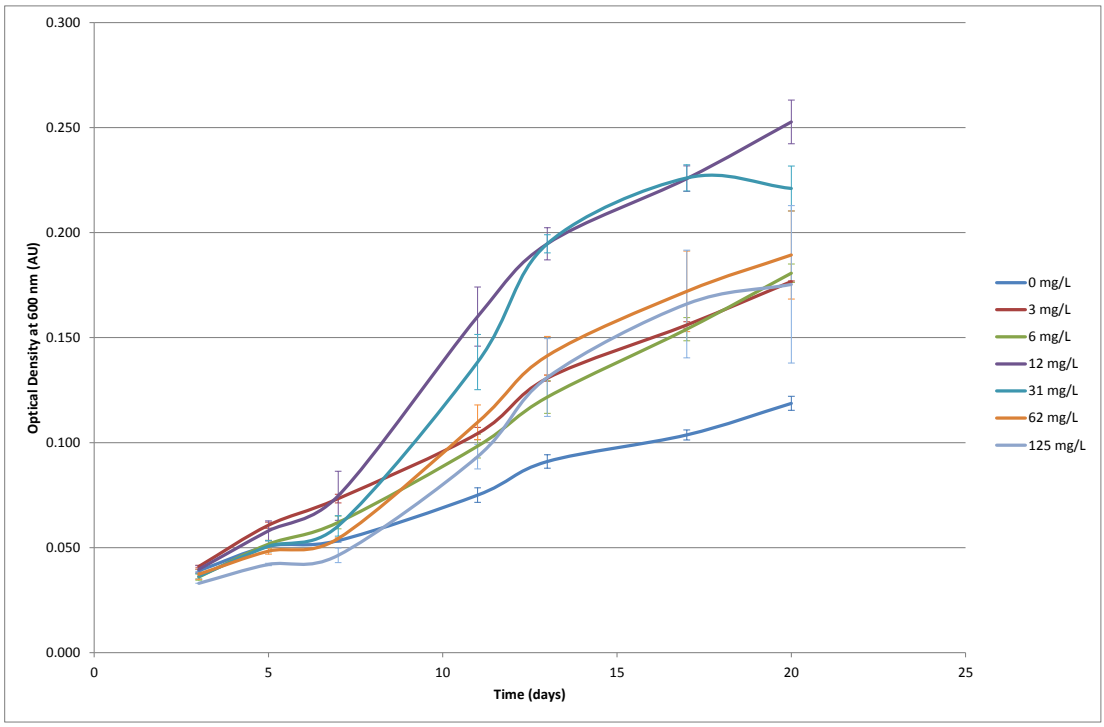

Figure 7-8 Growth of *Chlorella sp*. with different concentrations of NH_4Cl (bars represent standard error)

The results obtained from this experiment were broadly as expected – that this particular strain of *Chlorella* would not adapt particularly well to growth in NH_4Cl, although it does show best growth at concentrations of 12-62 mg NH_4Cl L^{-1}. The fact that all cultures have similar initial growth can probably be explained by the preferential use of nitrate stored within the cell. In fact, upon analysis of the data, it is assumed that growth on stored nitrate that has been released into the medium by ruptured cells is responsible for the growth observed for 0 mg NH_4Cl L^{-1}. We can,

therefore, think of the residual growth of 0.089 d^{-1} (Table 28) as entirely due to released or stored nitrate; according to the kinetic equation for nitrate growth developed earlier (Equation 7-6), this would correspond to a sodium nitrate concentration of 12.6 mg L^{-1} due to released nitrate, which is in broad agreement with the measured concentrations of released nitrate previously determined – i.e. 7-15 mg L^{-1} in the top row of Table 26.

As with the data for nitrates in Section 7.2.1 above, the experimental data for ammonium was used to find parameter values for inclusion in the process rate expression for the growth of algae on S_{NH4} in the integrated model. As described in detail above, the parameter values were found via a double-reciprocal plot of growth rate vs. substrate concentration. The specific growth rate, μ, is calculated directly from the experimental data and, in this case, uses the mean measurements from day 7 to day 13. As shown in Figure 7-8, there is some residual growth in ammonium-free medium and, as discussed earlier, in order to correct for this, growth rates were normalised to exclude growth seen at [S] = 0.

Initially, the experimental data was used to assess the fit of standard Monod type kinetics; the normalised growth rate, Nμ, was used in a Lineweaver-Burk plot (Figure 7-9) to determine μ_{max} and K_S.

Table 28 Growth rates of *Chlorella sp*. at different values of [S]

NH_4Cl Concentration ([S], mg/L)	**Experimental Growth Rate (μ, d^{-1})**	**Normalised Growth Rate (Nμ, d^{-1})**	**1/[S]**	**1/Nμ**
0	0.089	0.000	0.000	0.000
3.143	0.096	0.007	0.318	138.452
6.287	0.112	0.023	0.159	42.902
12.573	0.160	0.071	0.080	14.152
31.433	0.195	0.106	0.032	9.418
62.867	0.159	0.070	0.016	14.229
125.733	0.173	0.084	0.008	11.880

Taking into consideration the normalised growth rate, it was decided that only the points for 12-125 mg NH_4Cl L^{-1} should be plotted. As the growth for the three lower points was insignificant after normalisation, including these points may have led to artificially high or low parameters.

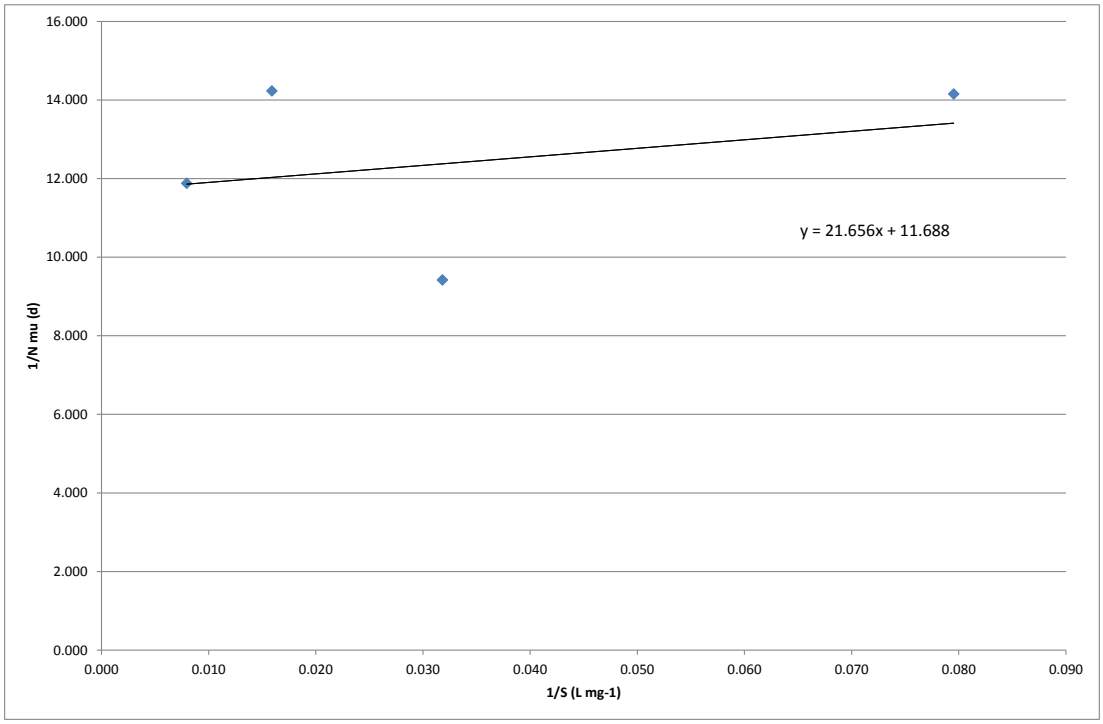

Figure 7-9 Double-reciprocal plot of *Chlorella sp*. growth data with NH_4Cl

Again using Equation 7-5, the intercept is equal to μ_{max}^{-1}:

$$\mu_{NH4} = c^{-1} = \frac{1}{11.688\ d} = 0.086\ d^{-1}$$

This value, in combination the gradient, can then be used to calculate the Monod constant for ammonium dependency, K_{NH4}.

$$K_{NH4} = \mu_{NH4} \times m = 0.086\ d^{-1} \times 21.656\ d\ mg\ L^{-1} = 1.86\ mg\ L^{-1}$$

It can be seen that the double reciprocal plot (Figure 7-9) is a very poor straight line and the resulting value of the Monod constant determined using this method is very low. In the second approach, therefore, Hill type kinetic equations of varying orders were manually adjusted to achieve a better fit to the data. Taking into account the fact that the half-velocity constant, K_S, is the value of [S] when $\mu / \mu_{max} = 0.5$, it was

observed from the normalised growth rates in Table 28 that K_{NH4} should be somewhere in the region of 6-12 mg NH_4Cl L^{-1}. By a process of trial and error, both K_S and μ_{max} can be tweaked until Monod parameters are reached that fit the experimental data. Using the Monod expression, Equation 7-4, the adjusted values of μ_{NH4} and K_{NH4} can be used to find a predicted growth rate for all values of [S]. If a plot of the normalised experimental and calculated growth rates is compared, we can get an idea of how close to the true value the parameters are; this is illustrated in Figure 7-10, below.

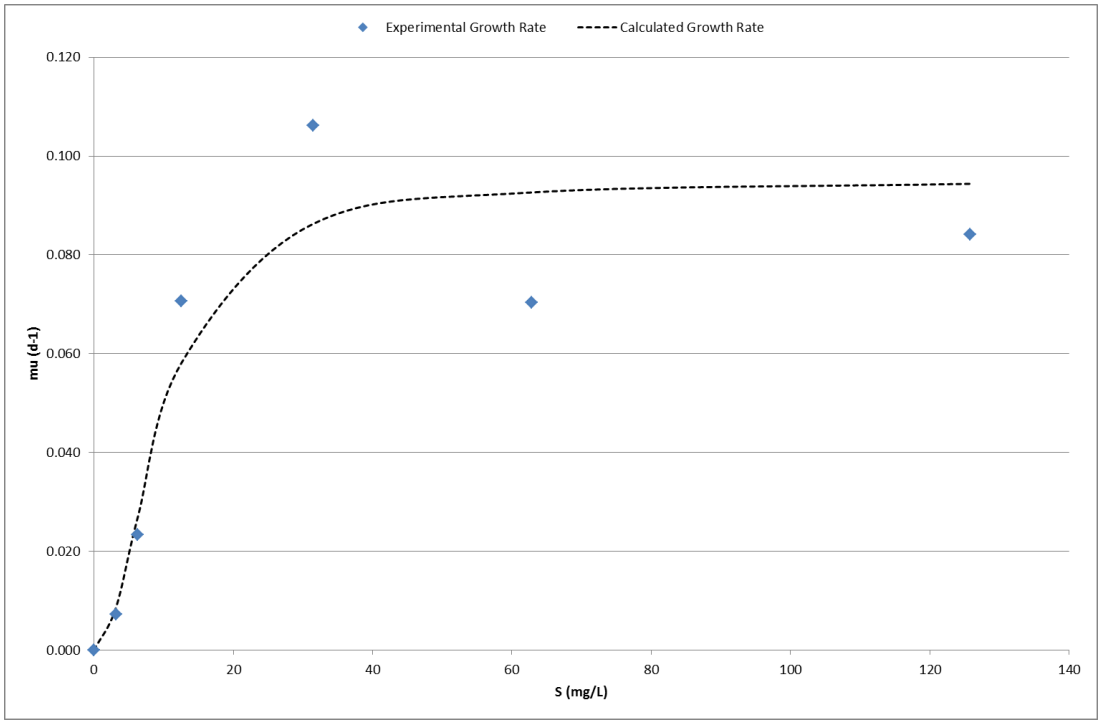

Figure 7-10 Comparison of experimental growth rate of algae on ammonium (diamonds) and the calculated values (continuous dashed line)

To produce this figure, parameters μ_{NH4} = 0.095 d^{-1} and K_{NH4} = 10.0 mg L^{-1} were used and the experimental growth rate is now tracked closely by the calculated growth rate. A co-operative exponent was required for this expression also, to provide a non-linear shape to the growth curve. In this instance, a value of *n = 2* was used to give the curve its sigmoidal shape. The fitted model of algal growth on ammonium, using Monod kinetics, is expressed as:

$$\mu = 0.095 \frac{[S]^2}{10.0^2 + [S]^2} \qquad \textbf{Equation 7-7}$$

In accordance with ASM3 conventions, the K_S value was adjusted to reflect the nitrogen content of the growth medium, i.e. the relative atomic mass of nitrogen with respect to the relative molecular mass of ammonium chloride.

$$K_{NH4} = \frac{10\ mg\ NH_4Cl\ L^{-1}}{53.46} \times 14 = 2.62\ mg\ N\ L^{-1}$$

This model (Equation 7-7) and its parameters were used in the mathematical expression for algal growth on ammonium for the integrated activated sludge and algal pond model.

7.2.3 Effect of carbon dioxide concentration on the growth of cells

The usual method in which to assess the effect of carbon dioxide upon an aqueous culture would be to aerate the growth medium with gas containing a known percentage of carbon dioxide gas (Spijkerman et al. 2011). However, because I wanted to know the exact concentration of carbon dioxide in the medium, a novel approach was taken whereby bottled, carbonated water was used to feed the algal cultures. Following a scouting experiment to ascertain that algal cultures would grow in commercially available sparkling water, cultures containing a known concentration of carbon dioxide were sampled at intervals over a period of 7 days. The growth rate was determined by measurement of the optical density of each sample at a wavelength of 600 nm – the mean optical density of the triplicate cultures can be seen in Table 29 and a table of raw data in Appendix L. A correction factor was calculated to compensate for the effect of daily dilution with water, as the cultures fed with greater volumes of sparkling water would be correspondingly less dense. This factor was used to produce a corrected OD_{600} value, which was plotted against time (days).

Table 29 Mean optical density of triplicate cultures of *Chlorella sp*. grown with different concentrations of CO_2

Culture ID	Mean OD_{600} at day:			Dilution correction factor for day:			Corrected mean OD_{600} at day:		
	1	4	7	1	4	7	1	4	7
0.6 mg/L	0.028	0.059	0.117	1.000	1.000	1.000	0.028	0.059	0.117
11 mg/L	0.029	0.077	0.176	1.000	1.005	1.010	0.029	0.078	0.178
24 mg/L	0.028	0.087	0.208	1.000	1.011	1.022	0.028	0.088	0.212
49 mg/L	0.027	0.107	0.285	1.000	1.023	1.046	0.027	0.109	0.298
126 mg/L	0.027	0.186	0.492	1.000	1.059	1.118	0.027	0.197	0.550
255 mg/L	0.027	0.278	0.780	1.000	1.119	1.238	0.027	0.311	0.965

The optical density measurements show a clear correlation between growth and availability of carbon dioxide – this relationship is illustrated in Figure 7-11. After one day of growth, the optical density measurements were very similar for all concentrations of CO_2. However, by day 4, a marked increase in growth can be seen in the cultures fed with more sparkling water. By the end of the experiment at day 7, the culture densities were spread out according to the concentration of carbon dioxide, reaching densities similar to those seen with sodium nitrate levels of over 50 mg $NaNO_3$ L^{-1}. The results obtained suggest that the growth rate of *Chlorella sp*. can be enhanced by elevated levels of carbon dioxide, when nitrate is not limiting.

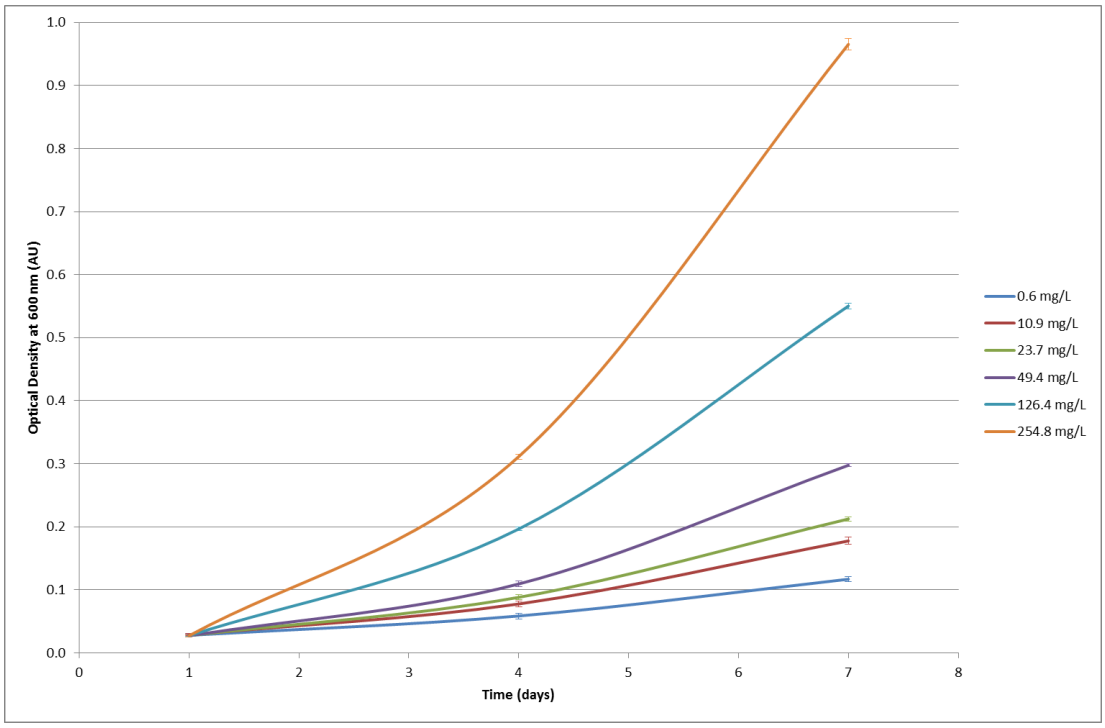

Figure 7-11 Growth of *Chlorella sp*. with different concentrations of CO_2 from carbonated water (bars represent standard error)

The specific growth rate, μ, between day 1 and day 7 was calculated directly from the experimental data as described in Equation 7-3 and is shown in the second column of Table 30. It can be seen that a single Monod type equation is not able to represent the data well since the growth rate at the atmosphere equilibrated concentration of CO_2 (i.e. 0.6 mg CO_2 L^{-1}) is highly significant being as much as 40% of the growth rate achieved by a CO_2 concentration of 255 mg L^{-1}, which is more than 400 times higher. If the atmospheric growth is subtracted from the other growth values to give normalised values, a very good fit is found by using a standard Monod equation as described below. In order to reflect this behaviour, two expressions will be required for the model of growth with respect to carbon dioxide: first, a so-called high affinity expression to represent the considerable growth that is achieved at atmospheric CO_2 concentrations or below; and secondly, an additional low affinity expression to take account of the additional growth observed at higher CO_2 concentrations.

Table 30 Growth rates of *Chlorella sp*. at different values of [S]

CO_2 Concentration ([S], mg/L)	Experimental Growth Rate (μ, d^{-1})	Normalised Growth Rate ($N\mu$, d^{-1})	1/[S]	$1/N\mu$	$N\mu$/[S]
0.6 mg/L	0.238	0.000	1.667	0.000	0.0
11 mg/L	0.304	0.066	0.092	15.216	6.0×10^{-3}
24 mg/L	0.340	0.101	0.042	9.857	4.3×10^{-3}
49 mg/L	0.398	0.160	0.020	6.264	3.2×10^{-3}
126 mg/L	0.500	0.262	0.008	3.816	2.1×10^{-3}
255 mg/L	0.594	0.356	0.004	2.811	1.4×10^{-3}

Note that growth data for CO_2 concentrations higher than atmospheric level only has been determined, so the low affinity expression (unlike the high affinity term) is supported by the data. The normalised growth rate, Nμ, in Table 30 is used in a Lineweaver-Burk plot (Figure 7-12) to determine μ_{max} and K_S.

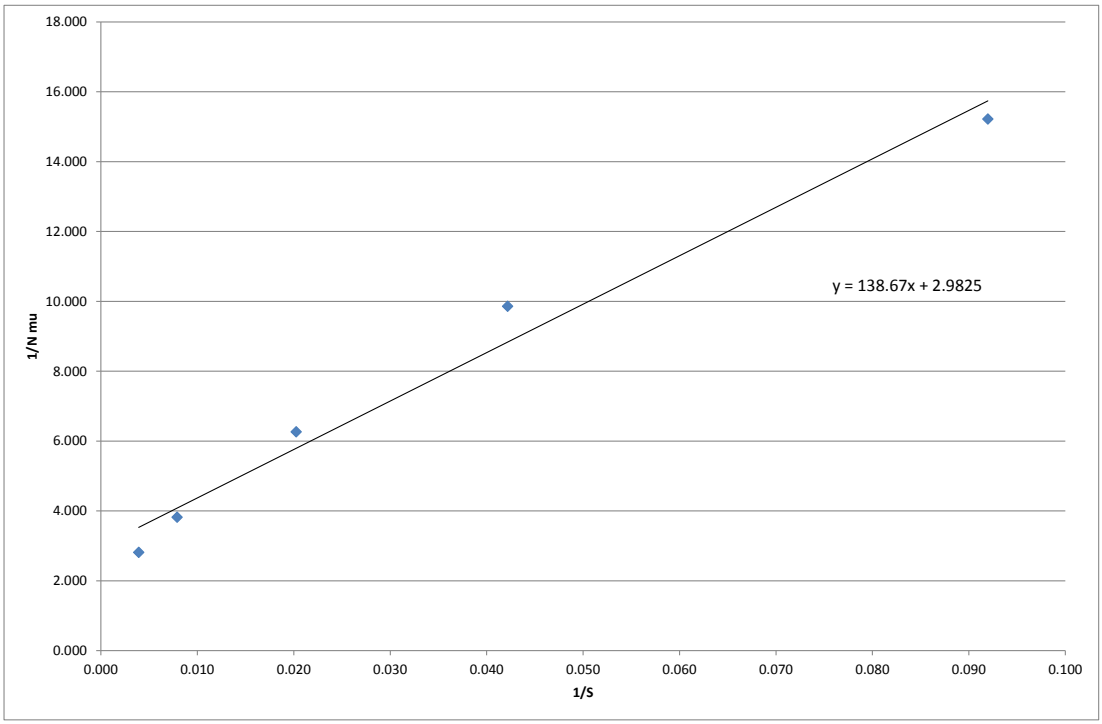

Figure 7-12 Double-reciprocal plot of CO_2 growth data

As shown in Equation 7-5, the intercept, c, is equal to μ_{max}^{-1}:

$$\mu_{CO2} = c^{-1} = \frac{1}{2.9825\ d} = 0.335\ d^{-1}$$

This value, in combination with the gradient, is then used to calculate the Monod constant for growth with carbon dioxide at elevated levels, K_{CO2}.

$$K_{CO2} = \mu_{CO2} \times m = 0.335\ d^{-1} \times 138.67\ d\ mg\ L^{-1} = 46.45\ mg\ L^{-1}$$

The growth at different concentrations of carbon dioxide was calculated using these parameters and plotted alongside the normalised growth values. These parameters were ill-fitting in relation to actual growth, so the Eadie-Hofstee method was followed to investigate alternative parameter values. The Eadie-Hofstee plot can be considered to be more robust against error-prone data than the Lineweaver-Burk plot because it gives equal weight to data points over the range of [S] and μ. However, a drawback of this method is that the independent variable, [S], is not represented separately in either axis – both are dependent upon rate – therefore any experimental error will be present in both axes. The values from an Eadie-Hofstee plot are interesting though and give a broader picture of trends in growth rate parameters (Figure 7-13).

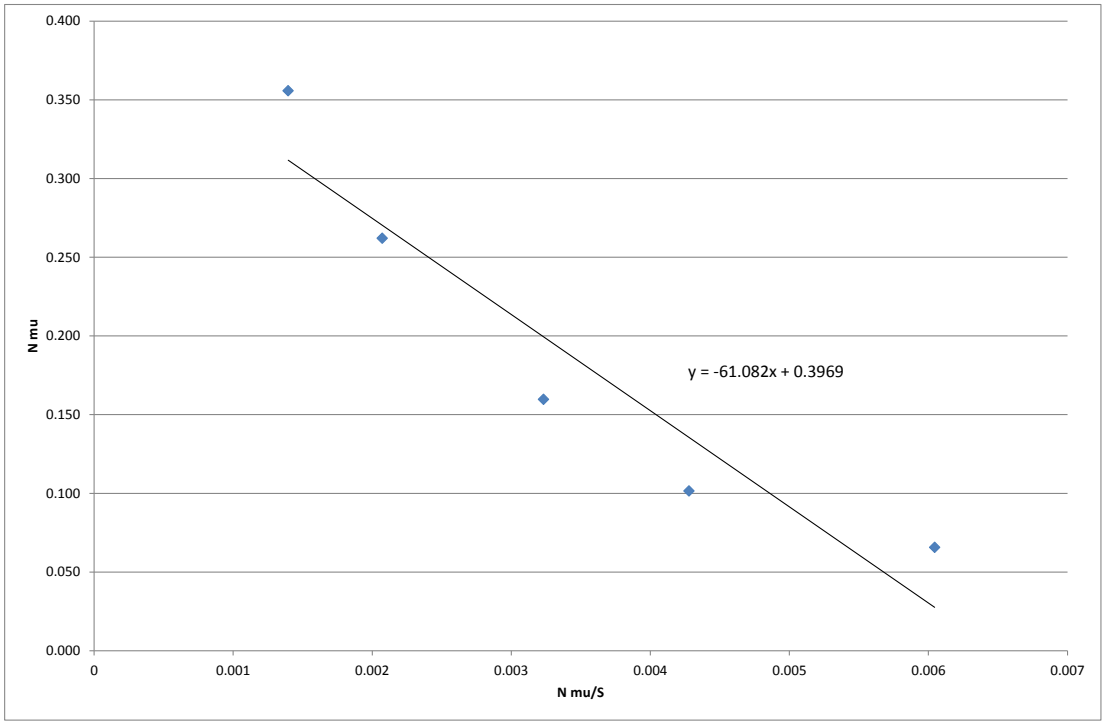

Figure 7-13 Eadie-Hofstee plot of CO_2 growth data

In a similar way to the Lineweaver-Burk plot, Monod parameter values are taken from the equation of the line, where $m = -K_S$ and $c = \mu_{max}$. Therefore, the parameter values from the Eadie-Hofstee plot would be K_{CO2} = 61.1 mg L^{-1} and μ_{max} = 0.40 d^{-1}. As mentioned in earlier sections, it is possible to manually adjust the Monod parameters to better fit the experimental results. Taking into account that both the K_S and μ_{max} values have increased, this information can be used to tweak the parameter values to find a model that fits the experimental data. Again using the Monod expression, Equation 7-4, with values obtained from the Lineweaver-Burk and Eadie-Hofstee plots as a basis for the parameters, a plot of the experimental and calculated growth rates can be compared.

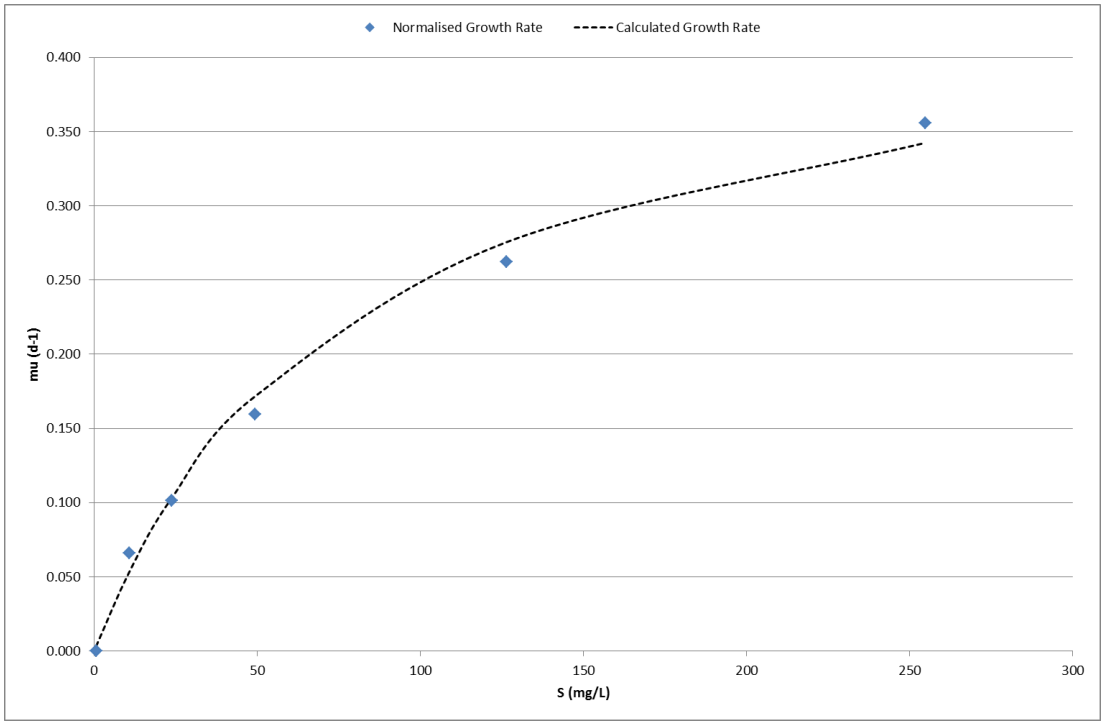

Figure 7-14 Comparison of normalised growth rate of algae on carbon dioxide (diamonds) and calculated values (continuous dashed line)

By using parameters μ_{CO2} = 0.4 d^{-1} and K_{CO2} = 80.0 mg L^{-1}, the experimental growth rate is tracked closely by the calculated growth rate (Figure 7-14). A co-operative exponent for the growth at elevated levels of carbon dioxide was not required.

If we now turn our attention to an expression for the high affinity growth observed for low levels of carbon dioxide (i.e. atmospheric or lower), we are limited by a lack of data. In fact, there is only a single measured data point for observed growth at

0.6 mg CO_2 L^{-1} that the expression must fit but, as photoautotrophic growth must drop to zero if there is no dissolved CO_2 present, another point can be extrapolated. At this juncture, it is useful to consider all experiments in order to deduce parameters from comparable experimental conditions. To illustrate:

Table 31 Experimental conditions and inferred kinetic parameters

Model Parameter	**Level of nutrient under test:**			**Experiment**
	$NaNO_3$	**NH_4Cl**	**CO_2**	
μ_{NO3} K_{NO3}	excess	-	atmospheric	1
μ_{NH4} K_{NH4}	-	excess	atmospheric	2
$\mu_{CO2\ atm}$ $K_{CO2\ atm}$	excess	-	atmospheric	3a (low CO_2)
μ_{CO2} K_{CO2}	excess	-	excess	3b (high CO_2)

Considering Table 31, we could argue that conditions were equivalent in Experiments 1 and 3a, where nitrate is not limiting and carbon dioxide is at atmospheric concentration in the growth medium. In this case, the maximum specific growth rate for carbon dioxide at atmospheric level could be adopted from Experiment 1, which would give the parameter $\mu_{CO2\_atm} = \mu_{NO3} = 0.27\ d^{-1}$. A Hill type function was chosen to switch on growth using a half-velocity constant that is half the concentration of dissolved carbon dioxide at atmospheric pressure, i.e $K_{CO2\ atm}$ = 0.3 mg CO_2 L^{-1}. Next, a sigmoidal shape is assumed for this high affinity growth similar to that observed with growth on both nitrate and ammonium with a co-operative exponent $n_{CO2} = n_{NO3} = 4$. The comparison of Experiments 1 and 3a is relevant to this particular species of *Chlorella*, which prefers nitrate to ammonium as its nitrogen source and is dependent upon nitrate for growth when carbon dioxide is not in excess. Although somewhat arbitrary, the description of growth for sub-atmospheric CO_2 concentration is not too critical since only higher than atmospheric concentrations will pertain for the algae in the integrated model.

The low and high affinity expressions can be combined to describe algal growth over a range of dissolved CO_2 concentrations, from zero to many times atmospheric pressure. The expression for high affinity growth at sub-atmospheric concentrations (Expression 1) is:

$$\mu_{atm} = 0.27\frac{[S]^4}{0.3^4 + [S]^4}$$

And the additional growth at elevated CO_2 levels, as supported by the experiments and analysis described above (Expression 2) is:

$$\mu_{elevated} = 0.4\frac{[S]}{80 + [S]}$$

The two expressions are combined to produce an overall model of algal growth on carbon dioxide.

$$\mu_{overall} = \left(0.27\frac{[S]^4}{0.3^4+[S]^4}\right) + \left(0.4\frac{[S]}{80+[S]}\right) \qquad \textbf{Equation 7-8}$$

It should be mentioned that the existence of both high and low affinity carbon substrate transporters in photosynthetic algae has been demonstrated in published research, such as the work of Moroney and Somanchi (1999) and Miyachi et al. (2003).

Equation 7-8 was used to produce a range of theoretical growth rate values, from 0-0.6 mg CO_2 L^{-1}, which were plotted and compared to the experimental data.

Table 32 Theoretical growth rates based on combined Monod expression for growth on CO_2

CO_2 Concentration ([S], mg/L)	Experimental Growth Rate (μ, d^{-1})	Expression 1 Growth Rate (μ_{atm}, d^{-1})	Expression 2 Growth Rate ($\mu_{elevated}$, d^{-1})	Predicted Growth Rate ($\mu_{overall}$, d^{-1})
0.0 mg/L	-	0.000	0.000	0.000
0.1 mg/L	-	0.003	0.000	0.004
0.2 mg/L	-	0.045	0.001	0.046
0.3 mg/L	-	0.135	0.001	0.136
0.4 mg/L	-	0.205	0.002	0.207
0.5 mg/L	-	0.239	0.002	0.242
0.6 mg/L	0.238	0.254	0.003	0.257
11 mg/L	0.304	0.270	0.048	0.318
24 mg/L	0.340	0.270	0.091	0.361
49 mg/L	0.398	0.270	0.153	0.423
126 mg/L	0.500	0.270	0.245	0.515
255 mg/L	0.594	0.270	0.304	0.574

We can see from the table above that Expression 1 cannot describe algal growth beyond atmospheric concentrations of CO_2, since it remains constant at its upper limit of 0.270 d^{-1}. On the other hand, Expression 2 does not take effect until the concentration of dissolved CO_2 is above 0.6 mg/L. This is illustrated in Figures 7-15 - 17, below.

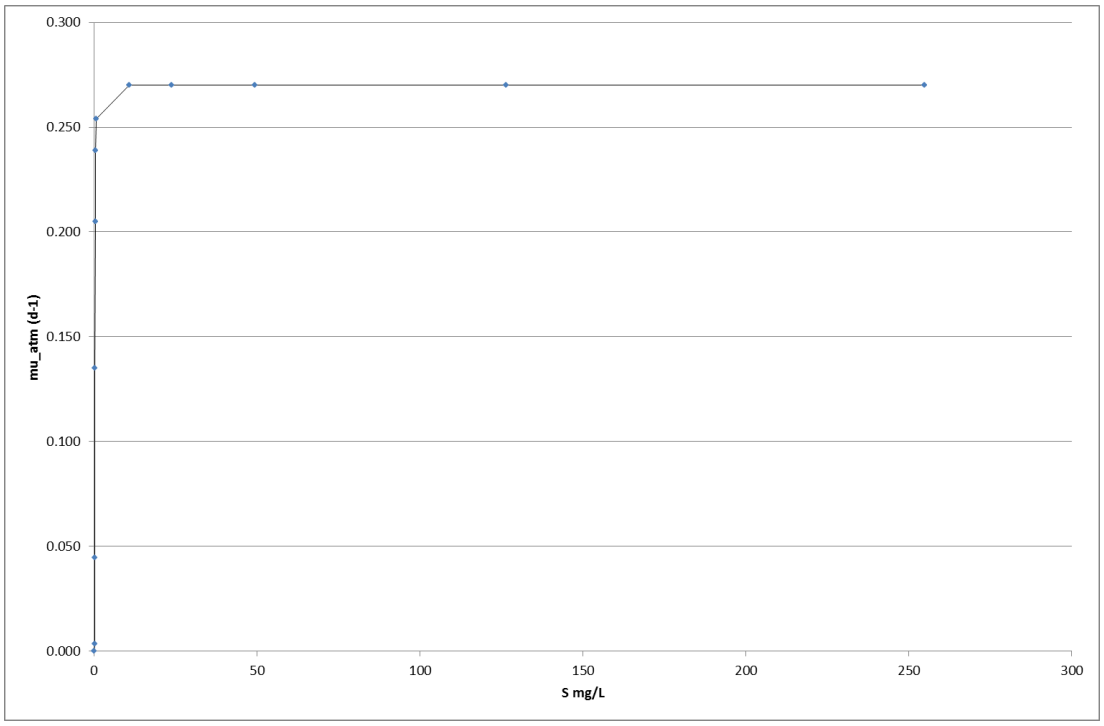

Figure 7-15 Expression 1 – growth rate at atmospheric CO_2

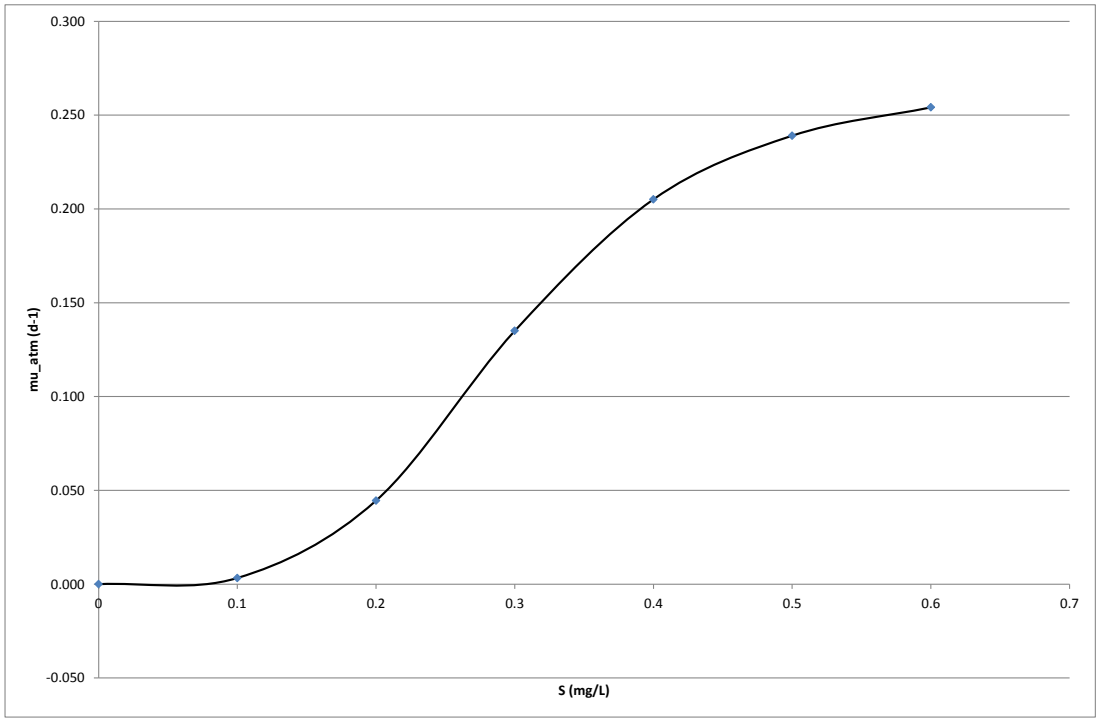

Figure 7-16 Close-up of Expression 1 to 0.6 mg CO_2 L^{-1}

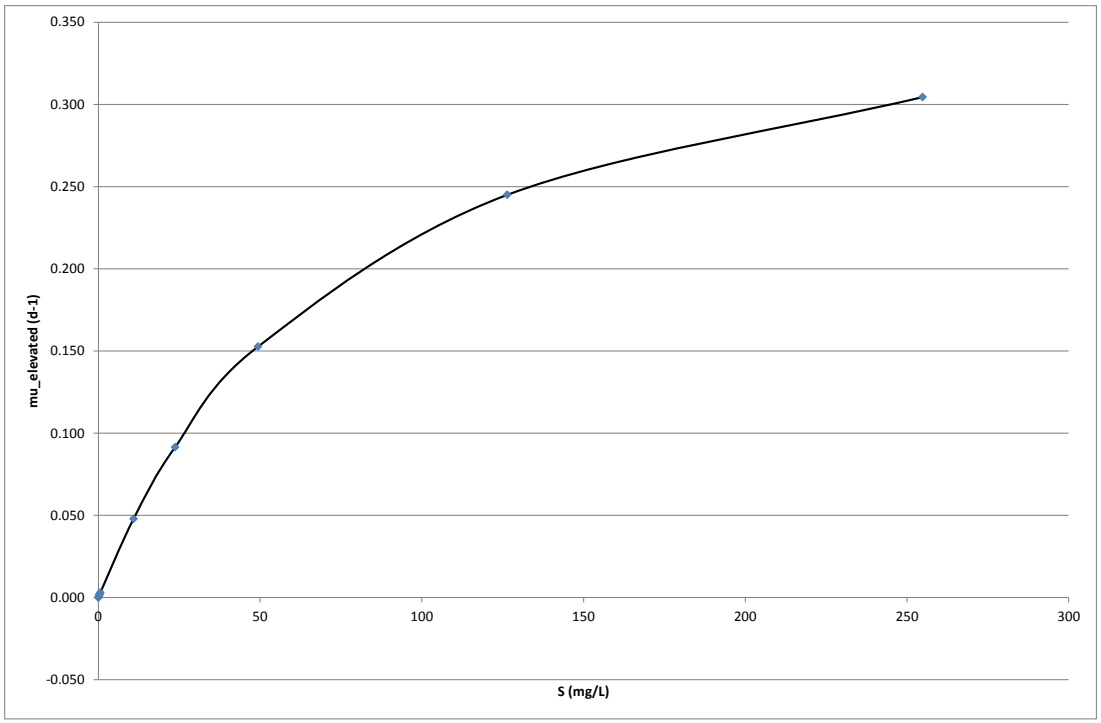

Figure 7-17 Expression 2 – growth rate at elevated CO_2

The combination of the high and low affinity terms gives a fuller picture of algal growth across a broad range of concentrations. This is illustrated in Figures 7-18 and 7-19, which compares the predicted values of $\mu_{overall}$ with the experimental data.

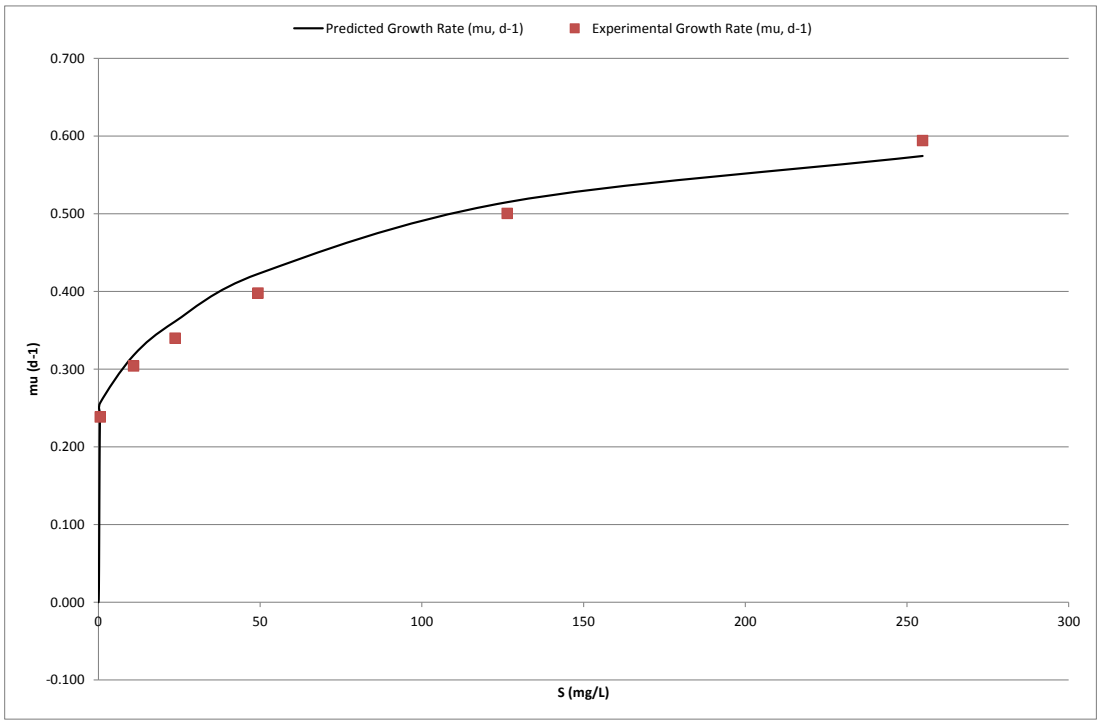

Figure 7-18 Comparison of predicted and experimental growth rates

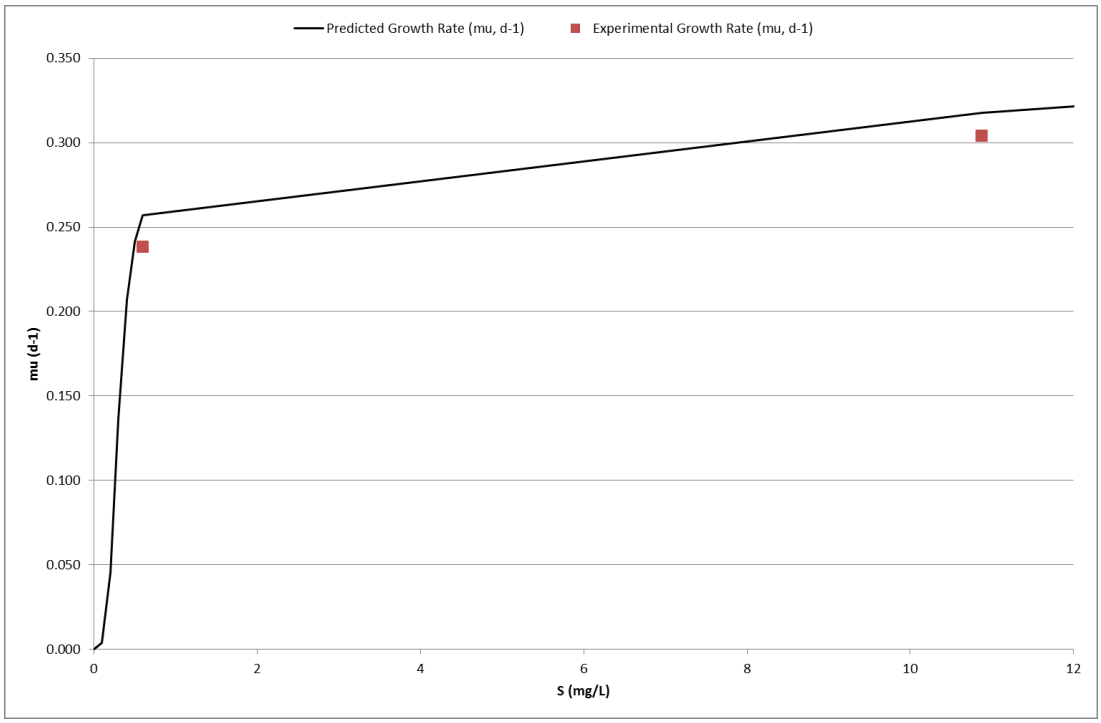

Figure 7-19 Close-up of predicted and experimental growth rates to 12 mg CO_2 L^{-1}

Considering Figure 7-18, the overall model for algal growth with carbon dioxide follows much the same rate as the experimental data, with a steep incline up to 0.6 mg CO_2 L^{-1} and a more gentle gradient thereafter. In accordance with the ASM3 convention for oxygen, which is measured as g O_2 m^{-3}, the K_S values will remain as carbon dioxide, i.e. g CO_2 m^{-3}. The model seen in Equation 7-8 and the parameters above were carried through for use in the integrated activated sludge and algal pond model. Two complete kinetic expressions for photoautotrophic growth limited by carbon dioxide, nitrate and ammonium are proposed in Chapter 8, Section 8.3.2: The use of experimental results in Monod expressions.

7.3 Discussion

7.3.1 Availability of nutrients in treated wastewater and the use of anoxic zones

The concentration of nitrate-nitrogen in the treated wastewater (secondary effluent) that would be routed into the algal pond depends upon the positioning of anoxic zones during the activated sludge process. Biological nitrogen removal can be regarded as a two-stage process: nitrification, where ammonium is converted to

nitrate by autotrophic bacteria, and denitrification, where nitrate is converted to nitrogen gas by heterotrophic bacteria (Henze et al. 2000; Tchobanoglous et al. 2004; Alasino et al. 2007). Nitrification requires aerobic conditions to proceed, whereas denitrification favours anoxic conditions but is dependent upon the availability of readily biodegradable organic substrates (S_S) and the amount of intracellular storage product (X_{STO}) within the heterotrophic cells.

Different configurations of activated sludge wastewater treatment plants have been designed to best deal with these processes, to produce an effluent that is both low in ammonium and nitrate. For example, putting the aerobic tank first produces nitrates that flow into the anoxic zone for conversion into nitrogen gas; however, there may not be enough biodegradable organic substrate left in the liquor to feed the denitrifying bacteria. Putting the anoxic zone first requires an internal recycle after the aerobic tank to provide nitrate in the pre-anoxic configuration; however, this arrangement can never produce a nitrate-free effluent. These systems are illustrated in Figure 7-20, below. Both arrangements have their pros and cons but, in the interests of algal growth using nitrate, a configuration where an aerobic zone is at the end of the sequence may be beneficial.

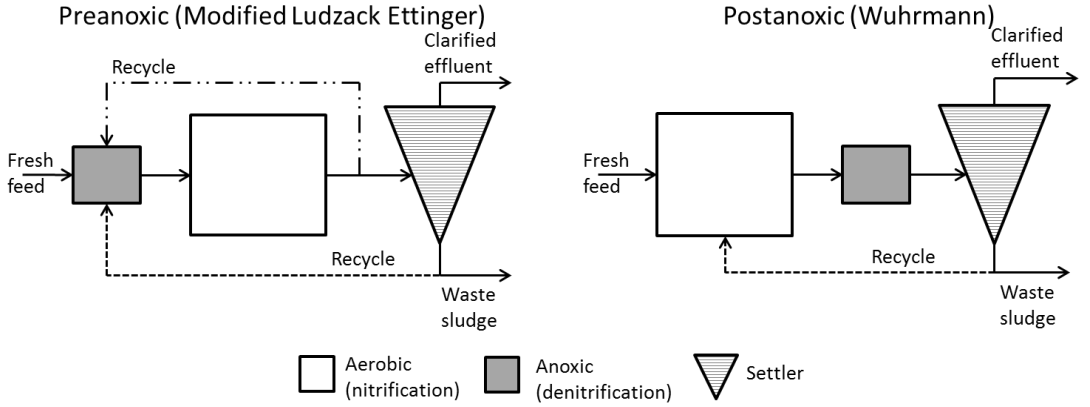

Figure 7-20 Pre- and post-anoxic activated sludge wastewater treatment plant configurations

Another approach to biological nitrogen removal is the use of a single tank that has aeration and non-aeration modes – the completely stirred alternating aerobic-anoxic (AAA) process (Balku and Berber 2006). In this system, the tank may be aerated for double the time that it is not; Balku and Berber's model uses a sequence

of 0.9 h non-aerated plus 1.8 h aerated, and achieves an effluent value of 6.3 g NO_3-N m^{-3} (mg/L) after 20 days in the aeration tank. Considering that a half-velocity constant of K_{NO3} = 2.47 mg N L^{-1} was obtained, a concentration of 6.3 mg NO_3-N L^{-1} would be adequate for algal growth. Again, this system may be beneficial for the diversion of effluent to an algal pond as the aeration sequence may be manipulated, depending on ammonium content of the influent, to favour a higher concentration of nitrate in the effluent. If the non-aerated period is reduced, or if an aerated period comes last in the sequence, then nitrate may not be fully denitrified and available for uptake by algal cells.

7.3.2 Further work

The results presented here could be strengthened in a number of ways. Initially, it would be interesting to repeat the nitrate and ammonium experiments to verify the results using an alternative species of algae with which to compare parameter values. It is impossible to predict from these results whether the K_S and μ_{max} values are typical for all species of algae, and a model that is suitable for many different species would be of most use to industry worldwide. Considering Table 21, the K_{NO3} and K_{NH4} parameter values come in at the lower end of the experimental concentration gradient. It may, therefore, be beneficial to reproduce these experiments with a narrower concentration gradient in order to examine algal growth at a more detailed level – say from 0-0.24 mM N – at intervals of 0.03 mM.

Another interesting experiment would be to examine the behaviour of algal growth at concentrations of carbon dioxide below typical atmospheric concentration, i.e. in the range of 0-0.6 mg CO_2 L^{-1}. This could be achieved by sparging and either aerating with a gas containing a known concentration of CO_2, or adding bicarbonate to produce a range of concentrations. At low levels of dissolved carbon dioxide, it has been assumed that growth follows the same pattern as nitrate, although in the experiments above the consequences of nutrient limitation have been measured by considering only a single nutrient at a time. If two nutrients were considered concurrently, we could gain insights into how low levels of nutrients limit algal growth or promote growth in the face of nutrient excess. To determine dependent

or independent colimitation of nitrate and carbon dioxide, for example, the concentration of nitrate could be varied at both high and low levels of carbon dioxide, and vice versa. This would provide a more detailed picture of when algal growth might stall and what actions can be taken to enhance growth under non-ideal conditions.

Other soluble substrates that are found in treated wastewater could also be the focus for further experimentation. For example, the Activated Sludge Model No. 2d presents a model that allows for simulation of biological phosphorus removal within activated sludge systems (Henze et al. 2000). Replacement of ASM3 in this work with $ASM2_D$, combined with detailed rate information on algal growth with phosphorus would provide the modeller with an alternative approach where biological phosphorus removal is of particular interest. In addition to this, algae may also derive additional energy for enhanced growth by heterotrophic utilisation of the biodegradable organic substrates found in treated wastewater. Although these will be at low levels in the secondary effluent flowing into the algal pond, there may be some additional growth on residual organic compounds not fully removed by the activated sludge process.

Specific data regarding the inhibition of growth by dissolved oxygen may also be a useful addition to the model. In this work, an inhibition parameter was adopted from the work of Marquez et al. (1995) that was determined for the cyanobacterium, *Spirulina platensis*. The method of sparging the algal culture with nitrogen and then oxygen, and using a dissolved oxygen sensor, would enable the determination of an inhibition constant for *Chlorella sp*. However, this idea is perhaps more relevant to cultures grown in tubular photo-bioreactors where there is no interaction with the environment and a build-up of O_2 is more likely; the culture instead passes though gas exchangers to remove O_2 and add CO_2 to the medium.

7.3.3 Summary

The algal growth rates presented here could be pessimistic since only photoautotrophic growth of the microalgae is considered – any possible

heterotrophic growth of the algae on the remaining soluble carbon substrates in the wastewater effluent has been ignored. However, the steady state value of S_{S_pl} obtained from the model (see Chapter 8) is low compared to that required for rapid heterotrophic growth. For example, experiments with glucose (Wan et al. 2011) reveal an optimum concentration of 10 g/L is beneficial for improved lipid yield. The organic substrate concentration in the algal pond is only 0.17 g/m^3 (mg/L), which is in agreement with Wang et al. (2010) who regards secondary effluent as having no significant carbon content. Still, these residual carbon substrates may contribute something to the sustained growth of algae in the integrated pond, for which further research is required.

Nevertheless, the data gathered in these experiments may be used to assist in the production of a suitable growth medium from wastewater effluent. Following treatment, the nitrate concentration should be measured to ascertain whether it is sufficient for algal growth. Supposing a dissolved nitrate concentration of 6.3 g NO_3-N m^{-3} was typical of secondary effluents arising from the activated sludge process (Balku and Berber 2006), this nitrate concentration would be sufficient to sustain algal growth, as the experimental results show that growth is switched on when the concentration of nitrate nitrogen is between 1.65-3.29 mg L^{-1}. Should a nitrate level be deemed insufficient for an algal culture to reach its maximum growth rate, it may be possible to adjust the plant settings to decrease nitrate removal. The addition of a synthetic nitrate component may also be considered if the cost of the supplement was outweighed by increased revenue from increased algal biomass production. Otherwise, toleration of slower growth, to avoid the extra cost of nitrate addition, may be preferable.

On the other hand, should the nitrate level far exceed algal requirements, dilution of the effluent, possibly with seawater, may be considered. This would increase the options available with respect to the species of algae that could be used in the process, as the plant operator would no longer be restricted to freshwater algae. It should be noted, however, that a marine alga may be undesirable in the wastewater treatment setting if AD forms part of the overall plant design. This is because high levels of sodium chloride in the growth medium of marine species can

be toxic to anaerobic microflora and can inhibit methane production (Sialve et al. 2009; Schwede et al. 2013).

In these experiments, the ability of *Chlorella sp*. to utilise dissolved carbon dioxide at elevated levels has been demonstrated. Although no measurements have been taken to determine the exact amount of carbon dioxide taken up by the algae, it can be seen by the increased growth rate that algae are able to utilise CO_2 when it is in excess. This is not the first time that algal cultures have been used to remove carbon dioxide from the atmosphere – research conducted by the USSR Academy of Sciences (Gitelson et al. 1976) showed that *Chlorella sp*. can be used to help maintain air quality within a hermetically sealed space, in which three men lived for a period of six months. Taking advantage of this particular quality, microalgal cultures may be used to help reduce the carbon footprint of wastewater treatment plants at the same time as producing an alternative to fossil fuels.

Many species of freshwater algae are known to contain lipid suitable for biodiesel production; these include *Botryococcus braunii*, *Nitzschia sp*. and other species of *Chlorella* (Belcher and Swale 1976; Chisti 2007). Other freshwater algae that may be considered for biodiesel production are *Chlamydomonas reinhardtii* (Hu et al. 2008; Li et al. 2010) and *Scenedesmus obliquus* (Gouveia and Oliveira 2009). Further research is necessary to determine the most suitable species of freshwater algae for growth in typical UK wastewater effluent; in addition to this, management of the use of a marine alga and the requisite manipulation with seawater on a typical UK wastewater treatment plant may be worthy of further research.

CHAPTER 8 - ACTIVATED SLUDGE ALGAL POND MODEL VERSION 3

8.1 Introduction

Following on from the laboratory work, the results of which can be seen in Chapter 7, the next stage of the modelling process was to include the experimentally-determined algal growth data in the model. This work was done in two stages: first, the liquid phases of the activated sludge and algal pond were integrated; second, algal growth expressions were added utilising dissolved substrates carried over from the activated sludge, combined with experimental data. Up until this point, the liquid phases of the two biological processes were not integrated, and the algal pond liquid phase was fixed, with no flow in or out. A screenshot of the model in Sentero can be seen in Figure 8-1.

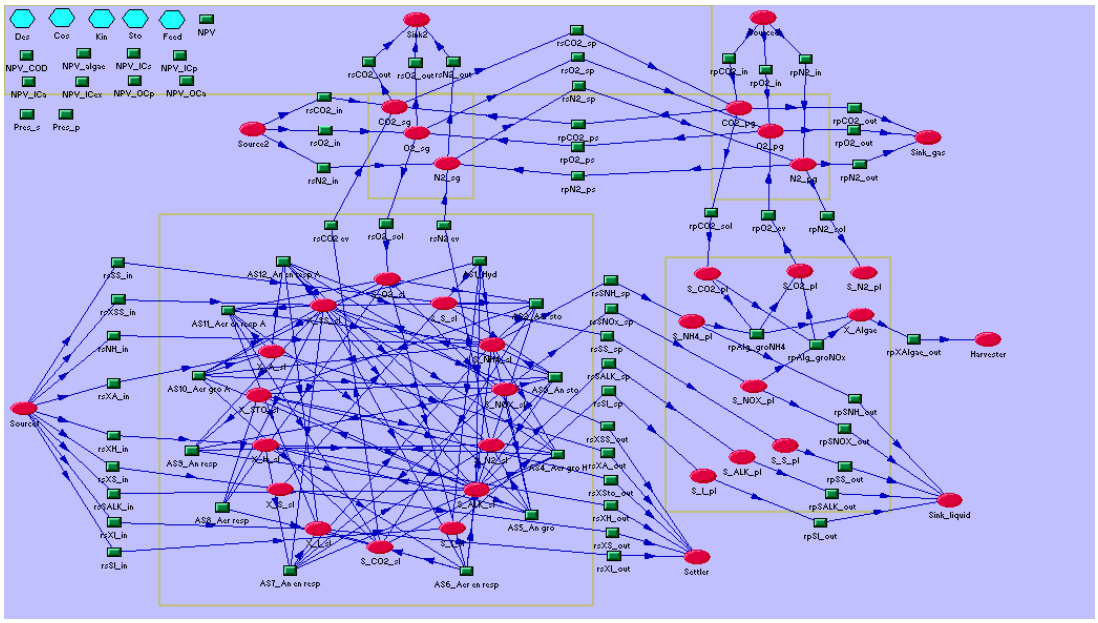

Figure 8-1 Reaction pathway of ASAPM v3

As one object of the integration is to use residual compounds within the treated wastewater to feed the algae, the transfer of water from the activated sludge to the algal pond was essential in meeting the targets of this research. The growth of algae had previously been described simply as a consumer of carbon dioxide and a producer of oxygen – integration of the liquid phase provides the opportunity to

make the algal growth rate expressions more realistic since, as well as a carbon source, algae also need a source of nitrogen to grow. This nitrogen can be provided by wastewater rather than by adding external sources such as fertilisers, which would be prohibitively expensive for large scale production. Note that the next most important element (i.e. the largest constituent of algal biomass after carbon, hydrogen, oxygen and nitrogen) is phosphorus. Although present in wastewater, its effect on algal growth is not considered in the expressions developed in this chapter. In other words, phosphorus is not deemed to be growth limiting in this work.

8.2 The Model

The form of the kinetic expressions fitted to the experimental algal growth data in this chapter are based on the type of Monod kinetics seen in the activated sludge and river water quality models. The arrangement of these expressions reflected the behaviour observed in laboratory experiments, using nitrogenous compounds typically found in treated wastewater. The process rates for growth on nitrate and ammonium were enhanced by including an expression for growth on carbon dioxide, to fully take advantage of all the benefits of integration of algal growth with wastewater treatment. The construction of these algal growth expressions will be discussed fully in Section 8.3.2.

The particulate algal substrate, X_{Alg_pl}, was added to the algal pond in order to monitor its growth; by including bulk transfer of X_{Alg_pl} into a harvester, the amount of algal biomass produced would be a measureable commodity. Another new species added to the algal pond was dissolved nitrogen, S_{N2_pl}. As an expression for the evolution of N_2 was necessary for ASAPM v2, it was felt that the equilibrium between nitrogen gas and dissolved nitrogen in the pond should be included for completeness, even though this substrate would not feature in any of the pond processes. The existing economic function for NPV_{algae} did not fit with the new algal growth expressions and the function was updated to measure the amount of algae collected in the Harvester and the CO_2 sequestered in the process. Investment and operating costs were updated to include the new liquid flows. In this final version,

all economic functions and parameter values were checked and compared to published values at the time of writing. A list of new processes and functions is given in Table 33.

Table 33 New reactions and pseudo-reactions for ASAPM v3

ρ/f	**Process/Function**	**Expression**
$rsSS_{sp}$	Flow of S_S from AS to pond	$S_{S\_sl}.L_{sp}$
$rsSNH_{sp}$	Flow of S_{NH4} from AS to pond	$S_{NH4\_sl}.L_{sp}$
$rsSNOx_{sp}$	Flow of S_{NOX} from AS to pond	$S_{NOX\_sl}.L_{sp}$
$rsSALK_{sp}$	Flow of S_{ALK} from AS to pond	$S_{ALK\_sl}.L_{sp}$
$rsSI_{sp}$	Flow of S_I from AS to pond	$S_{I\_sl}.L_{sp}$
$rpSS_{out}$	Removal of S_S	$S_{S\_pl}.Out_{pl}$
$rpSNH_{out}$	Removal of S_{NH4}	$S_{NH4\_pl}.Out_{pl}$
$rpSNOx_{out}$	Removal of S_{NOX}	$S_{NOX\_pl}.Out_{pl}$
$rpSALK_{out}$	Removal of S_{ALK}	$S_{ALK\_pl}.Out_{pl}$
$rpSI_{out}$	Removal of S_I	$S_{I\_pl}.Out_{pl}$
$rpN2_{sol}$	Dissolution of N_2 in algal pond	$V_{pl}.kLa_p(N2_{pg}.H_{N2} - S_{N2\_pl})$
$rpAlg_{groNH4}$	Algal growth on ammonium	$\left(\left(\mu_{CO2atm}\frac{S_{CO2\_pl}^{nco2}}{K_{CO2atm}^{nco2}+S_{CO2\_pl}^{nco2}}\right)+\mu_{CO2}\left(\frac{S_{CO2\_pl}}{K_{CO2}+S_{CO2\_pl}}\right)\right)\left(\mu_{NH4}\frac{S_{NH4\_pl}^{nnh}}{K_{NH4alg}^{nnh}+S_{NH4\_pl}^{nnh}}\right)\left(\frac{K_{O2alg}}{K_{O2alg}+S_{O2\_pl}}\right)X_{Algae}$
$rpAlg_{groNOx}$	Algal growth on nitrate	$\left(\left(\mu_{CO2atm}\frac{S_{CO2\_pl}^{nco2}}{K_{CO2atm}^{nco2}+S_{CO2\_pl}^{nco2}}\right)+\mu_{CO2}\left(\frac{S_{CO2\_pl}}{K_{CO2}+S_{CO2\_pl}}\right)\right)\left(\frac{S_{NOX\_pl}^{nno}}{K_{NOXalg}^{nno}+S_{NOX\_pl}^{nno}}\right)\left(\frac{K_{O2alg}}{K_{O2alg}+S_{O2\_pl}}\right)X_{Algae}$
$rpXAlgae_{out}$	Removal of algal biomass	$X_{algae}.Out_{pl}.alpha_{pond}$
NPV_{algae}	Value of biodiesel and CO_2 sequestration	$\Gamma.days_{algae}\left(\left(r_{algae}.Harvester.oil_{pc}\right)+\left(r_{CO2}\left(\left(CO2_{sg}(In_{sg}-Out_{sg})\right)-\left(CO2_{pg}(In_{pg}-Out_{pg})\right)\right)\right)\right)$
NPV_{ICex}	Investment cost of gas/ liquid exchange system	$-c_{ex}\left(G_{sp}^{\delta_{ex}}+G_{ps}^{\delta_{ex}}+L_{sp}^{\delta_s}\right)$
NPV_{OCp}	Operating cost of liquid pumping	$\Gamma.days_{COD}\left(-\alpha_E\left(kWh(In_{sl}+Out_{sl}+L_{sp}+Out_{pl})\right)\right)$

Additional parameter values for the new expressions are shown in Table 34 and are used in combination with existing values shown in Tables 11 and 16 in Chapters 5 and 6. The table includes design parameters obtained from the optimisation of ASAPM v2 – these are used here as start-up values for version 3 but will change later in this chapter as ASAPM v3 is optimised (Section 8.3.4).

Table 34 New and/or updated parameter values for ASAPM v3

Parameter	Description	Value	Units
Design Parameters			
G_{sp}	Gas flow from sludge tank to pond	7,709	$m^3\ d^{-1}$
G_{ps}	Gas flow from pond to sludge tank	647.6	$m^3\ d^{-1}$
In_{sg}	Gas flow from air to sludge tank	7,478	$m^3\ d^{-1}$
Out_{sg}	Gas flow from sludge tank to air	22.8	$m^3\ d^{-1}$
In_{pg}	Gas flow from air to pond	286.5	$m^3\ d^{-1}$
Out_{pg}	Gas flow from pond to air	7,428	$m^3\ d^{-1}$
V_{pl}	Volume of liquid in the pond	4,500	m^3
L_{sp}	Liquid flow from sludge tank to pond	1,000	$m^3\ d^{-1}$
Out_{pl}	Liquid flow from pond	1000	$m^3\ d^{-1}$
k_La_s	Mass transfer coefficient (sludge)	240	d^{-1}
$alpha_{pond}$	Settling parameter (pond)	1	-
Kinetic Parameters			
K_{CO2atm}	Saturation constant for atmospheric CO_2	0.3	g CO_2 m^{-3}
K_{CO2}	Saturation constant for elevated CO_2	80	g CO_2 m^{-3}
K_{NOXalg}	Saturation constant for NO_3	2.47	g NO_3 m^{-3}
K_{NH4alg}	Saturation constant for NH_4	2.62	g NH_4 m^{-3}
K_{O2alg}	Saturation constant for O_2 for algae	85.12	g O_2 m^{-3}
μ_{CO2atm}	Algal max growth rate at atmospheric CO_2	0.27	d^{-1}
μ_{CO2}	Algal max growth rate for elevated CO_2	0.40	d^{-1}
μ_{NH4}	Factor for algal growth rate on NH_4	0.35	d^{-1}
*n*co2	Co-operative exponent for atmospheric CO_2	4	-
*n*no	Co-operative exponent for nitrate	4	-
*n*nh	Co-operative exponent for ammonium	2	-

Parameter	Description	Value	Units
Cost Parameters			
r_{COD}	Revenue parameter, COD treatment	0.00064	€ g^{-1} COD_{XS}
r_{CO2}	Revenue parameter, carbon trading	$4.4x10^{-6}$	€ g^{-1} C
oil_{pc}	Fraction of algal biomass available as lipid	0.25	-
Stoichiometric Parameters			
i_{CO2NOx}	CO_2 content of algae in reaction with nitrate	1.54	g CO_2 (g X_{Algae})$^{-1}$
i_{CO2NH4}	CO_2 content of algae in reaction with ammonium	1.14	g CO_2 (g X_{Algae})$^{-1}$
i_{NO3}	NO_3 content of algae	0.06	g NO_3 (g X_{Algae})$^{-1}$
i_{NH4}	NH_4 content of algae	0.06	g NH_4 (g X_{Algae})$^{-1}$
Y_{alg}	Yield of algae	1	g X_{Algae} (g N)$^{-1}$
Y_{O2NOx}	Aerobic yield of algal biomass	1.24	g O_2 (g NO_X)$^{-1}$
Y_{O2NH4}	Aerobic yield of algal biomass	0.96	g O_2 (g NH_4)$^{-1}$

The kinetic parameters for algal growth that are listed in the above table are as detailed in Chapter 7. Further discussion on how these parameters are employed can be found in Section 8.3.2 of this chapter. The stoichiometric matrix for the updated reactions of ASAPM v3 is given in Appendix G and the table above shows the stoichiometric parameters associated with the algal growth expressions that are new to this version of the model. The values for these parameters are derived from the works of Ebeling et al. (2006) and Jupsin et al. (2003) and have been named in the style of ASM3.

8.3 Results

8.3.1 Intermediate model with integrated liquid phase

The premise behind this step of the modelling development was simple: to provide dissolved nutrients from the activated sludge to the pond for algal growth. As such, the results from the activated sludge and algal pond do not differ significantly to the results from ASAPM v2 but rather form a stepping-stone to further progression of

the model. It was interesting, however, to run a simulation of the intermediate model for comparison with ASAPM v2; in doing this, the behaviour of the ASM3 model could be checked in that it was still broadly similar to the previous version and that the bulk transfer expressions were carrying the soluble ASM components though to the algal pond. In making these changes, new parameters were added that affected the NPV of the overall process. A comparison of the results can be seen in Table 35, below.

Table 35 Comparison of ASAPM v2 with ASAPM v2/3 with integrated liquid phase

ASAPM v2				**ASAPM v2/3**			
ASM3 Component (g m^{-3})				**ASM3 Component (g m^{-3})**			
S_{O2_sl}	1.4	X_{I_sl}	1,943.1	S_{O2_sl}	1.4	X_{I_sl}	1,943.1
S_{I_sl}	30.0	X_{S_sl}	57.5	S_{I_sl}	30.0	X_{S_sl}	57.5
S_{S_sl}	0.2	X_{H_sl}	1,064.4	S_{S_sl}	0.2	X_{H_sl}	1,064.4
S_{NH4_sl}	0.5	X_{STO_sl}	116.3	S_{NH4_sl}	0.5	X_{STO_sl}	116.3
S_{NOX_sl}	16.7	X_{A_sl}	58.7	S_{NOX_sl}	16.7	X_{A_sl}	58.7
S_{ALK_sl}	2.1	X_{SS_sl}	10,769.2	S_{ALK_sl}	2.1	X_{SS_sl}	10,769.2
				S_{I_pl}	30.0	S_{NOX_pl}	16.7
				S_{S_pl}	0.2	S_{ALK_pl}	2.1
				S_{NH4_pl}	0.5		
NPV (€)				**NPV (€)**			
Total	1,065,001	Annual	85,460	Total	808,521	Annual	64,879
COD	1,284,836	Algae	1,648,153	COD	1,284,836	Algae	1,648,153
ICa	-1,133	ICex	-555,734	ICa	-1,133	ICex	-787,469
ICp	-738,220	ICs	-256,519	ICp	-738,220	ICs	-256,519
OCa	-291,638	OCp	-24,745	OCa	-291,638	OCp	-49,489

For this intermediate model, it can be seen that steady-state values for the ASM3 components are the same in both versions, and this includes the concentrations of dissolved substrates that are carried through to the algal pond. Although S_I, S_S, and S_{ALK} will not be used in the algal growth rate expressions, it was felt that by including these components the model would more accurately reflect the make-up of the water in the algal pond. In doing this, further research may find a way to

include dissolved carbonaceous material in the algal growth mechanism, although this is beyond the scope of this research.

Already we can see that integrating the liquid phases of the vessels brings about an increase in apparent cost but this is only because, in ASAPM v2, the cost of providing an external nitrogen source in the form of a fertiliser was ignored. The increase in apparent cost for ASAPM v2/v3 is due to capital and pumping costs associated with delivering wastewater to the algal pond. Firstly, there is an increase in the investment costs of the exchange mechanism, ICex – although this is a one-way flow as opposed to the two-way exchange modelled in the gas phase. By including this liquid flow from the activated sludge to the algal pond, extra costs have been incurred by directing the flow of treated wastewater to another vessel for further use before being discharged. Secondly, this diversion leads to an increase in the operating costs for pumping, as liquid pumping to and from the algal pond has been included. These new liquid flows are illustrated in Figure 8-1. The increase in costs is as a result of changes made to the economic function expressions, which can be seen in Table 33, above.

8.3.2 The use of experimental results in Monod expressions

Chlorella sp. was grown in the laboratory under various conditions in order to establish the relationship between its growth and nutrients arising from wastewater treatment. The result of these experiments was a collection of kinetic expressions that describe the growth behaviour of algae on nitrate, ammonium, and carbon dioxide at both atmospheric and elevated levels. The challenge was to combine these expressions to predict algal growth in a wastewater treatment setting, utilising the nutrients available to the culture, whilst maintaining kinetic laws. In addition to the growth expressions written as a result of the experiments, it was considered necessary to include an inhibition expression for dissolved oxygen. As the concept of gas exchange between wastewater treatment and algal growth depends upon the biological reactions occurring in vessels with enclosed headspaces, there is a danger of dissolved oxygen levels becoming high enough to inhibit algal growth. To address this possibility, an oxygen inhibition constant, K_I,

was adopted from the work of Marquez et al. (1995); in this work, I use the term K_{O2alg} in agreement with ASM3 nomenclature.

Ultimately, the process rate should be made up not only of growth on nitrate or ammonium but also of growth on carbon dioxide, as both nitrogen and CO_2 are used simultaneously by the algal culture. Indeed, carbon dioxide is fundamental to photosynthesis and autotrophic growth with the availability of other nutrients enhancing the rate of growth. For this reason, it was decided that the expression for carbon dioxide should make up the basis for both growth expressions, with the nitrogen source a multiplicative enhancement to it. As mentioned in the previous paragraph, inhibition by oxygen was included to limit growth should dissolved oxygen levels in the algal pond become too high. In keeping with the ASM3 format, the process rate expression was multiplied by the substrate involved in the reaction, X_{Algae}.

The native species of *Chlorella* used in the experiments grew preferentially on nitrate (NO_3) making this growth rate arguably the more important of the two nitrogen growth expressions. The common part of both expressions for growth on either nitrogen compound is the description of growth on carbon dioxide (Equation 7-8 in Chapter 7). For nitrate, the CO_2 term should be multiplied by Equation 7-6; however, as the maximum specific growth rate for carbon dioxide at atmospheric level was deemed equivalent to the maximum specific growth rate for nitrate, μ_{NO3} was excluded as this value already appears in the expression as μ_{CO2atm}. Including the oxygen inhibition expression and multiplication by the algal substrate, the following expression is constructed for growth on nitrate:

$$\mu_{NO3} = \left(\left(\mu_{CO2atm}\frac{S_{CO2\_pl}^{nco2}}{K_{CO2atm}^{nco2}+S_{CO2\_pl}^{nco2}}\right)+\mu_{CO2}\left(\frac{S_{CO2\_pl}}{K_{CO2}+S_{CO2\_pl}}\right)\right)\left(\frac{S_{NOX\_pl}^{nno}}{K_{NOXalg}^{nno}+S_{NOX\_pl}^{nno}}\right)\left(\frac{K_{O2alg}}{K_{O2alg}+S_{O2\_pl}}\right)X_{Algae}$$

The parameter values for this expression are explained in Chapter 7 and listed in Section 8.2 above (Table 34).

As residual ammonium will appear in treated wastewater and some growth was observed on this nutrient, a second growth expression was written for algal growth using ammonium (NH_4) as the nitrogen source. Again, the overall model of growth of algae on carbon dioxide was used as the basis, which was then multiplied by the expression for growth on NH_4 (Equation 7-7). However, instead of using the empirical value of $\mu_{NH4} = 0.095\ d^{-1}$, the parameter was adjusted – becoming a factor to illustrate that maximum growth on ammonium is less than that on nitrate. This factor was calculated by dividing the value for growth on ammonium at atmospheric CO_2, μ_{NH4}, by the atmospheric CO_2 growth rate, μ_{CO2atm}, in order to cancel out the term that appears in the first part of the CO_2 expression. Again including oxygen inhibition and the algal substrate, the following expression is created:

$$\mu_{NH4} = \left(\left(\mu_{CO2atm}\frac{S_{CO2\_pl}^{nco2}}{K_{CO2atm}^{nco2}+S_{CO2\_pl}^{nco2}}\right)+\mu_{CO2}\left(\frac{S_{CO2\_pl}}{K_{CO2}+S_{CO2\_pl}}\right)\right)\left(\mu_{NH4}\frac{S_{NH4\_pl}^{nnh}}{K_{NH4alg}^{nnh}+S_{NH4\_pl}^{nnh}}\right)\left(\frac{K_{O2alg}}{K_{O2alg}+S_{O2\_pl}}\right)X_{Algae}$$

For parameter values, again see Table 34 and Chapter 7.

These process rate expressions were built into the model with integrated liquid phase, ASAPM v2/3, and their behaviour in relation to dissolved nutrients monitored. In addition to changes made to the NPV functions for liquid exchange and pumping, the expression for revenue from algae and CO_2 sequestration was also updated and the results keenly observed.

8.3.3 Model with algal growth reactions

The addition of liquid transfer, algal growth and harvesting, and the adjustment of the NPV functions to reflect these changes marked the completion of the model for this research. Following on from the results presented in Section 8.3.1, it was necessary to ascertain the behaviour of the model with the updated algal growth reactions. Would there be sufficient carbon dioxide and residual nitrate in the wastewater effluent to grow algae? Would enough algae be produced to cover the

investment and operating costs of the algal pond and exchange mechanisms? In order to answer these questions, and to ensure that the algal growth process rates functioned correctly, a simulation using existing design parameters was completed and the results considered.

Table 36 Simulation results from ASAPM v3 with new algal growth rates

Activated Sludge Tank (Component, g m^{-3})		**Algal Pond (Component, g m^{-3})**		**NPV (€)**		**Headspace Pressure (mol m^{-3})**	
S_{O2_sl}	1.4	S_{O2_pl}	7.5	Total	50,928,073	Sludge	41.284
S_{I_sl}	30.0	S_{I_pl}	30.0	Annual	4,086,669	Pond	40.924
S_{S_sl}	0.2	S_{S_pl}	0.2	COD	669,077		
S_{NH4_sl}	0.5	S_{NH4_pl}	0.4	Algae	52,414,624		
S_{N2_sl}	14.2	S_{N2_pl}	14.0	ICs	-256,519		
S_{NOX_sl}	16.6	S_{NOX_pl}	7.5	ICp	-769,341		
S_{ALK_sl}	2.1	S_{ALK_pl}	2.1	ICa	-1,172		
S_{CO2_sl}	28.4	S_{CO2_pl}	0.5	ICex	-787,469		
X_{I_sl}	1,943.0	X_{Algae}	154.3	OCa	-291,638		
X_{S_sl}	57.5	X_{Algae} in Harvester	92,176,631.7	OCp	-49,489		
X_{H_sl}	1,064.7						
X_{STO_sl}	116.3						
X_{A_sl}	58.7						
X_{SS_sl}	10,769.2						

The results in the activated sludge tank of this final integrated model compare well with results from previous models, confirming that the ASM3 component is working as intended. More interesting is the comparison between S_{NH4}, S_{NOX} and S_{CO2} from the sludge tank to the algal pond – all substrates have reduced in concentration as a result of algal growth. The change in concentration of dissolved ammonium, S_{NH4}, is quite insignificant but the reduction in S_{NOX} is quite marked. This difference is due to the species of algae that was used to create the growth models – *Chlorella sp*. grew better on nitrate than ammonium and the model is written to reflect that preference. By transferring treated wastewater that contains a relatively high

concentration of dissolved nitrate to the algal pond, its concentration has been reduced to levels normally seen with wastewater treatment that includes anoxic periods/zones. As discussed in Chapter 7 (Section 7.3.1), low levels of S_{NOX} are normally associated with targeted anoxic treatment; the growth of an alga with a preference for nitrate may reduce the need for this. Balku and Berber (2006) quote an S_{NOX} concentration of 6.3 g m^{-3} in wastewater following anoxic treatment and the final value at steady state of 7.5 g m^{-3} is very close to this value. Thus, the algae are performing the useful secondary function of tertiary wastewater treatment by reducing the nitrate level from 16.6 g m^{-3} to 7.5 g m^{-3}.

The greatest difference between the sludge tank and algal pond is in the concentration of dissolved carbon dioxide, which decreases from 28.4 to 0.5 g CO_2 m^{-3}. This is translated into a significant yield of algal biomass, producing over 92,000 kg m^{-3} during the term of the project, which provides an income of over €52,000,000 over the investment period. After an adjustment to the parameter for revenue from wastewater treatment (r_{COD}) from version 1 to 3, the NPV_{COD} is lower than in earlier versions of the model, but the algal revenue more than makes up for the decrease. It is a possibility that the concentration of algal biomass may be lower if a Monod term for algal death had been included, as seen in the River Water Quality Model (Reichert et al. 2001). However, it was decided that the death term be excluded from this model, as algae would, in practice, be harvested quickly and not allowed to reach its full life-cycle as it would in a natural environment.

Considering the headspace pressure of the vessels shown in Table 36, the existing design parameters are already very close to ideal operating flow rates; the activated sludge tank is slightly above pressure and the algal pond slightly below. In order to address this minor issue, the model was optimised using Sentero's proximate parameter tuning programme in order to balance the headspace pressure while maintaining oxygen levels in the sludge tank and a high NPV.

8.3.4 Optimisation

The design parameters carried over from ASAPM v2 worked quite successfully in ASAPM v3, with dissolved oxygen being maintained in the sludge tank at a level

sufficient to maintain the biological reactions. This in turn produced enough carbon dioxide for transfer to the algal pond, which translated into many kilograms of algal biomass and a high overall NPV. However, as the pressure in the headspaces was not balanced, it was necessary to optimise the model for this feature. As the existing model parameters appeared to be quite close to the optimum, four proximate tuning analyses with different search parameters were tried in order to find a better solution.

Firstly, the model was optimised for total NPV, pressure in the headspaces and dissolved oxygen in the sludge tank; the values were set to €5,000,000, 41 mol m^{-3}, and 3 g O_2 m^{-3} respectively. The design parameters In_{sg}, G_{sp} and Out_{pg} had a tuning range of 1-500% and parameters G_{ps}, Out_{sg} and In_{pg} had a tuning range of 1-1000%; the difference in tuning range was chosen due to the difference in magnitude of the two groups and it was the intention that the first group of gas flow values should not become too large. A step length of 1 was selected. Following consideration of the results from this optimisation, it was decided that another tuning analysis should be run with S_{Ssl} as an alternative target to dissolved oxygen; the target value was 0.1 g S_{Ssl} m^{-3} and all other profiles remained the same. However, this analysis was completely unsuccessful with no solution being in any way beneficial. (Selected results from these analyses are shown in Table 37, below.)

The third analysis returned to the profiles chosen in the first, with some slight differences in the way the analysis was set up. Firstly, the design parameters In_{sg}, G_{sp} and Out_{pg} had a tuning range of 1-200% in order to maintain these gas flow values at a manageable rate. Secondly, the weightings of the target profiles were adjusted to reflect the importance of the outcome. For example, NPV was considered to be the least important as the tuning software did not struggle to produce a high NPV value and was assigned a weighting of 10. Next came S_{O2sl}, with an importance weighting of 100, as dissolved oxygen is crucial for bacterial growth in the sludge tank. Most important was the pressure constraint, with weightings of 1000, to reflect the requirement to obey physical laws within the vessels. This analysis gave a better result but the total NPV figure was not quite as good as that

shown in Table 36, so it was decided that a further proximate tuning analysis should be initiated. A screen shot of this final analysis can be seen in Figure 8-2, below.

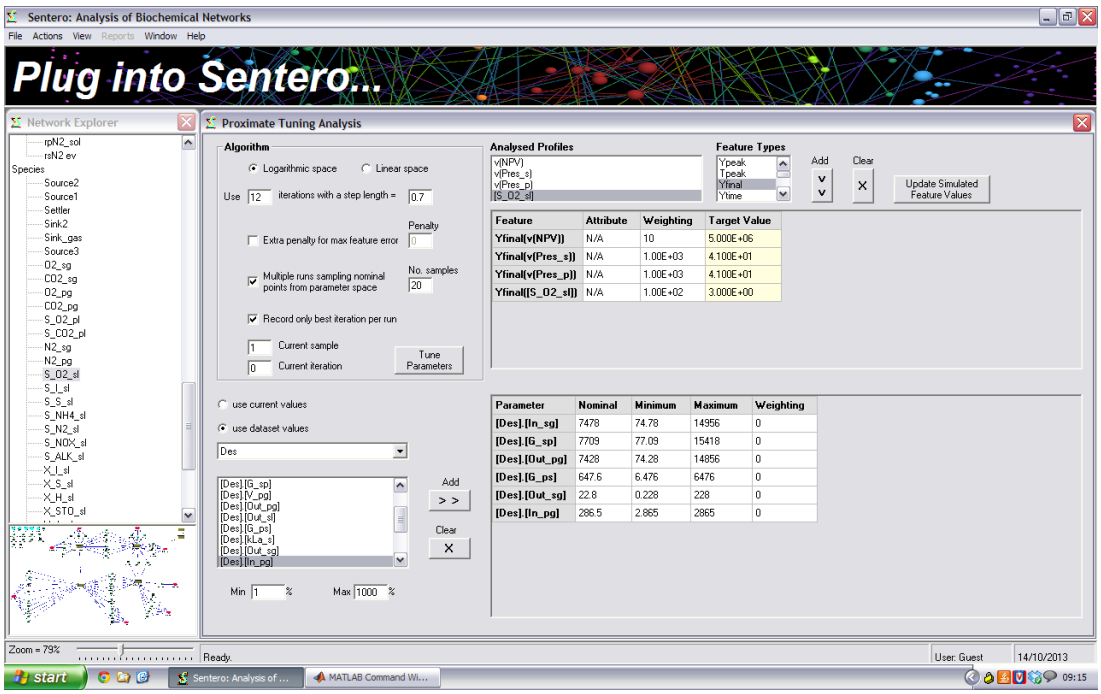

Figure 8-2 Final optimisation of ASAPM v3 with shortened step-length

This final analysis used all the same parameter profiles and values as laid out for the third analysis but with one difference – a step length of 0.7. It was anticipated that this shortened step length would enable the software to explore more carefully the space around the existing design parameter values. By taking relatively large steps of 1, the tuning software appeared to be missing the optimum value; however, as I did not wish to take such small steps that the optimum could not be reached, an intermediate value of 0.7 was chosen. A selection of results from all four tuning analyses can be seen in the table below.

Table 37 Selected results of parameter tuning analyses

	Parameter/Variable	Units	Run 1-18.3	Run 2-6.1	Run 3-12.17	Run 4-19.12
Design Parameters	G_{ps}	$m^3\ d^{-1}$	2,036.00	99.73	886.10	873.60
	G_{sp}	$m^3\ d^{-1}$	38,550.00	298.40	15,420.00	15,420.00
	In_{pg}	$m^3\ d^{-1}$	30.41	92.73	220.40	214.60
	In_{sg}	$m^3\ d^{-1}$	37,100.00	31,610.00	14,960.00	14,960.00
	Out_{pg}	$m^3\ d^{-1}$	36,550.00	783.00	14,760.00	14,770.00
	Out_{sg}	$m^3\ d^{-1}$	10.14	1.59	17.06	4.55
	Total gas pumping flow	$m^3\ d^{-1}$	**114,276.55**	**32,885.45**	**46,263.56**	**46,242.75**
Objective Function	Sludge-dissolved O_2 (S_{O2_sl})	$g\ m^{-3}$	2.70	-	2.17	2.17
	Organic substrates (S_{S_sl})	$g\ m^{-3}$	-	0.16	-	-
	$Pres_s$	$mol\ m^{-3}$	41.0	163.8	41.0	41.0
	$Pres_p$	$mol\ m^{-3}$	41.0	385.6	41.0	41.0
	Total NPV	k€	**47,920**	**1,939**	**50,870**	**50,914**

Considering the proximate parameter tuning results, the best of which are shown in Table 37, we can see that the total NPV never quite reaches the original high value found using the design parameters carried over from ASAPM v2. The value shown in Table 36 was €50,928,073 and the highest of the optimised values is €50,914,000. However, the gases in the headspace do now agree at 41 mol m^{-3} for Runs 1, 3 and 4, and all parameters for Runs 3 and 4 are very similar. As stated previously in this section, the optimisation results when tuned for organic substrates in the sludge tank (Run 2) are entirely unsuitable with high pressure and low NPV. A full steady-state simulation was run with the design parameters of Run 4-19.12 to obtain the final results for ASAPM v3.

Table 38 Simulation results of ASAPM v3 with optimisation Run 4-19.12

Activated Sludge Tank (Component, g m^{-3})		**Algal Pond (Component, g m^{-3})**		**NPV (€)**		**Headspace Pressure (mol m^{-3})**	
S_{O2_sl}	2.2	S_{O2_pl}	8.1	Total	50,914,158	Sludge	41.0
S_{I_sl}	30.0	S_{I_pl}	30.0	Annual	4,085,553	Pond	41.0
S_{S_sl}	0.2	S_{S_pl}	0.2	COD	669,079		
S_{NH4_sl}	0.4	S_{NH4_pl}	0.4	Algae	52,845,771		
S_{N2_sl}	13.9	S_{N2_pl}	13.8	ICs	-256,519		
S_{NOX_sl}	18.3	S_{NOX_pl}	9.0	ICp	-769,341		
S_{ALK_sl}	2.2	S_{ALKpsl}	2.2	ICa	-1,172		
S_{CO2_sl}	16.1	S_{CO2_pl}	0.5	ICex	-952,044		
X_{I_sl}	1,950.0	X_{Algae}	155.5	OCa	-572,128		
X_{S_sl}	57.6	X_{Algae} in Harvester	92,934,184.1	OCp	-49,489		
X_{H_sl}	1,050.3						
X_{STO_sl}	115.0						
X_{A_sl}	58.6						
X_{SS_sl}	10,768.4						

If the results from the optimised model are compared with the results prior to optimisation, it can be seen that the component concentration values for the activated sludge and algal ponds are broadly similar. The revenue for the treatment of wastewater (NPV_{COD}) is the same as the value seen in Table 36 and that, along with the dissolved and particulate activated sludge substrate concentrations, demonstrates that the ASM3 part of the model is functioning correctly. The change in gas flows has led to an increase in algal productivity, with the harvester containing a greater volume of algal biomass and the NPV_{Algae} value being slightly higher than seen previously. Both headspace values now come in at 41.0 mol m^{-3}; however, achieving this balance at the same time as maintaining S_{O2_sl} has led to an overall decrease in total NPV.

Looking back at the optimisation results for ASAPM v2 (Table 19), the optimum solution used a total gas pumping flow of 23,571.90 m^3 d^{-1}; the total gas pumping

flow required for ASAPM v3 was 46,242.75 m^3 d^{-1}. This doubling of gas flow as led to an increase in investment and operating costs and, in turn, a slight reduction in total NPV. Specifically, the costs that have risen are the investment cost of the gas/liquid exchange system (NPV_{ICex}) and the operating cost of aeration (NPV_{OCa}). The investment cost functions have the basic structure $IC_p = c_p Z_p^{\delta p}$, where c_p and δ_p are cost parameters and Z_p is the equipment characteristic dimension for unit p (Alasino et al. 2007). For this novel exchange system between the sludge tank and the algal pond, the characteristic quantity is flowrate, be that liquid (L_{sp}) or gas (G_{sp} and G_{ps}). As the flowrates between the tank headspaces have increased, installation costs should also rise to accommodate this extra capacity for pumping and pressure. Perhaps more intuitively, the operating costs of the aeration system have risen; NPV_{OCa}, which includes all gas flowrates, calculates the cost of aeration by multiplication with the energy term, *kWh*, and its corresponding unitary operation cost, α_E.

Although the investment cost of the exchange system has risen by almost 21% and the aeration costs by just over 96%, Total NPV is hardly affected at all. The value obtained by the non-optimised model was €50,928,073 (Table 36) with the optimised model reaching €50,914,158; this is a reduction of €13,915 over the project tem (20 years), or €1,117 per year. In percentage terms, the requirement for a balanced headspace costs the project approximately 0.027%.

8.4 Sensitivity Analysis

The Sentero modelling software allows us to calculate the effects of selected parameters upon the model outputs – i.e. the sensitivity of a function or species concentration to a change in a particular parameter. The parameters that give the model its novelty are of most interest in this work, and this would include design parameters for the gas exchange system and parameters that have been derived from experimental results. Additionally, it would be interesting to consider the effect of some cost parameters such as energy costs, revenue parameters and the percentage of oil recoverable from the algal cell.

To produce a sensitivity analysis, the Dynamic Metabolic Control Analysis function on Sentero is used and a local sensitivity analysis can be carried out for each output. In the example shown in Figure 8-3 below, a local sensitivity analysis will be calculated for three features: NPV, dissolved oxygen in the sludge tank (S_{O2_sl}) and dissolved carbon dioxide in the pond (S_{CO2_pl}). The analysis will be based on the perturbation, by 0.1% in this example, of selected parameters chosen from the Design Parameters dataset. In this work, first order sensitivities will be calculated and reported. Several analyses were run using selected parameters from the different datasets and choosing relevant outputs; two perturbation values (0.1% and 20.0%) were chosen for comparison. In producing such a large volume of data, only the sensitivities with a value greater than 0.05% will be highlighted and discussed; however all data is presented in Tables 39-41, below.

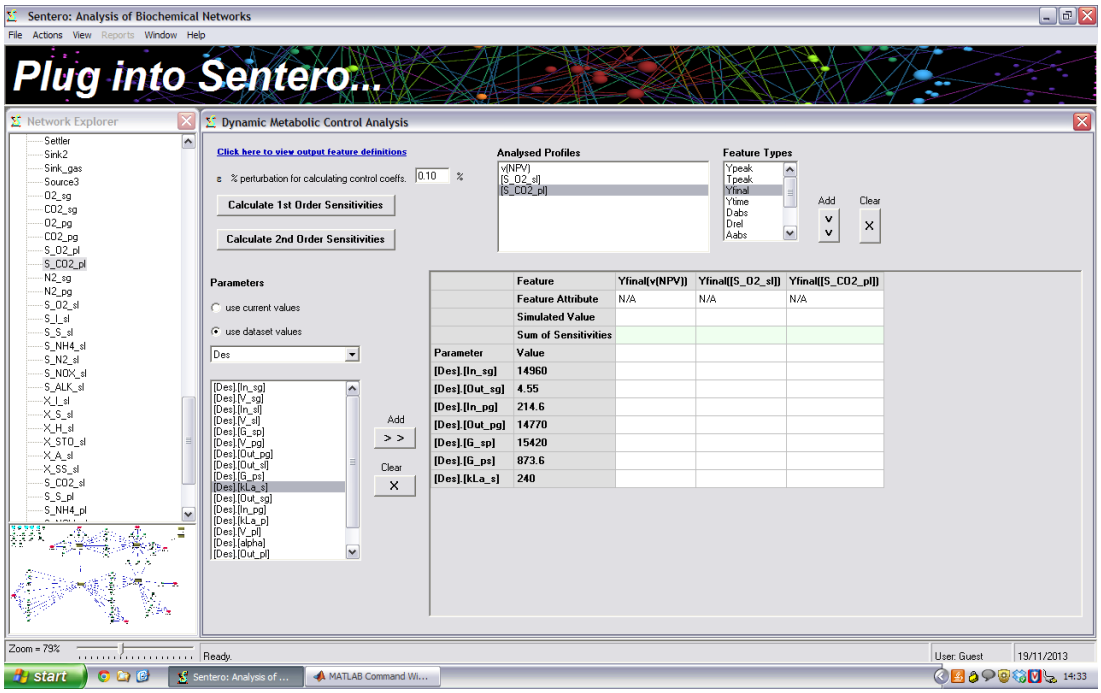

Figure 8-3 Screen shot of Dynamic Metabolic Control (Local Sensitivity) Analysis

Firstly, the Design Parameters dataset is considered, choosing the parameters that control the gas exchange system; because the oxygen mass transfer coefficient is very important for the treatment of domestic wastewater, the parameter k_La_s was also included in the analysis. Outputs that are affected by these parameters include the NPV functions and the concentrations of sludge-dissolved oxygen and pond-dissolved carbon dioxide. The headspace pressure of both vessels should also be

taken into account, which impacts indirectly upon the NPV of the project, as $Pres_s$ and $Pres_p$ are employed as equality constraints when optimising the model (see Section 5.3.2 Optimisation with NPV as objective function). It is entirely possible that a true optimum may never be found by the Proximate Parameter Tuning algorithm when an equality constraint is applied – in this case when $Pres_s$ and $Pres_p$ are equal to 41 mol m^{-3} – the result being a much narrower range in which parameters may be tuned. The results of the analysis of the Design Parameter dataset can be found in Table 39.

Table 39 Sensitivity analysis of steady state model outputs with design parameters at perturbation values of 0.1% and 20.0% (in brackets)

	NPV	**NPV_{COD}**	**NPV_{algae}**	**NPV_{ICs}**	**NPV_{ICp}**	**NPV_{ICa}**	**NPV_{ICex}**	**NPV_{OCa}**	**NPV_{OCp}**	**S_{O2_sl}**	**S_{CO2_pl}**	**$Pres_s$**	**$Pres_p$**
In_{sg}	1.70E-01 (2.22E-01)	2.10E-05 (2.82E-05)	1.68E-01 (2.18E-01)	0 (0)	0 (0)	0 (0)	0 (0)	-3.24E-01 (-3.24E-01)	0 (0)	3.46E+00 (3.11E+00)	1.76E-01 (1.46E-02)	1.01E+00 (1.01E+00)	1.00E+00 (9.99E-01)
Out_{sg}	-3.51E-04 (-3.51E-04)	-5.71E-09 (-5.71E-09)	-3.37E-04 (-3.37E-04)	0 (0)	0 (0)	0 (0)	0 (0)	-9.84E-05 (-9.84E-05)	0 (0)	-9.39E-04 (-9.39E-04)	-6.94E-05 (-6.94E-05)	-3.11E-04 (-3.11E-04)	-3.07E-04 (-3.07E-04)
G_{sp}	-1.27E-01 (-1.35E-01)	-1.82E-05 (-1.94E-05)	-1.14E-01 (-1.22E-01)	0 (0)	0 (0)	0 (0)	-2.54E-01 (-2.57E-01)	-3.33E-01 (-3.33E-01)	0 (0)	-3.00E+00 (-2.68E+00)	2.65E-02 (5.75E-02)	-9.96E-01 (-9.96E-01)	3.66E-03 (3.86E-03)
G_{ps}	5.48E-03 (5.47E-03)	1.09E-06 (1.09E-06)	6.80E-03 (6.81E-03)	0 (0)	0 (0)	0 (0)	-7.34E-02 (-7.39E-02)	-1.89E-02 (-1.89E-02)	0 (0)	1.78E-01 (1.78E-01)	-1.57E-03 (-1.58E-03)	5.64E-02 (5.64E-02)	-2.17E-04 (-2.17E-04)
In_{pg}	5.91E-04 (5.91E-04)	1.69E-08 (1.69E-08)	6.19E-04 (6.19E-04)	0 (0)	0 (0)	0 (0)	0 (0)	-4.64E-03 (-4.64E-03)	0 (0)	2.77E-03 (2.77E-03)	2.94E-03 (2.94E-03)	8.13E-04 (8.13E-04)	1.44E-02 (1.44E-02)
Out_{pg}	-7.85E-02 (-7.85E-02)	-1.09E-06 (-1.12E-06)	-7.22E-02 (-7.22E-02)	0 (0)	0 (0)	0 (0)	0 (0)	-3.19E-01 (-3.19E-01)	0 (0)	-1.79E-01 (-1.85E-01)	-1.92E-01 (-2.06E-01)	-5.64E-02 (-5.87E-02)	-1.00E+00 (-1.00E+00)
k_La_s	8.36E-02 (1.11E-01)	1.29E-05 (1.70E-05)	8.05E-02 (1.07E-01)	0 (0)	0 (0)	-1.44E-01 (-1.45E-01)	0 (0)	0 (0)	0 (0)	2.12E+00 (2.19E+00)	-1.86E-02 (-5.81E-02)	-2.48E-03 (-3.22E-03)	-2.37E-03 (-3.08E-03)

NB: sensitivities greater than 0.05 are highlighted

Looking at the values produced by the Control Analysis function, the first thing we notice is that the numbers are small – the largest being 3.46 for the sensitivity of S_{O2_sl} to In_{sg}. However, this value becomes smaller still when the perturbation is taken into consideration:

$$\%\ perturbation \times sensitivity = \%\ change\ in\ output \qquad \textbf{Equation 8-1}$$

So, continuing with this example, a 0.1% perturbation in In_{sg} would bring about a 0.346% change in dissolved oxygen in the sludge tank (S_{O2_sl}). Taking this into account, only values greater than 0.05 will be considered (highlighted in the results tables). Among the design parameters analysed, roughly one third of the results were deemed to be significant (27 out of 91 results) and of these, the values obtained were mostly negative (16 negative values vs. 11 positive). In theory, if an unconstrained optimum solution has been found by the Proximate Parameter Tuning algorithm, all sensitivity values would be negative as the parameter value is ideal and any adjustment would elicit a poorer result from the chosen output. However, the optimum solution was constrained to a narrow band of solutions, where $Pres_s$ and $Pres_p$ were equal to 41 mol m^{-3}. On a peak representing the optimum solution, the point where the equality constraint is satisfied may not be the highest point of the peak but the highest point that can be achieved within the given boundaries. This would then produce a positive value from a sensitivity analysis – where a percentage change in a parameter would produce a higher result for a given output. However, changing this parameter value may not then satisfy the equality constraint, making adjustment to the parameter unacceptable. Where sensitivity values are negative, it can be assumed that the parameter value is already at its optimum.

If we look along the rows of Table 39, it can be seen that the model is not sensitive to changes in the parameters Out_{sg} and In_{pg} – even at the higher perturbation of 20%. This can be explained by the fact that the value of these parameters is relatively low in comparison to the other gas flows (see Table 37, Run 4-19.12). Looking down the columns confirms that gas flow and aeration parameters do not affect the investment cost of the activated sludge tank and the algal pond (NPV_{ICs}

and NPV_{ICp}), nor do they affect the operating cost of the liquid pumping (NPV_{OCp}). Unsurprisingly, an increase in the aeration capacity of the sludge tank (k_La_s) and the gas exchange system (G_{sp} and G_{ps}) would lead to an increase the corresponding investment costs (NPV_{ICa} and NPV_{ICex}). The most significant parameters with respect to the operating cost of the aeration system (NPV_{OCa}) are In_{sg}, G_{sp} and Out_{pg} due to their relatively high starting point, meaning that even a 0.1% perturbation of the parameter value will equate to a noticeable increase in cost. It is interesting that no increase in any parameter leads to a significant increase in the revenue from wastewater treatment (NPV_{COD}). Even by adjusting parameters that increase dissolved oxygen in the sludge tank does not affect wastewater treatment revenue. This result implies that the reactions related to NPV_{COD}, i.e. the ASM3 reactions, are efficient and robust enough not to be significantly affected by external influences.

The outputs with the highest sensitivities are dissolved oxygen in the sludge tank (S_{O2_sl}) and the headspace pressures ($Pres_s$ and $Pres_p$). It is possible to increase dissolved oxygen by 0.346% with a 0.1% increase in In_{sg}, and 0.212% with a 0.1% increase in k_La_s. However, increasing In_{sg} and k_La_s increases both operating and investments costs, and any increase in In_{sg} increases both $Pres_s$ and $Pres_p$ by 0.1%. Considering that there is no benefit in doing this – i.e. no corresponding increase in NPV_{COD} – there seems little point in building tanks/ponds that cope with high or low pressures when the process runs effectively at atmospheric pressure. S_{O2_sl} may also be increased with an increase in G_{ps} but again, there is no monetary benefit to this - just an increase in operating costs and an imbalance in $Pres_s$. G_{sp} and Out_{pg} also affect $Pres_s$ and $Pres_p$ quite strongly and both effects are negative as gas is discharged from the vessels. As all sensitivity values are negative for these two parameters, it can be assumed that their values are optimal.

Quite interesting are the increases to be made in NPV_{Algae} and the corresponding increases to overall NPV. At first glance it is not obvious why an increase in In_{sg} and k_La_s, which both increase dissolved oxygen in the sludge tank, should lead to an increase in algal revenue. Considering the model for NPV_{Algae}:

$$\Gamma.days_{algae}\Bigg(\left(r_{algae}.Harvester.oil_{pc}\right) + \Bigg(r_{CO2}\Big(\left(CO2_{sg}\left(In_{sg}-Out_{sg}\right)\right)-\left(CO2_{pg}\left(In_{pg}-Out_{pg}\right)\right)\Big)\Bigg)\Bigg)$$

we can see that it includes a term for revenue from CO_2 sequestration (r_{CO2}). By increasing the flow of air into the sludge tank, the concentration of carbon dioxide in the headspace ($CO2_{sg}$) is also increased, thus boosting the revenue from carbon sequestration as the CO_2 is transferred from the sludge tank to the algal pond. In addition to this effect, k_La_s increases the dissolution of CO_2 from the sludge liquid into the headspace, again to be transferred to the algal pond. This can be seen in the process rate for the evolution of dissolved carbon dioxide ($rsCO2_{ev}$):

$$V_{sl}(kLa_s \times 0.91)\left(CO2_{sl}-CO2_{sg}.H_{CO2}\right)$$

So, whilst the increase in NPV_{Algae} may not be directly related to an increase in algal growth, by increasing the concentration of carbon dioxide in the headspace the revenue from carbon sequestration can be increased.

Secondly, the Cost Parameters dataset is considered, choosing parameters that are liable to fluctuation within the economy. This includes the updating term (Γ), unitary operation cost (α_E) and revenues from wastewater treatment, algal biodiesel and carbon sequestration. The effect of the percentage of available algal oil inside the algal cell (oil_{pc}) is also taken into account.

Table 40 Sensitivity analysis of steady state model outputs with cost parameters at perturbation values of 0.1% and 20.0% (in brackets)

	NPV	**NPV_{COD}**	**NPV_{algae}**	**NPV_{OCa}**	**NPV_{OCp}**
Γ	1.04E+00 (1.04E+00)	1.00E+00 (1.00E+00)	1.00E+00 (1.00E+00)	-1.00E+00 (-1.00E+00)	-1.00E+00 (-1.00E+00)
oil_{pc}	1.04E+00 (1.04E+00)	0 (0)	1.00E+00 (1.00E+00)	0 (0)	0 (0)
α_E	-1.22E-02 (-1.22E-02)	0 (0)	0 (0)	-1.00E+00 (-1.00E+00)	-1.00E+00 (-1.00E+00)
r_{COD}	1.31E-02 (1.31E-02)	1.00E+00 (1.00E+00)	0 (0)	0 (0)	0 (0)
r_{algae}	1.04E+00 (1.04E+00)	0 (0)	1.00E+00 (1.00E+00)	0 (0)	0 (0)
r_{CO2}	1.05E-04 (1.05E-04)	0 (0)	1.02E-04 (1.02E-04)	0 (0)	0 (0)

The sensitivity analysis of the cost parameters is much more straightforward than the design parameters, with all significant sensitivities (greater than 0.05) having a value proportional to the perturbation of the parameter, i.e. the sensitivity is equal, or approximately equal, to 1. The sensitivity values here are intuitive – an increase in α_E leads to an increase in operating costs, and increases in r_{COD} and r_{algae} lead to increases in NPV_{COD} and NPV_{Algae} respectively. Algal revenue can also be increased by a change in the percentage of lipid recovered from the algal cell (oil_{pc}). This parameter value is currently estimated at 0.25 and could be increased by either: selection of an algal species that has a very high lipid content, or an improvement in the process to extract lipid from the cell. We can see from Table 40 that NPV is not sensitive to changes in r_{CO2} – revenue derived from carbon trading is currently very low, with a parameter value of $r_{CO2} = 4.4x10^{-6}$ € g^{-1} C (Bloomberg 2013), meaning that even a 20% increase in this revenue would not significantly improve NPV.

The updating term, Γ, affects all NPV functions detailed in Table 40, and the change in NPV is proportional to the perturbation in parameter in each instance. The updating term is used to compute costs to the present value and is related to the

interest rate (or discount rate, *id*), as illustrated in Equation 3-11, Section 3.6 Process Economics. It is the sensitivity to the *id* component that is the most important, with the possibility for fluctuation in global interest rates to affect the overall Net Present Value of the project.

Finally, the Kinetic Parameters dataset is considered, focusing on parameters obtained experimentally using *Chlorella sp*. In this sensitivity analysis, the effects of specific growth rate (μ), saturation constant (K) and co-operative exponent (n) on NPV functions, substrate concentration and headspace pressure were investigated; the results are shown in Table 41, below. There are very few significant sensitivity values in this analysis, with only 14 out of 121 being greater than 0.05 for a perturbation of 0.1% and 15 out of 121 for a 20% perturbation. Looking along the rows, the most significant parameter is the specific growth rate for carbon dioxide at atmospheric concentration (μ_{CO2atm}) with the 20% perturbation values being particularly high. The parameters for growth at elevated levels of carbon dioxide, μ_{CO2} and K_{CO2}, do not impact significantly upon any of the outputs examined here. If we look down the columns of Table 41, it can be seen that the outputs most affected by changes in parameter values are dissolved carbon dioxide and ammonium in the algal pond (S_{CO2_pl} and S_{NH4_pl}). Dissolved oxygen in the sludge liquid (S_{O2_sl}), NPV of wastewater treatment (NPV_{COD}) and the headspace pressures ($Pres_s$ and $Pres_p$) are not significantly affected by any parameter.

Perhaps the most interesting parameter in this analysis is the specific growth rate for carbon dioxide at atmospheric concentration (μ_{CO2atm}) and its capacity to increase NPV and NPV_{Algae}. A 20% perturbation in this parameter could result in an increase in NPV of over €11m (€51m x 22% = €11,220,000) which is a substantial amount, even over a project term of 20 years. To obtain the maximum increase in NPV, the parameter value would need to increase from 0.27 d^{-1} to 0.324 d^{-1}. As the model stands, μ_{CO2atm} is an estimated parameter derived from μ_{NO3} following experiments in the laboratory (see Sections 7.2.1 and 7.2.3 for details). At the time of experimentation, analysis of the results and building those results into the model, the description of algal growth for sub-atmospheric CO_2 concentration was not seen as critical since only higher than atmospheric concentrations would apply

for the algae in the integrated model. It is, therefore, difficult to predict whether this 20% increase in parameter value might be achievable without further experimentation in the laboratory. Although an increase in specific growth rate of this magnitude may not be possible for the *Chlorella sp.* used in my experiments, it may well be feasible for another species of fast-growing algae. These results agree with those of Liu, J.Y. et al. (2013) since they demonstrate that lipid productivity and therefore profitability depend on growth rate, just as much as lipid content, or perhaps more so.

Table 41 Sensitivity analysis of steady state model outputs with kinetic parameters at perturbation values of 0.1% and 20.0% (in brackets)

	NPV	NPV_{COD}	NPV_{algae}	S_{CO2_pl}	S_{NH4_pl}	S_{NOX_pl}	X_{Algae}	Harvester	$Pres_s$	$Pres_p$	S_{O2_sl}
μ_{CO2atm}	8.56E-02 (1.10E+00)	4.58E-09 (5.07E-08)	8.24E-02 (1.05E+00)	-2.24E+00 (-4.32E+00)	-1.10E-02 (-1.27E-01)	-8.57E-02 (-8.01E-01)	8.36E-02 (1.12E+00)	8.25E-02 (1.05E+00)	3.68E-06 (4.06E-05)	7.97E-05 (8.80E-04)	7.52E-04 (8.32E-03)
K_{CO2atm}	-3.75E-02 (-3.75E-02)	-1.99E-09 (-1.99E-09)	-3.61E-02 (-3.61E-02)	9.74E-01 (9.75E-01)	4.78E-03 (4.78E-03)	3.73E-02 (3.73E-02)	-3.64E-02 (-3.64E-02)	-3.61E-02 (-3.61E-02)	-1.60E-06 (-1.60E-06)	-3.46E-05 (-3.46E-05)	-3.27E-04 (-3.27E-04)
n_{co2}	1.96E-02 (2.08E-02)	1.05E-09 (1.11E-09)	1.89E-02 (2.00E-02)	-5.12E-01 (-5.30E-01)	-2.52E-03 (-2.67E-03)	-1.96E-02 (-2.08E-02)	1.91E-02 (2.03E-02)	1.89E-02 (2.00E-02)	8.42E-07 (8.94E-07)	1.82E-05 (1.94E-05)	1.72E-04 (1.83E-04)
μ_{CO2}	8.97E-04 (8.97E-04)	4.78E-11 (4.80E-11)	8.64E-04 (8.64E-04)	-2.35E-02 (-2.35E-02)	-1.15E-04 (-1.15E-04)	-8.99E-04 (-8.99E-04)	8.76E-04 (8.77E-04)	8.64E-04 (8.64E-04)	3.86E-08 (3.86E-08)	8.35E-07 (8.35E-07)	7.88E-06 (7.89E-06)
K_{CO2}	-8.91E-04 (-9.23E-04)	-4.85E-11 (-4.94E-11)	-8.58E-04 (-8.89E-04)	2.33E-02 (2.42E-02)	1.15E-04 (1.19E-04)	8.93E-04 (9.25E-04)	-8.71E-04 (-9.02E-04)	-8.59E-04 (-8.89E-04)	-3.83E-08 (-3.97E-08)	-8.30E-07 (-8.59E-07)	-7.83E-06 (-8.11E-06)
K_{NOXalg}	-1.90E-03 (2.02E-03)	-1.02E-10 (-1.08E-10)	-1.83E-03 (-1.95E-03)	5.02E-02 (5.27E-02)	-2.56E-03 (-2.65E-03)	2.00E-03 (2.11E-03)	-1.85E-03 (-1.94E-03)	-1.83E-03 (-1.95E-03)	-8.04E-08 (-8.47E-08)	-1.75E-06 (-1.84E-06)	-1.68E-05 (-1.77E-05)
n_{no}	2.44E-03 (2.99E-03)	1.33E-10 (1.63E-10)	2.35E-03 (2.88E-03)	-6.51E-02 (-7.91E-02)	3.31E-03 (3.92E-03)	-2.60E-03 (-3.18E-03)	2.39E-03 (2.39E-03)	2.35E-03 (2.88E-03)	1.04E-07 (1.28E-07)	2.27E-06 (2.78E-06)	2.18E-05 (2.67E-05)
K_{O2alg}	7.52E-03 (8.18E-03)	4.02E-10 (4.37E-10)	7.25E-03 (7.88E-03)	-1.97E-01 (2.12E-01)	-9.67E-04 (-1.05E-03)	-7.54E-03 (-8.19E-03)	7.35E-03 (7.99E-03)	7.25E-03 (7.88E-03)	3.23E-07 (3.52E-07)	7.00E-06 (7.61E-06)	6.61E-05 (7.19E-05)
μ_{NH4}	2.59E-03 (2.62E-03)	3.11E-11 (3.21E-11)	2.50E-03 (2.52E-03)	-1.12E-02 (-1.13E-02)	-1.26E-01 (-1.26E-01)	3.28E-03 (3.29E-03)	1.68E-03 (1.68E-03)	2.50E-03 (2.52E-03)	1.10E-07 (1.10E-07)	2.04E-06 (2.04E-06)	5.26E-06 (5.27E-06)
K_{NH4alg}	-3.80E-03 (-3.90E-03)	-6.25E-11 (-6.47E-11)	-3.66E-03 (-3.76E-03)	2.20E-02 (2.27E-02)	2.47E-01 (2.58E-01)	-6.45E-03 (-6.66E-03)	-3.30E-03 (-3.40E-03)	-3.66E-03 (-3.76E-03)	-2.15E-07 (-2.22E-07)	-4.00E-06 (-4.13E-06)	-1.03E-05 (-1.06E-05)
n_{nh}	-6.60E-03 (-6.80E-03)	-1.25E-10 (-1.28E-10)	-6.36E-03 (-6.55E-03)	4.37E-02 (4.48E-02)	4.91E-01 (5.19E-01)	-1.28E-02 (-1.32E-02)	-6.54E-03 (-6.74E-03)	-6.36E-03 (-6.55E-03)	-4.27E-07 (-4.40E-07)	-7.93E-06 (-8.18E-06)	-2.05E-05 (-2.10E-05)

The output most often affected by changes in parameter value is dissolved carbon dioxide, S_{CO2_pl}. The previous paragraph discusses how an increase in μ_{CO2atm} has the potential to substantially increase NPV – with this comes greater demand for dissolved carbon dioxide, leading to a strongly negative response in the sensitivity analysis for this substrate. An increase in the co-operative exponent, i.e. n_{co2} or n_{no}, will also increase the rate of growth, having a negative impact on dissolved CO_2 and positive, if small, impact upon X_{Algae}. However, we can see the opposite of this is true for n_{nh} and its positive effect upon S_{NH4_pl}. Increasing this co-operative exponent slows growth, perhaps due to the sigmoidal nature of the growth curve, to a point where X_{Algae} and harvested algae are negatively affected. Conversely, this is not true for an increase in μ_{NH4}, due to the initial parameter value being so small as not to have an immediate effect on dissolved ammonium (see Section 8.3.2 for details of how μ_{NH4} is calculated).

An increase in the saturation constant, *K*, will have the effect of inhibiting growth and this is confirmed by the positive sensitivity results in dissolved carbon dioxide, ammonium and nitrate, and the negative sensitivity in X_{Algae}. An increase in *K* will have the effect of increasing the nutrient concentration at which the cells grow efficiently, therefore making the environment less amenable to algal growth. The only saturation constant for which this is not the case is the inhibition constant K_{O2alg}. Raising this parameter increases the concentration of dissolved oxygen that algae can tolerate, therefore allowing growth to continue for longer. The best way to determine if any of these parameter values may be changed is to further investigate algal behaviour in the laboratory. My experiments used a freshwater alga that is native to northern England and prefers nitrate to ammonium as its nitrogen source. Further experiments, either with *Chlorella sp*. or another species, might confirm the accuracy of the kinetic growth parameters or dictate that they should be adjusted to show a different prediction of growth and NPV.

8.5 Discussion

8.5.1 Reuse of treated wastewater and utilisation of nutrients

The broad aim of this research is to determine how well microalgae may grow in treated wastewater in an integrated activated sludge/algal pond system. One of the main barriers to mass cultivation of algae is the life-cycle burden with respect to water use. In a study by Clarens et al. (2010), it was calculated that the burden of algae on water was 12 ± 2.4 x 10^4 m^3 per functional unit (317 GJ) of energy – a significant burden when compared to other bioenergy feedstocks such as corn, canola and switchgrass. Water is a finite resource and is continually being used and reused in the domestic water cycle. In the UK, each of us produces an average of 150 L of wastewater per day, which is diverted to one of the 9,000 wastewater treatment works in the country (Water UK 2006). This continuous and reliable influx of water makes a wastewater treatment works the ideal site to construct an algal pond. Indeed, Lundquist et al. (2010) use microalgae for the treatment of secondary wastewater in a similar manner to the use of the activated sludge process. What this research seeks to explore is not only the utility of an available volume of water but also of residual compounds therein that are necessary for algal growth.

In domestic primary effluent, there are various compounds that are vital for the growth of microalgae; within the Activated Sludge Model No. 3 these are ammonium (S_{NH4}) and nitrate (S_{NOX}). Also present in wastewater are phosphorus-containing compounds – typically phosphates -$H_2PO_4^-$ and -HPO_4^{2-}. This is reflected in the growth medium used to grow *Chlorella sp*. in the laboratory to provide the kinetic data used in the model (see Chapter 4, Table 4). Phosphates are not modelled in the activated sludge algal pond model because the sludge compartment employs ASM3, from which phosphate reactions are omitted. Biological phosphorus removal is, however, included in $ASM2_D$ – an extension of ASM2 – although this model has been published as a basis for further model development only (Henze et al. 2000). It is for this reason that ASM3 was chosen in

preference, although later models of ASAPM have the potential to include phosphates as and when the activated sludge models are updated accordingly.

ASAPM uses the suggested starting concentrations of dissolved and particulate substrates given in ASM3, which reflects typical concentrations found in settled wastewater. In addition to this, kinetic expressions are used that were written for an alga that is native to northern England and prefers nitrate to ammonium as its nitrogen source. Considering the results of the model, shown in Table 38 above, it can be seen that the concentration of ammonium flowing into the algal pond from the sludge tank is already very low and might be very quickly used up by a strain of algae that prefers ammonium as its nitrogen source. Dissolved carbon dioxide and nitrate do not suffer from short supply, as they are constantly being produced during biological wastewater treatment, whereas ammonium is being removed. We can conclude, therefore, that a typical secondary effluent would be suitable for cultivating this particular species of *Chlorella*.

The starting concentrations of dissolved and particulate substrates may be adjusted in the model to suit a particular wastewater treatment facility and its typical intake, to determine the site's suitability for an algal pond extension. For example, if the ammonium intake were particularly low, the resulting nitrate flowing through to the algal pond would likely be correspondingly low. For the species of *Chlorella* used here, this may impact upon its growth and lead to much reduced mass of algae in the Harvester. If other factors made the site amenable to the construction of an algal pond, such as water flow/volume, sufficient and suitable land, etc., then addition of an external nutrient source may be considered – although the associated cost of this would need to be included in the model. Considering again the report by Lundquist et al. (2010), where microalgae are used as the secondary step in wastewater treatment, an alga that preferred ammonium as its nitrogen source would be required. It can be recognised from these examples that the options for the integration of algal cultivation and wastewater treatment are not only as proposed in this work but may be adjusted to suit different scenarios and locations.

8.5.2 Production of realistic model for use in the WWT industry

The key factor in producing a realistic model for use in the wastewater treatment industry was the application of a full integration between the activated sludge and algal pond, i.e. utilising evolved carbon dioxide and oxygen from the biological processes through a series of mass transfer reactions. Although many authors have mentioned the use of wastewater for algal growth in their research, Stephenson et al. (2010), Lundquist et al. (2010), Clarens et al. (2010) and Fortier and Sturm (2012) to name but a few, none have mentioned the possibility of using evolved CO_2 from the wastewater treatment process itself to feed the algae in a separate pond. It is regularly proposed that flue gases from other industries, such as fossil-fired power generation, cement manufacturing and fermentation processes, etc., are used in preference to chemical-grade CO_2, although the potential to use locally-produced carbon dioxide seems to have been overlooked.

Considering the uptake of carbon dioxide by the algal substrate in ASAPM, it is evident that CO_2 is central to the process, and this is confirmed by the sensitivity analysis. Looking back at the model's results (shown in Table 38, above), the final concentration of dissolved CO_2 in the sludge tank is 16.1 g m^{-3} and upon transfer to the algal pond, reduces to 0.5 g m^{-3}. This demonstrates the importance of the provision of a carbon source when growing algae as an industrial process. In Table 41, it was observed that the substrate S_{CO2_pl}, dissolved carbon dioxide in the algal pond, was strongly affected by changes in kinetic parameter values – the specific growth rate for carbon dioxide at atmospheric concentration (μ_{CO2atm}) in particular. Its capacity to increase revenue from algae was significant and an increase in μ_{CO2atm} may well be feasible for another species of fast-growing algae. However, with this comes greater demand for dissolved carbon dioxide, for which the model presented here will predict whether sufficient carbon dioxide is available from biological wastewater treatment to sustain algal growth.

To maintain its relevance to the wastewater treatment industry, it was decided that the growth of algae with NH_4 as well as NO_3 should be included (see Jupsin et al. (2003)) even though majority of NH_4 is removed by the activated sludge process. It

transpired that the growth route with NH_4 is less important for *Chlorella sp*., as determined by the laboratory experiments detailed in Chapters 4 and 7. However, including this growth route in the model provides the greatest flexibility with regard to alternative algal species, as well as providing relevant information on the final concentration of nitrogen compounds in the wastewater prior to discharge to surface water. As previously discussed in Chapter 7 (Section 7.3.1 Availability of nutrients in treated wastewater and the use of anoxic zones) care must be taken with the use of aerobic/anoxic biological wastewater treatment with respect to algal growth. Insufficient consideration of aeration procedures may result in little or no transfer of NO_3 from the sludge tank to the algal pond, which may result in a poor algal yield.

Perhaps more importantly is the profitability of such a venture to the investing party. To this end, a model of cost and revenue streams has been included and these values have been combined to give an overall Net Present Value for the fully integrated process. Great attention to detail was required to produce a realistic and up-to-date estimate of the economics involved, ensuring that the functions were constantly updated to reflect additional liquid/gas flows and parameter values at current market rates. Fundamentally, the wastewater treatment industry would like to know if enough revenue could be generated from algae to cover the investment and operating costs. Considering the results of ASAPM v3, shown in Table 38 above, it appears that an algal pond would be a worthwhile addition to biological wastewater treatment. If NPV_{Algae} was deducted from the total NPV value and the associated costs, ICp and ICex, removed, and taking into consideration the embedded portion in the operating costs that can be attributed to the algal pond, wastewater treatment alone would roughly break even and not result in either profit or loss.

It must be taken into account, however, that this basic model is designed to run at full capacity for 365 days of the year. This is achieved by the employment of cost parameters $days_{COD}$ and $days_{algae}$, both of which are set at 365 d in this proof-of-concept model. It is a very real possibility that the algal pond would not produce as much biomass during the winter months in the United Kingdom, thereby reducing

algal revenue. It is also a possibility that the activated sludge may not run all year round and may need periods of inactivity for maintenance, etc. It is for the industrial operator to decide when using the model the correct parameter values for $days_{COD}$ and $days_{algae}$, based on the operating requirements of a specific treatment works. This may change from one country to another and, indeed, from one site to another in the same country. The model presented here, therefore, represents the best case scenario and is by no means a guarantee of final income.

8.5.3 Further work

As previously stated in Section 8.5.1 above, ASAPM uses the suggested starting concentrations of dissolved and particulate substrates given in ASM3, reflecting typical concentrations found in primary effluent. This includes organic compounds such as the biodegradable substrates S_S and X_S, and the inert substrates S_I and X_I. As the alga used in this work is photoautotrophic, i.e. uses solar energy to produce biomass from carbon dioxide, it has no use for the organic substrates included in ASM3. Consequently, *Chlorella sp*. is unable to grow during the hours of darkness, with the result for the wastewater treatment industry that revenue from algae is not being exploited to its full potential. One possible solution to this is the use of a mixotrophic alga, i.e. a species that can make use of both organic and inorganic carbon.

Further research would be needed to explore this idea, to determine whether levels of dissolved organic substrates remaining in the secondary effluent are sufficient to sustain overnight growth. Phycoremediation, the utilisation of microalgae for the removal of nutrients in wastewater, is an accepted method of wastewater treatment and is used by Lundquist et al. (2010) in their assessment of algal biofuel production . However, during the activated sludge process, readily biodegradable substrates are reduced from 100 to 0.2 g COD m^{-3} (S_S, Tables 16 and 38) and, at these very low concentrations, may not lead to substantial overnight growth. Following laboratory experiments with a suitable organism, it may be possible to manipulate the duration of biological wastewater treatment to provide organic substrates to the algal pond at concentrations sufficient to produce significant

biomass during the hours of darkness. The model could be quite easily updated to include mixotrophic growth processes and the settling parameter, alpha, adjusted to denote a shorter treatment period.

As discussed in the Sensitivity Analysis (Section 8.4 above) the kinetic parameter μ_{CO2atm} is an estimated parameter derived from μ_{NO3} following experiments in the laboratory. The results of the analysis suggest that μ_{CO2atm} is a parameter of great significance to the profitability of the project and a small increase could potentially boost revenue by millions of Euros. At the time of experimentation, growth at sub-atmospheric concentrations of carbon dioxide was not seen as critical since only higher than atmospheric levels would apply for the algae in the integrated model. Further work in the laboratory, using CO_2 at low concentrations, would be required to confirm the validity of this estimated parameter in order to make the model more robust. In the case that the specific growth rate is confirmed and biomass production cannot be increased beyond values already predicted by the model, a different species of fast-growing algae may be considered. Again, it would be relatively easy to update model parameters to describe the growth of another algal species.

More extensive future work may involve the addition of an anaerobic digester and combined heat and power models. The idea of using digested algal cells to produce methane for use in power generation is discussed by Goldman (1979) and adopted by Lundquist et al. (2010). The addition of AD would provide the model user with a choice of ways in which to use algal biomass: either digest the algal cells whole with waste sludge to maximise methane production, or digest lipid-extracted algal cells in order to produce oil for biodiesel. In either case, methane from AD may be used in a generator to produce both heat and power for the biological reactions. If these extensions were added to the model, yet more CO_2 rich gas from the generator can be diverted to the algal pond in addition to that from biological wastewater treatment. With these opportunities to generate energy – from algal biodiesel, methane from the digestion of waste sludge and algal biomass, and heat and electricity from the methane – there is every possibility that a reduced carbon footprint from biological wastewater treatment should be achieved.

8.5.4 Summary

Considering the results obtained in ASAPM v2 (Chapter 6, Table 20), the predicted NPV can now be compared to that of this final version. In ASAPM v2, the Total NPV was €1,065,001 which has increased to €50,914,158 in ASAPM v3. This considerable difference is due to the inclusion of laboratory-determined kinetic expressions that accurately describe the growth of a native species of freshwater microalgae. The algal growth expressions in ASAPM v3 make full use of waste carbon dioxide and nitrogen products from the activated sludge process; this was not addressed in ASAPM v2 and resulted in a large underestimate of algal productivity. A constant supply of CO_2 to the algal pond is necessary for sustained growth, as confirmed by results where the final concentration of dissolved CO_2 in the sludge tank is 16.1 g m^{-3}, reducing to 0.5 g m^{-3} the algal pond. Consequently, the importance of carbon dioxide capture and transfer from the sludge tank to the algal pond cannot be understated.

Although an update in cost parameters led to a marked decrease in revenue from the treatment of wastewater from ASAPM v2 to v3, this was more than recompensed by the increase in revenue from algae. It must not be forgotten that cost parameter values are largely beyond our control, in particular: r_{COD}, r_{CO2}, r_{algae}, Γ, α_E, and all installation and operating costs (please see Chapter 3 for full descriptions). We are at the mercy of the global economy and market forces and must update the model to reflect current carbon trading prices, interest rates and energy costs, among others. Although the carbon trading price has fallen throughout the course of this research, the opposite scenario may also be true at some point in the future and, if this did occur, revenue from carbon sequestration may well rise.

This final version of the integrated activated sludge algal pond model is a representation of a process that is relevant to today's wastewater treatment industry. The first version of the model, ASAPM v1, was intended to act as an indicator for future patterns and predicted that exhaust gases from activated sludge would be useful in growing algae in a nearby pond; the second iteration of the

model confirmed the original findings and included a more robust version of the activated sludge process by employing the industry standard ASM3. ASAPM v3 includes integration of liquid flows and experimentally derived process rates for algal growth. The model is designed to flexible and easy to adjust to suit different wastewater treatment sites and their inputs and operating conditions. In addition to this, there is scope for further extension with AD and power generation, as deemed appropriate for the site in question. As such, ASAPM v3 may not be the final answer in integrated wastewater treatment and algal growth systems but perhaps a conceptual platform on which to build as the algal biofuel industry develops.

CHAPTER 9 - CONCLUSIONS AND RECOMMENDATIONS

9.1 Conclusions

In this work an economic model of integrated biological wastewater treatment and algal growth for biofuels has been produced. The Activated Sludge Algal Pond Model was built over three iterations and presents a novel method of gas transfer between the activated sludge and algal growth vessels. ASAPM includes the industry standard model of biological wastewater treatment, ASM3, which was validated separately prior to employment within ASAPM. Although there is no sample output included with ASM3, very similar results to other works that use the model were achieved – therefore verifying the accuracy of this work. A model is hereby presented that is useful and relevant to the wastewater industry in predicting the economic feasibility of integrating algal cultivation with the activated sludge process.

In addition to the use of gas transfer between the headspaces of the two vessels, the fact that two separate vessels have been modelled is a distinctive feature of this work. Commonly, when the integration of wastewater treatment and algal growth for biofuels is discussed, many researchers suggest the use of high rate algal ponds. In that scenario, the microorganisms responsible for treating the wastewater are mixed with the algae in one vessel. That approach is not adopted in this research due to problems encountered with the separation of algae from bacterial biomass. In this work the method of utilising algae for tertiary wastewater treatment is adopted to allow easier harvesting without the need for speciality flocculants. Included in ASAPM is a function to predict the Net Present Value of the project, and this value is further split into cost and revenue streams. This provides the opportunity to predict profits arising from the integration, through the sale of algal lipid for biodiesel; we are also able to observe capital and operating costs with a view to controlling excess expenditure. Being able to isolate the activated sludge and algal growth vessels by manipulation of parameters, the model has shown that it would not be economically feasible to build algal pond that is not integrated fully with the activated sludge process.

Within the algal pond model, original process rate expressions of algal growth have been written that are applicable to an alga native to northern England. This means that ASAPM is particularly relevant to the UK wastewater treatment industry as the species is accustomed to local environmental conditions, such as temperature and light availability. In order to write the kinetic expressions of algal growth, cultures of *Chlorella sp*. were fed with carbonated water to introduce dissolved carbon dioxide to the growth medium – a method novel, to the best of my knowledge, to this work. A sensitivity analysis of the model shows dissolved carbon dioxide in the pond to be a very important factor for algal growth – a small change in the specific growth rate at atmospheric levels of carbon dioxide results in a significant decrease in dissolved carbon dioxide, which in turn leads to a moderate increase in NPV. This highlights the ability of algae to make a significant impact on the carbon footprint of wastewater treatment by sequestration of carbon dioxide. The carbon capturing ability of algae cannot be understated, with a reduction in dissolved carbon dioxide from 16.1 to 0.5 g m^{-3} from the activated sludge tank to the algal pond.

In addition to dissolved carbon dioxide produced by biological wastewater treatment, ASAPM also describes growth of algae on other wastewater substrates – namely nitrate and ammonium. Although the particular species of algae used in this work, *Chlorella sp*., did not adapt well to growth on NH_4, this substrate has been included to increase model flexibility. This provides ASAPM with the ability to predict the nitrogen requirements of different species of algae with respect to secondary effluent and the concentrations of nitrogenous compounds therein. Secondary effluent is almost certainly a suitable medium in which to cultivate this particular species of *Chlorella*, although this may be subject to the aerobic/anoxic arrangement of the activated sludge process on a particular wastewater treatment plant.

Presented here is a model that is a conceptual platform which can perform in its own right, or may be used as a basis for a superstructure that integrates one or more further processes into the existing model. There is certainly scope to add more models – for example: AD and CHP, which are both complementary to a wastewater treatment setting. ASAPM might also be extended to include

biorefinery processes, such as harvesting and drying of algal biomass, conversion technologies (esterification) and extraction of nutritional supplements. If these extensions are not applicable to the site in mind for algal cultivation, there may be other factors that are important to a specific WWTP. One such factor may be the presence of high levels of phosphorus in the wastewater, which might require close monitoring. It would be relatively straightforward in that case to replace ASM3 in the activated sludge liquid phase with a model that tracked phosphorus compounds – $ASM2_D$, for example. Additional Monod expressions could be added to the existing algal growth rates to account for uptake of phosphorus by algae.

In summary, the main contributions of this work are: experimental work, to provide important parameters for algal growth; a modelling framework of an integrated activated sludge-algal pond system, enabling economic analysis; and results suggesting that such a system may be profitable. This work presents a working economic model of integrated biological wastewater treatment and algal growth for biofuels. The model is designed to be of use for the wastewater treatment industry as a decision-making tool for planning algal cultivation alongside the activated sludge process. ASAPM is flexible to different wastewater treatment scenarios with the inclusion of expressions and parameters that can be tweaked to fit specific operating conditions, influent concentrations or alternative microorganisms. The model may also be seen as a conceptual platform upon which to model a biorefinery system as a way to building a sustainable future for liquid fuels.

9.2 Recommendations for Further Work

Further work could be done on either or both aspects of this project – modelling and microalgae – to improve the Activated Sludge Algal Pond Model presented in this thesis. A sensitivity analysis of the final version of the model showed that the growth rate of *Chlorella sp*. with respect to carbon dioxide (μ_{CO2atm}) was particularly important to the profitability of the project. As the value of this parameter was estimated from growth on nitrate at atmospheric levels of CO_2, the algal growth models may benefit from further investigation using sub-atmospheric levels of carbon dioxide to feed the algal culture. These experiments did not form part of

the original proposal, as it was imagined that dissolved carbon dioxide would remain high due to its continuous evolution from wastewater bacteria. However, the final model shows that dissolved carbon dioxide in the algal pond is reduced from 16.1 to 0.5 g CO_2 m^{-3}, which is slightly below the concentration expected at atmospheric pressure. Determining growth of *Chlorella sp*. at these reduced levels may confirm or reject the validity of the parameter value used in this work.

Further experimental work to be undertaken might be the repetition of experiments to measure the growth rate of algae on ammonium and nitrate, in order to verify the values determined in the original work. Additionally, as the half-saturation constants, K_{NO3} and K_{NH4}, were established at the lower end of the experimental concentration gradient, it might be considered useful to experiment with lower concentrations of $NaNO_3$ and NH_4Cl. This, again, would enable the verification of the original results. Co-limitation experiments might also be interesting to give a more rounded picture of algal behaviour. For example, data from cultures grown with a gradient of nitrate against high and low dissolved carbon dioxide concentrations would serve to make Monod expressions of algal growth more true to dynamic conditions.

The current model of the integrated activated sludge and algal growth processes does not consider phosphorus-containing compounds, although phosphorus is a recognised substrate in wastewater treatment and nutrient in algal growth. If phosphorus were to be required for a specific wastewater treatment plant, ASM3 could be replaced by $ASM2_D$. This would make further laboratory experiments necessary to produce a Monod expression for the growth of *Chlorella sp*. on the phosphorus compounds commonly found in treated wastewater.

Experiments to determine if any heterotrophic growth by *Chlorella sp*. is possible would also be an interesting addition to ASAPM. Small amounts of residual carbonaceous compounds in the secondary effluent may be sufficient to maintain some growth of algae during the hours of darkness; using an alga that could grow over a 24 hour period may significantly improve biomass yield and, correspondingly, Net Present Value. The oxygen inhibition constant, K_{O2alg}, adopted in this work was

taken from the literature and originally determined for *Spirulina platensis*, which is a cyanobacterium or blue-green alga. An experiment to determine a specific oxygen inhibition constant for *Chlorella sp*. might make an interesting comparison to the value adopted in this work.

All of the experiments considered above are proposed for my chosen species of algae – *Chlorella sp*., which is native to the north of England. Of course, an alternative species could be considered with which to compare the results. If another, faster-growing, species were cultivated an increase in the growth rate parameter, μ, may result, which would in turn increase the biomass yield and NPV of the project. This may generate a second model specific to a different alga, or the data may be combined to yield averaged parameter values that would deliver a more general, less species-specific model of algal growth.

With regard to the model itself, the description of wastewater treatment presented here is somewhat simplified. There is only one WWT vessel, which describes aerobic biological wastewater treatment by way of ASM3. As discussed in Chapter 7, separate anoxic tanks are used to control denitrification in order to meet regulations for discharge of effluent into watercourses. The arrangement of separate aerobic and anoxic tanks can be seen in Figure 7-20 in Section 7.3.1. The addition of an anoxic zone, or indeed the use of an alternating aerobic-anoxic aeration sequence, would add that extra layer of detail. The inclusion of a settling tank – with settling described by the Takács model – would also provide another level of complexity for relevance to an actual WWTP.

The addition of further processes to the model may give a more comprehensive description of a wastewater treatment plant. Anaerobic digestion and combined heat and power generation are relevant to a wastewater treatment scenario as waste sludge is used as feedstock for AD and the resulting methane used for CHP. Algal biomass, with or without lipid, would also be a suitable feedstock for AD and heat and electricity from CHP would be useful in providing the energy needs of the integrated processes. Eventually, the construction of a superstructure model would be the ultimate aim for further work. Adopting a biorefinery approach, increasingly

seen in the literature, would include the downstream processing of algal lipid – from harvesting to transesterification – to illustrate the entire cycle of processes from the influx of wastewater to the production of a sustainable biodiesel.

REFERENCES

Akgul, O., Shah, N. and Papageorgiou, L. G. (2012) Economic optimisation of a UK advanced biofuel supply chain, *Biomass & Bioenergy*, **41**, 57-72.

Alasino, N., Mussati, M. C. and Scenna, N. (2007) Wastewater treatment plant synthesis and design, *Industrial & Engineering Chemistry Research*, **46**, 7497-7512.

Alasino, N., Mussati, M. C., Scenna, N. J. and Aguirre, P. (2010) Wastewater Treatment Plant Synthesis and Design: Combined Biological Nitrogen and Phosphorus Removal, *Industrial & Engineering Chemistry Research*, **49(18)**, 8601-8612.

Aleklett, K., Hook, M., Jakobsson, K., Lardelli, M., Snowden, S. and Soderbergh, B. (2010) The Peak of the Oil Age - Analyzing the word oil production Reference Scenario in World Energy Outlook 2008, *Energy Policy*, **38(3)**, 1398-1414.

Allen, M. B. (1956) General features of algal growth in sewage oxidation ponds, *California State Water Pollution Control Bd Publ*, **13**, 11-34.

Arbib, Z., Ruiz, J., Álvarez-Díaz, P., Garrido-Pérez, C. and Perales, J. A. (2014) Capability of different microalgae species for phytoremediation processes: Wastewater tertiary treatment, CO2 bio-fixation and low cost biofuels production, *Water Research*, **49**, 465-474.

Balku, S. and Berber, R. (2006) Dynamics of an activated sludge process with nitrification and denitrification: Start-up simulation and optimization using evolutionary algorithm, *Computers & Chemical Engineering*, **30(3)**, 490-499.

Barlow, J. L. (1993) Numerical Aspects of Solving Linear Least Squares Problems. In: *Handbook of Statistics: Computational Statistics* [Rao, C. R., ed]. Amsterdam, North-Holland. **9**.

Batstone, D. J., Keller, J., Angelidaki, I., Kalyuzhnyi, S. V., Pavlostathis, S. G., Rozzi, A., Sanders, W. T. M., Siegrist, H. and Vavilin, V. A., eds (2002) *Anaerobic Digestion Model No.1*, Scientific and Technical Report. London, IWA Publishing.

Belcher, H. and Swale, E. (1976) *Freshwater Algae*. London, Her Majesty's Stationery Office.

Bellarby, J., Wattenbach, M., Tuck, G., Glendining, M. J. and Smith, P. (2010) The potential distribution of bioenergy crops in the UK under present and future climate, *Biomass & Bioenergy*, **34(12)**, 1935-1945.

Bloomberg (2013) *Energy & Oil Prices - Emissions*. [online]. Available from: http://www.bloomberg.com/energy/ [Accessed 26 Jun 2013].

Bordel, S., Guieysse, B. and Munoz, R. (2009) Mechanistic Model for the Reclamation of Industrial Wastewaters Using Algal-Bacterial Photobioreactors, *Environmental Science & Technology*, **43(9)**, 3200-3207.

BP (2013) *BP Statistical Review of World Energy 2013*. London, plc, B.

Brennan, L. and Owende, P. (2010) Biofuels from microalgae-A review of technologies for production, processing, and extractions of biofuels and co-products, *Renewable & Sustainable Energy Reviews*, **14(2)**, 557-577.

Brownbridge, G., Azadi, P., Smallbone, A., Bhave, A., Taylor, B. and Kraft, M. (2014) The future viability of algae-derived biodiesel under economic and technical uncertainties, *Bioresource Technology*, **151**, 166-173.

Brune, D. E., Lundquist, T. J. and Benemann, J. R. (2009) Microalgal Biomass for Greenhouse Gas Reductions: Potential for Replacement of Fossil Fuels and Animal Feeds, *Journal of Environmental Engineering-Asce*, **135(11)**, 1136-1144.

Buhr, H. O. and Miller, S. B. (1982) A Dynamic Model Of The High Rate Algal Bacterial Waste Water Treatment Pond, *Water Research*, **17(1)**, 29-38.

Bumadian, M. M. (2011) *Molecular Identification and Physiological Characterisation of Extremely Halotolerant Bacteria Isolated from a Freshwater Environment*. PhD thesis, University of Sheffield.

Cantrell, K., Ro, K., Mahajan, D., Anjom, M. and Hunt, P. G. (2007) Role of thermochemical conversion in livestock waste-to-energy treatments: Obstacles and opportunities, *Industrial & Engineering Chemistry Research*, **46(26)**, 8918-8927.

Cao, J., Yuan, W. Q., Pei, Z. J., Davis, T., Cui, Y. and Beltran, M. (2009) A Preliminary Study of the Effect of Surface Texture on Algae Cell Attachment for a Mechanical-Biological Energy Manufacturing System, *Journal of Manufacturing Science and Engineering-Transactions of the Asme*, **131(6)**.

Chisti, Y. (2007) Biodiesel from microalgae, *Biotechnology Advances*, **25(3)**, 294-306.

Cirrincione, M., Pucci, M., Cirrincione, G. and Capolino, G. A. (2002) A new experimental application of least-squares techniques for the estimation of the induction motor parameters. In: *Conference Record of the 2002 IEEE Industry Applications Conference, Vols 1-4*]. New York, IEEE. p.1171-1180.

Clarens, A. F., Resurreccion, E. P., White, M. A. and Colosi, L. M. (2010) Environmental Life Cycle Comparison of Algae to Other Bioenergy Feedstocks, *Environmental Science & Technology*, **44(5)**, 1813-1819.

Cloud, L. (15 Jan 2013). *Life Sparkling Water*. Personal email to P. Uttley (dtp09pju@sheffield.ac.uk).

Copp, J. B., Jeppsson, U. and Rosen, C. (2003) *Towards an ASM1-ADM1 State Variable Interface for Plant-Wide Wastewater Treatment Modeling*: Proceedings of the 76th Annual WEF Conference and Exposition (WEFTEC) held in Los Angeles.

Corominas, L., Flores-Alsina, X., Snip, L. and Vanrolleghem, P. A. (2012) Comparison of different modeling approaches to better evaluate greenhouse gas emissions from whole wastewater treatment plants, *Biotechnology and Bioengineering*, **109(11)**, 2854-2863.

Cruwys, J. A., Dinsdale, R. M., Hawkes, F. R. and Hawkes, D. L. (2002) Development of a static headspace gas chromatographic procedure for the routine analysis of volatile fatty acids in wastewaters, *Journal of Chromatography A*, **945(1-2)**, 195-209.

Cubasch, U., Wuebbles, D., Chen, D., Facchini, M. C., Frame, D., Mahowald, N. and Winther, J.-G. (2013) Introduction. In: *Climate Change 2013: The Physical Science Basis. Contribution of Working Group I to the Fifth Assessment Report of the Intergovernmental Panel on Climate Change* [Stocker, T. F., Qin, D., Plattner, G.-K.et al, eds]. Cambridge, Cambridge University Press.

Demirbas, A. (2005) Biodiesel production from vegetable oils via catalytic and non-catalytic supercritical methanol transesterification methods, *Progress in Energy and Combustion Science*, **31(5-6)**, 466-487.

Demirbas, A. (2009) Political, economic and environmental impacts of biofuels: A review, *Applied Energy*, **86**, S108-S117.

Demirbas, A. (2011) Competitive liquid biofuels from biomass, *Applied Energy*, **88(1)**, 17-28.

Department for Energy and Climate Change (2009) *National Renewable Energy Action Plan for the UK*. 209/28/EC. London, HMSO.

Department for Energy and Climate Change (2012) *UK Bioenergy Strategy*. 12D/077. London, HMSO.

Department for Energy and Climate Change (2013) *Annual Energy Statement 2013*. Cm 8732. London, HMSO.

Dingstad, G. I., Westad, F. and Naes, T. (2004) Three case studies illustrating the properties of ordinary and partial least squares regression in different mixture models, *Chemometrics and Intelligent Laboratory Systems*, **71(1)**, 33-45.

Doran, P. M. (2006) *Bioprocess Engineering Principles*. London, Academic Press.

Ebeling, J. M., Timmons, M. B. and Bisogni, J. J. (2006) Engineering analysis of the stoichiometry of photoautotrophic, autotrophic, and heterotrophic removal of ammonia-nitrogen in aquaculture systems, *Aquaculture*, **257(1-4)**, 346-358.

Ekama, G. A. (2009) Using bioprocess stoichiometry to build a plant-wide mass balance based steady-state WWTP model, *Water Research*, **43(8)**, 2101-2120.

El-Halwagi, M. M. and Manousiouthakis, V. (1989) Synthesis Of Mass Exchange Networks, *Aiche Journal*, **35(8)**, 1233-1244.

El-Shorbagy, W., Arwani, A. and Droste, R. L. (2011) Optimal Sizing of Activated Sludge Processes with ASM3, *International Journal of Civil & Environmental Engineering*, **11(01)**, 19-55.

Encyclopedia Britannica (2014) *Activated Sludge Method*. [online]. Encyclopedia Britannica, Inc. Available from: http://www.britannica.com/EBchecked/media/19281/Primary-and-secondary-treatment-of-sewage-using-the-activated-sludge [Accessed 07 Feb 2014].

Flynn, K. J., Fasham, M. J. R. and Hipkin, C. R. (1997) Modelling the interactions between ammonium and nitrate uptake in marine phytoplankton, *Philosophical Transactions of the Royal Society of London Series B-Biological Sciences*, **352(1361)**, 1625-1645.

Fortier, M.-O. P. and Sturm, B. S. M. (2012) Geographic analysis of the feasibility of collocating algal biomass production with wastewater treatment plants, *Environmental science & technology*, **46(20)**, 11426-11434.

Frangopoulos, C. A. and Keramioti, D. E. (2010) Multi-Criteria Evaluation of Energy Systems with Sustainability Considerations, *Entropy*, **12(5)**, 1006-1020.

Friends of the Earth (2007) *Anaerobic Digestion*. London, Friends of the Earth.

Fukuda, H., Kondo, A. and Noda, H. (2001) Biodiesel fuel production by transesterification of oils, *Journal of Bioscience and Bioengineering*, **92(5)**, 405-416.

Funahashi, A., Tanimura, N., Morohashi, M. and Kitano, H. (2010) CellDesigner: a process diagram editor for gene-regulatory and biochemical networks, Tokyo, BIOSILICO.

Gebreslassie, B. H., Waymire, R. and You, F. Q. (2013) Sustainable Design and Synthesis of Algae-Based Biorefinery for Simultaneous Hydrocarbon Biofuel Production and Carbon Sequestration, *Aiche Journal*, **59(5)**, 1599-1621.

Gehring, T., Silva, J. D., Kehl, O., Castilhos, A. B., Costa, R. H. R., Uhlenhut, F., Alex, J., Horn, H. and Wichern, M. (2010) Modelling waste stabilisation ponds with an extended version of ASM3, *Water Science and Technology*, **61(3)**, 713-720.

Gillot, S., Vermeire, P., Jacquet, P., Grootaerd, H., Derycke, D., Simoens, F. and Vanrolleghem, P. A. (1999) Integration of wastewater treatment plant investment and operating costs for scenario analysis using simulation, *Mededelingen Faculteit Landbouwkundige en Toegepaste Biologische Wetenschappen Universiteit Gent*, **64(5a)**, 13-20.

Gilmour, D. J. (1990) Halotolerant and Halophilic Microorganisms. In: *Microbiology of Extreme Environments* [Edwards, C., ed]. Milton Keynes, Open University Press. p.147-177.

Giordano, M., Norici, A., Gilmour, D. J. and Raven, J. A. (2007) Physiological responses of the green alga Dunaliella parva (Volvocales, Chlorophyta) to controlled incremental changes in the N source, *Functional Plant Biology*, **34(10)**, 925-934.

Gitelson, II, Terskov, I. A., Kovrov, B. G., Sidko, F. Y., Lisovsky, G. M., Okladnikov, Y. N., Belyanin, V. N., Trubachov, I. N. and Rerberg, M. S. (1976) Life Support System with Autonomous Control Employing Plant Photosynthesis, *Acta Astronautica*, **3(9-10)**, 633-650.

Goldman, J. C. (1979) Outdoor Algal Mass Cultures - I. Applications, *Water Research*, **13(1)**, 1-19.

Gouveia, L. and Oliveira, A. C. (2009) Microalgae as a raw material for biofuels production, *Journal of Industrial Microbiology & Biotechnology*, **36(2)**, 269-274.

Gray, N. F. (1990) *Activated Sludge*. New York, Oxford University Press.

Great Britain (2008) *Climate Change Act 2008*. *Part 1*. London, HMSO.

Gujer, W., Henze, M., Mino, T. and van Loosdrecht, M. C. M. (2000) Activated Sludge Model No. 3. In: *Activated Sludge Models ASM1, ASM2, ASM2D and ASM3* [Henze, M., Gujer, W., Mino, T. and van Loosdrecht, M. C. M., eds]. London, IWA Publishing. p.99-121.

Guo, L., Porro, J., Sharma, K. R., Amerlinck, Y., Benedetti, L., Nopens, I., Shaw, A., Van Hulle, S. W. H., Yuan, Z. and Vanrolleghem, P. A. (2012) Towards a benchmarking tool for minimizing wastewater utility greenhouse gas footprints, *Water Science and Technology*, **66(11)**, 2483-2495.

Hager, W. W., Horst, R. and Pardalos, P. M. (1993) Mathematical Programming - A Computational Perspective. In: *Handbook of Statistics: Computational Statistics* [Rao, C. R., ed]. Amsterdam, North-Holland. **9**.

Harmand, J., Rapaport, A. and Trofino, A. (2003) Optimal design of interconnected bioreactors: New results, *Aiche Journal*, **49(6)**, 1433-1450.

Hauduc, H., Rieger, L., Takacs, I., Heduit, A., Vanrolleghem, P. A. and Gillot, S. (2010) A systematic approach for model verification: application on seven published activated sludge models, *Water Science and Technology*, **61(4)**, 825-839.

He, L., Subrarnanian, V. R. and Tang, Y. J. (2012) Experimental analysis and model-based optimization of microalgae growth in photo-bioreactors using flue gas, *Biomass & Bioenergy*, **41**, 131-138.

Heaven, S., Milledge, J. and Zhang, Y. (2011) Comments on 'Anaerobic digestion of microalgae as a necessary step to make microalgal biodiesel sustainable', *Biotechnol Adv*, **29(1)**, 164-167.

Henze, M., Gujer, W., Mino, T. and van Loosdrecht, M., eds (2000) *Activated Sludge Models ASM1, ASM2, ASM2D and ASM3*, Scientific and Technical Report. London, IWA Publishing.

Hiatt, W. C. and Grady, C. P. L. (2008) An Updated Process Model for Carbon Oxidation, Nitrification, and Denitrification, *Water Environment Research*, **80(11)**, 2145-2156.

Hosseini, S. A. and Shah, N. (2011) *Multiscale Modeling of Biorefineries*: Proceedings of the 21st European Symposium on Computer Aided Process Engineering held at Porto Carras Resort, Chalkidiki. Amsterdam, Elsevier B.V. **29**, p.1688-1692.

Hu, Q., Sommerfeld, M., Jarvis, E., Ghirardi, M., Posewitz, M., Seibert, M. and Darzins, A. (2008) Microalgal triacylglycerols as feedstocks for biofuel production: perspectives and advances, *Plant Journal*, **54(4)**, 621-639.

Iacopozzi, I., Innocenti, V., Marsili-Libelli, S. and Giusti, E. (2007) A modified Activated Sludge Model No. 3 (ASM3) with two-step nitrification-denitrification, *Environmental Modelling & Software*, **22(6)**, 847-861.

IEA (2008) *2008 World Energy Outlook 2008: Executive Summary*. Paris, Agency, I. E.

IEA (2010) *2010 World Energy Outlook: Executive Summary*. Paris, Agency, I. E.

IEA (2012) *2012 World Energy Outlook: Executive Summary,* . Paris, Agency, I. E.

IEA (2013a) *2013 World Energy Outlook: Executive Summary*. Paris, Agency, I. E.

IEA (2013b) *Key World Energy Statistics 2013*. Paris, Agency, I. E.

Intercontinental Exchange (2011) *Emissions*. [online]. Atlanta, Intercontinental Exchange, Inc. Available from: www.theice.com/emissions.jhtml [Accessed 02 Nov 2011].

Ji, M. K., Abou-Shanab, R. A. I., Kim, S. H., Salama, E. S., Lee, S. H., Kabra, A. N., Lee, Y. S., Hong, S. and Jeon, B. H. (2013) Cultivation of microalgae species in tertiary municipal wastewater supplemented with CO2 for nutrient removal and biomass production, *Ecological Engineering*, **58**, 142-148.

Jimenez, C., Cossio, B. R. and Niell, F. X. (2003) Relationship between physicochemical variables and productivity in open ponds for the production of Spirulina: a predictive model of algal yield, *Aquaculture*, **221(1-4)**, 331-345.

Johnson, M. B. and Wen, Z. Y. (2010) Development of an attached microalgal growth system for biofuel production, *Applied Microbiology and Biotechnology*, **85(3)**, 525-534.

Jupsin, H., Praet, E. and Vasel, J. L. (2003) Dynamic mathematical model of high rate algal ponds (HRAP), *Water Science and Technology*, **48(2)**, 197-204.

Kadam, K. L. (2002) Environmental implications of power generation via coal-microalgae cofiring, *Energy*, **27(10)**, 905-922.

Kawasaki, L. Y., Tarifeño-Silva, E., Yu, D. P., Gordon, M. S. and Chapman, D. J. (1982) Aquacultural approaches to recycling of dissolved nutrients in secondarily treated domestic wastewaters - I Nutrient uptake and release by artificial food chains, *Water Research*, **16(1)**, 37-49.

Keim, W. (2010) Petrochemicals: Raw material change from fossil to biomass?, *Petroleum Chemistry*, **50(4)**, 298-304.

Kemp, I. C. (2007) *Pinch Analysis and Process Integration*. Oxford, Butterworth-Heinemann.

Kiely, G. (1998) *Environmental Engineering*. Boston, Irwin/McGraw-Hill.

Kim, S., Kim, H., Ko, D., Yamaoka, Y., Otsuru, M., Kawai-Yamada, M., Ishikawa, T., Oh, H. M., Nishida, I., Li-Beisson, Y. and Lee, Y. (2013) Rapid Induction of Lipid Droplets in Chlamydomonas reinhardtii and Chlorella vulgaris by Brefeldin A, *Plos One*, **8(12)**.

Kjarstad, J. and Johnsson, F. (2009) Resources and future supply of oil, *Energy Policy*, **37(2)**, 441-464.

Kone, A. C. and Buke, T. (2010) Forecasting of CO2 emissions from fuel combustion using trend analysis, *Renewable & Sustainable Energy Reviews*, **14(9)**, 2906-2915.

Lanot, A. and McQueen-Mason, S. (2011) *Biorenewables: Improving crops and processes for integrated biorefineries*. York, Futures, C. f. L. C.

Lardon, L., Helias, A., Sialve, B., Stayer, J. P. and Bernard, O. (2009) Life-Cycle Assessment of Biodiesel Production from Microalgae, *Environmental Science & Technology*, **43(17)**, 6475-6481.

Lavigne, R. and Gloger, K. (2006) The Carbon Footprint of Wastewater Treatment, www.venturi-aeration.com.

Lawson, C. L. and Hanson, R. J. (1974) *Solving Least Squares Problems*. Englewood Cliffs, Prentice-Hall Inc.

Le Treut, H., Somerville, R., Cubasch, U., Ding, Y., Mauritzen, C., Mokssit, A., Peterson, T. and Prather, M. (2007) Historical Overview of Climate Change Science. In: *Climate Change 2007: The Physical Science Basis. Contribution of Working Group I to the Fourth Assessment Report of the Intergovernmental Panel on Climate Change* [Solomon, S., Qin, D., Manning, M.et al, eds]. Cambridge, Cambridge University Press.

Li, Y., Chen, Y.-F., Chen, P., Min, M., Zhou, W., Martinez, B., Zhu, J. and Ruan, R. (2011a) Characterization of a microalga Chlorella sp well adapted to highly concentrated municipal wastewater for nutrient removal and biodiesel production, *Bioresource Technology*, **102(8)**, 5138-5144.

Li, Y., Zhou, W., Hu, B., Min, M., Chen, P. and Ruan, R. R. (2011b) Integration of algae cultivation as biodiesel production feedstock with municipal wastewater treatment: Strains screening and significance evaluation of environmental factors, *Bioresource Technology*, **102(23)**, 10861-10867.

Li, Y. T., Han, D. X., Hu, G. R., Dauvillee, D., Sommerfeld, M., Ball, S. and Hua, Q. (2010) Chlamydomonas starchless mutant defective in ADP-glucose pyrophosphorylase hyper-accumulates triacylglycerol, *Metabolic Engineering*, **12(4)**, 387-391.

Liu, J. Y., Mukherjee, J., Hawkes, J. J. and Wilkinson, S. J. (2013) Optimization of lipid production for algal biodiesel in nitrogen stressed cells of Dunaliella salina using FTIR analysis, *Journal of Chemical Technology and Biotechnology*, **88(10)**, 1807-1814.

Liu, Y. M., Zhang, C. Y., Shen, X. P., Zhang, X. L., Cichello, S., Guan, H. B. and Liu, P. S. (2013) Microorganism lipid droplets and biofuel development, *Bmb Reports*, **46(12)**, 575-581.

Lizzul, A. M., Hellier, P., Purton, S., Baganz, F., Ladommatos, N. and Campos, L. (2014) Combined remediation and lipid production using Chlorella sorokiniana grown on wastewater and exhaust gases, *Bioresource Technology*, **151**, 12-18.

Llamas, A., Al-Lal, A. M., Hernandez, M., Lapuerta, M. and Canoira, L. (2012) Biokerosene from Babassu and Camelina Oils: Production and Properties of Their Blends with Fossil Kerosene, *Energy & Fuels*, **26(9)**, 5968-5976.

Lundquist, T. J., Woertz, I. C., Quinn, N. W. T. and Benemann, J. R. (2010) *A Realistic Technology and Engineering Assessment of Algae Biofuel Production*. San Luis Obispo, University, C. P. S.

Lunin, V. V., Sergeeva, Y. E., Galanina, L. A., Mysyakina, I. S., Ivashechkin, A. A., Bogdan, V. I. and Feofilova, E. P. (2013) Biodiesel fuel production from lipids of filamentous fungi, *Applied Biochemistry and Microbiology*, **49(1)**, 46-52.

MacKay, D. J. (2009) *Sustainable Energy - without the hot air*.]. Cambridge, UIT Cambridge Ltd.

Madigan, M. T., Martinko, J. M. and Parker, J. (2003) *Biology of Microorganisms*. Upper Saddle River, Pearson Education.

Marquez, F. J., Sasaki, K., Nishio, N. and Nagai, S. (1995) Inhibitory effect of oxygen accumulation on the growth of *Spirulina platensis*, *Biotechnology Letters*, **17(2)**, 225-228.

MathWorks (2013) MATLAB, Natick, MathWorks.

Matsuoka, S., Ferro, J. and Arruda, P. (2009) The Brazilian experience of sugarcane ethanol industry, *In Vitro Cellular & Developmental Biology-Plant*, **45(3)**, 372-381.

Miyachi, S., Iwasaki, I. and Shiraiwa, Y. (2003) Historical perspective on microalgal and cyanobacterial acclimation to low- and extremely high-CO_2 conditions, *Photosynthesis Research*, **77(2-3)**, 139-153.

Morgan, J. (2008) *Agriculture's Role in Energy Production from Biomass and Waste*. London, English Farming and Food Partnerships.

Morken, J., Sapci, Z. and Stromme, J. E. T. (2013) Modeling of biodiesel production in algae cultivation with anaerobic digestion (ACAD), *Energy Policy*, **60**, 98-105.

Moroney, J. V. and Somanchi, A. (1999) How do algae concentrate CO_2 to increase the efficiency of photosynthetic carbon fixation?, *Plant Physiology*, **119(1)**, 9-16.

Mussati, M., Gernaey, K., Gani, R. and Jorgensen, S. B. (2002) Computer aided model analysis and dynamic simulation of a wastewater treatment plant, *Clean Techn Environ Policy*, **4**, 100-114.

Mussati, M. C., Mussati, S. F., Alasino, N., Aguirre, P. and Scenna, N. (2005) *Optimal Synthesis of Acitvated Sludge Wastewater Treatment Plants for Nitrogen Removal*: Proceedings of the 2nd Mercosur Congress on Chemical Engineering and 4th Mercosur Congress on Process Systems Engineering held at Rio de JaneiroENPROMER, p.14-18.

Mutanda, T., Karthikeyan, S. and Bux, F. (2011) The Utilization of Post-chlorinated Municipal Domestic Wastewater for Biomass and Lipid Production by Chlorella spp. Under Batch Conditions, *Applied Biochemistry and Biotechnology*, **164(7)**, 1126-1138.

Nauha, E. K. and Alopaeus, V. (2013) Modeling method for combining fluid dynamics and algal growth in a bubble column photobioreactor, *Chemical Engineering Journal*, **229**, 559-568.

Nielsen, J. (2006) Microbial Process Kinetics. In: *Basic Biotechnology* [Ratledge, C. and Kristiansen, B., eds]. Cambridge, Cambridge University Press.

Nigam, P. S. and Singh, A. (2011) Production of liquid biofuels from renewable resources, *Progress in Energy and Combustion Science*, **37(1)**, 52-68.

Nolan, R. P. and Lee, K. (2011) Dynamic model of CHO cell metabolism, *Metabolic Engineering*, **13(1)**, 108-124.

Nopens, I., Batstone, D. J., Copp, J. B., Jeppsson, U., Volcke, E., Alex, J. and Vanrolleghem, P. A. (2009) An ASM/ADM model interface for dynamic plant-wide simulation, *Water Research*, **43(7)**, 1913-1923.

Nopens, I., Benedetti, L., Jeppsson, U., Pons, M. N., Alex, J., Copp, J. B., Gernaey, K. V., Rosen, C., Steyer, J. P. and Vanrolleghem, P. A. (2010) Benchmark Simulation Model No 2: Finalisation of plant layout and default control strategy, *Water Science and Technology*, **62(9)**, 1967-1974.

Oil-Price.net (2011) *Crude Oil and Commodity Prices*. [online]. Oil-Price.net. Available from: http://oil-price.net/ [Accessed 02 Nov 2011].

Olguin, E. J. (2012) Dual purpose microalgae-bacteria-based systems that treat wastewater and produce biodiesel and chemical products within a Biorefinery, *Biotechnology Advances*, **30(5)**, 1031-1046.

Osundeko, O., Davies, H. and Pittman, J. K. (2013) Oxidative stress-tolerant microalgae strains are highly efficient for biofuel feedstock production on wastewater, *Biomass and Bioenergy*, **56**, 284-294.

Park, J. B. K. and Craggs, R. J. (2007) Biogas production from anaerobic waste stabilisation ponds treating dairy and piggery wastewater in New Zealand, *Water Science and Technology*, **55(11)**, 257-264.

Petit, J. R., Jouzel, J., Raynaud, D., Barkov, N. I., Barnola, J. M., Basile, I., Bender, M., Chappellaz, J., Davis, M., Delaygue, G., Delmotte, M., Kotlyakov, V. M., Legrand, M., Lipenkov, V. Y., Lorius, C., Pepin, L., Ritz, C., Saltzman, E. and Stievenard, M. (1999) Climate and atmospheric history of the past 420,000 years from the Vostok ice core, Antarctica, *Nature*, **399(6735)**, 429-436.

Plambeck, J. A. (1995) *Introductory University Chemistry 1*. [online]. Edmonton, University of Alberta. Available from: http://dwb4.unl.edu/Chem/CHEM869J/CHEM869JLinks/www.chem.ualberta.ca/courses/plambeck/p101/p01182.htm [Accessed 18 Jun 2013].

Powell, N., Shilton, A. N., Pratt, S. and Chisti, Y. (2008) Factors influencing luxury uptake of phosphorus by microalgae in waste stabilization ponds, *Environmental Science & Technology*, **42(16)**, 5958-5962.

Rao, C. R. (1965) *Linear Statistical Inference and Its Applications*. New York, John Wiley & Sons, Inc.

Raynaud, D., Barnola, J. M., Chappellaz, J., Blunier, T., Indermuhle, A. and Stauffer, B. (2000) The ice record of greenhouse gases: a view in the context of future changes, *Quaternary Science Reviews*, **19(1-5)**, 9-17.

Reichert, P., Borchardt, D., Henze, M., Rauch, W., Shanahan, P., Somlyody, L. and Vanrolleghem, P. (2001) River water quality model no. 1 (RWQM1): II. Biochemical process equations, *Water Science and Technology*, **43(5)**, 11-30.

RFA (2014) *2012 World Fuel Ethanol Production*. [online]. Washington, D.C., Renewable Fuels Association. Available from: http://ethanolrfa.org/pages/World-Fuel-Ethanol-Production [Accessed 10 Feb 2014].

Rijckaert, A. (2009) Dutch aubergine grower pipes carbon dioxide into greenhouses, *The Telegraph*, Terneuzen.

Rosenberg, J. N., Mathias, A., Korth, K., Betenbaugh, M. J. and Oyler, G. A. (2011) Microalgal biomass production and carbon dioxide sequestration from an integrated ethanol biorefinery in Iowa: A technical appraisal and economic feasibility evaluation, *Biomass & Bioenergy*, **35(9)**, 3865-3876.

Rowe, R. L., Street, N. R. and Taylor, G. (2009) Identifying potential environmental impacts of large-scale deployment of dedicated bioenergy crops in the UK, *Renewable & Sustainable Energy Reviews*, **13(1)**, 260-279.

Santos, L. C. and Zemp, R. J. (2000) Energy and capital targets for constrained heat exchanger networks, *Bazilian Journal of Chemical Engineering*, **17**, 4-7.

Schwede, S., Rehman, Z. U., Gerber, M., Theiss, C. and Span, R. (2013) Effects of thermal pretreatment on anaerobic digestion of Nannochloropsis salina biomass, *Bioresource Technology*, **143**, 505-511.

Sergeeva, Y. E., Galanina, L. A., Andrianova, D. A. and Feofilova, E. P. (2008) Lipids of filamentous fungi as a material for producing biodiesel fuel, *Applied Biochemistry and Microbiology*, **44(5)**, 523-527.

Shanahan, P., Borchardt, D., Henze, M., Rauch, W., Reichert, P., Somlybody, L. and Vanrolleghem, P. (2001) River water quality model no. 1 (RWQM1): I. Modelling approach, *Water Science and Technology*, **43(5)**, 1-9.

Shiratake, T., Sato, A., Minoda, A., Tsuzuki, M. and Sato, N. (2013) Air-Drying of Cells, the Novel Conditions for Stimulated Synthesis of Triacylglycerol in a Green Alga, Chlorella kessleri, *Plos One*, **8(11)**.

Sialve, B., Bernet, N. and Bernard, O. (2009) Anaerobic digestion of microalgae as a necessary step to make microalgal biodiesel sustainable, *Biotechnology Advances*, **27(4)**, 409-416.

Smith, R. (2005) *Chemical Process Design and Integration*. Chichester, Wiley.

Solomon, B. D. (2010) Biofuels and sustainability. In: *Ecological Economics Reviews*]. Oxford, Blackwell Publishing. **1185:** p.119-134.

Sperandio, M. and Paul, E. (1997) Determination of carbon dioxide evolution rate using on-line gas analysis during dynamic biodegradation experiments, *Biotechnology and Bioengineering*, **53(3)**, 243-252.

Spijkerman, E., de Castro, F. and Gaedke, U. (2011) Independent Colimitation for Carbon Dioxide and Inorganic Phosphorus, *Plos One*, **6(12)**.

Staffordshire University (2011) *Biological wastewater treatment processes; secondary treatment*. *Distance Learning.* [online]. Stoke-on-Trent, Staffordshire University. Available from: http://www.staffs.ac.uk/schools/sciences/consultancy/dladmin/zCIWEMWWT/Activity5/act5.html [Accessed 20 Feb 2014].

Staine, F. and Favrat, D. (1996) Energy integration of industrial processes based on the pinch analysis method extended to include exergy factors, *Applied Thermal Engineering*, **16(6)**, 497-507.

Stephenson, A. L., Kazamia, E., Dennis, J. S., Howe, C. J., Scott, S. A. and Smith, A. G. (2010) Life-Cycle Assessment of Potential Algal Biodiesel Production in the United

Kingdom: A Comparison of Raceways and Air-Lift Tubular Bioreactors, *Energy & Fuels*, **24**, 4062-4077.

Strobel, G. A., Knighton, B., Kluck, K., Ren, Y. H., Livinghouse, T., Griffin, M., Spakowicz, D. and Sears, J. (2008) The production of myco-diesel hydrocarbons and their derivatives by the endophytic fungus Gliocladium roseum (NRRL 50072), *Microbiology-Sgm*, **154**, 3319-3328.

Sukenik, A., Levy, R. S., Levy, Y., Falkowski, P. G. and Dubinsky, Z. (1991) Optimizing Algal Biomass Production in an Outdoor Pond - A Simulation-Model, *Journal of Applied Phycology*, **3(3)**, 191-201.

Swana, J., Yang, Y., Behnam, M. and Thompson, R. (2011) An analysis of net energy production and feedstock availability for biobutanol and bioethanol, *Bioresource Technology*, **102(2)**, 2112-2117.

Tam, N. F. Y. and Wong, Y. S. (1996) Effect of ammonia concentrations on growth of Chlorella vulgaris and nitrogen removal from media, *Bioresource Technology*, **57(1)**, 45-50.

Tchobanoglous, G., Burton, F. L. and Stensel, H. D. (2004) *Wastewater Engineering: Treatment and Reuse*. New York, McGraw-Hill.

Tjan, W., Tan, R. R. and Foo, D. C. Y. (2010) A graphical representation of carbon footprint reduction for chemical processes, *Journal of Cleaner Production*, **18(9)**, 848-856.

United Nations (1998) *Kyoto Protocol to the United Nations Framework Convention on Climate Change*. Kyoto, United Nations.

United Nations (2013) *Carbon Dioxide Emissions*. *Millennium Development Goals Indicators.* [online]. New York, United Nations Statistics Division. Available from: http://mdgs.un.org/unsd/mdg/SeriesDetail.aspx?srid=749&crid= [Accessed 07 Feb 2014].

Vandevivere, P. and Verstraete, W. (2006) Environmental Applications. In: *Basic Biotechnology* [Ratledge, C. and Kristiansen, B., eds]. Cambridge, Cambridge University Press.

Vanrolleghem, P., Borchardt, D., Henze, M., Rauch, W., Reichert, P., Shanahan, P. and Somlyody, L. (2001) River water quality model no. 1 (RWQM1): III. Biochemical submodel selection, *Water Science and Technology*, **43(5)**, 31-40.

Vanrolleghem, P. A. and Gillot, S. (2002) Robustness and economic measures as control benchmark performance criteria, *Water Science and Technology*, **45(4-5)**, 117-126.

Vesilind, P. A., ed (2003) *Wastewater Treatment Plant Design*. Alexandria, Water Environment Federation/IWA Publishing.

Wan, M., Liu, P., Xia, J., Rosenberg, J. N., Oyler, G. A., Betenbaugh, M. J., Nie, Z. and Qiu, G. (2011) The effect of mixotrophy on microalgal growth, lipid content, and expression levels of three pathway genes in Chlorella sorokiniana, *Applied Microbiology and Biotechnology*, **91(3)**, 835-844.

Wang, L. A., Min, M., Li, Y. C., Chen, P., Chen, Y. F., Liu, Y. H., Wang, Y. K. and Ruan, R. (2010) Cultivation of Green Algae Chlorella sp in Different Wastewaters from Municipal Wastewater Treatment Plant, *Applied Biochemistry and Biotechnology*, **162(4)**, 1174-1186.

Wang, Y. P. and Smith, R. (1994) Waste-Water Minimization, *Chemical Engineering Science*, **49(7)**, 981-1006.

Water UK (2006) Wastewater treatment and recycling, Water UK, London.

Weissermel, K. (1980) Raw-Material Polymer Interrelations - Today's Choice - Tomorrow's Options, *Pure and Applied Chemistry*, **52(2)**, 265-276.

Wilkinson, S. J. (2009) Sentero: A Tool for the Analysis of Biochemical Networks, http://www.shef.ac.uk/polopoly_fs/1.48155!/file/Sentero.pdf.

Wilkinson, S. J., Benson, N. and Kell, D. B. (2008) Proximate parameter tuning for biochemical networks with uncertain kinetic parameters, *Molecular Biosystems*, **4(1)**, 74-97.

Woertz, I., Feffer, A., Lundquist, T. and Nelson, Y. (2009) Algae Grown on Dairy and Municipal Wastewater for Simultaneous Nutrient Removal and Lipid Production for Biofuel Feedstock, *Journal of Environmental Engineering-Asce*, **135(11)**, 1115-1122.

Yan, Y. J., Li, X., Wang, G. L., Gui, X. H., Li, G. L., Su, F., Wang, X. F. and Liu, T. (2014) Biotechnological preparation of biodiesel and its high-valued derivatives: A review, *Applied Energy*, **113**, 1614-1631.

Yang, A. (2011) Modeling and Evaluation of CO2 Supply and Utilization in Algal Ponds, *Industrial & Engineering Chemistry Research*, **50(19)**, 11181-11192.

Yen, H. W., Hu, I. C., Chen, C. Y., Ho, S. H., Lee, D. J. and Chang, J. S. (2013) Microalgae-based biorefinery - From biofuels to natural products, *Bioresource Technology*, **135**, 166-174.

Zamboni, A., Murphy, R. J., Woods, J., Bezzo, F. and Shah, N. (2011) Biofuels carbon footprints: Whole-systems optimisation for GHG emissions reduction, *Bioresource Technology*, **102(16)**, 7457-7465.

Zimmerman, W. B., Zandi, M., Tesar, V., Gilmour, D. J. and Ying, K. Z. (2011) Design of an airlift loop bioreactor and pilot scales studies with fluidic oscillator induced microbubbles for growth of a microalgae Dunaliella salina, *Applied Energy*, **88(10)**, 3357-3369.

APPENDICES

Appendix A – Process rates for the ASM3 model

ρ	Process	Process Rate
AS1	Hydrolysis	$k_H \frac{X_S/X_H}{K_X+(X_S/X_H)} X_H$
AS2	Aerobic storage of S_S	$k_{STO} \frac{S_{O2}}{K_{O2}+S_{O2}} \frac{S_S}{K_S+S_S} X_H$
AS3	Anoxic storage of S_S	$k_{STO}\, \eta_{NOX} \frac{K_{O2}}{K_{O2}+S_{O2}} \frac{S_{NOX}}{K_{NOx}+S_{NOX}} \frac{S_S}{K_S+S_S} X_H$
AS4	Aerobic growth	$\mu_H \frac{S_{O2}}{K_{O2}+S_{O2}} \frac{S_{NH4}}{K_{NH4}+S_{NH4}} \frac{S_{ALK}}{K_{ALK}+S_{ALK}} \frac{(X_{STO}/X_H)}{K_{STO}+(X_{STO}/X_H)} X_H$
AS5	Anoxic growth	$\mu_H\, \eta_{NOX} \frac{K_{O2}}{K_{O2}+S_{O2}} \frac{S_{NOX}}{K_{NOX}+S_{NOX}} \frac{S_{NH4}}{K_{NH4}+S_{NH4}} \frac{S_{ALK}}{K_{ALK}+S_{ALK}} \frac{(X_{STO}/X_H)}{K_{STO}+(X_{STO}/X_H)} X_H$
AS6	Aerobic endog. respiration	$b_{H,O2} \frac{S_{O2}}{K_{O2}+S_{O2}} X_H$
AS7	Anoxic endog. respiration	$b_{H,NOX} \frac{K_{O2}}{K_{O2}+S_{O2}} \frac{S_{NOX}}{K_{NOx}+S_{NOX}} X_H$
AS8	Aerobic respiration	$b_{STO,O2} \frac{S_{O2}}{K_{O2}+S_{O2}} X_{STO}$
AS9	Anoxic respiration	$b_{STO,NOX} \frac{K_{O2}}{K_{O2}+S_{O2}} \frac{S_{NOX}}{K_{NOx}+S_{NOX}} X_{STO}$
AS10	Aerobic growth of X_A	$\mu_A \frac{S_{O2}}{K_{A,O2}+S_{O2}} \frac{S_{NH4}}{K_{A,NH4}+S_{NH4}} \frac{S_{ALK}}{K_{A,ALK}+S_{ALK}} X_A$
AS11	Aerobic endog. respiration	$b_{A,O2} \frac{S_{O2}}{K_{A,O2}+S_{O2}} X_A$
AS12	Anoxic endog. respiration	$b_{A,NOX} \frac{K_{A,O2}}{K_{A,O2}+S_{O2}} \frac{S_{NOX}}{K_{A,NOX}+S_{NOX}} X_A$

Appendix B – Stoichiometric matrix for ASM3 and the ASAPM activated sludge liquid phase

Variable ρ	S_{O2}	S_S	S_{NH4}	S_{NOX}	S_{N2}	S_{ALK}	S_I	X_I	X_S	X_H	X_{STO}	X_A	X_{SS}	S_{CO2} (ASAPM only)
AS1	-	$1-f_{SI}$	$-(1-f_{SI}).i_{NSS}-f_{SI}.i_{NSI}+i_{NXS}$	-	-	$-(1-f_{SI}).i_{NSS}-f_{SI}.i_{NSI}+i_{NXS}.i_{Charge\_NHx}$	f_{SI}	-	-1	-	-	-	$-i_{SS,XS}$	-
AS2	$-(1-Y_{STO,O2})$	-1	i_{NSS}	-	-	$i_{NSS}.i_{Charge\_NHx}$	-	-	-	-	$Y_{STO,\ O2}$	-	$Y_{STO,O2}.i_{SS,STO}$	$(1-Y_{STO,CO2})$
AS3	-	-1	i_{NSS}	$-(1-Y_{STO,NOX})/(i_{NOxN2})$	$(1-Y_{STO,NOX})/(i_{NOxN2})$	$i_{NSS}.i_{Charge\_NHx}+(1-Y_{STO,NOX})/(i_{NOxN2}).i_{Charge\_NOx}$	-	-	-	-	$Y_{STO,NOX}$	-	$Y_{STO,NOX}.i_{SS,STO}$	-
AS4	$-(1-Y_{H,O2})/Y_{H,O2}$	-	$-i_{NBM}$	-	-	$-i_{NBM}.i_{Charge\_NHx}$	-	-	-	1	$-1/Y_{H,O2}$	-	$(-1/Y_{H,O2}).i_{SS,STO}+i_{SS,BM}$	$(1-Y_{H,CO2})/Y_{H,CO2}$
AS5	-	-	$-i_{NBM}$	$-(1-Y_{H,NOX})/Y_{H,NOX}.(1/i_{NOxN2})$	$(1-Y_{H,NOX})/Y_{H,NOX}.(1/i_{NOxN2})$	$-i_{NBM}.i_{Charge\_NHx}+(1-Y_{H,NOX})/Y_{H,NOX}.(1/i_{NOxN2}).i_{Charge\_NOx}$	-	-	-	1	$-1/Y_{H,NOX}$	-	$(-1/Y_{H,NOX}).i_{SS,STO}+i_{SS,BM}$	-
AS6	$-(1-f_{XI})$	-	$-f_{XI}.i_{NXI}+i_{NBM}$	-	-	$f_{XI}.i_{NXI}+i_{NBM}.i_{Charge\_NHx}$	-	f_{XI}	-	-1	-	-	$-i_{SS,BM}+f_{XI}.i_{SS,XI}$	$(1-f_{XI})$
AS7	-	-	$-f_{XI}.i_{NXI}+i_{NBM}$	$-(1-f_{XI})/(i_{NOxN2})$	$(1-f_{XI})/(i_{NOxN2})$	$(1-f_{XI})/(i_{NOxN2}).i_{Charge\_NOx}+f_{XI}.i_{NXI}+i_{NBM}.i_{Charge\_NHx}$	-	f_{XI}	-	-1	-	-	$-i_{SS,BM}+f_{XI}.i_{SS,XI}$	-
AS8	-1	-	-	-	-	-	-	-	-	-	-1	-	$-i_{SS,STO}$	1
AS9	-	-	-	$-1/(i_{NOxN2})$	$1/(i_{NOxN2})$	$1/(i_{NOxN2}).i_{Charge\_NOx}$	-	-	-	-	-1	-	$-i_{SS,STO}$	-
AS10	$-(-i_{COD\_NOx}-Y_A)/Y_A$	-	$-1/Y_A-i_{NBM}$	$1/Y_A$	-	$1/Y_A-i_{NBM}.i_{Charge\_NHx}+1/Y_A.i_{Charge\_NOx}$	-	-	-	-	-	1	$i_{SS,BM}$	$(-i_{COD\_NOx}-Y_A)/Y_A$

Variable **ρ**	**S_{O2}**	**S_S**	**S_{NH4}**	**S_{NOX}**	**S_{N2}**	**S_{ALK}**	**S_I**	**X_I**	**X_S**	**X_H**	**X_{STO}**	**X_A**	**X_{SS}**	**S_{CO2}** (ASAPM only)
AS11	$-(1-f_{XI})$	-	$-f_{XI}.\ i_{NXI}+i_{NBM}$	-	-	$1/Y_A-i_{NBM}.i_{Charge\_NHx}$	-	f_{XI}	-	-	-	-1	$-i_{SS,BM}$ $+f_{XI}.i_{SS,XI}$	$(1-f_{XI})$
AS12	-	-	$-f_{XI}.\ i_{NXI}+i_{NBM}$	$-(1-f_{XI})$ $/(i_{NOxN2})$	$(1-f_{XI})/(i_{NOxN2})$	$f_{XI}.i_{NXI}+i_{NBM}.i_{Charge\_NHx}$ + $(1-f_{XI})/(i_{NOxN2}).i_{Charge\_NHx}$	-	f_{XI}	-	-	-	-1	$-i_{SS,BM}$ $+f_{XI}.i_{SS,XI}$	-

Appendix C – Parameter values of the ASM3 model

Parameter	Description	Value	Units
Kinetic Parameters			
k_H	Hydrolysis rate constant	3	g COD_{XS} (g COD_{XH})$^{-1}$ d^{-1}
K_X	Hydrolysis saturation constant	1	g COD_{XS} (g COD_{XH})$^{-1}$
k_{STO}	Storage rate constant	5	g COD_{SS} (g COD_{XH})$^{-1}$ d^{-1}
ηNO_X	Anoxic reduction factor	0.6	-
K_{O2}	Saturation constant for S_{O2}	0.2	g O_2 m^{-3}
K_{NOX}	Saturation constant for S_{NOX}	0.5	g NO_3^- -N m^{-3}
K_S	Saturation constant for S_S	2	g COD_{SS} m^{-3}
K_{STO}	Saturation constant for X_{STO}	1	g COD_{XSTO} (g COD_{XH})$^{-1}$
μ_H	Heterotrophic max growth rate for X_H	2	d^{-1}
K_{NH4}	Saturation constant for S_{NH4}	0.01	g N m^{-3}
K_{ALK}	Saturation constant for alkalinity for X_H	0.1	mol HCO_3^- m^{-3}
$b_{H,O2}$	Aerobic endogenous respiration rate of X_H	0.2	d^{-1}
$b_{H,NOX}$	Anoxic endogenous respiration rate of X_H	0.1	d^{-1}
$b_{STO,O2}$	Aerobic respiration rate of X_{STO}	0.2	d^{-1}
$b_{STO,NOX}$	Anoxic respiration rate of X_{STO}	0.1	d^{-1}
μ_A	Autotrophic max growth rate of X_A	1	d^{-1}
$K_{A,NH4}$	Ammonium substrate saturation for X_A	1	g N m^{-3}
$K_{A,O2}$	Oxygen saturation for nitrifiers	0.5	g O_2 m^{-3}
$K_{A,ALK}$	Bicarbonate saturation for nitrifiers	0.5	mol HCO_3^- m^{-3}
$b_{A,O2}$	Aerobic endogenous respiration rate of X_A	0.15	d^{-1}
$b_{A,NOX}$	Anoxic endogenous respiration rate of X_A	0.05	d^{-1}
$K_{A,NOX}$	Saturation constant for S_{NOX} for X_A	0.5	g NO_3^- -N m^{-3}
Stoichiometric Parameters			
f_{SI}	Production of S_I in hydrolysis	0.0	g COD_{SI} (g COD_{XS})$^{-1}$
$Y_{STO,O2}$ ($Y_{STO,CO2}$)	Aerobic yield of stored product for S_S	0.85	g COD_{XSTO} (g COD_{SS})$^{-1}$
$Y_{STO,NOX}$	Anoxic yield of stored product for S_S	0.8	g COD_{XSTO} (g COD_{SS})$^{-1}$
$Y_{H,O2}$ ($Y_{H,CO2}$)	Aerobic yield of heterotrophic biomass	0.63	g COD_{XH} (g COD_{XSTO})$^{-1}$
$Y_{H,NOX}$	Anoxic yield of heterotrophic biomass	0.54	g COD_{XH} (g COD_{XSTO})$^{-1}$

Parameter	Description	Value	Units
Y_A	Aerobic yield of X_A	0.24	g COD_{Xns} (g N_{NOX})$^{-1}$
f_{XI}	Production of X_I in endogenous respiration	0.2	g COD_{XI} (g COD_{XBM})$^{-1}$
i_{NSS}	N content of S_S	0.03	g N (g COD_{SS})$^{-1}$
i_{NSI}	N content of S_I	0.01	g N (g COD_{SI})$^{-1}$
i_{NXS}	N content of X_S	0.04	g N (g COD_{XS})$^{-1}$
i_{NXI}	N content of X_I	0.02	g N (g COD_{XI})$^{-1}$
i_{NBM}	N content of biomass, X_H, X_{ns}, X_{nb}	0.07	g N (g COD_{XBM})$^{-1}$
$i_{SS,XI}$	Conversion factor X_I in X_{SS}	0.75	g X_{SS} (g X_I)$^{-1}$
$i_{SS,XS}$	Conversion factor X_S in X_{SS}	0.75	g X_{SS} (g X_S)$^{-1}$
$i_{SS,BM}$	Conversion factor biomass in X_{SS}	0.9	g X_{SS} (g X_{STO})$^{-1}$
$i_{SS,STO}$	Conversion factor X_{STO} in X_{SS}	0.6	g X_{SS} (g X_{Bio})$^{-1}$
$i_{NOx,N2}$	Conversion factor for NO_3 reduction to N_2	2.857	g COD_{Xns} (g N_{NOX})$^{-1}$
$i_{COD,NOx}$	Conversion factor for NO_3 in COD	-4.571	g COD_{Xns} (g N_{NOX})$^{-1}$
i_{Charge_NHx}	Conversion factor for NH_x in charge	0.071	Charge (g NH_x)$^{-1}$
i_{Charge_NOx}	Conversion factor for NO_3 in charge	-0.0714	Charge (g NO_3)$^{-1}$

Appendix D – Simulation results from the steady-state model

Species / **Time**	**A** ($g\ m^{-3}$)	**B** ($g\ m^{-3}$)	**O_2** ($g\ m^{-3}$)
0	0.0000	0.0000	0.0000
1	6.4450	80.0215	1.6528
2	6.4450	91.7234	1.6528
3	6.4450	93.3072	1.6528
4	6.4450	93.5214	1.6528
5	6.4450	93.5504	1.6528
6	6.4450	93.5544	1.6528
7	6.4450	93.5550	1.6528
8	6.4450	93.5550	1.6528
9	6.4450	93.5550	1.6528
10	6.4450	93.5550	1.6528
11	6.4450	93.5550	1.6528
12	6.4450	93.5550	1.6528
13	6.4450	93.5550	1.6528
14	6.4450	93.5550	1.6528
15	6.4450	93.5550	1.6528
16	6.4450	93.5550	1.6528
17	6.4450	93.5550	1.6528
18	6.4450	93.5550	1.6528
19	6.4450	93.5550	1.6528
20	6.4450	93.5550	1.6528

Appendix E – Stoichiometric matrix for ASAPM v1

Variable	**$CO2_{sg}$**	**$N2_{sg}$**	**$O2_{sg}$**	**$CO2_{sl}$**	**$O2_{sl}$**	**X_S**	**$CO2_{pg}$**	**$N2_{pg}$**	**$O2_{pg}$**	**$CO2_{pl}$**	**$O2_{pl}$**
ρ											
$rsN2_{in}$	-	$1/V_{sg}$	-	-	-	-	-	-	-	-	-
$rsO2_{in}$	-	-	$1/V_{sg}$	-	-	-	-	-	-	-	-
$rsCO2_{in}$	$1/V_{sg}$	-	-	-	-	-	-	-	-	-	-
$rsN2_{out}$	-	$-1/V_{sg}$	-	-	-	-	-	-	-	-	-
$rsO2_{out}$	-	-	$-1/V_{sg}$	-	-	-	-	-	-	-	-
$rsCO2_{out}$	$-1/V_{sg}$	-	-	-	-	-	-	-	-	-	-
$rsN2_{sp}$	-	$-1/V_{sg}$	-	-	-	-	-	$1/V_{pg}$	-	-	-
$rsO2_{sp}$	-	-	$-1/V_{sg}$	-	-	-	-	-	$1/V_{pg}$	-	-
$rsCO2_{sp}$	$-1/V_{sg}$	-	-	-	-	-	$1/V_{pg}$	-	-	-	-
$rpN2_{ps}$	-	$1/V_{sg}$	-	-	-	-	-	$-1/V_{pg}$	-	-	-
$rpO2_{ps}$	-	-	$1/V_{sg}$	-	-	-	-	-	$-1/V_{pg}$	-	-

Variable ρ	$CO2_{sg}$	$N2_{sg}$	$O2_{sg}$	$CO2_{sl}$	$O2_{sl}$	X_S	$CO2_{pg}$	$N2_{pg}$	$O2_{pg}$	$CO2_{pl}$	$O2_{pl}$
$rpCO2_{ps}$	$1/V_{sg}$	-	-	-	-	-	$-1/V_{pg}$	-	-	-	-
$rpN2_{in}$	-	-	-	-	-	-	-	$1/V_{pg}$	-	-	-
$rpO2_{in}$	-	-	-	-	-	-	-	-	$1/V_{pg}$	-	-
$rpCO2_{in}$	-	-	-	-	-		$1/V_{pg}$	-	-	-	-
$rpN2_{out}$	-	-	-	-	-	-	-	$-1/V_{pg}$	-	-	-
$rpO2_{out}$	-	-	-	-	-	-	-	-	$-1/V_{pg}$	-	-
$rpCO2_{out}$	-	-	-	-	-	-	$-1/V_{pg}$	-	-	-	-
$rsO2_{sol}$	-	-	$-1/V_{sg}$	-	$1/V_{sl}$	-	-	-	-	-	-
$rsCO2_{ev}$	$1/V_{sg}$	-	-	$-1/V_{sl}$	-	-	-	-	-	-	-
$rpO2_{ev}$	-	-	-	-	-	-	-	-	$1/V_{pg}$	-	$-1/V_{pl}$
$rpCO2_{sol}$	-	-	-	-	-	-	$-1/V_{pg}$	-	-	$1/V_{pl}$	-
$rpAlg_{gro}$	-	-	-	-	-	-	-	-	-	-1	1

Variable	**$CO2_{sg}$**	**$N2_{sg}$**	**$O2_{sg}$**	**$CO2_{sl}$**	**$O2_{sl}$**	**X_S**	**$CO2_{pg}$**	**$N2_{pg}$**	**$O2_{pg}$**	**$CO2_{pl}$**	**$O2_{pl}$**
ρ											
$rsXS_{in}$	-	-	-	-	-	$1/V_{sl}$	-	-	-	-	-
$rsXS_{hyd}$	-	-	-	1	$-O2_{req}$	-1	-	-	-	-	-
$rsXS_{out}$	-	-	-	-	-	$-1/V_{sl}$	-	-	-	-	-

Appendix F – Additional stoichiometry for ASAPM v2

		S_{O2}	S_S	S_{NH4}	S_{NOX}	S_{N2}	S_{ALK}	S_I	X_I	X_S	X_H	X_{STO}	X_A	X_{SS}	S_{N2_sl}	$N2_{sg}$
In_z	Inflow of substrates	-	$1/V_{sl}$													
Out_{Sz}	Outflow of soluble substrates	-	$1/V_{sl}$						-	-	-	-	-	-		
Out_{Xz}	Outflow of particulates	-	-	-	-	-	-	-	$1/V_{sl}$							
$rsN2_{ev}$	Evolution of N_2 from AS tank	-	-	-	-	-	-	-	-	-	-	-	-	-	$-1/V_{sl}$	$1/V_{sg}$

Appendix G – Additional stoichiometry for ASAPM v3

	S_{S_sl}	S_{NH4_sl}	S_{NOX_sl}	S_{ALK_sl}	S_{I_sl}	S_{O2_pl}	S_{S_pl}	S_{NH4_pl}	S_{NOX_pl}	S_{ALK_pl}	S_{I_pl}	S_{CO2_pl}	X_{Algae_pl}	S_{N2_pl}	N_{2_pg}
$rsSS_{sp}$	$-1/V_{sl}$	-	-	-	-	-	$1/V_{pl}$	-	-	-	-	-	-	-	-
$rsSNH_{sp}$	-	$-1/V_{sl}$	-	-	-	-	-	$1/V_{pl}$	-	-	-	-	-	-	-
$rsSNOx_{sp}$	-	-	$-1/V_{sl}$	-	-	-	-	-	$1/V_{pl}$	-	-	-	-	-	-
$rsSALK_{sp}$	-	-	-	$-1/V_{sl}$	-	-	-	-	-	$1/V_{pl}$	-	-	-	-	-
$rsSI_{sp}$	-	-	-	-	$-1/V_{sl}$	-	-	-	-	-	$1/V_{pl}$	-	-	-	-
$rpSS_{out}$	-	-	-	-	-	-	$-1/V_{pl}$	-	-	-	-	-	-	-	-
$rpSNH_{out}$	-	-	-	-	-	-	-	$-1/V_{pl}$	-	-	-	-	-	-	-
$rpSNOx_{out}$	-	-	-	-	-	-	-	-	$-1/V_{pl}$	-	-	-	-	-	-
$rpSALK_{out}$	-	-	-	-	-	-	-	-	-	$-1/V_{pl}$	-	-	-	-	-
$rpSI_{out}$	-	-	-	-	-	-	-	-	-	-	$-1/V_{pl}$	-	-	-	-
$rpN2_{sol}$	-	-	-	-	-	-	-	-	-	-	-	-	-	$1/V_{pl}$	$-1/V_{pg}$
$rpAlg_{groNH4}$	-	-	-	-	-	Y_{O2NH4}	-	$-i_{NH4}$	-	-	-	$-i_{CO2}$	Y_{alg}	-	-
$rpAlg_{groNOx}$	-	-	-	-	-	Y_{O2NOx}	-	-	$-i_{NO3}$	-	-	$-i_{CO2}$	Y_{alg}	-	-
$rpXAlgae_{out}$	-	-	-	-	-	-	-	-	-	-	-	-	$-1/V_{pl}$	-	-

Appendix H – Raw data: optical density measurements at 600 nm (calculated starting OD = 0.011 AU)

Culture ID		**Value**	**Day 3**	**Day 5**	**Day 7**	**Day 10**	**Day 12**	**Day 14**	**Day 18**	**Day 20**	**Day 24**	**Day 26**	**Day 28**	**Day 35**
0.0 mg $NaNO_3$ L^{-1}	A	OD_{600}	0.034	0.046	0.062	0.083	0.087	0.111	0.107	0.109	0.124	0.130	0.133	0.141
(0.0 mM $NaNO_3$)	B	OD_{600}	0.035	0.043	0.052	0.066	0.068	0.084	0.090	0.092	0.097	0.109	0.096	0.109
	C	OD_{600}	0.032	0.044	0.055	0.071	0.077	0.092	0.076	0.068	0.037	0.028	0.018	0.016
		Mean	0.034	0.044	0.056	0.073	0.077	0.096	0.091	0.090	0.086	0.089	0.082	0.089
		sd	0.002	0.002	0.005	0.009	0.010	0.014	0.016	0.021	0.045	0.054	0.059	0.065
		se	0.001	0.001	0.003	0.005	0.005	0.008	0.009	0.012	0.026	0.031	0.034	0.037
		se %	2.620	1.989	5.259	6.879	7.096	8.370	9.849	13.264	29.895	34.940	41.166	42.281
5.0833 mg $NaNO_3$ L^{-1}	A	OD_{600}	0.043	0.073	0.094	0.139	0.143	0.171	0.179	0.191	0.215	0.235	0.239	0.273
(0.0598 mM $NaNO_3$)	B	OD_{600}	0.034	0.067	0.093	0.121	0.122	0.155	0.163	0.175	0.198	0.223	0.222	0.253
	C	OD_{600}	0.044	0.073	0.096	0.124	0.126	0.170	0.178	0.186	0.210	0.240	0.249	0.277
		Mean	0.040	0.071	0.094	0.128	0.130	0.165	0.173	0.184	0.208	0.233	0.237	0.268
		sd	0.006	0.003	0.002	0.010	0.011	0.009	0.009	0.008	0.009	0.009	0.014	0.013
		se	0.003	0.002	0.001	0.006	0.006	0.005	0.005	0.005	0.005	0.005	0.008	0.007
		se %	7.884	2.817	0.935	4.350	4.939	3.130	2.985	2.568	2.429	2.168	3.330	2.773

Culture ID		Value	Day 3	Day 5	Day 7	Day 10	Day 12	Day 14	Day 18	Day 20	Day 24	Day 26	Day 28	Day 35
10.1667 mg $NaNO_3$ L^{-1}	A	OD_{600}	0.049	0.092	0.160	0.209	0.233	0.292	0.317	0.372	0.446	0.507	0.535	0.625
(0.1196 mM $NaNO_3$)	B	OD_{600}	0.051	0.101	0.134	0.160	0.176	0.217	0.243	0.265	0.301	0.314	0.326	0.374
	C	OD_{600}	0.036	0.068	0.103	0.136	0.147	0.194	0.210	0.236	0.272	0.292	0.313	0.362
		Mean	0.045	0.087	0.132	0.168	0.185	0.234	0.257	0.291	0.340	0.371	0.391	0.454
		sd	0.008	0.017	0.029	0.037	0.044	0.051	0.055	0.072	0.093	0.118	0.125	0.149
		se	0.005	0.010	0.016	0.021	0.025	0.030	0.032	0.041	0.054	0.068	0.072	0.086
		se %	10.373	11.321	12.450	12.761	13.630	12.626	12.325	14.212	15.845	18.409	18.381	18.899
20.3333 mg $NaNO_3$ L^{-1}	A	OD_{600}	0.042	0.080	0.124	0.189	0.220	0.273	0.291	0.328	0.373	0.409	0.433	0.482
(0.2392 mM $NaNO_3$)	B	OD_{600}	0.046	0.079	0.123	0.189	0.210	0.272	0.293	0.323	0.371	0.406	0.422	0.476
	C	OD_{600}	0.039	0.075	0.126	0.196	0.221	0.279	0.299	0.331	0.377	0.418	0.435	0.493
		Mean	0.042	0.078	0.124	0.191	0.217	0.275	0.294	0.327	0.374	0.411	0.430	0.484
		sd	0.004	0.003	0.002	0.004	0.006	0.004	0.004	0.004	0.003	0.006	0.007	0.009
		se	0.002	0.002	0.001	0.002	0.004	0.002	0.002	0.002	0.002	0.004	0.004	0.005
		se %	4.790	1.958	0.709	1.220	1.618	0.796	0.817	0.713	0.472	0.877	0.940	1.029

Culture ID		Value	Day 3	Day 5	Day 7	Day 10	Day 12	Day 14	Day 18	Day 20	Day 24	Day 26	Day 28	Day 35
50.8333 mg $NaNO_3$ L^{-1}	A	OD_{600}	0.042	0.079	0.131	0.213	0.275	0.360	0.458	0.511	0.584	0.650	0.689	0.782
(0.5980 mM $NaNO_3$)	B	OD_{600}	0.062	0.110	0.179	0.311	0.370	0.458	0.519	0.582	0.648	0.697	0.732	0.833
	C	OD_{600}	0.053	0.088	0.134	0.245	0.313	0.389	0.457	0.517	0.597	0.642	0.671	0.778
		Mean	0.052	0.092	0.148	0.256	0.319	0.402	0.478	0.537	0.610	0.663	0.697	0.798
		sd	0.010	0.016	0.027	0.050	0.048	0.050	0.036	0.039	0.034	0.030	0.031	0.031
		se	0.006	0.009	0.016	0.029	0.028	0.029	0.021	0.023	0.020	0.017	0.018	0.018
		se %	11.051	9.972	10.489	11.256	8.645	7.224	4.289	4.236	3.203	2.588	2.595	2.220
101.6667 mg $NaNO_3$ L^{-1}	A	OD_{600}	0.014	0.011	0.008	0.013	0.013	0.045	0.113	0.169	0.274	0.350	0.397	0.651
(1.1961 mM $NaNO_3$)	B	OD_{600}	0.051	0.091	0.155	0.305	0.376	0.472	0.582	0.657	0.809	0.922	0.998	1.213
	C	OD_{600}	0.056	0.108	0.172	0.336	0.418	0.517	0.637	0.714	0.880	0.984	1.059	1.244
		Mean	0.040	0.070	0.112	0.218	0.269	0.345	0.444	0.513	0.654	0.752	0.818	1.036
		sd	0.023	0.052	0.090	0.178	0.223	0.260	0.288	0.300	0.331	0.350	0.366	0.334
		se	0.016	0.037	0.064	0.126	0.157	0.184	0.204	0.212	0.234	0.247	0.259	0.236
		se %	40.221	52.324	57.104	57.805	58.539	53.442	45.862	41.264	35.800	32.865	31.627	22.782

Culture ID		Value	Day 3	Day 5	Day 7	Day 10	Day 12	Day 14	Day 18	Day 20	Day 24	Day 26	Day 28	Day 35
203.333 mg $NaNO_3$ L^{-1}	A	OD_{600}	0.056	0.116	0.172	0.330	0.428	0.518	0.654	0.740	0.967	1.179	1.357	1.732
(2.3922 mM $NaNO_3$)	B	OD_{600}	0.057	0.109	0.174	0.324	0.425	0.514	0.615	0.710	0.829	1.022	1.200	1.608
	C	OD_{600}	0.042	0.104	0.130	0.431	0.541	0.651	0.746	0.984	1.323	1.477	1.585	1.756
		Mean	0.052	0.110	0.159	0.362	0.465	0.561	0.672	0.811	1.040	1.226	1.381	1.699
		sd	0.008	0.006	0.025	0.060	0.066	0.078	0.067	0.150	0.255	0.231	0.194	0.079
		se	0.005	0.003	0.014	0.035	0.038	0.045	0.039	0.087	0.147	0.133	0.112	0.046
		se %	9.372	3.173	9.041	9.597	8.216	8.024	5.782	10.694	14.155	10.884	8.095	2.700

Appendix I – Raw data: optical density measurements at 232 nm

Culture ID		**Value**	**Day 3**	**Day 5**	**Day 7**	**Day 10**	**Day 12**	**Day 14**	**Day 18**	**Day 20**	**Day 24**	**Day 26**	**Day 28**	**Day 35**
0.0 mg $NaNO_3$ L^{-1}	A	OD_{232}	0.142	0.171	0.161	0.171	0.117	0.188	0.206	0.202	0.154	0.181	0.176	0.219
(0.0 mM $NaNO_3$)	B	OD_{232}	0.062	0.086	0.070	0.070	0.052	0.086	0.093	0.087	0.084	0.104	0.076	0.095
	C	OD_{232}	0.053	0.078	0.068	0.074	0.065	0.087	0.088	0.100	0.098	0.112	0.097	0.143
		Mean	0.086	0.112	0.100	0.105	0.078	0.120	0.129	0.130	0.112	0.132	0.116	0.152
		sd	0.049	0.052	0.053	0.057	0.034	0.059	0.067	0.063	0.037	0.042	0.053	0.063
		se	0.028	0.030	0.031	0.033	0.020	0.034	0.039	0.036	0.021	0.024	0.030	0.036
		se %	33.019	26.648	30.775	31.448	25.459	28.117	29.866	28.042	19.094	18.471	26.169	23.697
5.0833 mg $NaNO_3$ L^{-1}	A	OD_{232}	0.069	0.091	0.063	0.075	0.060	0.088	0.094	0.093	0.120	0.102	0.101	0.120
(0.0598 mM $NaNO_3$)	B	OD_{232}	0.053	0.129	0.066	0.069	0.061	0.084	0.093	0.102	0.118	0.110	0.097	0.127
	C	OD_{232}	0.109	0.078	0.061	0.068	0.064	0.084	0.099	0.100	0.114	0.111	0.097	0.112
		Mean	0.077	0.099	0.063	0.071	0.062	0.085	0.095	0.098	0.117	0.108	0.098	0.120
		sd	0.029	0.027	0.003	0.004	0.002	0.002	0.003	0.005	0.003	0.005	0.002	0.008
		se	0.017	0.015	0.001	0.002	0.001	0.001	0.002	0.003	0.002	0.003	0.001	0.004
		se %	21.628	15.403	2.294	3.093	1.949	1.563	1.947	2.775	1.503	2.645	1.356	3.621

Culture ID		Value	Day 3	Day 5	Day 7	Day 10	Day 12	Day 14	Day 18	Day 20	Day 24	Day 26	Day 28	Day 35
10.1667 mg $NaNO_3$ L^{-1}	A	OD_{232}	0.115	0.091	0.063	0.073	0.076	0.100	0.107	0.122	0.155	0.143	0.135	0.173
(0.1196 mM $NaNO_3$)	B	OD_{232}	0.111	0.081	0.060	0.073	0.074	0.106	0.108	0.110	0.128	0.111	0.101	0.129
	C	OD_{232}	0.108	0.103	0.068	0.072	0.070	0.105	0.104	0.116	0.137	0.119	0.116	0.143
		Mean	0.111	0.092	0.064	0.073	0.073	0.104	0.106	0.116	0.140	0.124	0.117	0.148
		sd	0.004	0.011	0.004	0.001	0.003	0.003	0.002	0.006	0.014	0.017	0.017	0.022
		se	0.002	0.006	0.002	0.000	0.002	0.002	0.001	0.003	0.008	0.010	0.010	0.013
		se %	1.821	6.938	3.665	0.459	2.405	1.790	1.130	2.986	5.669	7.733	8.384	8.750
20.3333 mg $NaNO_3$ L^{-1}	A	OD_{232}	0.174	0.162	0.101	0.088	0.081	0.113	0.108	0.137	0.160	0.144	0.130	0.181
(0.2392 mM $NaNO_3$)	B	OD_{232}	0.176	0.166	0.103	0.083	0.082	0.112	0.124	0.137	0.151	0.148	0.144	0.165
	C	OD_{232}	0.196	0.172	0.081	0.084	0.089	0.114	0.148	0.124	0.160	0.155	0.135	0.166
		Mean	0.182	0.167	0.095	0.085	0.084	0.113	0.127	0.133	0.157	0.149	0.136	0.171
		sd	0.012	0.005	0.012	0.003	0.004	0.001	0.020	0.008	0.005	0.006	0.007	0.009
		se	0.007	0.003	0.007	0.002	0.003	0.001	0.012	0.004	0.003	0.003	0.004	0.005
		se %	3.859	1.744	7.393	1.797	2.996	0.511	9.177	3.266	1.911	2.157	3.004	3.032

Culture ID		Value	Day 3	Day 5	Day 7	Day 10	Day 12	Day 14	Day 18	Day 20	Day 24	Day 26	Day 28	Day 35
50.8333 mg $NaNO_3$ L^{-1}	A	OD_{232}	0.455	0.451	0.379	0.274	0.225	0.191	0.217	0.219	0.250	0.249	0.237	0.290
(0.5980 mM $NaNO_3$)	B	OD_{232}	0.445	0.412	0.315	0.181	0.131	0.146	0.177	0.171	0.195	0.226	0.205	0.255
	C	OD_{232}	0.459	0.460	0.375	0.263	0.215	0.188	0.187	0.160	0.213	0.206	0.207	0.259
		Mean	0.453	0.441	0.356	0.239	0.190	0.175	0.194	0.183	0.219	0.227	0.216	0.268
		sd	0.007	0.026	0.036	0.051	0.052	0.025	0.021	0.031	0.028	0.022	0.018	0.019
		se	0.004	0.015	0.021	0.029	0.030	0.015	0.012	0.018	0.016	0.012	0.010	0.011
		se %	0.919	3.340	5.809	12.259	15.660	8.300	6.206	9.880	7.381	5.473	4.784	4.127
101.6667 mg $NaNO_3$ L^{-1}	A	OD_{232}	0.825	0.881	0.860	0.866	0.862	0.861	0.849	0.815	0.758	0.693	0.633	0.409
(1.1961 mM $NaNO_3$)	B	OD_{232}	0.816	0.869	0.778	0.624	0.570	0.553	0.454	0.371	0.280	0.306	0.313	0.405
	C	OD_{232}	0.830	0.824	0.750	0.584	0.562	0.499	0.359	0.267	0.293	0.315	0.323	0.427
		Mean	0.824	0.858	0.796	0.691	0.665	0.638	0.554	0.484	0.444	0.438	0.423	0.414
		sd	0.007	0.030	0.057	0.153	0.171	0.195	0.260	0.291	0.272	0.221	0.182	0.012
		se	0.004	0.017	0.033	0.088	0.099	0.113	0.150	0.168	0.157	0.128	0.105	0.007
		se %	0.497	2.022	4.146	12.743	14.849	17.682	27.081	34.695	35.435	29.116	24.832	1.636

Culture ID		Value	Day 3	Day 5	Day 7	Day 10	Day 12	Day 14	Day 18	Day 20	Day 24	Day 26	Day 28	Day 35
203.333 mg $NaNO_3$ L^{-1}	A	OD_{232}	1.480	1.567	1.479	1.389	1.389	1.318	1.279	1.165	0.915	0.683	0.482	0.795
(2.3922 mM $NaNO_3$)	B	OD_{232}	1.479	1.535	1.466	1.379	1.345	1.324	1.291	1.184	1.005	0.823	0.607	0.800
	C	OD_{232}	1.494	1.529	1.462	1.271	1.242	1.167	1.002	0.824	0.590	0.688	0.730	1.047
		Mean	1.484	1.544	1.469	1.346	1.325	1.270	1.191	1.058	0.837	0.731	0.606	0.881
		sd	0.008	0.020	0.009	0.065	0.075	0.089	0.164	0.203	0.218	0.079	0.124	0.144
		se	0.005	0.012	0.005	0.038	0.044	0.051	0.094	0.117	0.126	0.046	0.072	0.083
		se %	0.326	0.764	0.349	2.806	3.287	4.045	7.928	11.058	15.065	6.270	11.807	9.445

Appendix J – Raw data: mg $NaNO_3$ L^{-1} calculated from OD_{232} measurements, using $y = -0.0536x^2 + 0.6824x$

Culture ID	Day 3	Day 5	Day 7	Day 10	Day 12	Day 14	Day 18	Day 20	Day 24	Day 26	Day 28	Day 35
0-A	17.987	21.736	20.440	21.736	14.775	23.947	26.299	25.775	19.535	23.036	22.386	28.003
0-B	7.779	10.820	8.791	8.791	6.516	10.820	11.711	10.948	10.566	13.113	9.551	11.966
0-C	6.642	9.805	8.537	9.297	8.158	10.948	11.075	12.603	12.348	14.135	12.220	18.115
5-A	8.664	11.456	7.905	9.424	7.526	11.075	11.838	11.711	15.160	12.858	12.730	15.160
5-B	6.642	16.314	8.284	8.664	7.652	10.566	11.711	12.858	14.903	13.880	12.220	16.057
5-C	13.752	9.805	7.652	8.537	8.031	10.566	12.475	12.603	14.391	14.008	12.220	14.135
10-A	14.519	11.456	7.905	9.171	9.551	12.603	13.496	15.416	19.664	18.115	17.085	21.996
10-B	14.008	10.185	7.526	9.171	9.297	13.369	13.624	13.880	16.186	14.008	12.730	16.314
10-C	13.624	12.986	8.537	9.044	8.791	13.241	13.113	14.647	17.343	15.031	14.647	18.115
20-A	22.126	20.570	12.730	11.075	10.185	14.263	13.624	17.343	20.311	18.244	16.443	23.036
20-B	22.386	21.088	12.986	10.439	10.312	14.135	15.672	17.343	19.147	18.760	18.244	20.958
20-C	24.991	21.866	10.185	10.566	11.202	14.391	18.760	15.672	20.311	19.664	17.085	21.088
50-A	60.002	59.442	49.470	35.280	28.792	24.338	27.741	28.003	32.092	31.959	30.373	37.416
50-B	58.603	54.015	40.773	23.036	16.571	18.502	22.516	21.736	24.860	28.924	26.168	32.754

Culture ID	Day 3	Day 5	Day 7	Day 10	Day 12	Day 14	Day 18	Day 20	Day 24	Day 26	Day 28	Day 35
50-C	60.563	60.703	48.922	33.816	27.478	23.947	23.817	20.311	27.216	26.299	26.429	33.285
100-A	114.979	123.930	120.551	121.514	120.872	120.711	118.792	113.400	104.510	94.588	85.621	53.600
100-B	113.557	121.996	107.608	84.291	76.392	73.933	59.862	48.374	36.080	39.562	40.503	53.047
100-C	115.770	114.821	103.276	78.427	75.233	66.206	46.736	34.348	37.818	40.773	41.852	56.095
200-A	235.675	255.519	235.454	216.213	216.213	201.803	194.142	172.661	129.460	93.081	63.799	110.260
200-B	235.454	248.064	232.601	214.145	207.210	202.997	196.481	176.154	144.470	114.662	81.790	111.043
200-C	238.780	246.687	231.728	192.592	187.027	173.027	143.961	114.821	79.302	93.834	100.208	151.673

Appendix K – Raw data: optical density measurements at 600 nm (calculated starting OD = 0.020 AU)

Culture ID		**Value**	**Day 3**	**Day 5**	**Day 7**	**Day 11**	**Day 13**	**Day 17**	**Day 20**
0.0 mg NH_4Cl L^{-1}	A	OD_{600}	0.040	0.050	0.054	0.069	0.096	0.099	0.122
(0.0 mM NH_4Cl)	B	OD_{600}	0.038	0.050	0.052	0.075	0.085	0.105	0.112
	C	OD_{600}	0.039	0.052	0.054	0.081	0.092	0.107	0.122
		Mean	0.039	0.051	0.053	0.075	0.091	0.104	0.119
		sd	0.001	0.001	0.001	0.006	0.006	0.004	0.006
		se	0.001	0.001	0.001	0.003	0.003	0.002	0.003
		se %	1.480	1.316	1.250	4.619	3.532	2.319	2.809
3.1433 mg NH_4Cl L^{-1}	A	OD_{600}	0.042	0.061	0.073	0.105	0.133	0.159	0.177
(0.0588 mM NH_4Cl)	B	OD_{600}	0.040	0.058	0.070	0.099	0.128	0.154	0.177
	C	OD_{600}	0.041	0.063	0.077	0.109	0.131	0.155	0.176
		Mean	0.041	0.061	0.073	0.104	0.131	0.156	0.177
		sd	0.001	0.003	0.004	0.005	0.003	0.003	0.001
		se	0.001	0.001	0.002	0.003	0.001	0.002	0.000
		se %	1.408	2.395	2.765	2.785	1.112	0.979	0.189

Culture ID		Value	Day 3	Day 5	Day 7	Day 11	Day 13	Day 17	Day 20
6.2867 mg NH_4Cl L^{-1}	A	OD_{600}	0.035	0.054	0.066	0.096	0.122	0.155	0.186
(0.1175 mM NH_4Cl)	B	OD_{600}	0.039	0.053	0.064	0.109	0.135	0.163	0.184
	C	OD_{600}	0.034	0.048	0.056	0.090	0.108	0.144	0.172
		Mean	0.036	0.052	0.062	0.098	0.122	0.154	0.181
		sd	0.003	0.003	0.005	0.010	0.014	0.010	0.008
		se	0.002	0.002	0.003	0.006	0.008	0.006	0.004
		se %	4.243	3.592	4.928	5.703	6.408	3.576	2.420
12.5733 mg NH_4Cl L^{-1}	A	OD_{600}	0.037	0.051	0.062	0.148	0.187	0.226	0.270
(0.2350 mM NH_4Cl)	B	OD_{600}	0.043	0.067	0.098	0.188	0.210	0.236	0.254
	C	OD_{600}	0.039	0.056	0.064	0.144	0.187	0.215	0.234
		Mean	0.040	0.058	0.075	0.160	0.195	0.226	0.253
		sd	0.003	0.008	0.020	0.024	0.013	0.011	0.018
		se	0.002	0.005	0.012	0.014	0.008	0.006	0.010
		se %	4.447	8.148	15.644	8.780	3.938	2.687	4.122

Culture ID		**Value**	**Day 3**	**Day 5**	**Day 7**	**Day 11**	**Day 13**	**Day 17**	**Day 20**
31.4333 mg NH_4Cl L^{-1}	A	OD_{600}	0.034	0.048	0.057	0.113	0.195	0.229	0.235
(0.5875 mM NH_4Cl)	B	OD_{600}	0.037	0.048	0.054	0.145	0.202	0.214	0.228
	C	OD_{600}	0.038	0.056	0.070	0.157	0.187	0.235	0.200
		Mean	0.036	0.051	0.060	0.138	0.195	0.226	0.221
		sd	0.002	0.005	0.009	0.023	0.008	0.011	0.019
		se	0.001	0.003	0.005	0.013	0.004	0.006	0.011
		se %	3.308	5.263	8.139	9.493	2.226	2.763	4.838
62.8667 mg NH_4Cl L^{-1}	A	OD_{600}	0.036	0.051	0.055	0.099	0.128	0.137	0.184
(1.1751 mM NH_4Cl)	B	OD_{600}	0.042	0.048	0.054	0.104	0.137	0.203	0.228
	C	OD_{600}	0.034	0.046	0.054	0.126	0.159	0.176	0.156
		Mean	0.037	0.048	0.054	0.110	0.141	0.172	0.189
		sd	0.004	0.003	0.001	0.014	0.016	0.033	0.036
		se	0.002	0.001	0.000	0.008	0.009	0.019	0.021
		se %	6.438	3.006	0.613	7.562	6.515	11.138	11.068

Culture ID		**Value**	**Day 3**	**Day 5**	**Day 7**	**Day 11**	**Day 13**	**Day 17**	**Day 20**
125.7333 mg NH_4Cl L^{-1}	A	OD_{600}	0.033	0.041	0.047	0.105	0.151	0.217	0.244
(2.3502 mM NH_4Cl)	B	OD_{600}	0.033	0.042	0.040	0.089	0.148	0.145	0.167
	C	OD_{600}	0.033	0.043	0.052	0.086	0.094	0.136	0.115
		Mean	0.033	0.042	0.046	0.093	0.131	0.166	0.175
		sd	0.000	0.001	0.006	0.010	0.032	0.044	0.065
		se	0.000	0.001	0.003	0.006	0.019	0.026	0.037
		se %	0.000	1.375	7.511	6.319	14.138	15.441	21.372

Appendix L – Raw data: optical density measurements at 600 nm (calculated starting OD = 0.018 AU)

Culture ID		**Value**	**Day 1**	**Day 4**	**Day 7**
0.6 mg CO_2 L^{-1}	A	OD_{600}	0.033	0.054	0.112
	B	OD_{600}	0.024	0.054	0.114
	C	OD_{600}	0.027	0.068	0.125
		Mean	0.028	0.059	0.117
		sd	0.005	0.008	0.007
		se	0.003	0.005	0.004
		se %	9.449	7.955	3.454
10.9 mg CO_2 L^{-1}	A	OD_{600}	0.032	0.084	0.184
	B	OD_{600}	0.026	0.068	0.179
	C	OD_{600}	0.028	0.080	0.165
		Mean	0.029	0.077	0.176
		sd	0.003	0.008	0.010
		se	0.002	0.005	0.006
		se %	6.153	6.216	3.231

Culture ID		Value	Day 1	Day 4	Day 7
23.7 mg CO_2 L^{-1}	A	OD_{600}	0.032	0.093	0.215
	B	OD_{600}	0.026	0.079	0.203
	C	OD_{600}	0.025	0.090	0.206
		Mean	0.028	0.087	0.208
		sd	0.004	0.007	0.006
		se	0.002	0.004	0.004
		se %	7.901	4.873	1.733
49.4 mg CO_2 L^{-1}	A	OD_{600}	0.031	0.116	0.286
	B	OD_{600}	0.025	0.101	0.280
	C	OD_{600}	0.026	0.104	0.288
		Mean	0.027	0.107	0.285
		sd	0.003	0.008	0.004
		se	0.002	0.005	0.002
		se %	6.790	4.283	0.844

Culture ID		**Value**	**Day 1**	**Day 4**	**Day 7**
126.4 mg CO_2 L^{-1}	A	OD_{600}	0.030	0.181	0.496
	B	OD_{600}	0.025	0.185	0.484
	C	OD_{600}	0.027	0.191	0.497
		Mean	0.027	0.186	0.492
		sd	0.003	0.005	0.007
		se	0.001	0.003	0.004
		se %	5.316	1.565	0.848
254.8 mg CO_2 L^{-1}	A	OD_{600}	0.030	0.282	0.765
	B	OD_{600}	0.024	0.271	0.786
	C	OD_{600}	0.028	0.282	0.789
		Mean	0.027	0.278	0.780
		sd	0.003	0.006	0.013
		se	0.002	0.004	0.008
		se %	6.453	1.317	0.968